Mass Spectrometry and Gas Chromatography in Chemical Analysis and Identification; Experimental Factors and Case Studies

by

Noel William Davies, B.Sc.Agr.(Hons)

Submitted in fulfilment of the requirements for the degree of
Doctor of Philosophy
University of Tasmania, November, 1993

This thesis contains no material that has been accepted for the award of a higher degree or graduate diploma in any tertiary institution. To the best of my knowledge and belief, the thesis contains no material previously published or written by another person, except where due reference is made in the text of the thesis.

Noel William Davies

This thesis may be made available for loan and limited photocopying in accordance with the Copyright Act 1968.

Noel William Davies

ABSTRACT

This thesis is based on developments in mass spectrometry (MS), gas chromatography (GC) and combined gas chromatography-mass spectrometry (GC-MS) as analytical techniques, and specific applications of these developments and traditional MS and GC-MS to the analysis of organic samples. The majority of this work has been published in the refereed scientific literature.

A detailed theoretical study was undertaken into the relationships between chromatographic resolution in combined GC-MS and carrier gas flow rate. The influence that the type of GC-MS interface has on optimum flow rate requirements was quantified. A simple equation relating column length, column 'hold-up' time and volumetric flow rates in directly coupled capillary GC-MS was derived, facilitating the setting of the appropriate optimum gas flow in this mode.

Average linear gas velocities and flow rates required to deliver optimum performance for a variety of column diameters, carrier gases and types of GC-MS interface were reported, together with the 'hold-up' times and inlet pressures necessary to deliver these values. The dependence between carrier gas flow rates, average linear velocities and temperature programming was determined for a number of GC-MS interface and flow control combinations. Discrimination caused by the 'open-split' interface in GC-MS was examined, and a numerical relationship was established between GC oven temperature and effluent yield in temperature programmed analyses.

A GC-MS screening procedure for a large group of target analytes was created using a 'bench-top' quadrupole mass spectrometer, enabling automatic detection at trace levels of genuine or potential 'positives' from crude extracts. Two representative ions of the target substance had to occur in the correct ratio and at a specific and automatically adjusted retention time for a 'positive' report. For maximum sensitivity a number of time windows were created, and selected ion monitoring of the two characteristic ions for each target compound was carried out. Although the protocol was developed for screening extracts of biological fluids for drugs, it could be applied to screening for target compounds from any matrix.

The technique of 'Selected Reaction Monitoring' of fragmentations within the first field-free region of a double-focussing instrument of Nier-Johnson geometry was developed, and applied to the quantitative determination

of drugs and drug metabolites from body fluid extracts using stable isotope labelled internal standards. This method, an aspect of the now widely adopted 'Mass Spectrometry/Mass Spectrometry' (MS/MS) techniques, greatly increased the specificity of the detection of target compounds. Warfarin from human blood and N-hydroxy phenacetin from human urine were quantified by this technique. These two examples were among the first to use a conventional geometry mass spectrometer in this way for the simultaneous monitoring of daughter ions from different parents from the first field-free region of the spectrometer.

Conventional low and high resolution MS and GC-MS were applied to the analysis of essential oils, wasp secretions and plant gums and waxes. The essential oils of six hop cultivars were analysed in detail, particularly with respect to the levels of selinene isomers. Commercial extracts of *Boronia megastigma* flowers were analysed by GC-MS; (Z)-heptadec-8-ene and dodecyl acetate were identified as major components, together with the new oxygenated sesquiterpene 'sesquicineole' in some clones, and some fifty other volatile components.

A library of several hundred reference mass spectra was compiled to enable analyses on a range of essential oils to be undertaken. This was made available to the MS community via the U.S. National Institutes of Standards and Technology (NIST) database. A collection of 'Kováts' GC retention indices, important corroborative evidence for the MS identification of essential oil related compounds, was obtained from a diverse range of literature sources for 400 mono- and sesquiterpenes. This collection of data was published as a review article.

Based on MS evidence in conjunction with microchemical reactions and subsequent comparison with authentic standards, (E,E)-2,8-dimethyl-1,7-dioxaspiro[5.5]-undecane, (E,E)-2-ethyl-7-methyl-1,6-dioxaspiro[4.5]-decane, (Z,E)-2,8-dimethyl-1,7-dioxaspiro[5.5]undecane and 2-methyl-6-pentyl-3,4-dihydro-2H-pyran were identified in the mandibular gland secretions of parasitic wasps. The structures of three new cycloartenone related triterpenes from *Gardenia* species were determined primarily by MS from first principles; these were 9,19-cyclolanostan-3,24-dione, 9,19-cyclolanost-24-en-3,23-dione, and 9,19-cyclolanostan-3,23-dione.

ACKNOWLEDGMENTS

I would like to acknowledge my colleagues in various research projects at the University of Tasmania included as part of this thesis; in particular Associate Professor Stuart McLean of the School of Pharmacy, and Professor Bob Menary and Dr. John Madden of the Department of Agricultural Science.

Mr. John Bignall, as Officer-in-Charge of Mass Spectrometry in the Central Science Laboratory during the period of my Research Fellowship (1979-1984), was a valued colleague. Mr. Mike Power provided invaluable technical support for the organic mass spectrometers in the Central Science Laboratory.

I am indebted to Emeritus Professor Ken Cavill from the University of N.S.W. for the experience gained in gas chromatography, mass spectrometry, sample extractions, purifications and organic synthesis while working on the chemistry of insect secretions under his direction from 1975 to 1979. I would like to acknowledge Dr. Joe Brophy, Mr. Derek Nelson and Mr. Ray Lidgard of the Organic Mass Spectrometry section at the University of N.S.W., by whom I was introduced to the theory and practice of organic mass spectrometry.

I would like to thank Professor Jim Reid, Professor John Bremner, Associate Professor Stuart McLean, Professor Paul Haddad and Mr. Jim Hutton for supporting my candidature, and Professor Haddad for his comments during the preparation of this thesis.

CONTRIBUTIONS TO JOINT PUBLICATIONS BY THE CANDIDATE

Eight of the fourteen publications used as the basis of this thesis involved joint authorship. In almost all of these cases the candidate was the senior and corresponding author. The following section outlines the various contributions of the candidate and others to these publications.

An automated screening procedure (Neill *et al.*, 1991) was the result of an Australian Research Council Grant of $37,000 to Associate Professor Stuart McLean (School of Pharmacy, University of Tasmania) and the candidate. The grant provided funds for the purchase of the necessary equipment (GC autosampler), and a part-time graduate assistant, Mr. Glen Neill, who worked under the joint supervision of the candidate and Associate Professor McLean.

The candidate wrote the flow-chart and subsequent Pascal macro that enabled the procedure to function, chose the diagnostic target ions, determined the empirical formulae of target ions, and was responsible for the overall supervision of all GC and MS aspects of the project, and the writing of a substantial portion of the submitted manuscript. Mr. Neill was responsible for the day to day preparation, extraction, derivatization and injection of samples, and the building of the database of mass spectra and retention times. Associate Professor McLean also wrote a substantial portion of the manuscript. The candidate was the author for correspondence.

The first application from the selected reaction monitoring procedure (Davies, Bignall and Roberts, 1983), involving the quantitative determination of warfarin from crude plasma extracts by a direct insertion probe technique. This project resulted from a request to the candidate from Dr. Mike Roberts of the School of Pharmacy at the University of Tasmania for the development of a quantitative assay for this drug. The blood samples were provided by Dr. Roberts, who wrote the clinical aspects in the introduction.

This request came at a time when the candidate had been working as a Research Fellow towards using the selected reaction monitoring technique for a range of applications, in consultation with Mr. John Bignall, the officer-in-charge of the MS facility. Useful discussions were held with Mr. Bignall throughout this work. For the warfarin paper, the candidate undertook all the experimental work, did the literature review, prepared the figures, wrote the majority of the manuscript, and was the corresponding author.

For the determination of N-hydroxy phenacetin (NHP) by selected reaction monitoring (Davies, Veronese and McLean, 1984) the candidate was responsible for all mass spectrometry aspects of this project, including the writing of those sections for the manuscript. Dr. Maurice Veronese, who was at the time a Ph.D. student of Associate Professor Stuart McLean, was investigating the differences in drug metabolism and response between individuals for a range of drugs (Veronese, 1988). Part of this work was the investigation of phenacetin metabolism; the determination of NHP in clinical samples formed part of a detailed pharmacological study of several metabolites by Dr. Veronese.

The candidate developed the NHP assay and used it on samples supplied by Dr. Veronese. These had been taken from thin layer plates after it was determined that analyses on crude extracts could not be adequately undertaken; sample extractions, enzyme hydrolyses and purifications were undertaken by Dr. Veronese. While the clinical results of this assay were part of Dr. Veronese's thesis, the candidate suggested, developed and undertook the assay when it was determined that thermal instability rendered N-methoxyphenacetin (NMP) (the derivative of NHP used for analysis) unsuitable for conventional capillary GC-MS analysis. The synthesis of both the standard and deuterated NMP was undertaken by Associate Professor McLean, and the article was jointly written by Associate Professor McLean and the candidate.

The short note outlining the advantages of accelerating voltage adjustments to obtain spectra of the daughter ions of several parent ions via linked scans using the same magnetic field to electric sector voltage ratio (Davies *et al.*, 1982*a*) resulted from discussions between the candidate, Mr. John Bignall and Mr. Ross Lincolne. The candidate wrote the manuscript for this note and was the corresponding author.

Dr. John Madden, of the Department of Agricultural Science, and the candidate worked together on the determination of the chemistry and biological significance of mandibular gland secretions of parasitic wasps (Davies and Madden, 1985). The candidate undertook all aspects of the chemical analysis, the literature review pertaining to the chemistry of wasp secretions and any other insects in which the detected compounds had been found, and the writing up of all matters relating to the chemistry of the secretions. Dr. Madden provided the samples and undertook all experimental work on insect behaviour as well as the writing up of all the biological and behavioural aspects.

The analysis by GC-MS of essential oils derived from hops grown in Tasmania (Davies and Menary, 1982) was undertaken with Professor Bob Menary of the Department of Agricultural Science, as part of a wider program looking at a range of commercial essential oils by GC-MS. The candidate was responsible for all analytical aspects of this paper, and much of the literature search. Pure α- and β-selinene were isolated by preparative GC from rosewood and celery oils respectively. Professor Menary provided the hop oil samples, much of the background information on hop varieties and origins of aroma compounds, and the discussion of 'aroma' type hops. The candidate wrote the majority of the manuscript and was the corresponding author.

The analysis of *Boronia megastigma* (Davies and Menary, 1983*b*) was also undertaken in collaboration with Professor Menary. Apart from the original isolation of the extract, the candidate undertook all the experimental aspects outlined in the paper, including the identification of all the listed components by GC-MS and ancillary techniques, was responsible for the majority of the literature survey and most of the text of the manuscript, and was the corresponding author.

The characterization of gums obtained from the various Gardenia species (Davies *et al.*, 1992) was a collaborative project between the candidate and colleagues at the University of the South Pacific in Fiji. Partially purified samples were provided by the group in Fiji, and the candidate undertook the identification of new and known triterpenes based on interpretation of GC-MS and MS data from first principles and comparison with reference spectra. The candidate undertook the literature review for known work in the area of triterpene and steroid fragmentation mechanisms.

In correspondence with Professor Subranamiam Sotheeswaran the candidate indicated the structures and devised the MS fragmentation schemes. For 9,19-cyclolanost-24-en-3,23-dione, NMR data from a partially purified fraction was used to assign the double bond position in the side chain. Professor Sotheeswaran provided a first draft of the manuscript, which was substantially modified and corrected by the candidate, and for which the candidate provided the structural and MS fragmentation diagrams.

Almost all of the references are the result of the candidate's own literature searches at the time of the original research, or subsequently for this thesis. Some of the references on phenacetin metabolism were obtained from Associate Professor Stuart McLean, and the reference to earlier German work on characterization of

hop varieties from their essential oils was obtained from Professor Bob Menary.

CONTENTS

1. INTRODUCTION

Scope and Limitations

This thesis is based on research undertaken at the University of Tasmania over thirteen years prior to enrolment. The majority of this work has been published in the refereed scientific literature, and has been submitted under the University of Tasmania rules for Research Higher Degrees based on published work.

The text of the thesis summarizes the work in each section, and refers the reader to the relevant publications; it does not attempt to present the work in each section in full detail where this is present in the published work. The principal publications have been incorporated in full into an appendix, which nevertheless constitutes an important part of the thesis.

Significant advances in organic mass spectrometers have occurred since much of the work described was carried out. Applications of mass spectrometry/mass spectrometry (MS/MS) using 'selected reaction monitoring' in conjunction with stable isotope labelled internal standards have become relatively commonplace, and modern instrument hardware and software accommodate this mode; the examples described here, dating back some ten years, were among the first to illustrate the utility of this technique on a conventional geometry mass spectrometer, and predated the commercial availability of the technique.

General Background

MS has traditionally provided a high degree of specificity and sensitivity to the detection and determination of known compounds. Information provided by empirical formulae of molecular and fragment ions via accurate mass measurement, and the study of specific fragmentation pathways yields a wealth of structural information for unknown organic compounds (Beynon, 1960; Budzikiewicz *et al.*, 1964; Beynon *et al.*, 1968; Waller, 1972; McLafferty, 1980*a*; McLafferty and Turecek, 1993).

The coupling of mass spectrometry with gas chromatography (GC-MS) provided the ability to integrate the excellent separation capabilities of GC with the powerful identification capacity of MS, enabling the direct analyses of complex mixtures. Numerous books and reviews have been written in this area, both on general and specific applications (e.g. Junk, 1972; McFadden, 1973; Karasek and Clement, 1988). The introduction of capillary GC-MS, beginning in the 1960's (McFadden *et al.*, 1963;

Teranishi *et al.*, 1963), had a major impact on the amount of information that could be obtained from a single analysis, due to the improved chromatographic separations provided by capillary columns. GC-MS has subsequently had an enormous impact as an analytical technique in clinical, environmental, forensic and natural product chemistry.

The applications of MS as an analytical technique for organic compounds have continued to expand; benchtop quadrupole and ion trap instruments now make the technique available to a much wider range of institutions and researchers than was previously possible. Advances in ionization modes and chromatographic coupling such as Fast Atom Bombardment, Liquid Secondary Ion MS, Thermospray and Electrospray liquid chromatography interfaces have enabled the analysis of a range of biochemicals and macromolecules that were previously not suited to MS. Numerous reviews have been written on these developments (e.g. Burlingame *et al.*, 1990; 1992), and a recent overview of the practical techniques used in organic MS has been published (Chapman, 1991), including reference to some of the original work described in this thesis.

Research areas

The overall theme of the individual and collaborative research undertaken since 1979 has been the *development* of a number of theoretical and practical aspects of MS and GC as techniques for the determination and analysis of organic compounds, in both chromatographically coupled (GC-MS) and MS only modes, and the *application* of these techniques and conventional MS and GC-MS to the analysis of organic samples in several disciplines. The work described in this thesis has been divided into three major subheadings; the development of certain theoretical and practical considerations in gas chromatography relevant to the coupling of this technique with MS; the development of specific GC-MS and mass spectrometry/mass spectrometry (MS/MS) techniques of relevance to a wide range of analyses; and the specific applications of these developments and conventional MS and GC-MS to specific analytical problems.

Under *theoretical considerations* has been included the chromatographic optimization of GC-MS systems based on carrier gas flow rate and GC oven temperature programming parameters. The determination of analyte yield using the 'open-split' interface in capillary GC-MS and the quantitative implications of this have also been included under theoretical development.

The *analytical technique development* category includes the development of an automated screening procedure for a complex range of target compounds using GC-MS, and the use of 'selected reaction monitoring' methods (MS/MS) for enhanced specificity in the determination of target compounds from relatively crude matrices. The applications of the latter technique to the analysis of warfarin in human blood plasma and N-hydroxy phenacetin in human urine have also been included in this section.

Other applications discussed relate to the use of MS in the analysis of a range of known and new natural products. These include; secretions involved in communication in parasitic wasps; the general application to essential oils and other plant extracts; essential oils from hops (*Humulus lupulus*); solvent extracts of *Boronia megastigma* flowers; and bud exudates from several Fijian *Gardenia* species. The development of relevant mass spectral and Kováts' retention index databases has been included under the general application of these techniques to essential oils and other plant extracts.

Background to Research Undertaken

During a five year Research Fellowship in Mass Spectrometry in the Central Science Laboratory (CSL) at the University of Tasmania, MS and GC-MS were introduced as analytical methods to a number of academic departments and projects, and basic research was undertaken in several areas. Existing research projects from within academic departments at the University were also supported, and the full potential of the then recently acquired Vacuum Generators (VG) 7070F double focussing mass spectrometer was developed. The application of GC-MS to the analysis of essential oils and related products commenced during this period, and the characterization of parasitic wasp secretions also formed part of the Research Fellowship.

Although the general technique of capillary GC-MS was well established by 1979, a number of contributions to the literature towards achieving optimum chromatographic performance were made during the period of the Research Fellowship. In particular, relationships between carrier gas flow rate, carrier gas linear velocity, oven temperature programming and type of capillary GC-MS interface were quantified. This in turn enabled optimum separations to be obtained under a variety of widely differing conditions.

Development of the then new technique of 'selected reaction monitoring' on mass spectrometers of conventional Nier-Johnson geometry was also undertaken,

using fragmentations occurring in the first field-free region of the spectrometer. This work included some of the first applications of this technique in conjunction with stable isotope dilution for quantitative determinations.

Appointment in 1984 as Officer-in-Charge of the MS facility in the CSL at the University of Tasmania saw the continued participation in collaborative research with colleagues from several disciplines in which MS was used to solve specific analytical problems, as well as further independent research relating to the techniques of gas chromatography and mass spectrometry. This period included the development of the automated GC-MS drug screening procedure. The principal areas of collaborative applications were in the disciplines of Agricultural Science, Pharmacy, Plant Science and Chemistry.

Publications

The individual and collaborative work outlined above on the development and analytical applications of MS and GC led to 36 publications in refereed international journals, and 32 presentations at national and international conferences. This thesis is based on fourteen articles directly relevant to the central theme, which in most cases involved sole or senior authorship. These publications are included in full in Appendix B.

A further 18 collaborative publications relating to the application of MS and GC to the analysis of a range of natural products and xenobiotics have been listed in Appendix A.

2. THEORETICAL CONSIDERATIONS IN GAS CHROMATOGRAPHY-MASS SPECTROMETRY

i) Chromatographic Optimization

a) Carrier Gas Flow Rate Determination in Directly Coupled GC-MS

Capillary GC-MS as a tool for organic analysis was first introduced in the 1960's (McFadden *et al.*, 1963; Teranishi *et al.*, 1963) using a time-of-flight mass spectrometer, and was subsequently used with quadrupole and magnetic sector mass spectrometers. Capillary GC-MS subsequently became a much more widespread technique during the late 1970's and early 1980's after the introduction of benchtop quadrupole and ion trap instruments made it affordable by many laboratories.

Obtaining and maintaining the best possible chromatographic separation of components for a given column remained of fundamental importance in the analysis of complex mixtures by capillary GC-MS; failure to do this can easily result in the mass spectra of unresolved components being recorded, complicating the interpretation of the data.

During this period there were substantial improvements made in the manufacture and performance of capillary GC columns in terms of the maximum resolution, including the introduction of fused silica capillary column technology (Dandenau and Zerenner, 1979; Dandenau *et al.* 1979; Lipsky *et al.*, 1980). One of the limitations of magnetic sector mass spectrometers for capillary GC-MS had been their inability to scan fast enough to keep pace with the narrow peak width of high resolution capillary columns, resulting in distorted spectra and effectively degraded chromatographic resolution.

Laminated magnet technology was introduced commercially during this same period, making magnetic sector mass spectrometers capable of scanning fast enough to cope with high resolution capillary chromatography peak widths. Various MS modes could be used in conjunction with the capillary GC separations, such as low and high mass resolution scanning, low and high mass resolution selected ion monitoring (SIM) and, for double focussing spectrometers, linked scans of magnetic field and electric sector to probe fragmentation pathways (Boyd and Beynon, 1977).

However, the introduction of the mass spectrometer to the chromatographic system has the potential to significantly degrade the chromatographic resolution, due to possible diffusion of separated components along the length of any

transfer lines, and the inherent operating pressure difference between the gas chromatograph and the mass spectrometer (McFadden, 1979, p.5).

Some commercial GC-MS capillary column interface designs of the mid to late 1970's, including that on the VG 7070F in the CSL, resulted in a substantial loss of chromatographic resolution. Some, including that on the VG 7070F, also resulted in a significant degree of discrimination against relatively non-volatile material that could otherwise pass through a GC column. For example, the heavier petroleum hydrocarbons in oil and sediment samples could not be adequately transmitted through the manufacturer's interface on the VG 7070F, with significant peak broadening and reduction in peak area occurring before n-triacontane. Modified interfaces were reported for some commercial instruments (e.g. Rose, 1983) that overcame some of these deficiencies.

One of the first priorities as Research Fellow in the CSL at the University of Tasmania in 1979 was the improvement in the chromatographic resolution in the capillary GC-MS mode of the then recently acquired VG 7070F double-focussing mass spectrometer. This instrument was supplied with a capillary column interface containing a glass lined tubing connection from the end of the capillary column to a 0.15mm diameter 'jet' situated just before the ion source, and remote from the end of the glass capillary column. The jet offered a fine restriction into the mass spectrometer, providing a large pressure drop across its length.

This maintained the pressure at the end of the capillary column at or near one atmosphere, such that the chromatographic separation was theoretically the same as when connected to a conventional GC detector. However, in practice this arrangement resulted in a considerable 'unswept' dead volume between the end of the column and the jet, which led to a significant loss of chromatographic resolution. By replacing this jet with one of *wider* bore (1mm), and thereby directly exposing the capillary column to the MS vacuum, maximum resolution could be achieved without substantial band broadening in the interface. This results from the effective 'sweeping' of the dead volume by the relatively high vacuum extending back to the end of column; as the pressure in the column approaches zero, linear gas velocities approach or exceed supersonic speeds.

Under these conditions, residence time in the transfer line is minimized by *increasing* the diameter (and therefore also the conductance) of the tubing; the traditional chromatographic approach of minimizing 'dead volume' in the connecting plumbing becomes

counterproductive. In the original modification to the VG7070, prior to the advent of fused silica columns, the glass capillary column terminated in the GC oven and was connected by a piece of 3mm internal diameter glass-lined steel tubing to the 1mm diameter ion source re-entrant. Subsequently fused silica capillary columns were threaded directly into the ion source.

The direct coupling of capillary columns to mass spectrometers, without the use of some device to provide a pressure drop from one atmosphere to ion source pressure at the end of the column, was not in widespread use in 1979.

Early research (Sellier and Guiochon, 1970) on direct coupling of capillary GC to mass spectrometers, in which the GC column was exposed to the vacuum of the mass spectrometer, concluded that the optimum average carrier gas velocity, as determined from 'van Deemter' plots of the Height Equivalent to a Theoretical Plate (HETP) versus average velocity (Giddings, 1965), was the same as the optimum value with the end of the column at or near atmospheric pressure. The latter situation occurs in normal GC and also in coupled GC-MS where there is a restriction with the appropriate conductance prior to the mass spectrometer.

Subsequently it was shown that this work had reached the incorrect conclusion due to the limited pumping capacity of the authors' mass spectrometer and their use of relatively long capillary columns, which substantially reduced the observable difference in effect between having atmospheric pressure or a vacuum at the end of the column (see discussion below, and Figure 2). It was determined (Hatch and Parrish, 1978; Cramers *et al.*, 1981) that it was in fact the *volumetric* flow of gas, as measured at atmospheric pressure, that needed to be held constant between the two modes of operation to maintain the highest possible number of theoretical plates.

Directly coupled capillary GC-MS therefore inevitably requires higher average carrier gas velocities than normal GC, the extent of the difference depending on the column's length and diameter (Hatch and Parrish, 1978). These higher optimum gas velocities result in correspondingly shorter analysis times, and this fact was one of the driving forces behind some of these early developments; the work of Hatch and Parrish was not specifically aimed at GC-MS coupling, but rather at the advantages in speed of analysis of running any capillary GC column with the outlet held at very low pressure. However, directly coupled capillary GC-MS may result in a theoretically larger HETP than is achievable with atmospheric outlet pressure, and hence lower efficiency

per unit length and lower total plate count. Expressed in terms of the total number of theoretical plates, Cramers *et al.* (1981) calculated that it was possible under vacuum GC conditions to obtain 87.5% of the resolution achieved with atmospheric outlet pressure. In practice they found no measurable decrease in performance.

From this work it was shown that there was no 'universal' optimum average velocity for any particular carrier gas as was originally thought, but rather a volumetric flow rate optimum for a given column and carrier gas regardless of the method of GC-MS interfacing. 'Flow rate' in this context refers to the actual *flux* of gas (e.g. in mL min^{-1} measured at atmospheric pressure), and not the 'average' flow rate, which is simply the volume of the column divided by the retention time of an unretained peak. Since optimum flow rates for various carrier gases and column types were known (e.g. Grob and Grob, 1981), the simplest solution for setting flow rates in directly coupled capillary GC-MS would be to measure the volumetric flow and adjust it till the correct value is reached. An added advantage of being able to determine flow rates in directly coupled capillary GC-MS is the ability to readily stay within the pumping capacity of the system.

However, this parameter can not be measured easily by the traditional methods, such as using some form of flow-meter, since the only access to the effluent is from the rotary pump, which gives a very erratic flow resulting in both very imprecise and inaccurate measurements. A relationship for directly coupled GC-MS between various more easily measured parameters and the volumetric flow rate was therefore sought.

The starting point for this relationship was Poiseuille's equation for 'viscous' flow in long, open cylindrical tubes (Dushman, 1962), and the fact that flow rate of gas through a tube is the product of the tube's conductance and the pressure drop across it (Holland, 1974, p.26). It was well established that the flow in capillary GC columns was viscous (McFadden, 1973, p.125). While the situation in the last few centimetres of wider bore columns approaches molecular flow conditions, this contributes a negligible amount to the overall time that a component spends in the GC-MS system.

Poiseuille's equation can be expressed (Cramers *et al.*, 1981);

$$\bar{\upsilon} = \frac{3d^2(P_i^2 - P_o^2)^2}{128\eta L(P_i^3 - P_o^3)} \qquad (1)$$

where $\bar{\upsilon}$ is the average linear velocity, d is column diameter, P_i is inlet pressure, P_o is outlet pressure, L is column length and η is the carrier gas viscosity at the column temperature. Since $\bar{\upsilon} = L/t_a$ where t_a is the 'hold-up' time (the time taken for an unretarded component such as air to pass through the column), equation 1 can be rearranged and expressed in terms of t_a;

$$t_a = \frac{128\eta L^2(P_i^3-P_o^3)}{3d^2(P_i^2-P_o^2)^2} \quad (2)$$

The expression for flow rate (Q) based on the product of the conductance of the column (Holland, 1974, p.26) and the pressure drop across the column (P_i-P_o) is;

$$Q = \frac{\pi d^4(P_i^2-P_o^2)}{256\eta L} \quad (3)$$

Rearrangement of equation 3 allows expression in terms of P_i;

$$P_i = \left[\frac{256\eta LQ}{\pi d^4} + P_o^2\right]^{1/2} \quad (4)$$

Substitution of equation 4 in equation 2, for the specific case when $P_o = 0$, resulted in the derivation of the expression;

$$t_{a,vac} = \frac{8}{3}\left[\frac{\pi\eta L^3}{Q}\right]^{1/2} \quad (5)$$

where $t_{a,vac}$ is the hold-up time under directly coupled GC-MS. This expression enabled ready conversion between required flow rates and optimum average linear gas velocity for any column and carrier gas in directly coupled GC-MS. i.e. for any flow rate Q_{vac}, the average velocity under directly coupled GC-MS ($\bar{\upsilon}_{vac}$) will be;

$$\bar{\upsilon}_{vac} = \frac{3}{8}\left[\frac{Q_{vac}}{\pi\eta L}\right]^{1/2} \quad (6)$$

Rearrangement of equation 5 also allows expression of the flow rate in directly coupled capillary GC-MS (Q_{vac}) in terms of the length of the column, the air peak time and the carrier gas viscosity, without any reference to column diameter or inlet pressure;

$$Q_{vac} = \frac{64\pi\eta L^3}{9(t_{a,vac})^2} \quad (7)$$

The removal of all reference to the column internal diameter and inlet pressure in equations 5 and 7 was not expected; a previous published relationship (Sellier and Guiochon, 1970) had incorporated both inlet pressure and column diameter terms. This relationship of flow rate being proportional to the cube of the column length divided by the square of the 'dead time' enabled the volumetric flow rate as measured at atmospheric pressure to be readily determined from accessible parameters, with no reference to the column's internal diameter or inlet pressure as was previously required.

The relationship further simplified to;

$$Q_{vac} = \frac{kL^3}{(t_{a,vac})^2} \quad (8)$$

where k is a constant for any particular carrier gas at a given temperature. For helium, k = 0.2568 at 20°C for the answer to be expressed directly in the convenient units of mL atm minute^{-1}. For example, the flow rate through a directly coupled 30m column of any diameter using helium as carrier gas, with the column held at 20°C, and with an experimentally determined hold-up time of 70 seconds, is (0.2568 x ($30^3/70^2$)) = 1.41 mL atm minute^{-1}.

The hold-up time for air was plotted against flow rate for vacuum GC for representative column lengths and carrier gases (Figure 1).

Plots showing the additional velocity required under direct coupling to correspond to the same flow rate as average velocities measured with the column outlet at atmospheric pressure were also generated for a range of representative column lengths, diameters and carrier gases (Figure 2). These enabled simple prediction of the optimum average velocity for a number of common situations.

To convert directly from a known optimum average carrier gas velocity with atmospheric outlet pressure to the corresponding optimum average velocity under conditions of direct coupling requires an iterative solution to a polynomial function. Rearrangement of equation 2, using the optimum value for $\bar{u}$ with atmospheric outlet pressure ($\bar{u}_{opt,atm}$), and substituting $t_a = \bar{u}/L$, gives:

$$\frac{128\eta L\bar{\upsilon}_{opt,atm}}{3d^2} = \frac{(P_{i,opt,atm}^2 - P_{atm}^2)^2}{P_{i,opt,atm}^3 - P_{atm}^3} \qquad (9)$$

where $P_{i,opt,atm}$ is the inlet pressure required to give the optimum velocity with atmospheric outlet pressure, and P_{atm} is atmospheric pressure. An iterative solution to this equation yields a value for $P_{i,opt,atm}$. The optimum hold-up time under directly coupled conditions, $t_{a,opt,vac}$, can be found directly from this via substitution in the expression (Cramers *et al.*, 1981);

$$t_{a,opt,vac} = \frac{L(P_{i,opt,atm}^2 - P_{atm}^2)^{3/2}}{\bar{\upsilon}_{opt,atm}(P_{i,opt,atm}^3 - P_{atm}^3)} \qquad (10)$$

The subsequent commercial introduction of flexible fused silica capillary columns enabled columns to be threaded right into the ion source of the mass spectrometer, and direct coupling became and remains one of the most common methods of interfacing GC with MS.

This work was published in *Analytical Chemistry* (Davies, 1984*a*)[1]. It presented a simple solution to the otherwise difficult task of experimentally determining carrier gas flow rates in directly coupled capillary GC-MS, and enabled conditions to be chosen so that near to optimum flow rates could be employed for any given analysis. This then ensured the best possible chromatographic resolution of closely eluting components for a particular carrier gas for any given set of GC oven temperature parameters. While the known optimum average linear velocity could be used under atmospheric outlet pressure to set appropriate conditions for analysis, this was not true for directly coupled GC-MS. In this case optimum values varied widely depending on the length and diameter of the column, and had not been established for many cases.

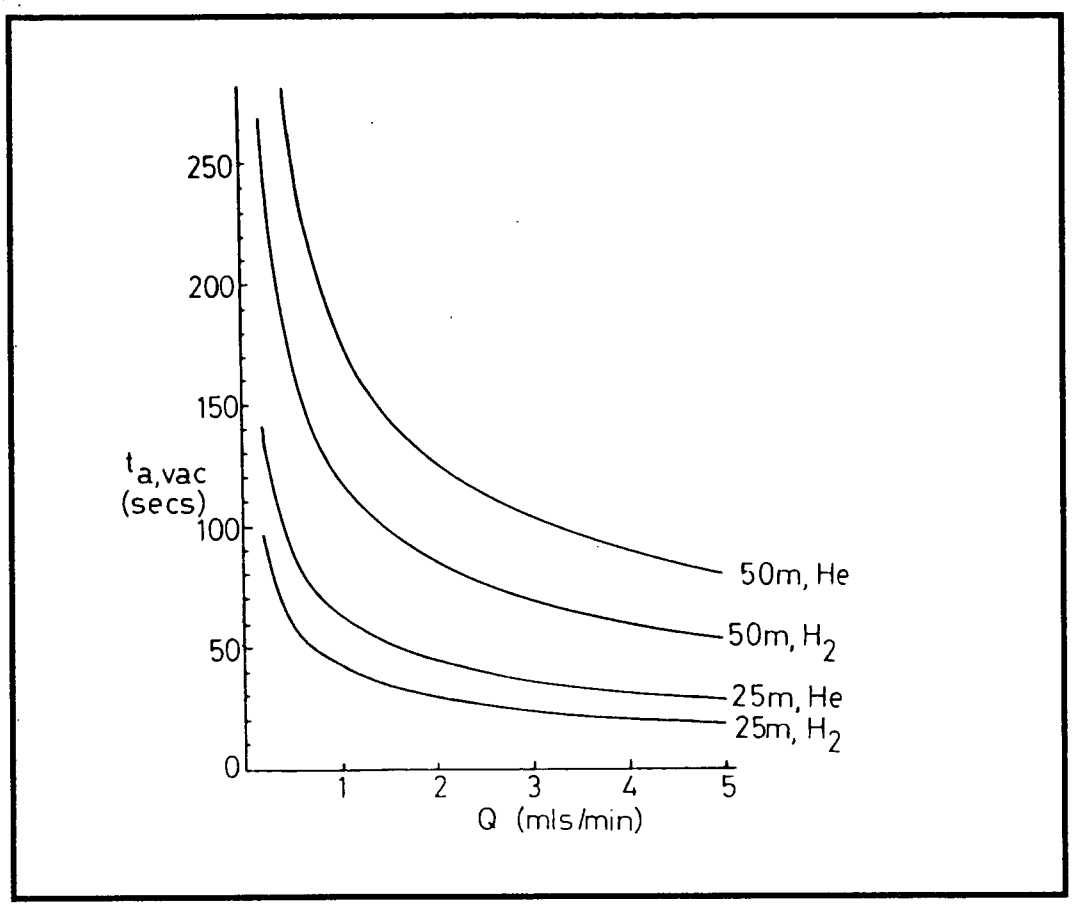

Figure 1

Plots of the air peak 'hold-up' time, $t_{a,vac}$, for directly coupled capillary GC-MS that will result in the given flow rates for 25m and 50m columns of any diameter consistent with viscous flow, with hydrogen and helium carrier gases, based on equation 5 derived above.

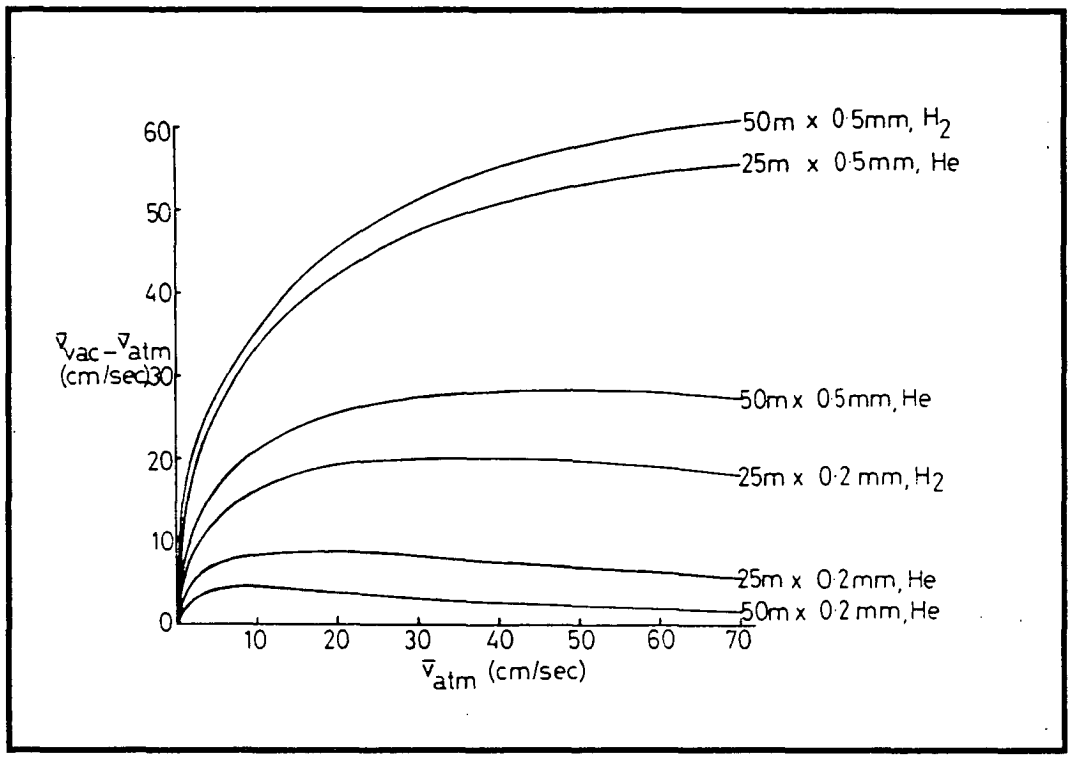

Figure 2

Plots of the additional average velocity required under directly coupled GC-MS to maintain the same flow rate relative to normal atmospheric outlet pressure GC for the specific column lengths, diameters and carrier gases indicated.

b) Temperature Programming and Carrier Gas Flow Rates in Gas Chromatography

A further fundamental aspect affecting the separation of individual components in any particular analysis is the rate at which the GC oven temperature is ramped. Until the relatively recent commercial introduction of electronic inlet pressure programming (Hermann *et al.*, 1990; Wylie *et al.*, 1991), most commercial gas chromatographs employed a constant head pressure to regulate carrier gas flow through capillary columns. Where a mass flow controller existed in the line, it was generally employed to control the *total* gas flow (i.e. including the 'split vent' portion of flow through a split/splitless injector), and not the actual column flow. A direct consequence of temperature programming under circumstances where the column head pressure is constant is that the flow rate and average linear velocity will fall as the column temperature rises, due to the increased viscosity of the gas with rising temperature (Ettre, 1984).

An article in *Analytical Chemistry* (Jones *et al.*, 1983) attempted to determine the best theoretical combination of flow rate and temperature program rate to yield optimized chromatographic resolution. This article plotted the separation number ('TZ') (Kaiser, 1961), a measure of a column's separating efficiency, against both temperature program rate and carrier gas flow rate in three dimensions, in an attempt to find the optimum combination of conditions.

However, there were a number of misconceptions in this article, and correspondence with the journal was entered into on the matter by the candidate. One of the major problems associated with the article by Jones *et al.* was that the authors failed to recognize the fact that the flow rate and average linear velocity were varying during any temperature programmed part of the analysis, and that this introduced an extra degree of complication in any procedure designed to optimize performance for a wide range of compounds of different retention times.

Specifically, their attempt to specify a flow rate (in reality an *initial* flow rate) and temperature program rate combination that was ideal for all compounds made no sense in the light of the fact that compounds eluting at higher temperatures will experience overall lower flow rates. Moreover, the rate of temperature programming also influences the column temperature at which a given component will elute, and hence the range of flow rates that the sample has been exposed to.

Jones *et al.* were invited by the editor of *Analytical Chemistry* to respond to these comments prior to their publication, and the original draft by the candidate was modified slightly based on the information contained in their reply. This article appeared soon after in *Analytical Chemistry* (Davies, 1984*b*)[2].

Further complications in the article by Jones and coworkers arose from the possible confusion between the concept of 'average flow rate' and 'measured flow rate'. The former is defined simply as the volume of the column divided by the retention time of an air peak, and does not represent a *quantity* of gas per unit of time, while the latter is the flow rate that can be measured at the end of the column at atmospheric pressure. If the temperature at which the measurement is made is known, then this defines the actual quantity of gas flowing per unit of time. The use of the term 'flow rate' without further definition implies the *measured* flow rate to most chromatographers; Jones *et al.* were talking about 'average flow rate', which will be substantially different from measured flow rate for all columns that have any appreciable pressure drop across their length.

Jones *et al.* (1987) subsequently published a second article investigating the effects on separation number of starting temperatures in association with temperature *and* pressure programming, in which these factors were more fully addressed.

c) General Effects of Interface, Method of Flow Control and Temperature Programming on Capillary GC-MS

A more detailed study of the effect of GC-MS interface type, the type of flow control and the effects of temperature programming on carrier gas flow rates was undertaken. The effects and implications of various combinations of these for optimizing chromatographic resolution were examined in some detail.

This work, published in *Journal of Chromatography* (Davies, 1985)[3], summarized a number of theoretical considerations which had not been addressed in the literature up to that point relevant to both GC and GC-MS, and presented detailed practical information to enable optimized performance to be achieved under a variety of differing conditions.

The article specifically addressed two areas; the effects that the type of GC-MS interface (such as direct coupling, capillary leak and open-split) would have on optimum average gas velocities and flow rates, and the effect that temperature programming of the GC oven, in combination with different types of flow control and GC-MS interface, would have on flow rate and average velocity parameters. The possible consequences of these effects on separation efficiency were also addressed. The points at which sub-atmospheric inlet pressure would be required to deliver desired flow rates were set out for a broad range of columns and carrier gases, enabling any potential problems to be avoided by suitable choice of column lengths and diameters.

The flow rates required to correspond to a particular optimum average carrier gas velocity with atmospheric outlet pressure were calculated, using the iterative solution to equation 9 to calculate $P_{i,opt,atm}$ and substituting this value in equation 3. The results of this procedure are shown in Figure 3, and illustrate the slight increase in flow rate required to deliver the same average velocity for increasing column lengths. The hold-up times, inlet pressures required with atmospheric pressure outlet pressure and with direct coupling were also plotted for the same range of columns.

Figure 4 shows the average velocities required for directly coupled columns of the stated diameters to correspond to the flow rates generated by the average velocity 25cm s^{-1} for helium and 50 cm s^{-1} for hydrogen. Dotted regions in these graphs represent column lengths that would require sub-atmospheric inlet pressure. Where such control is available, wide bore columns clearly provide the potential for very rapid analyses.

The effect of temperature programming on flow rates was investigated in some detail, including the different effects caused by the method of flow control and the type of GC-MS interface. While the theoretical optimum average velocity does actually increase very slightly with increasing column temperature (Guiochon, 1966), due to the dependence of the diffusion coefficient in the gas on temperature, the following discussion only looks at actual trends caused by temperature programming.

From equation 1, $\bar{u}$ will fall in an inversely proportional manner to the increase in carrier gas viscosity with temperature if the inlet pressure is held constant. This 'isobaric' governing of the flow through capillary columns remains one of the most common methods of flow control. Similarly, from equation 3, Q will also fall in an inverse proportional manner with increased gas viscosity. This effect is illustrated in Figure 5(a). The flow rate as measured after cooling to room temperature (Q_{end}) will be lower still by the ratio of the two absolute temperatures, due to the contraction of the gas (Charles' law). This is illustrated in Figure 5(b).

Where the column flow rate is regulated by a mass flow controller, or as is now possible by electronic pressure programming to maintain constant flow (Hermann *et al.*, 1990; Wylie *et al.*, 1991), an entirely different set of conditions prevail. A point that was perhaps not well appreciated is that under these operating conditions average carrier gas velocity $\bar{u}$ will not be constant but will increase, sometimes substantially, depending on the length and diameter of the column. If constant flow is maintained through a thermally isolated device, then from consideration of Charles' law, the flow rate (but not the average velocity or average flow rate) through the column will be greater by the ratio of the absolute temperature change of the GC oven, as illustrated in Figure 5(d).

When columns are directly coupled to a mass spectrometer, a constant relationship for the change in average velocity exists for all cases, as is shown in Figure 5(e). This follows from equation 7. Substituting $K = 64\pi L/9$ and $\bar{u} = L/t_a$ gives;

$$Q_1 = K\eta_1\bar{u}_1^2 \qquad (11)$$

and

$$Q_2 = K\eta_2\bar{u}_2^2 \qquad (12)$$

where Q_1 is the flow rate at some initial temperature T_1 with carrier gas viscosity η_1 and average velocity $\bar{u}_1$, and Q_2 is the flow rate at a higher temperature T_2 with carrier gas viscosity η_2 and average velocity $\bar{u}_2$. Since $Q_2 = Q_1.(T_2/T_1)$ when Q_{end} is held constant (from Charles' law),

substitution and expressing in terms of $\bar{u}_1$ and $\bar{u}_2$ and taking the ratio gives;

$$\bar{u}_2/\bar{u}_1 = \frac{\eta_1 T_2}{\eta_2 T_1} \qquad (13)$$

The change in average velocity and average flow rate with increased column temperature under conditions of mass flow control (Q_{end} held constant) and atmospheric outlet pressure needs independent consideration. When the column outlet is at atmospheric pressure, the situation is more complex, and the increase in velocity with temperature depends on column length, diameter and initial velocity. From equation 1, where $\bar{u}_2$, P_2 and η_2 are the average carrier gas velocity, inlet pressure and viscosity at a temperature T_2, and $\bar{u}_1$, P_1 and η_1 are the corresponding values for an initial temperature T_1;

$$\bar{u}_2/\bar{u}_1 = \frac{\eta_1 (P_2^2 - P_o^2)^2 (P_1^3 - P_o^3)}{\eta_2 (P_1^2 - P_o^2)^2 (P_2^3 - P_o^3)} \qquad (14)$$

P_1 and P_2 can be calculated from equation 4;

$$P_1 = \left[\frac{256 \eta_1 L Q_1}{\pi d^4} + P_o^2 \right]^{1/2} \qquad (15)$$

and, since $Q_2 = (T_2/T_1) Q_1$ when Q_{end} is constant;

$$P_2 = \left[\frac{256 \eta_2 L Q_1 T_2}{\pi d^4 T_1} + P_o^2 \right]^{1/2} \qquad (16)$$

To illustrate this effect, the following describes the specific case of a 25m, 0.32mm internal diameter column with a flow rate of helium at 20°C of 3 mL atm minute^{-1}, programmed with mass flow control to 200°C and with atmospheric outlet pressure.

Working in SI units;
$\eta_1 = 1.941.10^{-5}$ kg m^{-1}s^{-1}
$\eta_2 = 2.672.10^{-5}$ kg m^{-1}s^{-1}
$T_1 = 293$
$T_2 = 473$
$Q_1 = 3 \times 1.6885.10^{-3} = 5.065$ m^3 Pa s^{-1}
$Q_2 = 3 \times (473/293) \times 1.6885.10^{-3} = 8.177$ m^3 Pa s^{-1}
$P_o = 1.013.10^5$ Pa

L = 25 m
d = 0.00032 m

From equation 15, P_1 = 171,300 Pa absolute (70 kPa above atmospheric pressure).

From equation 16, P_2 = 229,600 Pa absolute (128.3 kPa above atmospheric pressure).

Substitution of these values in equation 14 gives;

$$\bar{\upsilon}_2/\bar{\upsilon}_1 = 1.29$$

The same answer can be achieved working from consideration of expressions for 'average' flow rates (James and Martin, 1952). In this case the ratio of the average flow rates $Q_{av,1}$ and $Q_{av,2}$ is given by;

$$\frac{Q_{av,2}}{Q_{av,1}} = \frac{T_2(P_2^2 - P_o^2)(P_1^3 - P_o^3)}{T_1(P_2^3 - P_o^3)(P_1^2 - P_o^2)} \quad (17)$$

Since $\bar{\upsilon} = Q_{av}/A$ where A is the cross sectional area of the column, the ratio of the average velocities is the same as the ratio of the average flow rates. Substitution of the specific values for P_1 and P_2 derived for the above example yields a calculated ratio for average flow rates of 1.29.

With electronic pressure control, the rate of pressure increase can be set such that either Q or $\bar{\upsilon}$ is held constant after appropriate calculations are made, although pre-programmed 'constant flow' conditions result in constant Q_{end}, giving mass flow control. The specific values for P_1 and P_2 calculated for the example above are precisely the values calculated and set by the electronic pressure control module on a HP 5890 series II split/splitless injector when 'constant flow' of 3mL atm minute^{-1} was requested for a column of the stated dimensions, and the oven was ramped from 20°C to 200°C.

To achieve constant velocity in this case, substituting in equation 1 and setting $\bar{\upsilon}_1 = \bar{\upsilon}_2$ and solving for P_2 results in a value of only 98kPa above atmospheric pressure (rather than the 128kPa required for constant flow), corresponding in a fall in Q_{end} to 2.1 mL atm minute^{-1}. While a modest rise in average carrier gas velocity with temperature as a result of 'constant flow' conditions may help to offset the rise required in optimum average velocities by higher temperatures (Guiochon, 1966), in most cases the actual rise will greatly exceed any required increase.

The lower the initial inlet pressure, the larger the relative increase in velocity will be. Figure 6 shows this effect for a range of columns and conditions.

From Figure 5a, 5d and Figure 6 it can be seen that average velocities and flow rates can be either doubled or halved in extreme cases, resulting in inevitable deterioration in GC resolution as values move away from optimum.

A rearrangement of equations derived in the course of this work enabled the calculation of the precise length of a piece of tubing of given internal diameter necessary to give atmospheric pressure at the end of the column for a given flow rate; this is the case in the 'capillary leak' interface.

$$L = \frac{\pi d^4 P_{atm}^2}{256 \eta Q_{opt}} \qquad (18)$$

where d is the tubing internal diameter, P_{atm} is atmospheric pressure and Q_{opt} the optimum flow rate.

These equations and figures resulted in a clarification of the relationships between flow rate, average linear velocity and temperature programming for a range of possible situations, for both conventional capillary GC and capillary GC-MS with various types of interface and carrier gas flow control. A quick consultation of the resulting figures enabled the choice of appropriate starting conditions for optimum separations to be readily made when installing a column for an analysis. In cases where average linear velocity varies substantially during the course of oven temperature programming, the appropriate parameters can be set at the midpoint of the temperature range to minimize degradation of chromatographic performance.

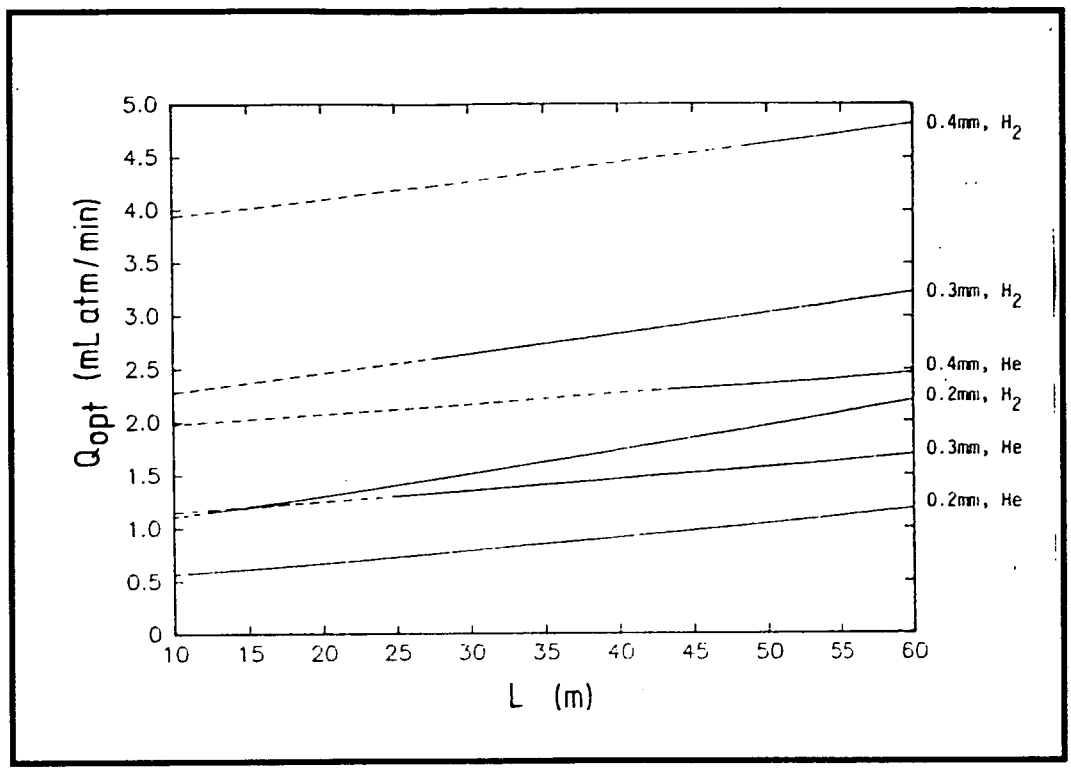

Figure 3

Flow rates required to deliver average velocities of 25cm s^{-1} for helium and 50 cm s^{-1} for hydrogen for the column internal diameters, lengths and carrier gases indicated with atmospheric pressure at the column outlet. When these same flow rates are applied to directly coupled GC-MS, the dotted regions represent situations which would require a column inlet pressure of less than one atmosphere.

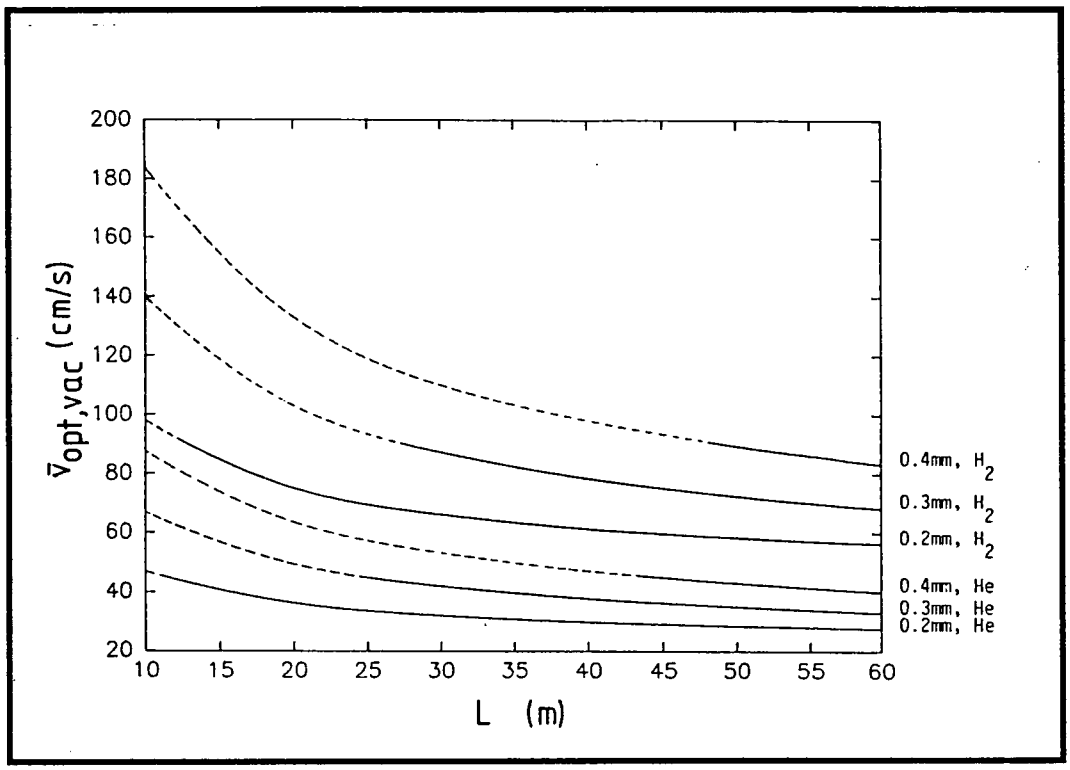

Figure 4

Average linear carrier gas velocities required for different column lengths, diameters and carrier gases to provide flow rates under directly coupled GC-MS corresponding to average velocities of 25 cm s^{-1} for helium and 50 cm s^{-1} for hydrogen under atmospheric outlet pressure. Dotted regions represent column lengths that would require sub-atmospheric inlet pressure.

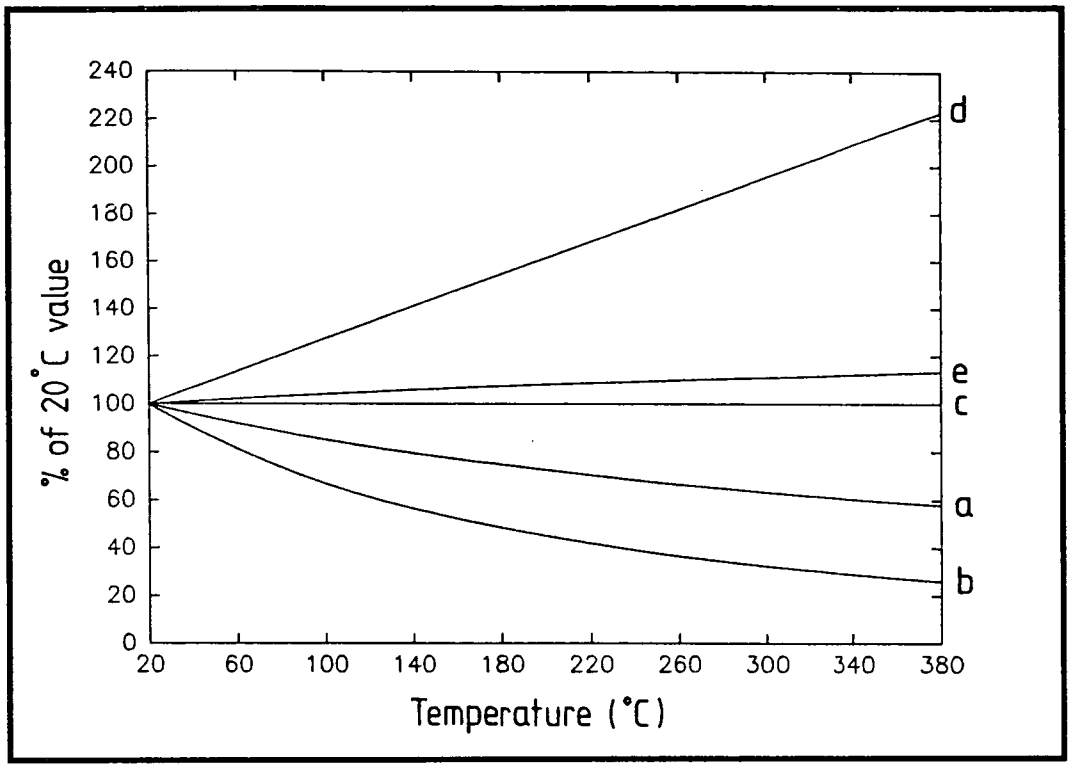

Figure 5

Effects of temperature programming on various parameters after flow-rate has been set, for different flow control and GC-MS interface combinations. The vertical axis shows the values as a percentage of any initial value at 20°C.

(a) flow rate as measured at atmospheric pressure and column temperature, average flow rate and average linear velocity with isobaric pressure control and any interface.

(b) flow rate as measured at atmospheric pressure and room temperature with isobaric pressure control and any interface.

(c) flow rate as measured at atmospheric pressure and room temperature with mass flow control and any interface.

(d) flow rate as measured at column temperature and atmospheric pressure with mass flow control and any interface.

(e) average flow rate and average linear velocity with mass flow control and direct coupling.

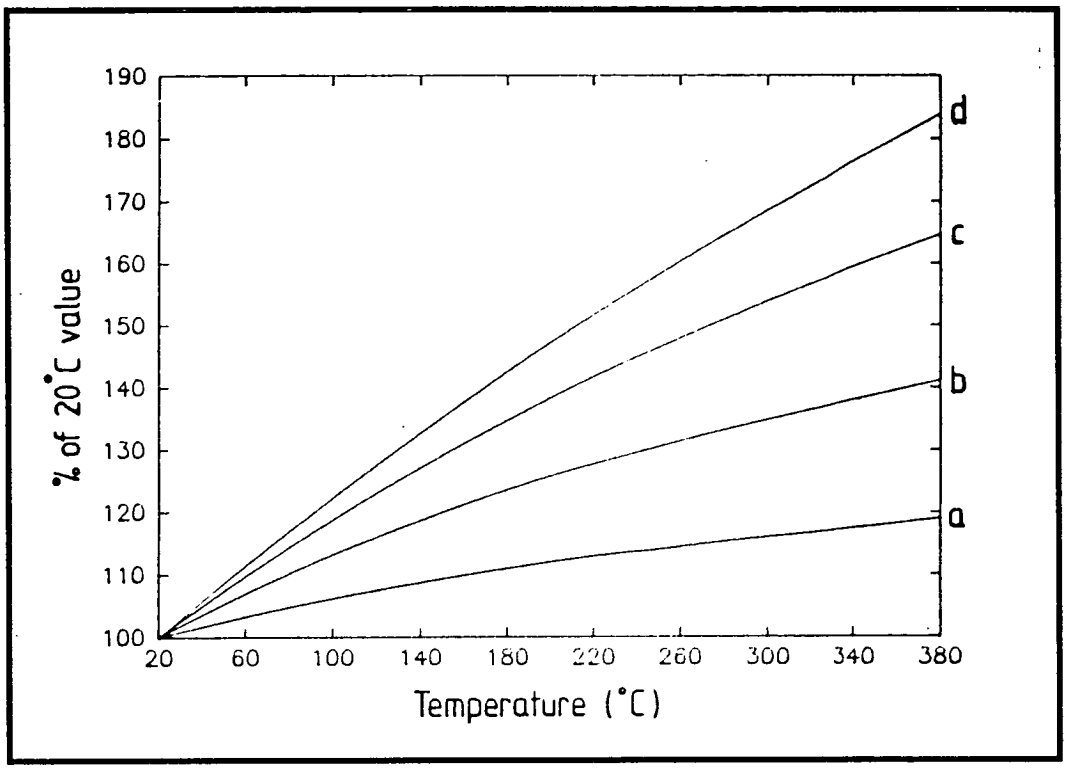

Figure 6

Increase in average carrier gas velocity ($\bar{\upsilon}$) and average flow rate (Q_{av}) under conditions of mass flow control and atmospheric outlet pressure for the range of columns and starting conditions indicated.

a) 50m x 0.2mm, initial $\bar{\upsilon}$ = 50 cm s^{-1} hydrogen, initial Q_{av} = 0.94 mL atm min^{-1}
b) 25m x 0.2mm, initial $\bar{\upsilon}$ = 50 cm s^{-1} hydrogen, initial Q_{av} = 0.94 mL atm min^{-1}
c) 25m x 0.3mm, initial $\bar{\upsilon}$ = 50 cm s^{-1} hydrogen, initial Q_{av} = 2.12 mL atm min^{-1}
d) 25m x 0.5mm, initial $\bar{\upsilon}$ = 30 cm s^{-1} helium, initial Q_{av} = 3.53 mL atm min^{-1}

ii) Yield and Quantitative Considerations for the Open-Split Interface

A further aspect of coupled GC-MS that was investigated was the performance of the 'open-split' interface, which had been in commercial use for more than a decade after its first description (Henneberg *et al.*, 1975). A schematic diagram of an open-split interface is shown in Figure 7. Maximizing the yield of analyte to the mass spectrometer and also the quantitative performance in temperature programmed GC were investigated by both theory and experiment, and published in the *Journal of Chromatography* (Davies, 1988)[4].

Equations were derived to enable compensation for the change in yield of analyte to either the mass spectrometer or a second detector run in parallel with the mass spectrometer when the carrier gas inlet pressure was isobaric and the interface was held at constant temperature. The changes in the flow rate through the column at different oven temperatures were used as the starting point for these relationships.

The flow rate F_b through the column at some elution temperature T_b (in Kelvin), as measured after cooling to room temperature, and representing the actual flux of gas, will be (Davies, 1985);

$$F_b = \frac{\eta_a T_a F_a}{\eta_b T_b} \qquad (19)$$

where F_a is the flow rate through the column at temperature T_a, and η_a and η_b are the carrier gas viscosities at T_a and T_b respectively. When T_a equals room temperature, F_a can be measured by disconnecting the column, and hence the flow to the mass spectrometer (F_m) can be determined from $F_a - F_{sa}$ where F_{sa} is the flow rate from the vent at the column temperature T_a. The various flow rates discussed are illustrated in Figure 7.

The percentage yield of effluent to the mass spectrometer (Y_a) at temperature T_a can then be calculated as;

$$Y_a = \frac{100 F_m}{F_p + F_a} \qquad (20)$$

where F_p is the flow rate of any added purge or make-up gas.

Gas viscosities can be calculated to within 1% of their experimentally determined values (Weast, 1984, p. F-43)

for the normal GC temperature range from the relationship $\eta = kT^{0.7}$ where η is viscosity, k a different constant for each gas and T the absolute temperature. This relationship is in close agreement with previously published data (Ettre, 1984). Substituting in equation 19 the appropriate value of T for each viscosity value, and substituting the result in the expression to calculate Y_b, the percentage yield of effluent to the mass spectrometer at temperature T_b gives;

$$Y_b = \frac{100F_m}{F_p + F_a(T_a/T_b)^{1.7}} \quad (21)$$

The yield ratio at the different temperatures is therefore;

$$Y_b/Y_a = \frac{F_p + F_a}{F_p + F_a(T_a/T_b)^{1.7}} \quad (22)$$

Yield was determined experimentally by physically measuring the only readily accessible parameters; F_a, F_{sa}, F_{sb} and F_p. This results in an agreement of better than 3% between theoretical and measured yields. If greater accuracy is required, then a better approximation of the relationship between temperature and the viscosity of a specific gas can be used (Ettre, 1984).

A calculated yield of more than 100% from this equation indicated that the mass spectrometer will be drawing in some air rather than venting excess helium, a situation which should naturally be avoided by the addition of some 'purge' or make-up gas.

The second equation, derived along similar lines, enables correction for changes in peak areas on a second detector such as a Flame Ionization Detector run in parallel from the effluent split away from the mass spectrometer;

$$Y_{sb}/Y_{sa} = \frac{(F_p + F_a)[F_a(T_a/T_b)^{1.7} + F_{sa} - F_a]}{F_{sa}[F_p + F_a(T_a/T_b)^{1.7}]} \quad (23)$$

where Y_{sb} and Y_{sa} are the percentage of total flow going to the second detector at temperatures T_b and T_a respectively, and F_{sa} is the absolute flow rate to the second detector at temperature T_a.

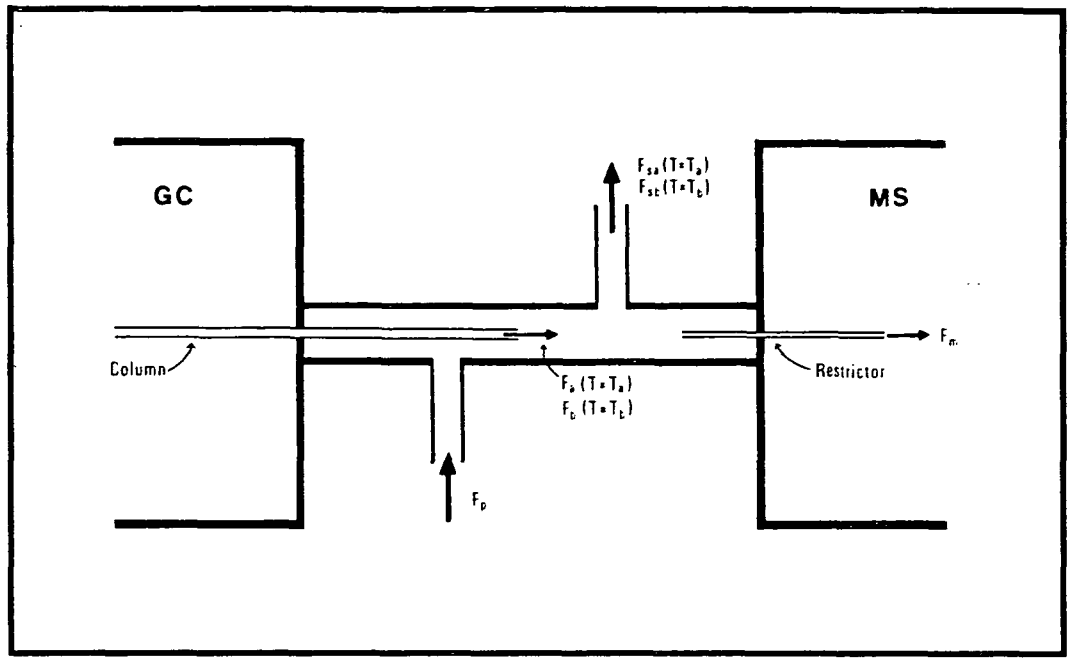

Figure 7

Schematic diagram of an open-split interface, indicating the gas flows referred to at the oven temperatures defined in the text.

This trend towards higher yields of analyte to the mass spectrometer with increasing column temperature can mask potential problems of injector discrimination against higher-boiling materials which can occur using traditional split/splitless injectors. This can have serious effects on quantitative GC-MS analysis. Some publications in this area (e.g. Wetzel and Kuster, 1983) have neglected this aspect of yield variation when looking at discrimination against higher boilers. The effect due to the increase in yield in the high temperature end of the analysis compensating for possible losses in sample transfer caused by condensation may have caused a significant underestimation of discrimination in these cases.

Since the response of a mass spectrometer for n-alkanes in the relevant boiling range (approximately C10 to C50), based on ionization cross sections and electron multiplier responses, is essentially proportional to the total mass of hydrocarbon and independent of molecular weight (Beynon, 1960, p.240), the true level of discrimination can be established by applying the appropriate correction factor based on equation 22 to each alkane in a standard solution.

Figure 8 illustrates the close agreement between experimental and calculated yield changes with GC oven

temperature for open-split interfaces in which the GC has isobaric pressure control. The yields were determined experimentally by measuring F_{sa}, F_a and F_p for a given T_a and F_{sb} for a range of values of T_b; F_m was determined from the difference between F_a and F_{sa}.

Where the open-split interface, including the restrictor to the mass spectrometer, is incorporated into the GC oven there will be no change in yield with temperature programming and isobaric pressure control. Under these circumstances, the flow through the column and restrictor will be equally affected by temperature changes.

With mass flow control or electronic pressure programming to provide constant flow, the flux of gas is constant at different oven temperatures, and the yield to the mass spectrometer will not vary regardless of the position of the interface. Under these circumstances the considerations outlined above do not apply.

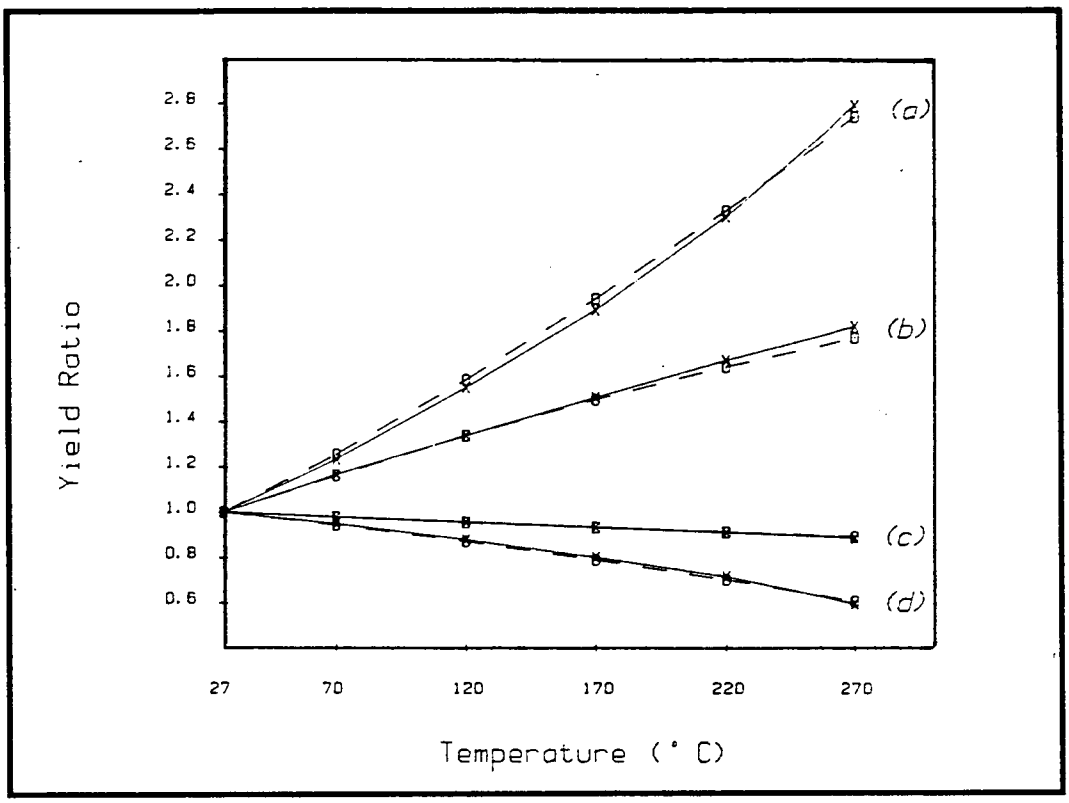

Figure 8

Calculated (circles and dotted lines) and experimental (crosses and solid lines) yield changes that occur during temperature programming with an open-split interface held at constant temperature with isobaric control of flow rates.

(*a*) the relative increase in yield of effluent to the mass spectrometer with no added purge gas.
(*b*) the relative increase in yield of effluent to the mass spectrometer with a purge gas set at 1.3 mL atm minute^{-1}, an initial column flow rate of 2.83 mL atm minute^{-1} and an initial yield of 12.4%.
(*c*) the relative decrease in yield to a second detector for the conditions given in *b*.
(*d*) the relative decrease in yield to a second detector for all cases where no added purge gas is used.

3. DEVELOPMENT OF ANALYTICAL TECHNIQUES

i) Development of an Automated Screening Procedure

As part of a research project aimed at identifying drugs other than alcohol that might be a contributory cause to road accidents, in collaboration with Associate Professor Stuart McLean of the School of Pharmacy at the University of Tasmania, the development of an automated screening protocol for human blood and tissue extracts based on capillary GC-MS on a Hewlett-Packard 5970B benchtop mass spectrometer was undertaken.

Preliminary research on the potential relationship between drugs (other than alcohol) and road accidents had been undertaken by a collaborative team at the University of Tasmania. This study, which was reported in *The Medical Journal of Australia* (McLean *et al.*, 1987), relied on a nitrogen specific Flame Thermionic GC detector for preliminary screening, followed by GC-MS analysis of all samples showing potential positives for drugs.

There were, however, some disadvantages using this preliminary screening method, including many apparent false positive drug findings. In addition, non-nitrogenous drugs such as Δ-9 tetrahydrocannabinol (THC), the active constituent of *Cannabis sativa*, and non-steroidal anti-inflammatory agents such as ibuprofen, ketoprofen and naproxen could not be detected. THC was determined in this preliminary study by a separate immunological screening procedure.

It was therefore decided to develop an automated GC-MS analysis and reporting protocol enabling a reasonably large number of samples to be screened directly for a large number of target substances by this relatively specific and sensitive method. The development was not only aimed towards the Drugs and Driving project, but had widespread relevance. Many forensic laboratories lack the equipment and/or staff resources for carrying out full toxicological screens targeting individual drugs or classes of drugs based on the traditional range of tests such as HPLC, TLC, radioimmunoassay and other immunological tests.

While never intended to be a panacea for drug analyses at trace levels, the automated GC-MS screen nevertheless suited the requirements and resources of the Drugs and Driving project. The results of this study were reported in an article in *Journal of Chromatography (Biomedical Applications)* (Neill *et al.*, 1991)[5].

The first stage of the project was to fully develop all aspects relating to the acquisition and processing of data by the benchtop GC-MS system. This initially required the acquisition of reference mass spectra and GC retention data for some 120 drug standards. Appropriate derivatives were selected where necessary to improve chromatographic performance. Derivatization procedures used, based on work undertaken at the University of Sydney (Vine and Watson, 1983), included methylation of carboxylic acid groups and trifluoroacetylation of alcohols and amines. The chromatographic performance of each drug was also carefully monitored, due to the potential for irreversible adsorption and/or thermal degradation of various polar drugs.

The second stage was the development of a data editing procedure to enable positive drug findings to be automatically detected and the results directly reported from the analysis of relatively crude body fluid and tissue extracts. In conjunction with this, data acquisition programs for trace drug analysis by selected ion monitoring (SIM) were also developed, based on standard retention times and choosing two diagnostic ions per target drug.

A procedure for automatically correcting retention times for any drift was also employed, by incorporating n-decane (C10) and n-triacontane (C30) in each sample vial and comparing the retention times of these peaks against the 'standard' retention times obtained at the beginning of the project.

While automation was a standard feature of the quantitative software supplied with the Hewlett-Packard 5970B GC-MS system used in this study, it was not capable of doing the job required. The quantitative software was geared towards *expecting* to find target compounds, whereas in any screening procedure, the majority of target substances tested for will inevitably be absent. It was imperative that the screening method be capable of detecting genuine drugs without numerous false positive reports. Most false positives equally had to be able to be eliminated by visual inspection of the chromatograms.

Figure 9 shows the flow chart devised to carry out the automated drug identification procedure, which was based on searching for the appearance of two diagnostic ions at the right retention time, *after* adjustment of the time scale based on the two hydrocarbon markers. The peak area ratios for the two diagnostic ions also had to fall between predetermined limits. A Pascal 'macro' was then written to enable chromatograms to be generated and searched for the presence of each target drug based on this flow chart.

Figure 10 shows the portion of the macro that was replicated for each drug with appropriate values for the variables in each case. A brief preliminary section automatically identifies the retention times of n-decane and n-triacontane, used to correct for any drift in retention times.

Figures 11 and 12 show the results of a typical automated analysis and data editing session on a forensic blood sample. This sample had previously been examined for the presence of any drugs by normal GC-MS with manual editing of peaks by an experienced chemist, and had come up with a negative result, based on the inspection of the mass spectra of all the major and obvious minor peaks. Figure 11 shows the Total Ion Chromatogram (TIC), with the inset diagram displaying an expansion of the relevant region where diazepam was subsequently detected at 23.84 minutes by the automated editing protocol, as shown in Figure 12. In this example Figure 12 was the entire report.

The work was extended to include a series of selected ion time windows, with up to 20 ions per window, to enable the maximum possible sensitivity for up to 80 target drugs in the data acquisition phase of the work. Figures 13 and 14 show the results of the analysis of a liver extract from a different subject in which both diazepam and nordiazepam were detected. The TIC in this case is simply the summation of the ions *monitored* in each window, and not the total ions in the spectrometer. A false 'probable' positive for the drug haloperidol ('H' on the chromatogram) was also reported, but visual inspection of the resulting chromatograms in the report indicated this could not be genuine, since the chromatograms for the two diagnostic ions did not quite match.

This whole procedure could be readily applied to screen for target substance from a variety of sample matrices.

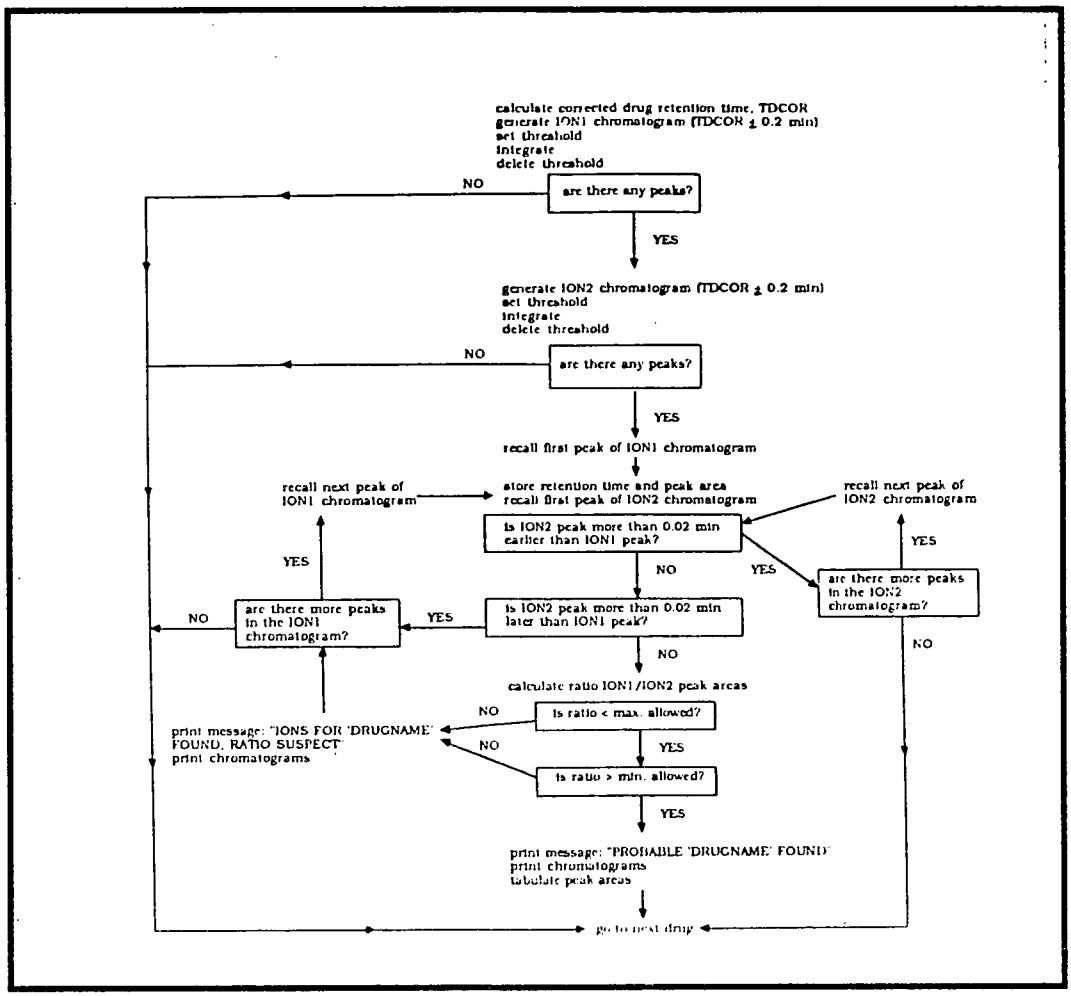

Figure 9

Flow chart showing the scheme for automated drug identification.

```
TD=DRUGTIME
TDCOR=(A+((TD-TC10)/(TC30-TC10))*(B-A))
CH TDCOR-0.2:TDCOR+0.2, ION1
THRESH THRESH1, TD-1
INT
THRESH THRESH1, -(TD-1)
N=NPEAKS
IF NPEAKS>0
 CH TDCOR-0.2:TDCOR+0.2, ION2
 THRESH THRESH2, TD-1
 INT
 THRESH THRESH2, -(TD-1)
 NB=NPEAKS
 IF NPEAKS>0
  EX
  Z=1
  WHILE N>0
   PE Z
   RO -1
   P1=PEAK_AREA
   RT=RET_TIME
   EX
   Y=1
   M=NB
   WHILE M>0
    PE Y
    RO -1
    IF RT-RET_TIME<0.02
     IF RT-RET_TIME>-0.02
      P2=PEAK_AREA
      ARATIO=P1/P2
      IF ARATIO < MAXRATIO
       IF ARATIO > MINRATIO
        WRITELN 701,"PROBABLE DRUGNAME  FOUND"
        WRITELN 701,#10,#10,#10
        N=0
        P=2
       ENDIF
      ENDIF
      IF P=1
       WRITELN 701,"****************************************"
       WRITELN 701,"IONS FOR DRUGNAME FOUND, RATIO SUSPECT"
       WRITELN 701,"****************************************"
       WRITELN 701,#10,#10,#10,#10
      ENDIF
      MERGE
      CLEAR 3
      CLEAR Y
      CLEAR Z
      DR 3,X
      SCR
      WRITELN 701,#10,#10
      IF P=2
       TAB RESULTS, PRINTER:
       WRITELN 701,#10,#10,#10
       WRITELN 701,"****************************************"
       WRITELN 701,#10,#10,#10,#10
       P=1
      ENDIF
     ENDIF
     M=0
    ELSE
     Y=Y+1
     M=M-1
    ENDIF
   ENDWHILE
   Z=Z+1
   N=N-1
   EX
   ENDWHILE
  ENDIF
 ENDIF
```

Figure 10

Drug Editing 'Macro'. The macro is replicated for each drug with the following variables substituted:

DRUGTIME - the standard drug retention time, based on the specific retention times 6.06 minutes and 27.65 minutes for decane and triacontane respectively.

ION1	-	the *m/z* value of the principal diagnostic ion
THRESH1	-	the integration threshold to use for ION1
ION2	-	the *m/z* value of the second diagnostic ion
THRESH2	-	the integration threshold to use for ION2
MAXRATIO	-	the maximum allowable ratio for the peak areas of ION1/ION2
MINRATIO	-	the minimum allowable ratio for the peak areas of ION1/ION2
DRUGNAME	-	the name of the target drug

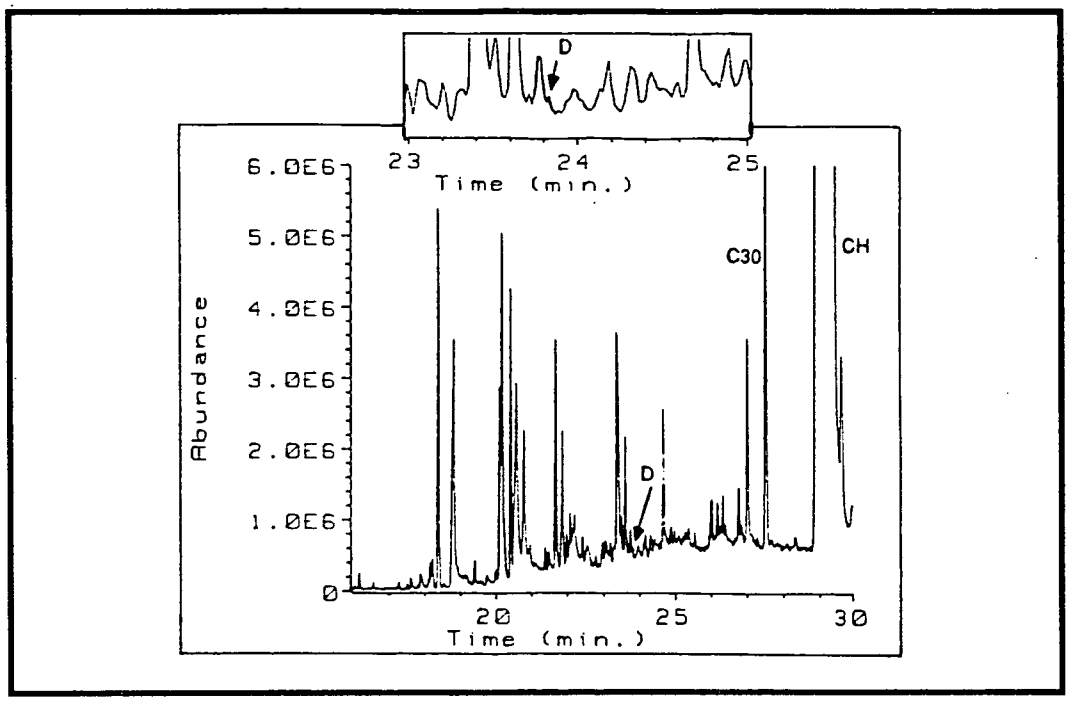

Figure 11

Portion of the Total Ion Chromatogram of an extract of a forensic blood sample. The inset diagram shows the expansion of the region where diazepam was subsequently detected by the automated editing protocol. 'D' indicates diazepam, 'C30' the triacontane time reference peak and 'CH' cholesterol.

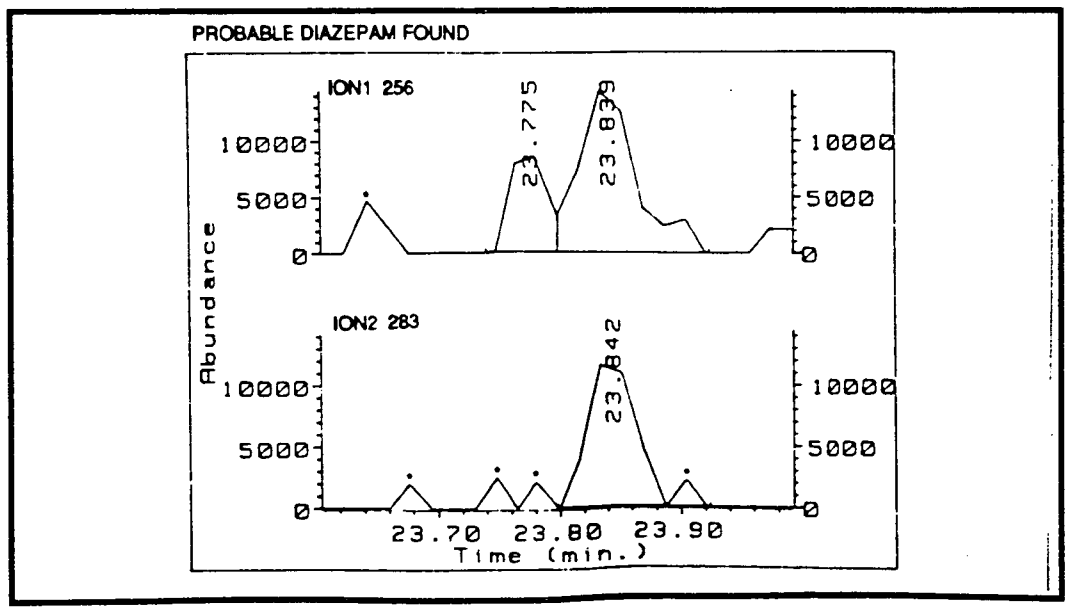

Figure 12

The entire report of the automated editing protocol for the same sample, showing the probable detection of diazepam and the relevant ion chromatograms.

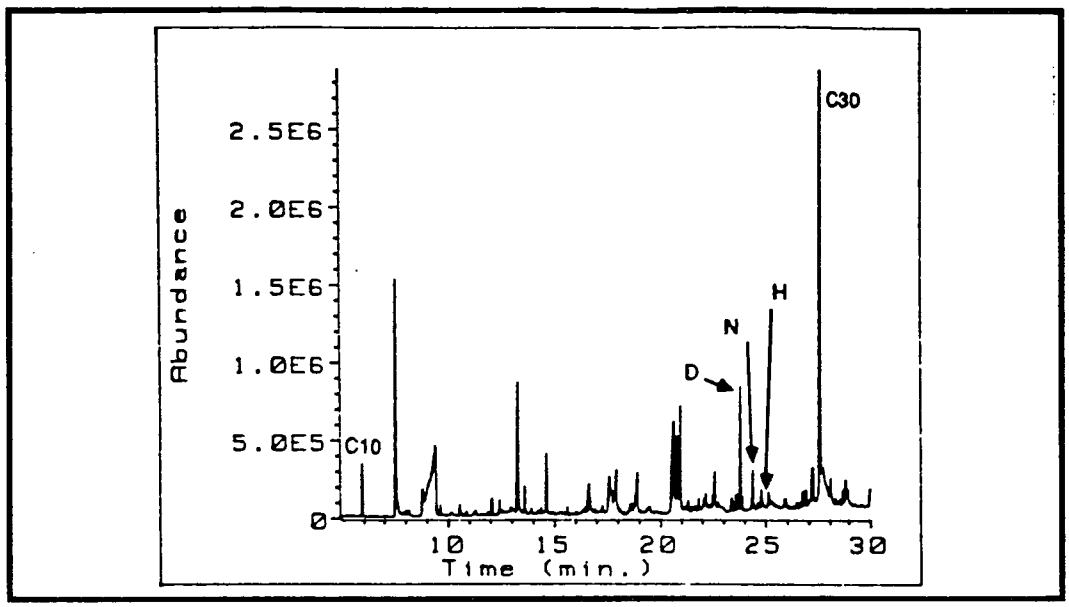

Figure 13

Portion of the 'Total Ion Chromatogram' of an extract of a forensic liver extract acquired in the selected ion monitoring screening mode, indicating the probable drugs detected; diazepam (D), nordiazepam (N) and the false positive report for haloperidol (H) (see text). C10 and C30 are the time reference peaks n-decane and n-triacontane respectively.

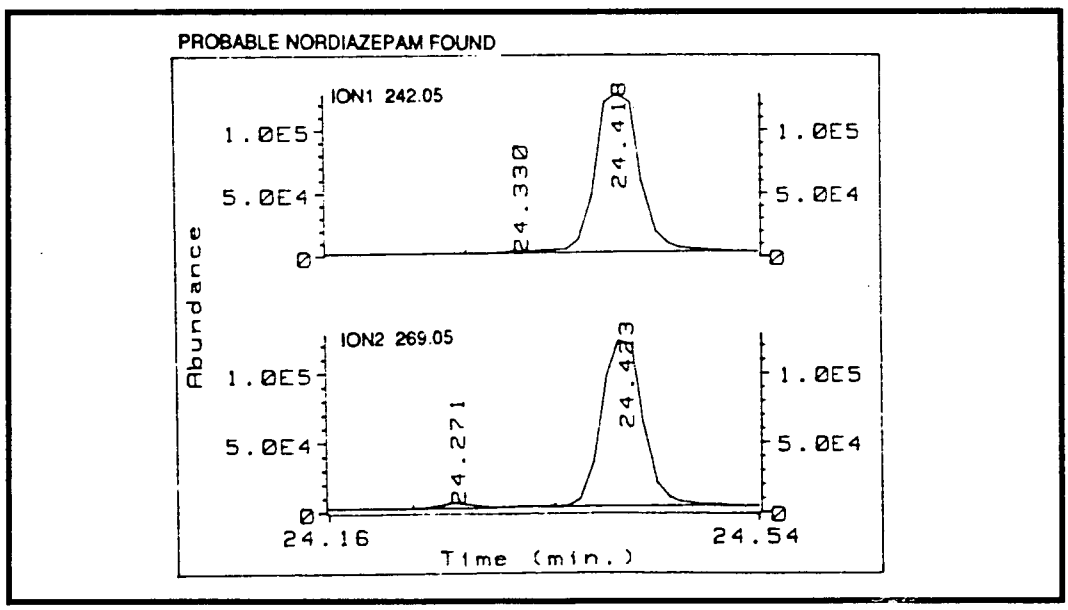

Figure 14

Portion of the report of the automated editing protocol from the selected ion monitoring acquisition mode, showing the detection of nordiazepam and the two relevant ion chromatograms giving good visual confirmation.

ii) MS/MS Techniques

a) Background

Research was undertaken in the area of analytical applications of metastable or collisionally induced fragmentations in the first field-free region of double-focussing mass spectrometers of conventional Nier-Johnson geometry. Double focussing mass spectrometers with this geometry, in which the electric sector (*E*) preceded the magnetic sector (*B*) (Figure 15), represent the majority of high resolution instruments sold.

The monitoring of daughter ions formed by fragmentations after the ion source was first applied to instruments of reverse geometry, in which the magnetic sector precedes the electric sector, by groups led by McLafferty (McLafferty and Bockhoff, 1978) and Cooks (Kondrat *et al.*, 1978). In these cases the aim was to provide greater specificity for both the detection and quantitative determination of target compounds. There are numerous examples in the literature beginning in the late 1970's and early 1980's of the application of this technique to the direct analysis of crude biological extracts or even intact tissue samples on instruments of reversed geometry (e.g. McClusky *et al.*, 1978; Youssefi *et al.*, 1979; McLafferty, 1980*b*; Glish *et al.*, 1980), and an early overview of the subject was published (Cooks, 1979).

The greater specificity is gained from the fact that ions formed in this way will be transmitted at a lower energy from the 'main beam' daughter ions formed in the ion source, and the amount of kinetic energy lost specifically relates the daughter ion *m/z* value back to its parent ion (e.g. Beynon *et al.*, 1968, p58);

$$KE_d = (m_d/m_p) . KE_p$$

where KE_d is the kinetic energy of the daughter ion, KE_p the kinetic energy of the parent ion and m_d and m_p the *m/z* values of the daughter and parent ions respectively.

The use of tandem mass spectrometers for the determination of fragmentation pathways and/or the structural analysis of individual ions in the scanning mode, as well as the analytical application of detecting and quantifying target substances by focussing on specific parent ion-daughter ion fragmentations became known as 'MS/MS' (Kondrat and Cooks, 1978).

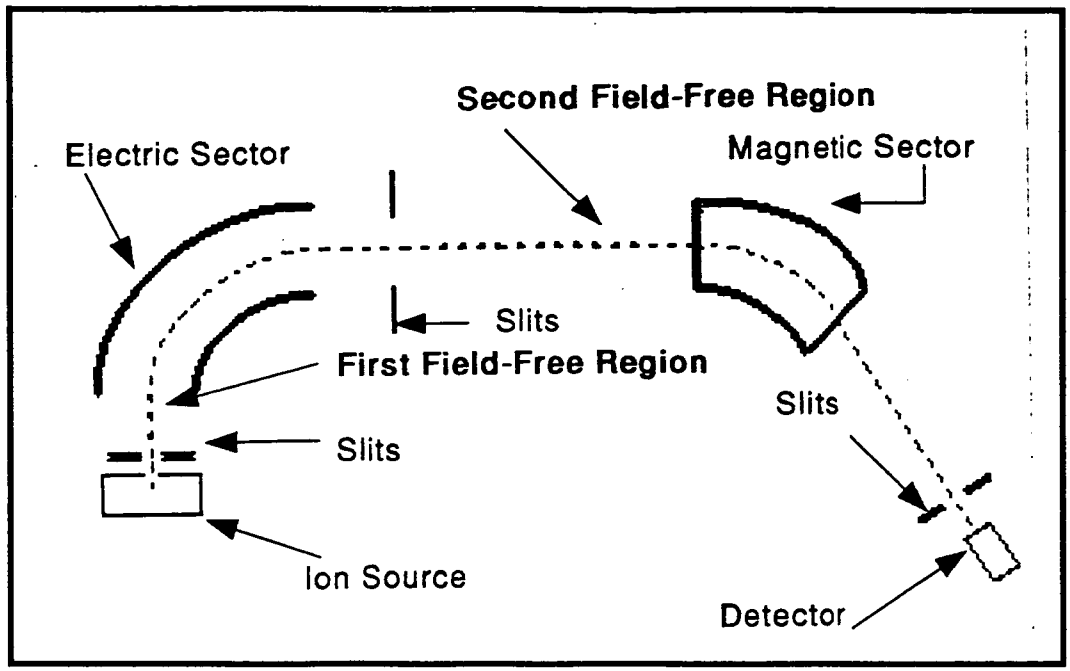

Figure 15

Schematic Diagram of a Nier-Johnson Mass Spectrometer

In reversed geometry instruments, this was accomplished by choosing a suitable parent ion using the magnetic sector, and either acquiring a full 'Mass-analysed Ion Kinetic Energy Spectroscopy' (MIKES) (Beynon and Cooks, 1971) spectrum by scanning the electric sector voltage, or more typically for target compound detection by switching to one or more voltages to focus known daughter ions. The parent ion in these cases could itself have arisen by one or more previous fragmentations, while the daughter ions are formed in the second field-free region of the spectrometer.

In instruments of conventional Nier-Johnson geometry, second field-free region daughter ions resulting from the fragmentation of metastable precursors cannot be focussed independently of the main beam, but rather give rise to the classic broad 'metastable' peaks in analogue spectra; these are usually intentionally filtered out in digitized spectra by parameters associated with peak width. However, fragmentations that occur in the first field-free region, immediately following the ion source, can be focussed away from the main beam either by scanning the accelerating voltage (V) alone to produce spectra of parent ions of given daughters, or by the various 'linked scans' of the magnetic and electric sectors to produce spectra of parent ions of given daughters or daughter ions of given parents (Boyd and Beynon, 1977; Millington and Smith, 1977), and constant neutral losses (Zackett *et al.*, 1979; Lacey and McDonald, 1979).

To focus individual fragmentations within the first field-free region there are in fact an infinite number of combinations of *B*, *E* and *V* that can be used (e.g. Lacey and McDonald, 1977). Only by scanning *B* or by holding the ratio *V/E* constant while scanning *V* can the 'main beam' ions formed within the ion source be focussed.

It was realized in the late 1970's and early 1980's that monitoring ions derived from fragmentations within the first field-free region of conventional geometry instruments would provide an extra dimension of specificity in the determination of target compounds by both GC-MS and direct insertion probe MS (Gaskell *et al.*, 1978, 1979, 1980*b*; Harvey *et al.*, 1980; Chess and Gross, 1980). In these publications single decompositions or decompositions to more than one daughter ion derived from the same parent were monitored, or else the same daughter ion from different parent ions was monitored.

The ions were focussed either by accelerating voltage 'defocusing' or by switching both the magnetic and electric sectors together such that there was no change in the ratio of their field values (the '*B/E*' scan). The technique has been variously named 'metastable decomposition monitoring', 'metastable peak monitoring', 'metastable ion detection', 'selected reaction monitoring' and 'selected decomposition monitoring'. The last two can apply to either unimolecular or collision induced fragmentations, while the others can strictly only be applied to unimolecular fragmentations.

b) Quantitative Selected Reaction Monitoring (SRM)

In work carried out in 1981, this technique was applied to a range of experimental qualitative and quantitative determinations. The starting point for each case was the acquisition of *B/E* scans from the molecular ion and high mass daughter ions from reference standards of the substances under investigation, and of prospective substances for use as internal standards.

For the initial unpublished quantitative analyses, an internal standard having an ion at the same *m/z* value as the chosen parent ion of the target substance was used, which did *not* have any interference at the daughter ion *m/z* value(s) chosen for monitoring.

A series of compounds was investigated, including an unpublished homoerythrina alkaloid in crude solvent extracts of *Athrotaxis selaginoides* (King Billy Pine). The new alkaloid was subsequently determined to have structure (I) (Panichanun and Bick, 1984), and was named selaginoidine. The work on quantitative analysis of this alkaloid was presented at the 1981 conference of the Australian and New Zealand Society for Mass Spectrometry (Davies and Bignall, 1981).

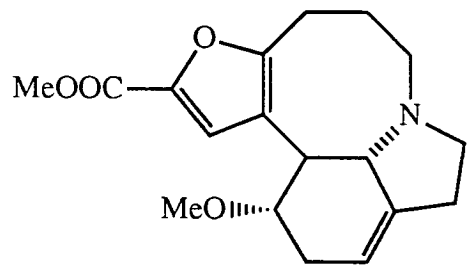

I

The normal mass spectrum of selaginoidine had a molecular ion at *m/z* 317 (10%), and prominent ions at *m/z* 286 (18), 259 (100), 258 (90) and 244 (10). *B/E* linked scan from the molecular ion at *m/z* 317 showed a single prominent first field-free region fragmentation for the loss of 58 ($COOCH_2$) to 259, and this was chosen as the target reaction from the alkaloid for monitoring.

As an internal standard, a substance with a different and characteristic fragmentation from *m/z* 317 was required. It was found that the pesticide Dicophane (DDT) had a small but significant ion at *m/z* 317 $[M-Cl]^+$, and a *B/E* linked scan from this ion indicated a daughter ion at *m/z* 282 $[(M-Cl)-Cl]^{+\cdot}$.

The alkaloid was then quantified in a series of crude extracts from a number of genotypes. A small amount of

purified material was available, and so a standard curve was constructed over the range 2ng → 20ng alkaloid per microlitre. Linear regression gave the relationship $y = 0.014 + 0.033x$ (correlation coefficient 0.995) where y was the concentration of alkaloid in ng μl^{-1}, and x the ratio of the m/z 259 to m/z 282 daughter ions from m/z 317.

A 5µl aliquot a solution containing 1mg mL^{-1} of crude extract and 1mg mL^{-1} of DDT was loaded onto the direct insertion probe, and the daughter ions at m/z 282 (internal standard) and m/z 259 were alternately monitored with a 300ms dwell time per channel. Standard deviation over 20 replicates was 8%, within the requirements of a rapid screening technique.

Additional qualitative confirmation of compound identity in this technique is contained in the distillation profile of the sample off the direct insertion probe, which must closely match that of a reference sample of the target substance.

c) Selected Reaction Monitoring Using Stable Isotope Labelled Internal Standards

The use of stable isotope labelled internal standards for quantitative determination by GC-MS had become a routine procedure by 1980. The advantages that these bring to GC-MS analyses are equally valid to selected reaction monitoring. In work presented as a poster at the 8th International Mass Spectrometry Conference, Gaskell and coworkers discussed the advantages of multiple metastable peak monitoring with the use of stable isotope labelled internal standards, using the measurement of testosterone in human plasma as an example (Gaskell *et al.*, 1980*a*).

In almost all cases, the use of isotope labelled internal standards will require the monitoring of two or more parent ion/daughter ion decompositions; only in cases where the label is lost will the daughter ions be the same. The spectrometer therefore has to be controlled in such a way as to alternately bring these different fragmentations to focus.

The information inherent in tracking ion intensity versus the values of B, E and V can be represented in a three dimensional ion 'surface' by appropriate choice of axes, such as those proposed by Lacey and McDonald (1977). In this representation, intensity is plotted as contour lines versus ρ and μ where $\rho = (V_o/V)(E/E_o)$ and $\mu = (E_o/E)m_B$ where V_o and E_o are values of V and E at which the main beam of ions formed within the ion source is transmitted, and m_B is the mass of singly charged ions transmitted when $V=V_o$ and $E=E_o$. Figure 16 schematically illustrates this approach using a portion of the ion 'surface' for a mixture of warfarin (II) and its pentadeuterated analogue (III).

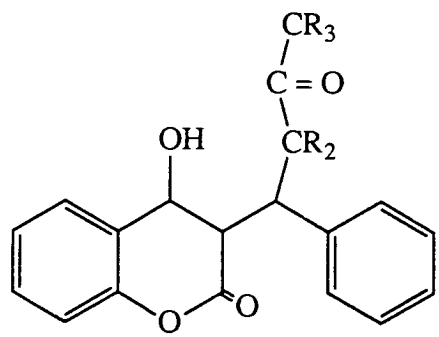

II R=H

III R=D

Other approaches have also been used for the three dimensional representation of ion current surfaces (Kiser *et al.*, 1969; Farncombe *et al.*, 1982). These approaches show that there are an infinite number of combinations of E, B and V that can be used to focus these independent first field-free region fragmentations; synchronized

switching of any two of the three variables to appropriate values will allow the required first field-free region fragmentations to be focussed.

The normal advantages and disadvantages of changing particular variables apply. Switching *V* can result in significant loss of sensitivity if relatively large changes are made. However, the difference required to focus stable isotope labelled ions and the corresponding unlabelled ions is minimal. Switching of the magnetic field suffers from the limitation of how quickly the field will stabilize at the new value, and can be limiting for capillary column peak widths. Again, the change in the field required to alternately focus labelled and unlabelled ions is minimal.

Importantly, complete mapping of ion current surfaces in this way enables various artifact peaks found in normal linked scans to be recognized for what they are; e.g. intersection of 'ridges' caused by fragmentations occurring within the electric sector, or detection of daughter ions from parent ions near to the target parent ion in mass, but not resolved because of the relatively poor energy discrimination of the technique (Lacey and McDonald, 1977, 1978, 1980). The dotted lines in Figure 16 show where constant parent ion scans (*B/E* constant) from the molecular ions *m/z* 308 and *m/z* 313 respectively intersect features on the ion current surface.

Commercial instruments prior to the early 1980's did not have the capability of synchronizing the switching of more than one independent variable from among *E*, *B* and *V*, since the analytical applications were not foreseen when the instruments were designed. In the published abstract of the work described by Gaskell and coworkers discussed above (Gaskell *et al.*, 1980*a*), no experimental details were presented other than the statement that switching between the separate metastables was under computer control.

The ability to independently control more than one variable at a time was not a standard feature of the instrument and the software described, and yet synchronized switching of at least two of the three variables among *B*, *E* and *V* is required to alternately focus two unrelated fragmentations. The VG 7070 with VG 2035 datasystem mentioned was the same configuration as used in the CSL. Even with the optional feature of a digital scan control system, only one independent variable at a time could be controlled. It was therefore not clear how the independent control had been achieved by Gaskell's group; it had presumably involved significant electronic and software modifications.

Gaskell subsequently published a technique for dual metastable peak monitoring by switching E and V (Thorne and Gaskell, 1985), which allows rapid switching between target daughter ions as no change in magnetic field is required.

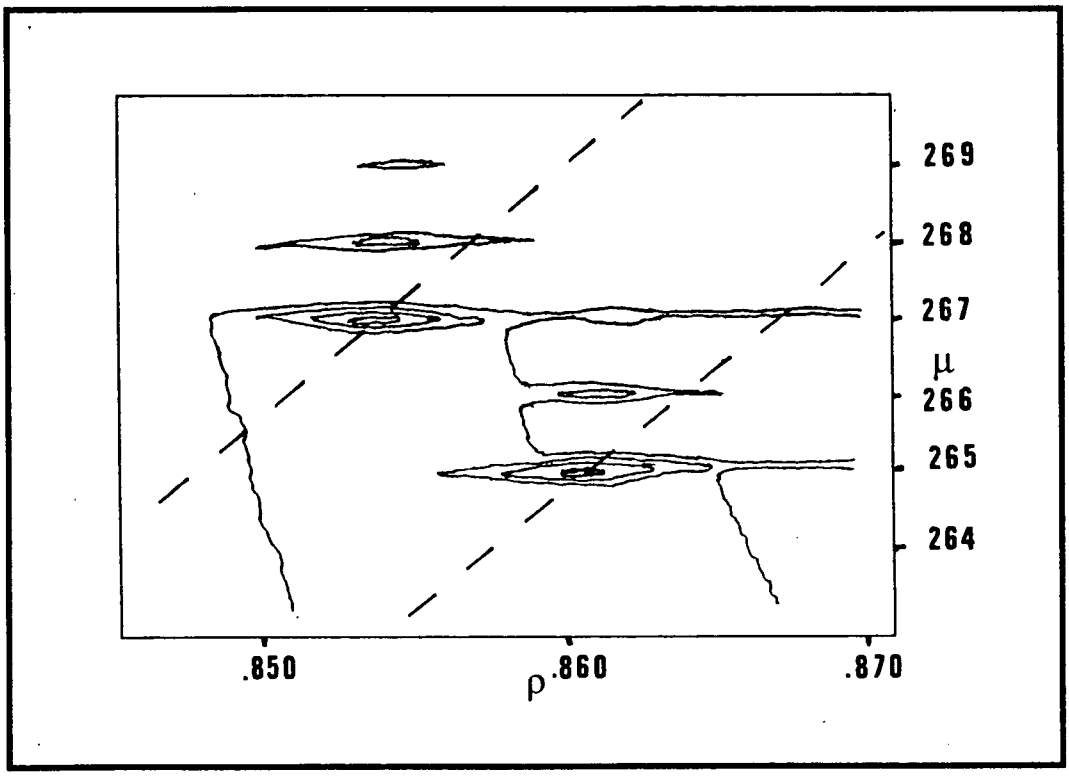

Figure 16

Portion of the ion current surface for a mixture of the drug warfarin (II) and its pentadeuterated analogue (III). The major ions present are from the metastable decompositions m/z 308 $\rightarrow$ m/z 265 and m/z 313 $\rightarrow$ m/z 267, plus fragmentations from the natural isotopic parent ions at m/z 309, 310, 314 and 315. $\rho = (V_o/V)(E/E_o)$ and $\mu = (E_o/E)m_B$ where V_o and E_o are values of V and E at which main beam ions are transmitted, and m_B is the mass of singly charged ions transmitted when $V=V_c$ and $E=E_o$.

d) Warfarin Determination in Crude Plasma Extracts by SRM

While the VG7070 was not initially designed to undertake multiple reaction monitoring, the considerations outlined above meant that it was possible provided two independent variables from *E*, *B* and *V* could be controlled.

An assay was developed for the direct quantitative determination of the anticoagulant drug warfarin (II) in crude extracts of human blood plasma. Warfarin is used in the clinical management of thromboembolic disorders such as strokes and heart attacks. This assay utilized the metastable losses of CH_3CO and CD_3CO from the molecular ions of warfarin and its deuterated analogue (III) respectively, and represented one of the first applications of direct quantitative determinations using unrelated parent-daughter fragmentations on a normal geometry instrument. A cycle of 2 seconds was achieved on a standard instrument with no modifications. This work was published in *Biomedical Mass Spectrometry* (Davies *et al.*, 1983)[6].

The synchronization in this case was accomplished by having two 'blank' channels in the magnet switching mode between the two analytical channels, during which the accelerating voltage was switched to the appropriate preset values. The fragmentations chosen for monitoring were *m/z* 308 $\rightarrow$ *m/z* 265 ($[M - CH_3CO]^{+\cdot}$) for warfarin and the corresponding *m/z* 313 $\rightarrow$ *m/z* 267 for the internal standard D5-warfarin, based on a full *B/E* scan from the warfarin molecular ion. The deuterated warfarin was prepared directly from warfarin by isotope exchange using a previously published method (Duffield *et al.*, 1979).

(An editorial change altered the submitted figures substantially, resulting in erroneous linked scan data being published for warfarin. A spectrum showing full peak profiles had been submitted, partly since that was the manner in which the data had been acquired, and partly to illustrate the good daughter ion resolution. The sides of the peaks at *m/z* 265 and *m/z* 266 were redrawn by the journal as four individual centroided peaks, implying the presence of significant daughter ions from *m/z* 308 at *m/z* 267 and *m/z* 268, which did not exist. This was noted in the returned proofs, and a request was made that the correct original figure be restored, but this was not carried out.)

It was first necessary to confirm that extracts of plasma from subjects not on warfarin therapy contained minimal interference at these positions on the ion current surface - i.e. whether the signal was due to the specified fragmentations or to fragmentations within the electric sector or during acceleration which might

contribute to the ion current at these points (Lacey and McDonald, 1977).

Human plasma samples (1 mL) were acidified to pH 3, 2μg (nominal) of internal standard was added, and the sample was extracted with 250 μL of chloroform. A one μL aliquot of the organic layer was loaded onto the direct insertion probe, and the solvent allowed to evaporate before analysis.

Figure 17 shows the ion current profiles for the target fragmentation in a blank plasma extract, as well as individual plasma extracts that had been spiked with only labelled warfarin (looking for potential interferences in the *m/z* 308 → *m/z* 265 channel), only unlabelled warfarin, and a patient sample showing both the labelled and unlabelled warfarin. The observable response in the *m/z* 308 → *m/z* 265 channel in the sample that had only been spiked with labelled warfarin is mainly attributable to the *m/z* 313 → *m/z* 267 fragmentation within the electric sector from the labelled warfarin. This effectively placed a lower limit of detection on the assay of 0.2μg mL^{-1}.

A standard curve was constructed using plasma samples spiked with between 0.5μg and 5μg of warfarin, and (nominally) 2μg of D5-warfarin. A linear regression on this data gave the relationship $y = 0.11 + 0.63x$ (correlation coefficient 0.998), where y is the concentration of warfarin plasma in μg mL^{-1}, and x is the ratio of peak areas of the *m/z* 308 → *m/z* 265 channel to the *m/z* 313 → *m/z* 267 channel. The coefficient of variation on replicate analyses of the same extract was 7.2% (n=5).

This method was then applied to a number of clinical plasma samples, where levels of between 0.5μg and 1μg mL^{-1} were recorded.

Great caution is required in using direct insertion probe MS/MS for quantitative work in pharmacology; not only must blank samples be free of any appreciable signal at the relevant points on the ion current surface, but also care must be taken that no metabolite of the target compound could give rise to a measurable signal at these points. In the case of warfarin, it was established that no known metabolite would produce the fragmentation *m/z* 308 → *m/z* 265. It was noted that the fragmentation *m/z* 310 → *m/z* 265 was known for the two diastereomers produced by biological reduction of the ketone group to the corresponding alcohol (Trager *et al.*, 1970), and that due to the inherent energy spread of the ions, resulting in relatively poor parent ion specificity, that a very

small contribution to the nominal *m/z* 308 → *m/z* 265 fragmentation would occur from this source.

The first draft of this paper was received by the editors in November 1982, just prior to the publication of plans for an electronic device that had been designed to allow switching to unrelated first field free region daughter ions on a similar instrument (Durden, 1982), and after a presentation at the 1981 American Society for Mass Spectrometry conference in Minneapolis (Durden, 1981). This device enabled isotope labelled internal standards to be employed for quantitative determinations by MS/MS, with full automation of the peak switching.

This approach then enabled the direct quantitative determination of specific target substances in relatively crude matrices with stable isotope labelled internal standards, either by combined GC/MS/MS or direct insertion probe MS/MS. For best results the former required fast scanning magnets (not present on the 7070F) and electronic synchronization of the switching of two voltage sources; the latter was possible with a degree of manual initialization and no modifications to the instrument or software. The technique proved invaluable in the solution of specific problems.

The ability to carry out selected reaction monitoring is now a routine feature of most commercial instruments.

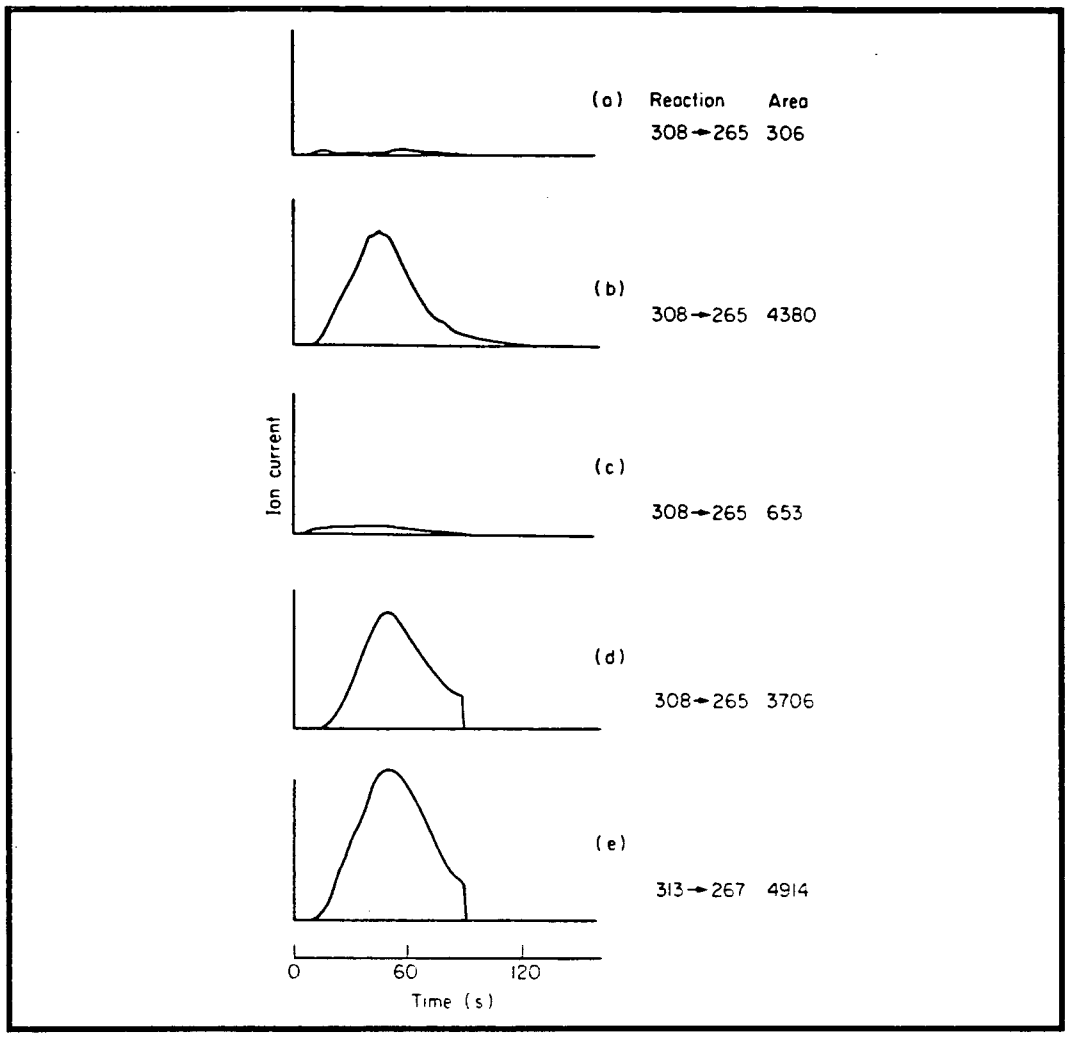

Figure 17

Ion profiles and areas for the indicated decompositions for warfarin in blood plasma extracts;

a) warfarin channel, blank plasma only
b) warfarin channel, plasma spiked with 1 µg/mL of warfarin
c) warfarin channel, blank plasma spiked with deuterated warfarin only
d) warfarin channel, plasma from a patient on warfarin therapy
e) deuterated warfarin channel, from the same direct probe insertion experiment as 'd'

e) N-Hydroxyphenacetin Determination in Urine Extracts

A subsequent application of selected reaction monitoring included the quantitative determination of the thermally sensitive N-hydroxyl metabolite of phenacetin in enzymically hydrolysed urine extracts, which was published in *Journal of Chromatography (Biomedical Applications)* (Davies *et al.*, 1984)[7].

Phenacetin had already been largely discontinued as a clinical analgesic due to the known or suspected toxic side-effects (Gillette *et al.*, 1982). However, the proposed mechanism of toxicity, via N-hydroxylation, had never been conclusively demonstrated *in vivo* in any mammal prior to work undertaken with Associate Professor Stuart McLean, in which the occurrence of N-hydroxyphenacetin (NHP) (IV) was demonstrated conclusively for the first time *in vivo* in rats (McLean *et al.*, 1981). This reactive metabolite was thought to be responsible for carcinogenic, mutagenic and hepatic toxicity effects, but had only been positively identified previously from *in vitro* studies.

Earlier publications had reported the presence of NHP as an *in vivo* metabolite of phenacetin in man (Belman *et al.*, 1968; Klutch and Bordun, 1968), but this work was subsequently criticized for the lack of specificity in the assays used (Weisburger and Weisburger, 1973; Macklin and Welch, 1980).

However, variable decomposition in the GC injection port of the methylated derivative, N-methoxyphenacetin (NMP) (V), to phenacetin (VI) and 2-methoxyphenacetin (2MP) (VII) was noted in the original study (McLean *et al.*, 1981), making quantitative work via GC-MS difficult. Selected reaction monitoring from the direct insertion probe overcame the problems associated with decomposition on GC analysis, and for the human urine was used to conclusively prove the presence of this metabolite, and subsequently to quantify it (Davies *et al.*, 1984)[7].

While the most intense ion in the full *B/E* scan from the molecular ion of NMP corresponded to the loss of ketene after hydrogen transfer, this fragmentation was also observed to be strong in standard samples of both the 2- and 3-methoxy isomers from which it had to be distinguished. The proposed mechanism for this process for acetanilide (Tomer *et al.*, 1973) is a direct transfer of an acetyl hydrogen to the nitrogen, followed by breaking of the N-C bond.

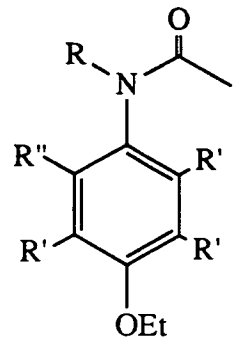

IV R=OH, R',R"=H

V R=OMe, R',R"=H

VI R,R',R" = H

VII R,R'=H, R"=OMe

VIII R=OMe, R',R"=D

However, there was a relatively intense ion at *m/z* 135 in the *B/E* scan from the molecular ion at *m/z* 209 in NMP (18% intensity relative to the daughter ion at *m/z* 167) that was not present in the other two isomers. High resolution mass measurement indicated that the loss of 74 mass units corresponded to the loss of *both* the methoxy and acetyl moieties. It clearly required the very rapid consecutive loss of the two groups within the first field free region of the spectrometer, a phenomenon that is known to produce daughter ions of the correct 'apparent' *m/z* value and energy (Jennings, 1966).

Under these circumstances the 'grand-daughter' ion behaves for the purposes of detection as though it was a single fragmentation, even in cases where neither of the individual losses is observed in the *B/E* scan. In the case of NMP, small daughter ions corresponding to the individual losses of the acetyl and methoxy groups were observed in the *B/E* scan from the molecular ion.

As part of the preliminary work on this metabolite, the mass spectrum of NMP was characterized in detail using high resolution mass spectrometry and a series of *B/E* linked scans to assign fragmentation pathways, since *any* characteristic daughter ion could be used for the assay, not just those from the molecular ion. Major differences in the *B/E* linked scans from the NMP daughter ion at *m/z* 179 and the phenacetin molecular ion at *m/z* 179 indicated these ions to be of different structures. Daughter ions from adjacent parents (particularly *m/z* 135, 136, 137 and 138) were subsequently assigned unequivocally from a series of B^2/E scans from the respective daughter ions. Figure 18 shows the principal fragmentation pathway of NMP based on this work, with some possible ion structures.

A comparison with similar work undertaken on the isomeric 2- and 3-methoxy phenacetin resulted in the choice of the daughter ion at *m/z* 135, as discussed above, to be the most useful diagnostic ion.

Preliminary trials of enzymically hydrolysed blank urine extracts indicated there was some interference for the

m/z 209 → *m/z* 135 fragmentation. Although this interference had a significantly higher boiling point than NMP and hence a much slower distillation profile from the direct insertion probe, it would have made accurate quantitation difficult. A preliminary purification by thin-layer chromatography subsequently eliminated this interference.

Initially N-butyryl-4-aminobenzoic acid (4-BABA) was used as an internal standard, with the fragmentation *m/z* 221 → *m/z* 151 ($[M - C_4H_6O]^{+\cdot}$) from the methylated derivative (4-BAMB) being monitored along with the NMP fragmentation *m/z* 209 → *m/z* 135. Good linearity was achieved for a standard curve of NMP in urine with 4-BABA added as internal standard (correlation coefficient = 0.9993). However, the distillation profiles of the two compounds off the direct insertion probe were significantly different. An ion source temperature of 120°C was necessary to maintain a minimum peak width of about 20 seconds and hence an adequate sampling rate on the relatively volatile NMP peak. Under these conditions the 4-BAMB took several minutes to completely evaporate from the probe tip without supplementary heating, which was undesirable in that it would introduce a much greater fraction of other urine components into the ion source, and also increase the time between analyses.

Tetra-deuterated NMP (DNMP, 98% $^2H_4$) (VIII) was subsequently made available as the internal standard, following its synthesis by Associate Professor Stuart McLean. This resulted in a significant improvement in the precision and accuracy of the assay. This improvement was a result of the essentially identical distillation profiles of the analyte and internal standard, and the better compensation for losses and variability during workup and sampling for MS/MS analysis. Figure 19 shows the normal mass spectrum of NMP and DNMP, and the metastable loss employed for quantitative monitoring.

A standard curve was generated by the addition of between 1 and 20 µg of NMP and 5 µg of DNMP to 2 mL of blank urine. Linear regression on peak areas gave a slope of 0.191, a *y*-intercept of 0.03 and a correlation coefficient of 0.9983. The coefficient of variation (C.V.) on repeated analysis of the same extract was 1.94% (n=8), while the C.V. on extracts of eight replicate 2 mL aliquots of the same urine sample was 9.2%.

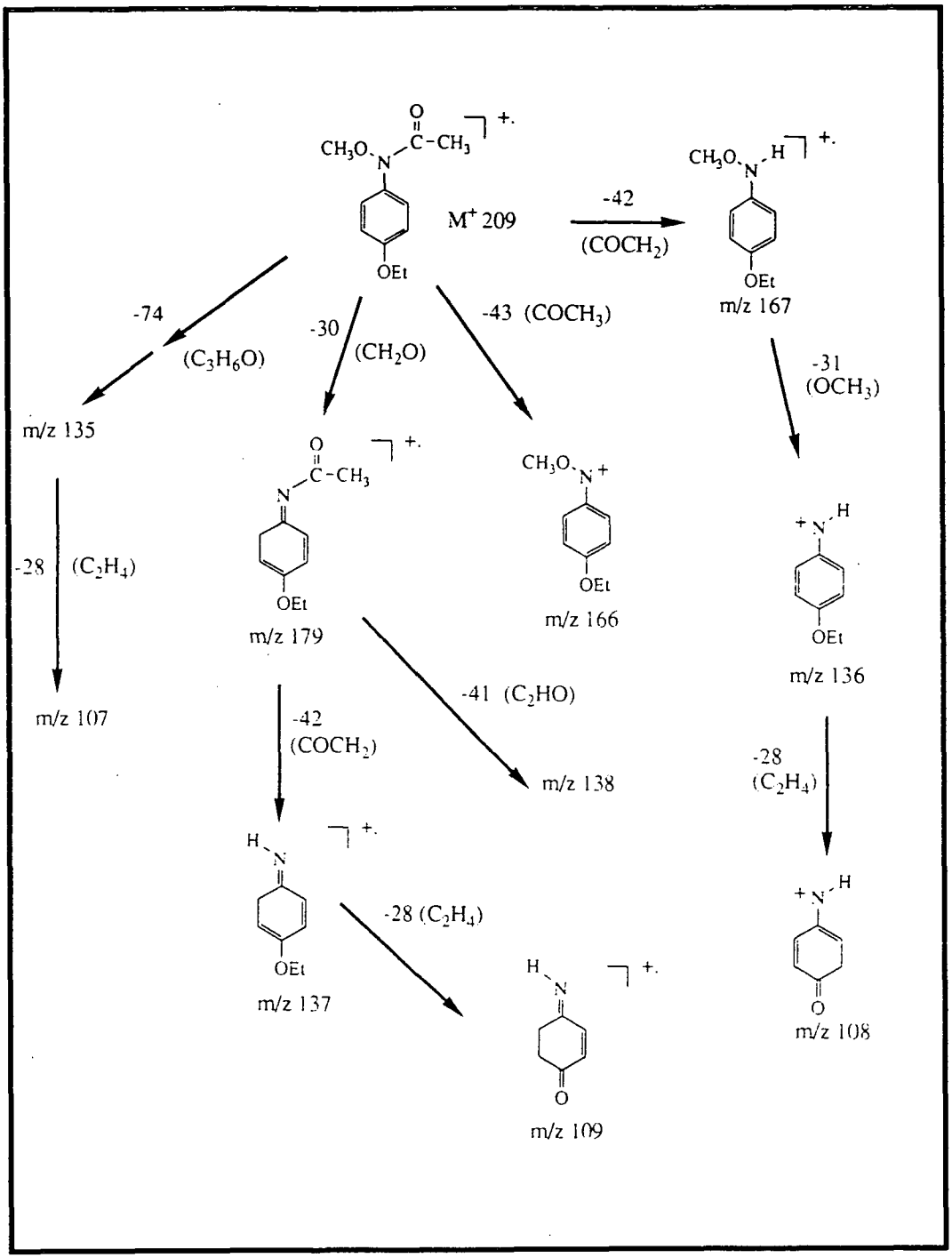

Figure 18

Mass spectral fragmentation scheme for NMP as determined from high resolution MS and a series of *B/E* and B^2/E linked scans.

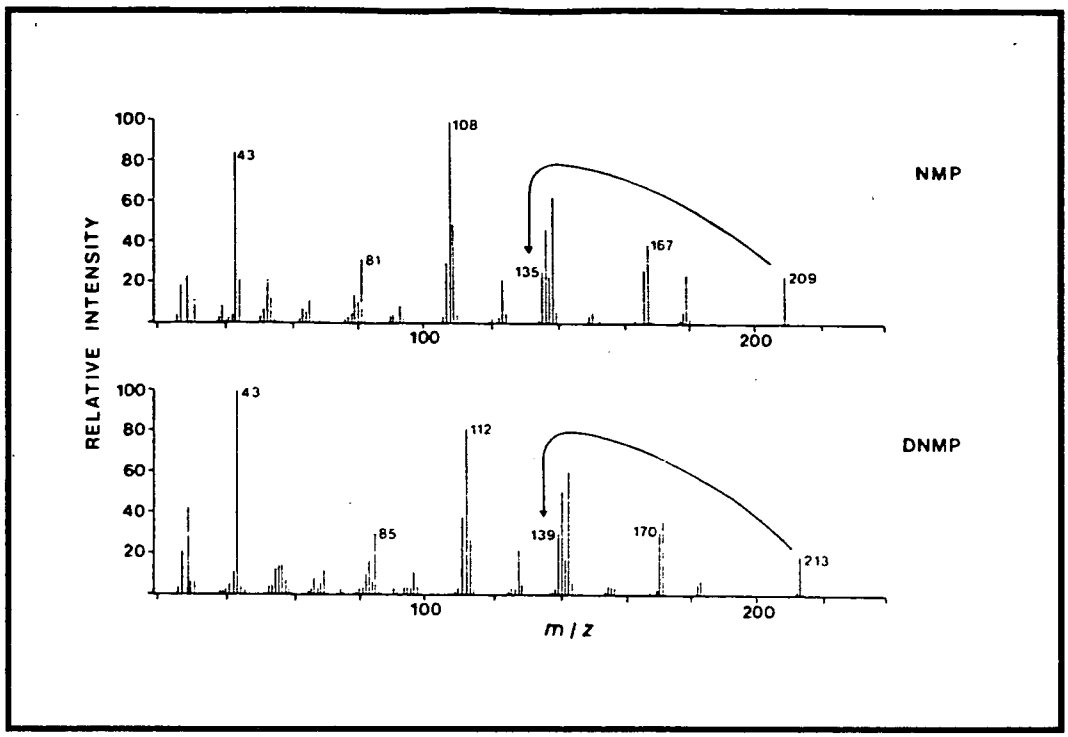

Figure 19

Mass spectra of NMP (V) and tetradeuterated NMP (VIII), illustrating the two metastable fragmentations used for the assay.

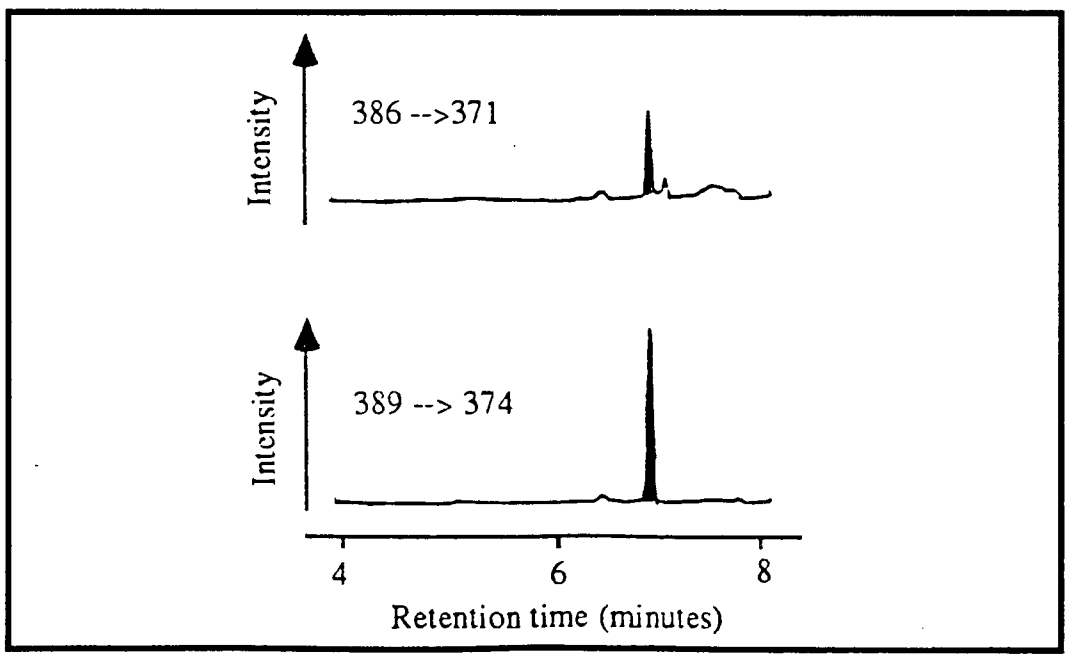

Figure 20

GC/MS/MS chromatograms for the fragmentations *m/z* 386 → 371 for THC (IX) and 389 → 374 for $^{2}H_{3}$THC (X) from a crude plasma extract.

f) Flexible Control of *B*, *E* and *V*

The MS/MS work was subsequently extended to enable switching to any point on the three dimensional 'ion surface' on an ageing conventional instrument with a minimum of modification by independent control of *B*, *E* and *V*. This work was presented as a poster at the 11th International Mass Spectrometry Conference in Bordeaux in 1988 (Davies, 1988)[8]. Examples used in this work included the quantitative determination of Δ-9 tetrahydrocannabinol (THC) (IX), the active constituent of cannabis, from human blood extracts by isotope dilution GC/MS/MS.

Metastable mapping of the mass spectrum of camphor was also illustrated, by acquiring a series of magnet scans with the value of *E* stepped down by 0.05% between successive scans. Each scan taken in this manner is a slice through the ion current surface (as illustrated and defined in Figure 16 for warfarin), parallel to the μ axis.

Figure 20 shows the chromatograms for the fragmentations *m/z* 386 → *m/z* 371 from the molecular ion of the trimethylsilyl derivative of THC, and the corresponding fragmentation for the trideuterated internal standard (X), from an unpurified whole blood extract. The levels were 2.5ng mL^{-1} blood for THC and (nominally) 10ng mL^{-1} of internal standard. This monitoring was achieved by independent control of *V* and *E*, with no magnetic field switching, so that cycle times were compatible with GC peak widths. Low resolution normal selected ion monitoring for this compound frequently has numerous interfering substances at the same or similar retention time for the main beam ions *m/z* 386, 371, 343 and 303 normally monitored.

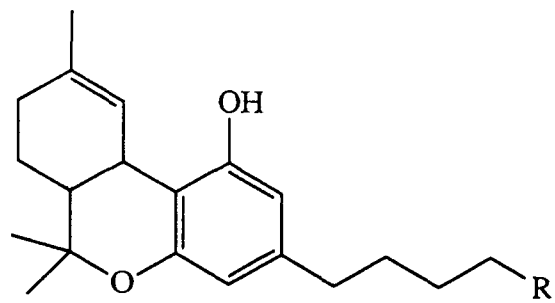

IX R=CH_3

X R=CD_3

While analysis of crude mixtures by MS/MS via the direct insertion probe (as distinct from GC/MS/MS) has fallen into some disfavour, due to the relatively high load of organic matter that is vaporized into the spectrometer resulting in potential problems with ion source and

flight tube contamination, it nevertheless has a place for some samples.

A recent book (Busch *et al.*, 1988) presents an overview of the many diverse aspects of MS/MS, including the various other instrument types that are also capable of this technique. These include triple quadrupole, multi-sector and hybrid instruments that provide separation of generations of ions in *space*, and ion cyclotron resonance and quadrupole ion trap instruments that provide the separation in *time*.

g) Accelerating Voltage Adjustments in *B/E* Scans

A short note published in *Organic Mass Spectrometry* (Davies *et al.*, 1982*a*)[9] was also relevant to the monitoring of metastable or collisionally induced fragmentations in the first field-free region of a Nier-Johnson double-focussing mass spectrometer. This note pointed out the advantages of using a single *B/E* ratio and small accelerating voltage adjustments to focus new parent ions for the generation of multiple linked scans from different parent ions from the same compound without tedious refocussing, resetting of a new *B/E* ratio and recalibration of the mass scale. This accelerating voltage adjustment was in fact the mechanism that was employed for the multiple reaction monitoring assay for warfarin discussed above.

The principal application of the voltage adjustment technique was to the acquisition of a number of full *B/E* linked scans from different parent ions over a period of only a few seconds. This was important where as much structural information as possible was required on very limited amounts of sample. Appropriate voltages to select different parent ions could be pre-set, for example, into separate channels of a Multiple Ion Detection (MID) unit or other multichannel device, and then selected by push-button operation during the magnet reset time.

A range of *B/E* scans could then be acquired with absolutely no delay between them other than the normal magnet reset time. This naturally required that the normal linkage of *E* with *V* was removed (Davies, 1989)[8] such that the MID system controlled only *V*, while the single *B/E* ratio was controlled in the normal manner by the linked scan unit of the spectrometer.

Working with a scan rate of 1 second per decade, linked scans acquiring the daughters of eight different parent ions could be achieved in a total of ten to fifteen seconds, which was well within the normal distillation profile of a single loading of the direct insertion probe. The technique is naturally limited to parent ions that are not grossly different in *m/z* value, to minimize losses in sensitivity caused by ion source defocussing effects of the lower accelerating voltage.

In practice parent ions could differ in *m/z* value by a ratio of 40% and still achieve acceptable results. Defocussing caused by changes in accelerating voltage could be minimized by tuning the ion source with the accelerating voltage set to the middle of the range to be used. The technique was particularly useful where only a

very small quantity of sample was available, and the maximum amount of linked scan data was required.

While mass spectrometers at the time were heading toward full digital control enabling loading of different *B/E* ratios for successive constant parent ion scans with different parents selected, the software and hardware capability of the VG 7070F resulted in delays of up to one minute while each change in ratio was downloaded, making it an impractical technique.

Current generation double-focussing mass spectrometers, with the associated advances in computer technology, generally enable totally flexible control of *B*, *E* and *V*, and also have the capacity for the necessary parameters for different *B/E* ratios to be rapidly loaded, obviating the need for the voltage adjustment technique.

h) Instrumentation and Techniques Used for MS/MS Work

Preliminary work on selected reaction monitoring was carried out on a VG 7070F mass spectrometer with 2035 datasystem, a Linked Scan control unit and Multiple Ion Detection (MID) unit. A Digital Scan control unit was subsequently installed on this instrument in 1982.

In initial experiments on multiple reaction monitoring from the same precursor, the *B/E* scan was selected in the normal manner, focussing the chosen main beam ion, and channels in the MID unit were set for the *apparent* *m/z* values of the daughter ions (i.e. at m_d^2/m_p where m_d is the *m/z* value of the daughter ion and m_p the *m/z* value of the precursor ion). Standard magnet switching selected ion monitoring (SIM) was employed. A minimum dwell time of 300ms per channel was chosen, due to the relatively long 'settling' time required by the older style, solid core magnet. This was sufficient to adequately switch the magnetic field over the very small range required to alternately focus ions differing only by the replacement of several hydrogens with deuterium.

In subsequent experiments looking at daughters from unrelated precursors, the ions were focussed by one of the following methods. In the first method, the linked scan unit was employed as described above, in addition to the use of two separate accelerating voltage channels (unlinked from *E*) switched in synchronization with the MID unit control of the relevant *B/E* channels. The use of accelerating voltage adjustments enabled different precursors to be selected, while maintaining the same mass axis (Davies *et al.*, 1982*a*), precluding the need to download different calibration files.

The accelerating voltage for the second precursor m_{p2} was set to $(m_{p2}/m_{p1})V_1$ where m_{p1} was the *m/z* value of the first precursor, and V_1 the accelerating voltage at which this main beam ion was focussed. Two extra channels were incorporated into the magnet SIM mode, during which the accelerating voltage was alternated. This avoided the need for precise synchronization of the *V* and *B/E* switching. This technique was used for the warfarin assay (Davies *et al.*, 1983).

In the second method, a Digital Scan control unit was used to control the switching of *B/E*, and the MID unit was used to set up independent channels for *V*. This was the method used for the NMP assay (Davies *et al.*, 1984). Alternatively, to avoid any switching of the magnetic field (Thorne and Gaskell, 1985), the Digital Scan unit was used to control *E*, and the MID unit was used to

control *V*. This was the method used for GC/MS/MS, such as for THC in human blood plasma discussed above.

4. APPLICATIONS

i) Parasitic Wasp Secretions

The specificity and sensitivity of GC-MS as an analytical technique makes it the method of first choice for the characterization of the secretions used by insects in behavioural control. These include sex pheromones, trail pheromones, alarm substances, defensive secretions and other behaviour modifying chemicals. They often occur at only trace levels, and in many cases exhibit extreme biologically activity at these levels. Several reviews of the area have been published (Silverstein, 1982; Baker and Herbert, 1984).

Research was commenced in 1981 aimed at identifying the chemistry of the mandibular gland secretions of two species of introduced parasitic wasps, which are important in the biological control of the *Sirex* wood wasp, a serious pest of *Pinus radiata* plantations. These secretions, obtained experimentally by 'milking' the fluid exuded from disturbed insects into glass micro capillaries, are implicated in the courtship and mating behaviour of the insects (Madden, personal communication). The chemical and behavioural results of this research were presented in an article in *Journal of Chemical Ecology* (Davies and Madden, 1985)[10].

One of the species, *Rhyssa persuasoria*, produced a secretion in which there were two principal volatile components. The first of these gave a mass spectrum with base peak *m/z* 59, and ions at *m/z* 31(42%), 39(17), 41(28), 43(49) and 87(5). This was identified as 3-hydroxy-3-methylbutan-2-one by comparison with reference spectra (Stenhagen *et al.*, 1974) and subsequently with an authentic sample (a gift from Prof. W. Francke). The second compound had a base peak at *m/z* 43, and ions at *m/z* 41(60), 55(30), 58(15), 69(26), 108(19), 111(15) and 126(7). This was identified from reference spectra and an authentic sample (a gift from Prof. G.W.K. Cavill) as 6-methylhept-5-en-2-one. After its first identification as a natural product in the defensive secretion of ants (Cavill and Ford, 1953), this ketone has been associated with the alarm and defensive secretions of numerous insects.

The second species, *Megarhyssa nortoni*, also produced 6-methylhept-5-en-2-one, as well as pentan-2-one and a series of compounds which could not be readily identified form reference data or from first principles. Three of these had similar mass spectra, with prominent ions at *m/z* 112 and *m/z* 115 and apparent molecular ions at *m/z* 184 (Figures 21, 22 and 23). A fourth compound, which

appeared to be unstable and diminished fairly rapidly upon storage, had a related but significantly different spectrum (Figure 24).

Accurate mass measurements on the molecular ion at *m/z* 184 of the first three compounds gave the empirical formulae $C_{11}H_{20}O_2$, while the fourth compound had an apparent molecular ion at *m/z* 168 with the formula $C_{11}H_{20}O$. The prominent fragment ions at *m/z* 112 and 115 were found to be $C_7H_{12}O$ and $C_6H_{11}O_2$ respectively.

The first three of these compounds all failed to form any ester, methoxime or trimethylsilyl derivatives, or to change upon hydrogenation or saponification. Bicyclic acetals or ethers were therefore suggested as possible candidates. Consultation with colleagues involved in insect chemistry (Brophy, personal communication) confirmed that a number of bicyclic acetals had recently been identified in insect secretions, and an examination of the literature (Francke *et al.*, 1978, 1979, 1980) showed that these compounds did in fact match closely the reported mass spectra of (E,E)-2,8-dimethyl-1,7-dioxaspiro[5.5]undecane (XI), (E,E)-2-ethyl-7-methyl-1,6-dioxaspiro[4.5]decane (XII) and (Z,E)-2,8-dimethyl-1,7-dioxaspiro[5.5]undecane (XIII) respectively. Comparison of GC and MS data with authentic standards provided by Professor Francke of the University of Hamburg confirmed these three identifications.

The fragmentation under electron impact of alkyl spiroacetals was studied by Francke *et al.* (1979). The diagnostic ion at *m/z* 112 in these three isomers is due to the extrusion of acetaldehyde and ethylene via electron transfer around the 6-membered ring. The ion at *m/z* 115 results from elimination of C_5H_9 after hydrogen transfer.

The fourth, unstable compound appeared to be related to an unknown isolated with these same spiroacetals (Bergstrom *et al.*, 1982). The identification of this compound had not been published prior to the dispatch of the original manuscript; however, the structure had just been determined to be 2-methyl-6-pentyl-3,4-dihydro-2H-pyran (XIV) (Francke, personal communication).

The unknown from *Megarhyssa* was confirmed to be identical by GC and MS by comparison with a synthetic sample of this enolether. Professor Francke generously let the identification of this pyran in *Megarhyssa nortoni* be published simultaneously with his report on cyclic enolethers from insects (Francke *et al.*, 1985) in which the identification of the pyran as a new natural product first appeared.

Other compounds identified in *Megarhyssa* were undecan-2-one and undecan-2-ol, which are biogenetically related to the spiroacetals.

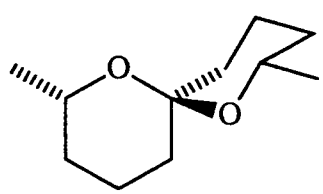

XI

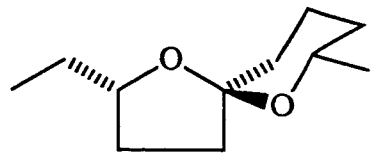

XII

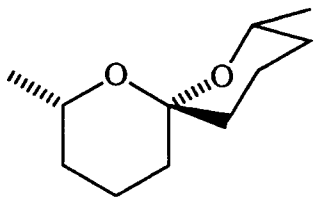

XIII

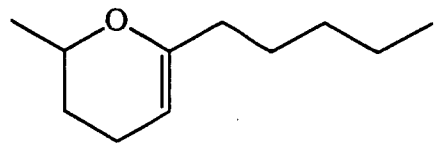

XIV

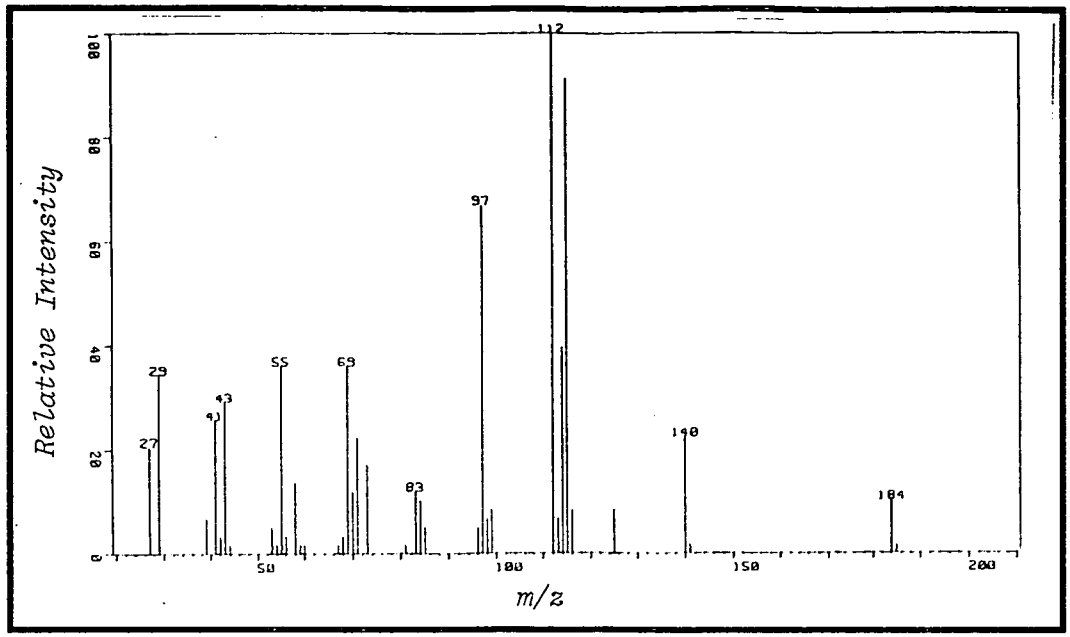

Figure 21

Mass spectrum of *M. nortoni* compound identified as (E,E)-2,8-dimethyl-1,7-dioxaspiro[5.5]undecane (XI)

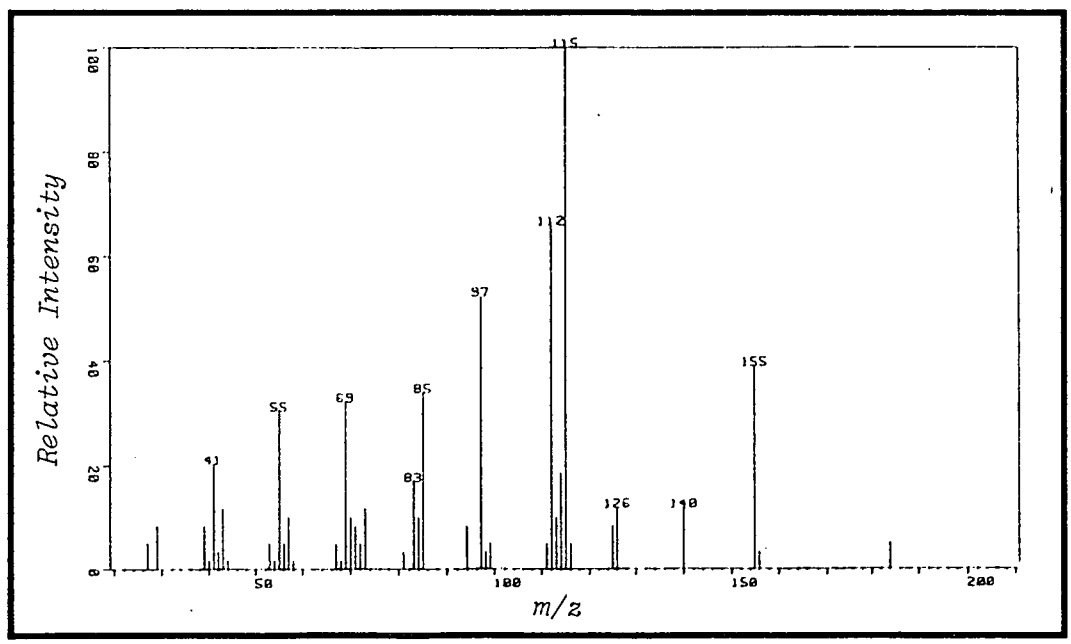

Figure 22

Mass spectrum of *M. nortoni* compound identified as (E,E)-2-ethyl-7-methyl-1,6-dioxaspiro[4.5]decane (XII)

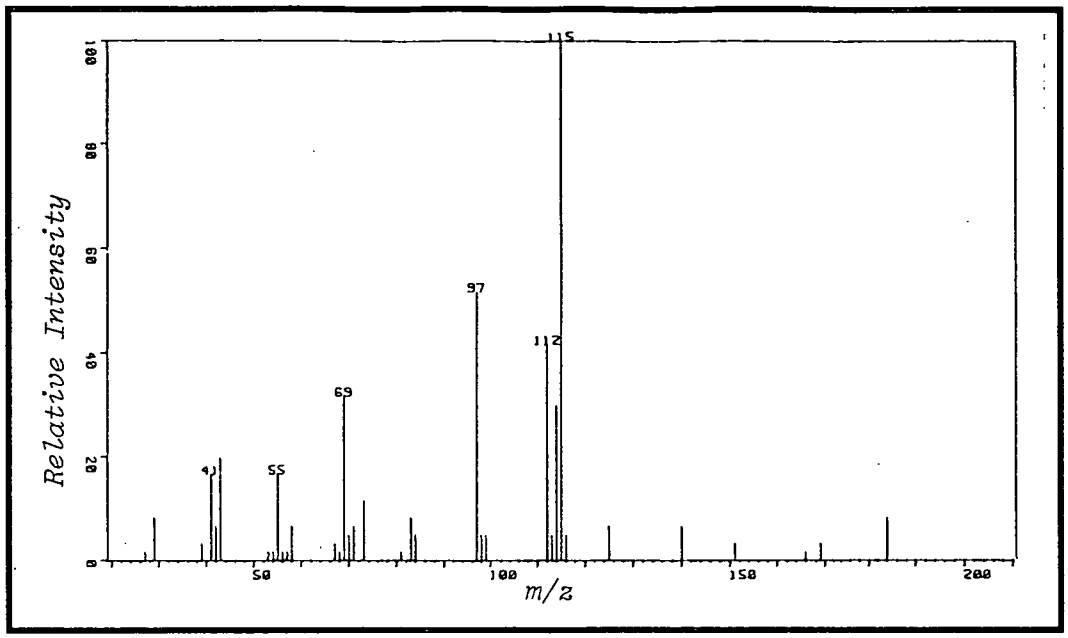

Figure 23

Mass spectrum of *M. nortoni* compound identified as (Z,E)-2,8-dimethyl-1,7-dioxaspiro[5.5]undecane (XIII)

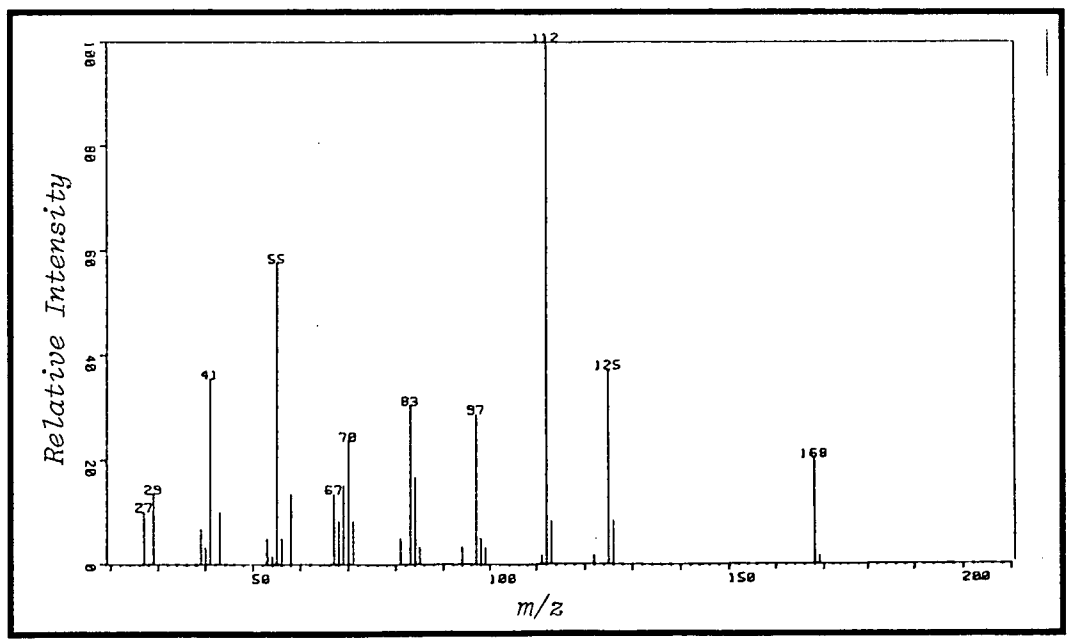

Figure 24

Mass spectrum of *M. nortoni* compound identified as 2-methyl-6-pentyl-3,4-dihydro-2H-pyran (XIV)

ii) Essential Oils and Related Plant Extracts

The detailed chemical characterization of essential oils and volatile plant extracts formed an important part of research activities during the period of the Research Fellowship. This work was principally done in collaboration with Professor R. Menary of the Department of Agricultural Science at the University of Tasmania, who provided most of the samples.

The characterization of essential oils forms an area of specialization within the field of GC-MS analysis. The requirement for this degree of specialization is in part due to the enormous range of potential terpenoid and other compounds likely to be found in essential oils and related products, and the relatively poor range of commercially available reference mass spectral data for these compounds. Furthermore, the mass spectra of terpenes are in many cases very similar, due both to the minor structural differences between some isomers, and to intramolecular rearrangements after ionization resulting in bond migration, yielding in some cases identical ion structures. Many terpenes exist in several diastereomeric forms with almost identical mass spectra (e.g. the sesquiterpene alcohols globulol, ledol, viridiflorol and epiglobulol; the monoterpene alcohols menthol, neomenthol, isomenthol and neoisomenthol).

There are also potential problems with artifacts caused by thermal rearrangements within the GC injection port or the GC-MS interface, such as the Cope rearrangement of Germacrene A, Germacrene B and bicyclogermacrene to β-elemene, γ-elemene and bicycloelemene respectively (Clark *et al.*, 1987; LeQuere and Latrasse, 1990).

The number of biogenetically feasible monoterpenes and sesquiterpenes is very large; there are over 100 reported carbon skeletons for sesquiterpenes. Even considering only hydrocarbons, alcohols and ketones, there are many thousand possible structures; mass spectral and GC data have only been reported in the general literature for a very small fraction of these. (Some of the large international flavour and fragrance companies have developed extensive libraries of both mass spectral and GC data for terpenes and other volatile compounds likely to be found in essential oils and related plant extracts, but due to commercial considerations do not release this information.)

Correct identification of known essential oil components therefore requires great care, often requiring the use of Kováts' retention indices (Kováts, 1958) in conjunction

with mass spectral data, and possibly direct comparison with authentic standards.

The difficulties of structural assignment of novel terpenes based on MS evidence alone have been outlined by Enzell *et al.* (1972). In general, monoterpenes and sesquiterpenes lack strong fragmentation-directing groups.

A considerable amount of development was therefore required to build up a suitable database of reference data on known terpenoids and other essential oil compounds either from the literature, or by acquiring data from pure samples or essential oils of known composition. This was done for both GC data, using Kováts' retention indices, and mass spectra. The former was ultimately published in 1990 as a review of 900 indices of 400 different terpenes in *Journal of Chromatography* (Davies, 1990)[11], to facilitate analytical work in this area. This review was based on a personal database of literature values for retention indices built up over the preceding ten years. The mass spectral data was developed as a database acquired from literature sources, colleagues, individual reference compounds and commercial essential oils of known composition, against which unknown compounds could be searched using commercial software (VG 2035 datasytem).

Apart from data generated on the VG 7070F (see Appendix C), the major sources for the mass spectral database were Brophy (personal communication), Hirose (1967), Moshonas and Lund (1970), Stenhagen *et al.* (1974), Heller and Milne (1978, 1980), Kennett *et al.* (1977*a*, 1977*b*, 1980, 1982), ten Noever de Brauw *et al.* (1979, 1982, 1986), Jennings and Shibamoto (1980), Swigar and Silverstein (1981), Ramaswami *et al.* (1986) and Adams (1989). Some sixty other literature references to mass spectra of individual terpenes or groups of terpenes and other essential oil compounds were used in the compilation of this database. This data has since been made available to other researchers in the area of essential oil analysis, and is incorporated into the database of the Laboratory for Aroma Research of the French National Institute for Agronomic Research (INRA) in Dijon, France.

Novel terpenes, which are often encountered in studies of essential oils from Australian native species (e.g. Southwell, 1978, 1987; Lassak and Southwell, 1977), will generally require classical isolation and structural elucidation by MS, IR and NMR for unequivocal structural assignments; this is seldom possible by MS alone from first principles.

Table 1 summarizes the range of commercial and experimental oils that were analysed during the period 1979-1992 using a combination of the mass spectral and Kováts' index databases described above.

During the course of this research on essential oils, a considerable number of errors in reference mass spectra in the EPA/NIH Mass Spectral Database (Heller and Milne, 1978, 1980) (subsequently incorporated into the NIST/EPA/MSDC Mass Spectral Database) and the Wiley Registry of Mass Spectral Data (Stenhagen *et al.*, 1974) were identified and noted in correspondence to the editors.

Acradenia frankliniae	*hops*
Artemisia afra	*Huon Pine*
Athrotaxus cuppressoides	*hyssop*
Athrotaxus selaginoides	*jasmine*
Bedfordia salicina	*kaprao*
Beyeria viscosa	*lemon*
bitter fennel	*Leptospermum lanigerum*
blackcurrant buds	*Leptospermum sericea*
Boronia megastigma	*lime*
Boronia pilosa	*marjoram*
buchu	*Melaleuca dissitiflora*
bush basil	*Melaleuca uncinata*
Callitris rhomboidea	*onion*
Calotis	*orange*
caraway	*Osmanthus*
celery herb	*palmerosa*
celery seed	*parsley herb*
chamomille	*parsley seed*
clary sage	*peppermint*
coriander	*Phebalium squameum*
cornmint (Mentha arvensis)	*pine-needle*
Dalmatian sage	*Podocarpus lawrencii*
Drimys lanceolata	*Prostanthera lasianthos*
Eucalyptus citriodora	*rosemary*
Eucalyptus delegatensis	*sage*
Eucalyptus globulus	*spearmint*
Eucalyptus macarthuri	*summer savory*
Eucalyptus nitens	*sweet basil*
Eucalyptus ovata	*sweet fennel*
Eucalyptus polybractea	*sweet marjoram*
Eucalyptus pulchella	*tarragon*
Eucalyptus radiata	*thryptomene*
Eucalyptus regnans	*thyme*
Eucalyptus smithii	*ti-tree (Melaleuca alternifolia)*
Eucalyptus tenuiramis	*verticordia*
Eucalyptus viminalis	*vetiver*
ginger	*wormwood (Artemisia absinthium)*
	Zieria arborescens

Table 1

Commercial and experimental essential oils analysed during the period 1980-1992 using the mass spectral and Kováts' index databases described.

a) Essential Oils from Hops

The first specific oils for which the results were published were distilled from commercially grown hops (*Humulus lupulus*) (Davies and Menary, 1982)[12]. Clarification of the composition of hop essential oils from various cultivars grown in Tasmania was undertaken, particularly with respect to the level of selinene isomers. The levels of α- and β-selinenes (XV and XVI) were of particular interest from the point of view of 'aroma' characteristics of the hops (Menary, personal communication), and ultimately of the beer brewed using particular hop cultivars. Other selinenes that were also of interest with respect to 'aroma' character were selina-4(14),7(11)-diene and selina-3,7(11)-diene.

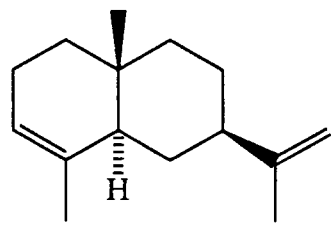

XV

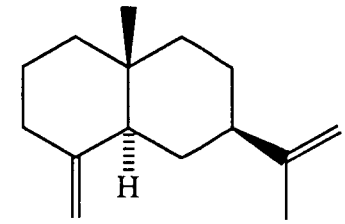

XVI

What appeared to be the same compounds had been ambiguously identified in Europe as 'posthumulenes' (Maier, 1978), and it was determined from reference standards that there were serious errors in much of the readily available published reference spectra for both α-selinene (Moshonas and Lund, 1970) and β-selinene (Heller and Milne, 1978,1980; Stenhagen *et al.*, 1974), although summarized spectra had been published that were substantially correct for α-selinene (Hirose, 1967) and β-selinene (e.g. Schreier *et al.*, 1976; Moshonas and Lund, 1970).

The correct mass spectra, obtained from pure samples of α- and β-selinene isolated by preparative GC from rosewood and celery oils respectively, are shown in Figures 25 and 26. The incorrect published spectra for these two sesquiterpenes were possibly based on erroneous identifications or thermal degradation within the MS. Reference mass spectra for selina-4(14),7(11)-diene and selina-3,7(11)-diene were obtained from a sample of oil from the hop variety 'Sunshine'.

Approximately fifty other volatile compounds in the hop oils were fully or partially characterized on the basis of GC and MS evidence.

Some published correspondence was entered into as a result of this work, regarding the possible role of sesquiterpenes as constituents of the hop 'aroma' character of certain beers (Clarke, 1982; Davies and Menary, 1983*a*).

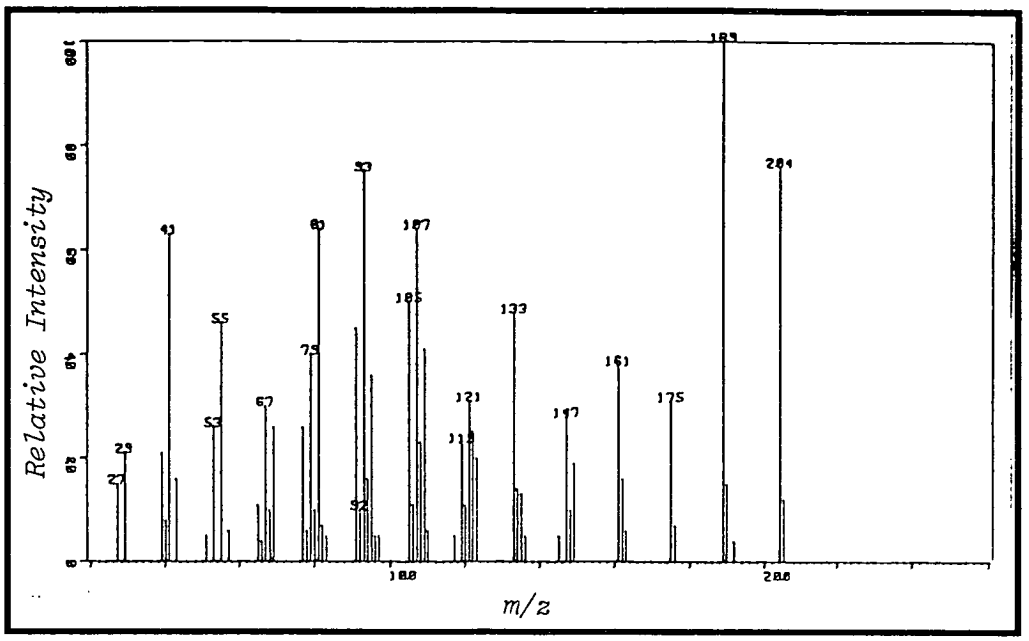

Figure 25

Mass spectrum of α-selinene (XV)

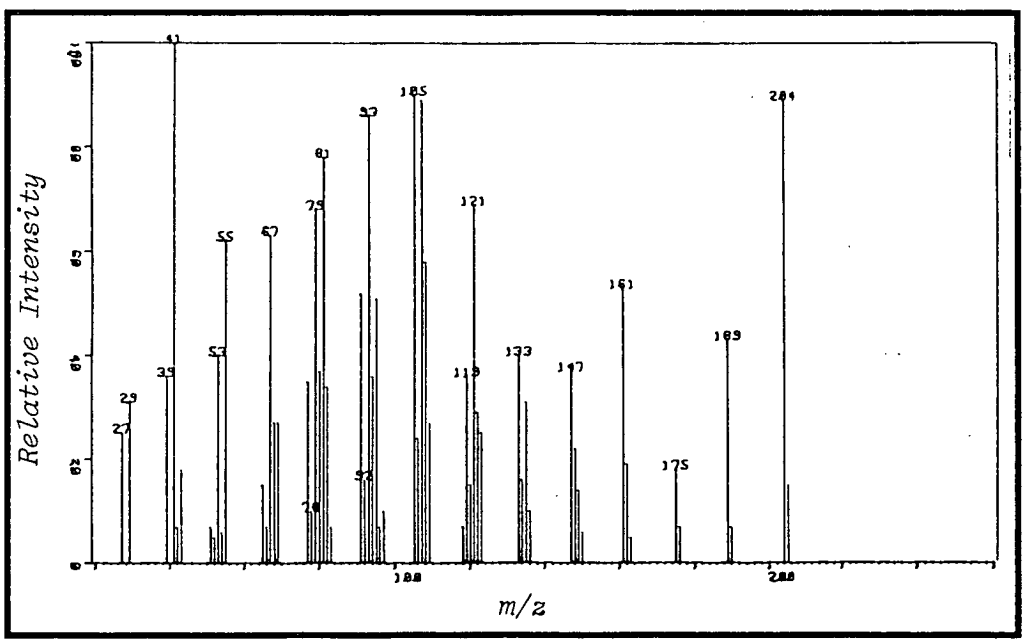

Figure 26

Mass spectrum of β-selinene (XVI)

b) *Boronia megastigma* Floral Concretes

The 'concrete' obtained by the solvent extraction of *Boronia megastigma* flowers is of interest to perfumers and flavorists due to its intense aroma and flavour enhancing characteristics. From pioneering studies done in the 1920's (Penfold, 1927) it was known to be the first natural source of β-ionone, but very little other chemistry had ever been carried out on this product. As part of the ongoing development of an essential oils industry in Tasmania, the *Boronia* concrete was characterized in some detail (Davies and Menary, 1983*b*)[13].

The organoleptic quality of the concrete, which is used as a flavour enhancer in foods and beverages, and to a lesser extent in perfumery products (Menary, personal communication) was of great importance from a marketing point of view. It was quickly established by GC analyses that there was a great deal of chemical diversity among the trial populations of *Boronia megastigma*, and detailed chemical investigations were undertaken with a view to correlating chemical composition with organoleptic properties.

Among the major components in all clones examined was the simple alkene (Z)-heptadec-8-ene. The double bond position of this compound was determined by the technique of methoxymercuration-demercuration (Blomquist *et al.*, 1980), followed by GC-MS analysis of the products.

A single, substantial GC peak was obtained following the methoxymercuration-demercuration of the heptadecene peak isolated by preparative GC, with prominent ions at *m/z* 143 (39%), 157(60%) and 171 (35%). The strong ion at 157 could be best interpreted as arriving from alpha cleavage to the methoxy group (on both sides) from 9-methoxyheptadecane, whereas the ions at *m/z* 143 and 171 could be interpreted as alpha-cleavage on both sides to the methoxy group in 8-methoxyheptadecane. The mixed product of 8- and 9-methoxyheptadecanes was consistent with a heptadec-8-ene.

The *cis* double bond geometry was determined by the characteristic band in the Raman spectrum at 1657 cm^{-1}, and the absence of *trans* absorptions between 1665 and 1676 cm^{-1}, in a sample purified by micro-preparative GC. While this compound could be readily obtained biosynthetically from the decarboxylation of oleic acid, it had only been reported twice before in plants.

Among the compounds identified as a major component in one particular chemotype was a new sesquiterpene (XVII) which was given the trivial name 'sesquicineole', due to its close structural relationship to the common

monoterpene 1,8-cineole (XVIII). This structure was not confirmed by any independent spectroscopic means.

The mass spectrum of the parent compound is given in Figure 27. The empirical formula $C_{15}H_{26}O$ was determined by accurate mass measurement. Upon hydrogenation in the GC injection port (80% Chromosorb W, 20% (5% Pd on carbon), 200°C, hydrogen carrier gas) a dihydro derivative was obtained (M^+ 224, *m/z* 43, 95, 139, 209), indicating a single double bond, with no effect on the major ion at 139, which was found to be $C_9H_{15}O$. A mixture of trans- and cis- bisabolane (XIX, XX) was obtained upon pre-column hydrogenolysis (80% Chromosorb W, 20% (5% Pd on carbon), 300°C, hydrogen carrier gas).

Precolumn hydrogenations and hydrogenolyses were based on the work of Beroza and Sarmiento (1963; 1966), with some modifications to the catalyst. These reactions were carried out using the packed column injection port of a Pye 204 GC, with a 1.8 metre packed (3% SE30 on Chromosorb W) stainless steel column (one eighth inch outside diameter) coupled to a VG 7070F mass spectrometer via a glass jet separator, using hydrogen as carrier gas. Model compounds were tested prior to analysis of the unknowns to ensure that adequate conversions were occurring.

Attempted formation of oxime and trimethylsilyl derivatives resulted in no change, indicating the oxygen function was not present as a carbonyl or alcohol. This evidence indicated the compound to be a cyclic ether with a C_6H_{11} side chain, and a bisabolane skeleton. The strength of the ion at *m/z* 139 indicated that the ether function was likely to join to carbon 8. Biosynthetic considerations indicated the 1,8 cyclic ether as described. Subsequent trials with 1,8-cineole as a model confirmed the behaviour of this compound under the hydrogenolysis conditions employed, yielding a mixture of cis- and trans- p-menthane.

Other compounds found included methyl jasmonate (XXI) and a previously undescribed isomer of methyl jasmonate. Again the structural assignment for methyl jasmonate was based primarily on mass spectral evidence from first principles, since no reference spectra were available until after the preliminary structural assignment. Due to the occurrence of only a single peak in the hydrogenated product, the minor isomer most likely contained a *trans* double bond, rather than being a stereoisomer on the cyclopentanone ring.

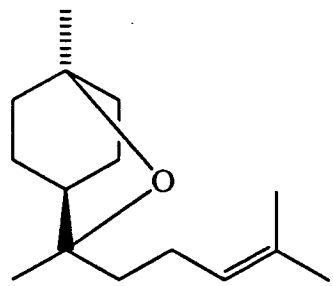

XVII

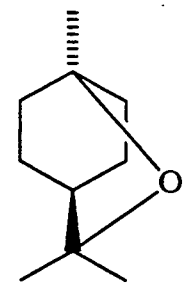

XVIII

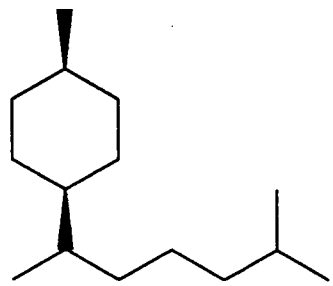

XIX

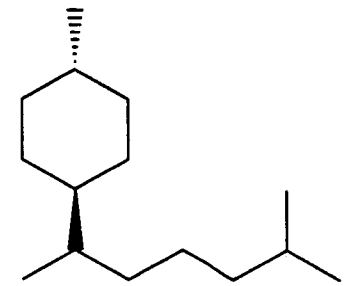

XX

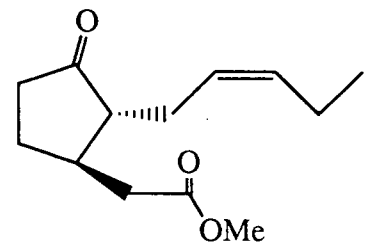

XXI

The molecular formula ($C_{13}H_{20}O_3$) was determined by accurate mass measurement, as were the formulae of key fragment ions at *m/z* 83 (C_5H_7O), *m/z* 151 ($C_{10}H_{15}O$) and *m/z* 156 ($C_8H_{12}O_3$). The prominent ion at *m/z* 83 suggested the compounds could be substituted cyclopentanones. A C_5H_9 side chain adjacent to the carbonyl could be responsible for a McLafferty rearrangement peak at *m/z* 156. The additional subunit present ($C_3H_5O_2$), as shown by the losses from the molecular ion and the ion at *m/z* 156, and presence of diagnostic peaks at *m/z* 59 and *m/z* 74, suggested a methyl ester function. Hydrogenation (5% Pd on carbon, in solution) of the concrete and subsequent GC-MS analysis confirmed the presence of a double bond in the C_5H_9 portion of the molecule. Methyl jasmonate was found to be the only known natural product satisfying these criteria, and the identification was confirmed from GC retention data and mass spectra of methyl jasmonate from a sample of Egyptian jasmine 'absolute'.

Two other volatile components could not be characterized by comparison with readily available reference data.

These showed *m/z* 82(100%), 71(77), 43(58), 67(42), 55(16), 59(8) and *m/z* 71(100%), 82(77), 43(86), 67(59), 55(14), 119(19), 134(9) and 152(trace) respectively. Both of these had no apparent molecular ion, and had strong similarities to the mass spectrum of 'hotrienol' (3,7-dimethyl-1,5,7-octatriene-3-ol).

However, the Kováts' index of hotrienol was much lower than either unknown. Subsequent comparison with authentic hotrienol confirmed that both eluted well after this compound. There were two known hydrated forms of hotrienol; 2,6-dimethyl-3,7-octadiene-2,6-diol and 3,7-dimethyl-1,7-octadiene-3,6-diol, that had been first reported from ho-leaf oil (*Cinnamomum camphora*) (Takaoka and Hiroi, 1976), and subsequently in Muscat of Alexandria grapes and wine (Williams *et al.*, 1980). Due to the ready dehydration of alcohols to alkenes on electron impact ionization, it was probable that the mass spectra of these diols would not be dissimilar to that of hotrienol, although no reference MS data were available. They would also be expected to elute considerably later than hotrienol on both polar and non-polar columns, consistent with the observed unknowns.

Synthetic samples of these two diols and hotrienol were obtained from Dr. Pat Williams of the Australian Wine Research Institute. The first unknown from *Boronia* was found to match exactly by GC and MS to 3,7-dimethyl-1,7-octadiene-3,6-diol. The second unknown eluted well after both diols on a non-polar methyl silicone GC phase, but *before* the 3,7-dimethyl-1,7-octadiene-3,6-diol on a Carbowax 20M column, indicating it to be less polar than the diol, but with a higher boiling point. A mono- or di-acetate of 3,7-dimethyl-1,7-octadiene-3,6-diol was a possible inference from this data.

Other major components present in all clones included the simple esters dodecyl acetate and tetradecyl acetate. Since it is known that in its native Western Australia *Boronia megastigma* is only pollinated by a single species of night-flying moth (Menary, personal communication), it is possible that these esters are present as specific sex pheromone mimics to attract the moth. Long chain saturated and unsaturated acetates are commonly found as Lepidopteran sex pheromones (Tumlinson, 1988).

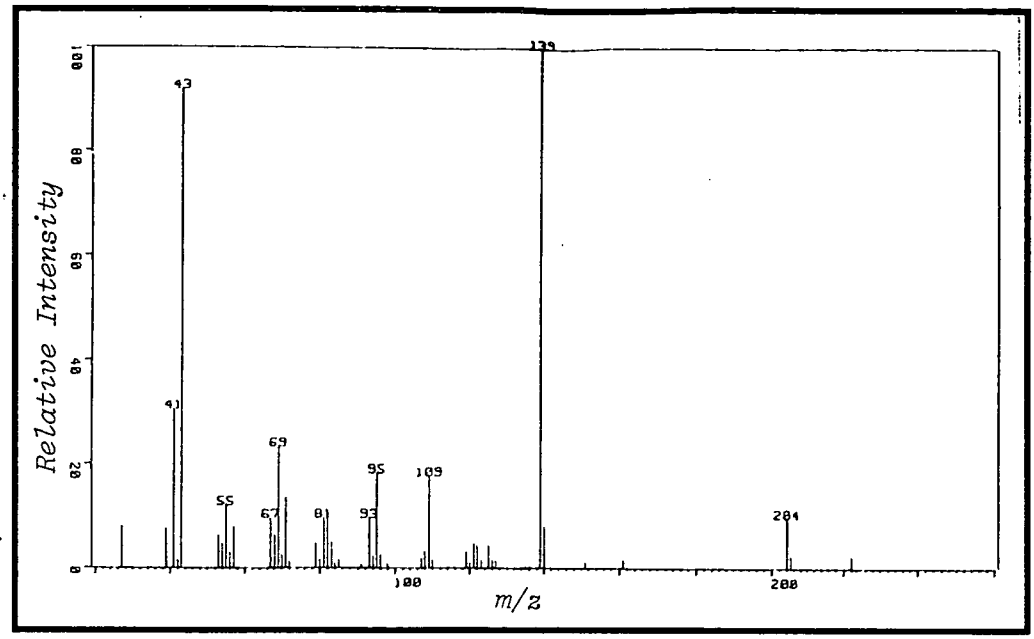

Figure 27

Mass spectrum of sesquicineole (XVII)

c) *Gardenia* Exudates

Collaborative natural product research with Professor Subranamiam Sotheeswaran from the University of the South Pacific in Fiji, including the provision and interpretation from first principles of mass spectral data, was undertaken over a number of years. As part of this work, extracts from a number of plants indigenous to Fiji were analysed by capillary GC-MS and direct insertion probe MS for known and new natural products. Structures of known and new triterpenes were assigned primarily on the basis of mass spectral information. While NMR data has also been used, the samples were not always pure enough for direct structural assignments by this method; it was used rather to back up the assignments based on the MS data. The first of this work to be published was the identification of cycloartenone (XXII) and three new related triterpenes in the bud exudates of six *Gardenia* species (Davies *et al.*, 1992)[14].

Cycloartenone was characterized by a molecular ion at m/z 424.370 ($C_{30}H_{48}O$ requires 424.3705), and ions at 340.278 ($C_{24}H_{36}O$), 313.250 ($C_{22}H_{33}O$), 311.235 ($C_{22}H_{31}O$) and 286.265 ($C_{21}H_{34}$). The fragmentation under electron impact conditions of the cycloartane skeleton has been studied extensively (Audier *et al.*, 1966; Aplin and Hornby, 1966). The effect on fragmentation of double bond position in attached side-chains at C-17 in related sterols has also been studied in detail (Wyllie and Djerassi, 1968). Figure 28 summarizes some of the characteristic fragment ions for cycloartenone and related triterpenes. One ion in particular, designated as ion 'a' (m/z 286 for cycloartenone), is known to be formed as a result of the cyclopropane bridge. Ion 'b' (m/z 313 for cycloartenone) results from the loss of the side chain at C-17, while ion 'c' arises from the Δ^{24} double bond in cycloartenone. The equivalent ions arise in other Δ^{24} triterpenes and sterols (Wyllie and Djerassi, 1968).

Three unknown compounds designated here as A, B and C (mass spectra Figures 29, 30 and 31) had the empirical formulae of their molecular and major diagnostic fragment ions determined by high resolution MS. The characteristic cycloartane fragmentation ion 'a', in which the A ring is completely lost, was found in each case. Compounds A and C were unaffected by catalytic hydrogenation, while compound B was converted to compound C. A literature search revealed no known cycloartane related triterpenes with the relevant formulae for the side chains at C-17 for compounds A and C. A cycloartane triterpene assigned the trivial name 'schizandraflorin' had been identified in *Schizandra grandiflora* (Talapatra *et al.*, 1982), with

a $\Delta^{20(21)}$, 24-one cycloartane structure (XXIII). However, the published mass spectrum of this compound was significantly different from that of compound B.

The structures of compounds A, B and C were determined by mass spectrometry from first principles, based on the characteristic fragmentations discussed above, and further fragment ions resulting from simple cleavage and McLafferty rearrangement ions (McLafferty, 1962, p. 93). The structure of compound A was determined to be the new natural product 9,19-cyclolanostan-3,24-dione (XXIV). Accurate mass data indicated the molecular ion to be *m/z* 440.363, indicating $C_{30}H_{48}O_2$ (requires 440.3654). Standing out from the general triterpene skeleton hydrocarbon ions were ions at *m/z* 43.055 (C_3H_7), 71.051 (C_4H_7O), 127.112 ($C_8H_{15}O$), 302.262 ($C_{21}H_{34}O$), 313.249 ($C_{22}H_{33}O$) and 354.290 ($C_{25}H_{38}O$). Figure 32 summarizes the case for the identification of this compound.

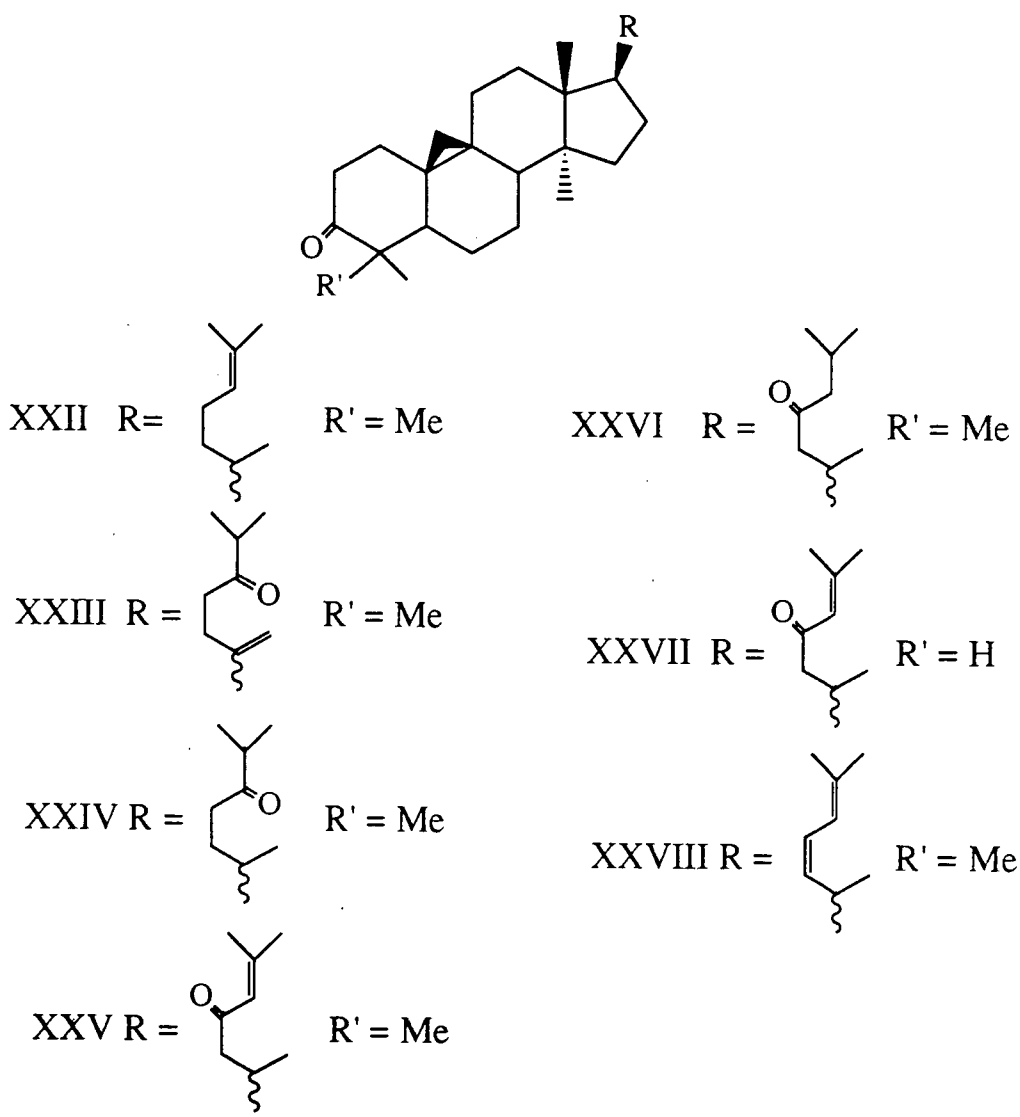

Figure 33 summarizes the case for compound B to be 9,19-cyclolanost-24-en-3,23-dione (XXV), another new natural

product. The position of the double bond assignment in the side chain was confirmed by proton NMR (δ_H 6.07 for the olefinic proton adjacent to the carbonyl group). Accurate mass data for this compound indicated M^+ 438.351 ($C_{30}H_{46}O_2$) and significant ions at *m/z* 83.050 (C_5H_7O), 98.073 ($C_6H_{10}O$), 125.098 ($C_8H_{13}O$), 300.244 ($C_{21}H_{32}O$) and 340.275 ($C_{24}H_{36}O$).

Figure 34 shows the case for compound C, which was found to be the new triterpene 9,19-cyclolanostan-3,23-dione (XXVI). Accurate mass data indicated M^+ 440.364 ($C_{30}H_{48}O_2$ requires 440.3654), and significant ions at *m/z* 85.067 (C_5H_9O), 127.112 ($C_8H_{15}O$), 302.263 ($C_{21}H_{34}O$), 313.247 ($C_{22}H_{33}O$) and 340.278 ($C_{24}H_{36}O$).

Further new triterpenes characterized as minor components in the exudates by mass spectra from first principles were C-4 nor-9,19-cyclolanost-24-en-3,23-dione (XXVII) and cycloartdienone (XXVIII).

In the published paper, an editorial decision was made not to include the MS fragmentation schemes or any discussion of the key ions; this left no explanation in the text as to the relevance of the indicated ions.

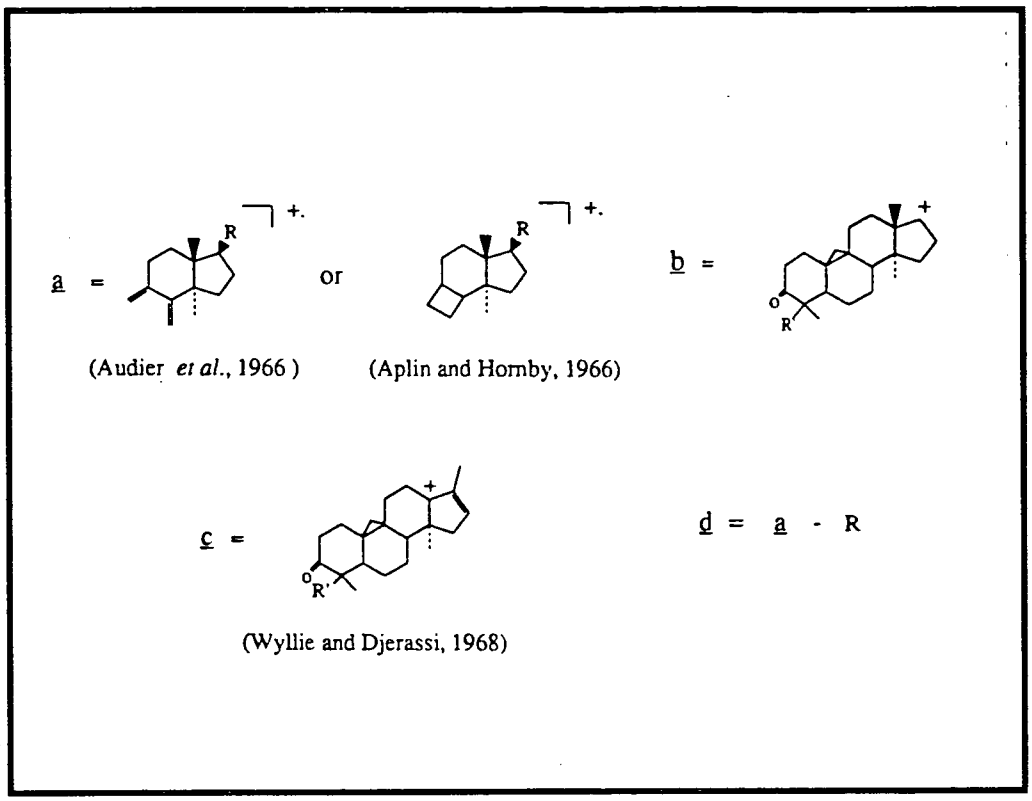

Figure 28

Key Fragment Ions for cycloartenone and related compounds

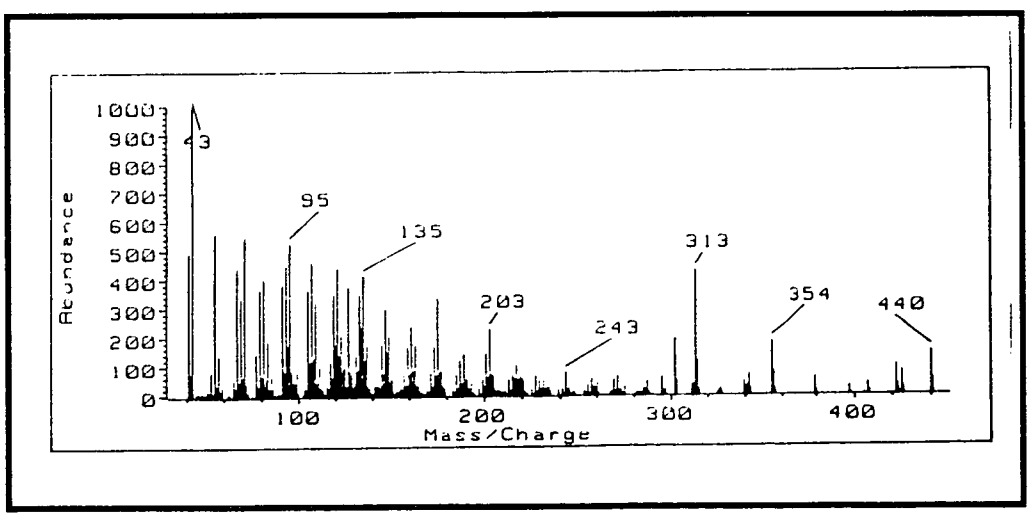

Figure 29

Mass spectrum of compound A (9,19-cyclolanostan-3,24-dione) (XXIV)

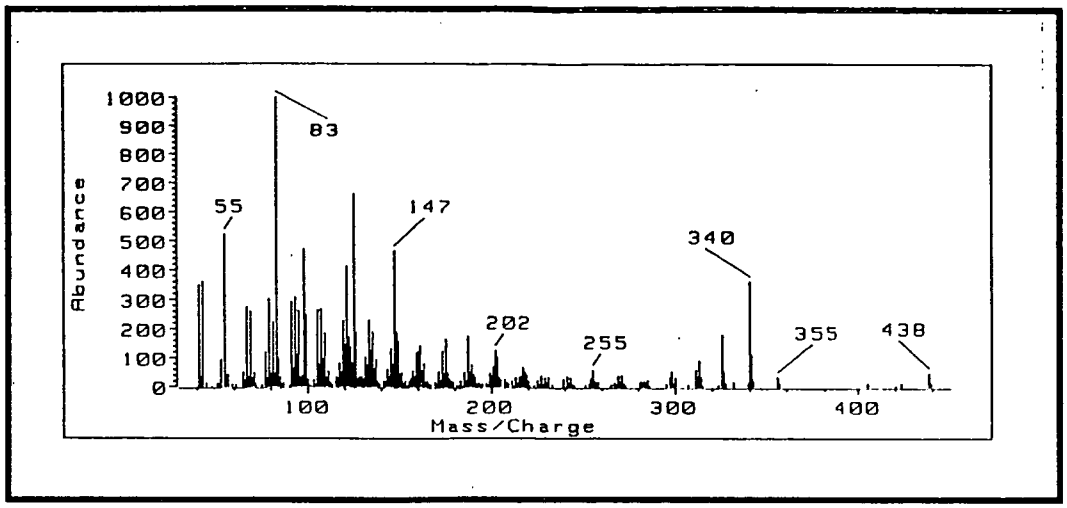

Figure 30

Mass spectrum of compound B (9,19-cyclolanost-24-en-3,23-dione) (XXIV)

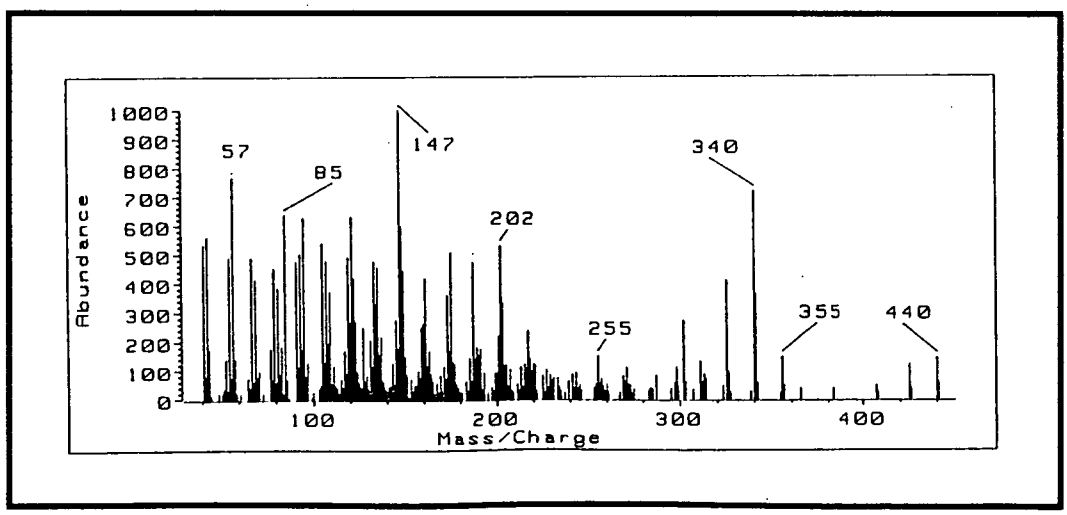

Figure 31

Mass spectrum of compound C (9,19-cyclolanostan-3,23-dione) (XXV)

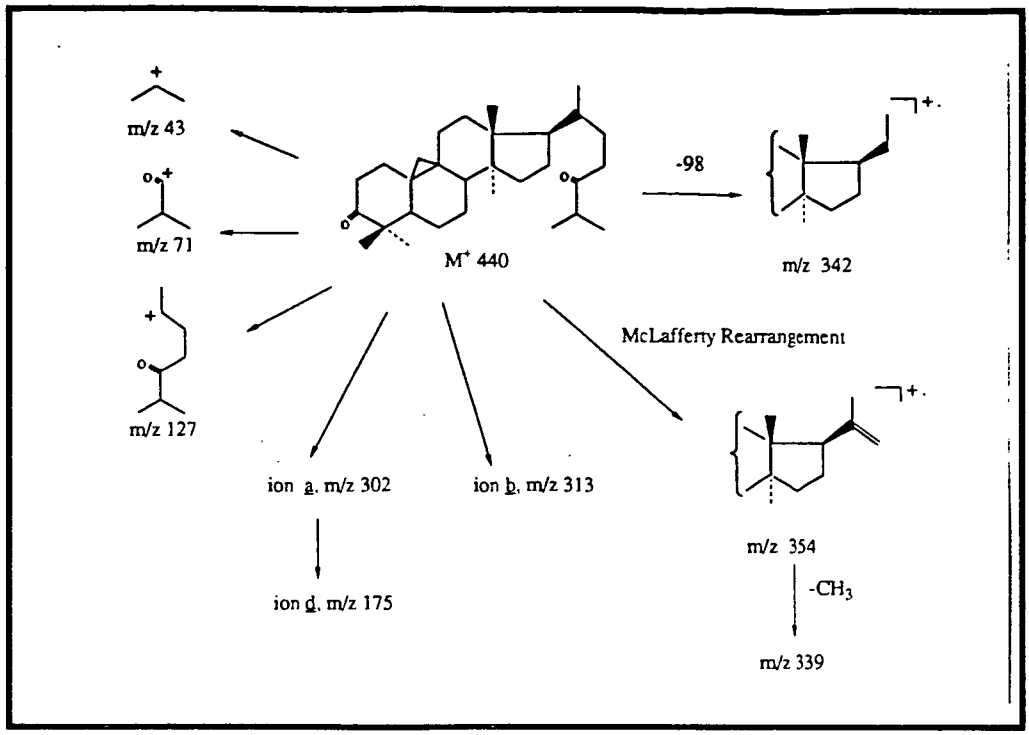

Figure 32

Mass Spectral Fragmentation Scheme for (9,19-cyclolanostan-3,24-dione)

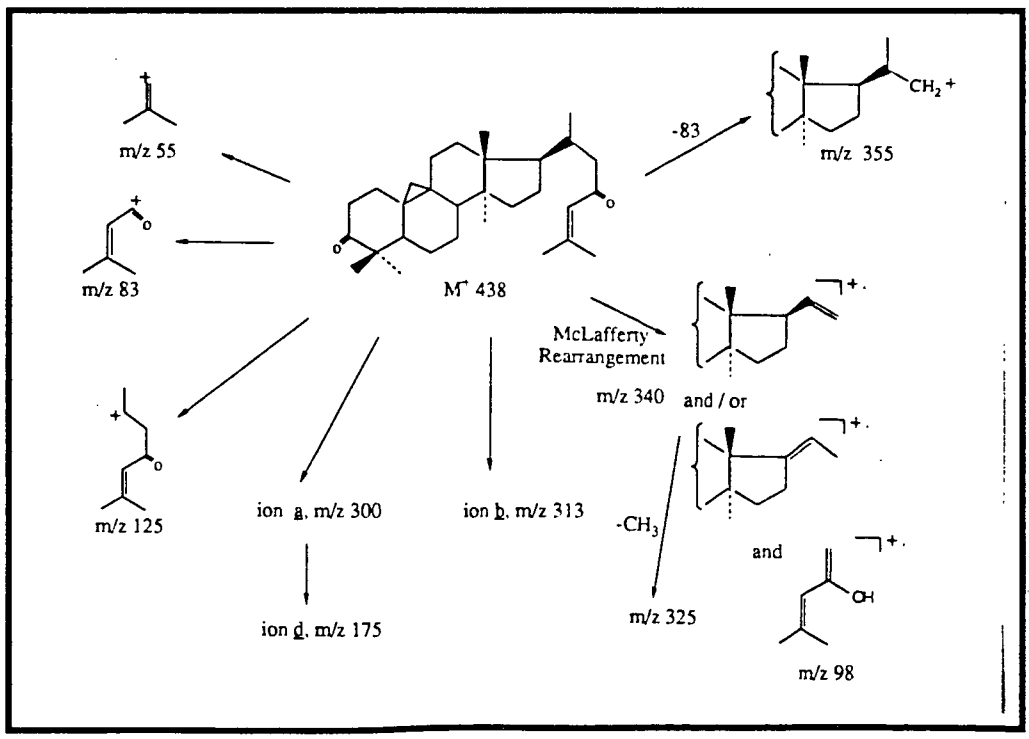

Figure 33

Mass Spectral Fragmentation Scheme for (9,19-cyclolanost-24-en-3,23-dione)

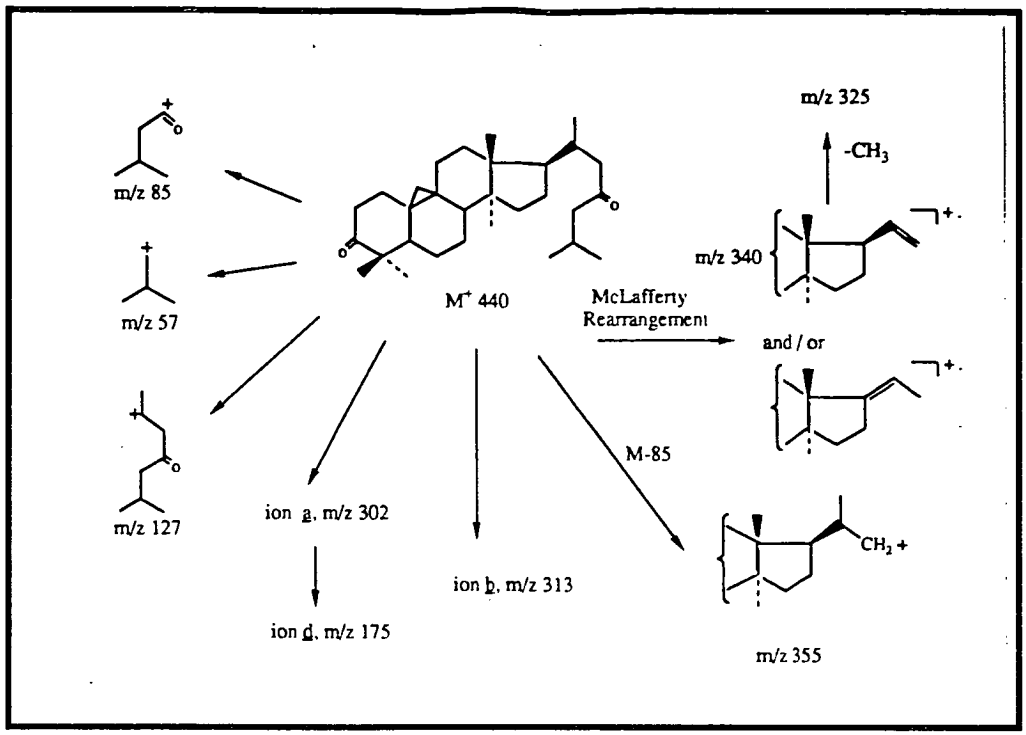

Figure 34

Mass Spectral Fragmentation Scheme for (9,19-cyclolanostan-3,23-dione)

iii) Contributions to the NIST/EPA/MSDC Mass Spectral Database

Several hundred full mass spectra acquired on the VG7070F in the CSL were incorporated into the database discussed above in section 4(ii). These spectra, obtained either from certified reference standards or from compounds otherwise unambiguously identified, were acquired during work on essential oil compositions, the potential involvement of drugs other than alcohol in road traffic accidents (McLean *et al.*, 1987; Neill *et al.*, 1991), the metabolic fate of phenacetin (McLean *et al.*, 1981) and related drugs, and forensic drug analyses.

Approximately three hundred mass spectra, predominately of natural products, drugs and drug metabolites, were submitted to the NIST/EPA/MSDC mass spectral database (Lias and Stein, 1990, 1992).

An eight peak version of these spectra (as distinct from spectra entered from literature sources and acquired from colleagues) is presented in Appendix C, indexed by name, major ions and molecular weight. A significant proportion were not present in the published mass spectral databases (Stenhagen *et al.*, 1974; Heller and Milne, 1978, 1980, 1982; Mass Spectrometry Data Centre, 1983; ten Noever de Brauw *et al.*, 1979, 1982, 1986; Kennett *et al.*, 1977*a*, 1977*b*, 1980, 1982), and so formed an integral part of the analytical strategy for essential oils and drugs.

The mass spectra of a series of N-arylacetylhydroxamic acids, acetamidophenols and their methyl derivatives, which formed part of the contributed data, were published separately together with a discussion of diagnostic fragment ions and their implications in drug metabolism studies (Davies *et al.*, 1982*b*).

Table 2 lists those compounds for which spectra were incorporated into the released versions of the NIST/EPA/MSDC database.

Table 2

acetanilide, 2,4-dihydroxy-
acetanilide, 2,4-dimethoxy-
acetanilide, 2-hydroxy-4-chloro-
acetanilide, 2-methoxy-4-chloro-
acetanilide, 3,4-dihydroxy-
acetanilide, 3,4-dimethoxy-
acetanilide, 3-methylthio-4-methoxy
acetanilide, N-hydroxy-3,4-dichloro-
acetanilide, N-hydroxy-4-chloro
allopurinol
benezene, 2,3,4,5-tetramethoxy allyl-
benzenesulfonamide, 2-hydroxy-4-acetylamino-
benzenesulfonamide, 2-methoxy-4-acetylamino-
benzenesulfonamide, N-hydroxy-4-acetylamino-
benzenesulfonamide, N-methoxy-4-acetylamino-
benzofuran, 3,6-dimethyl-, 2,3,3a,4,5,7a-hexahydro-
benzoic acid, 4-acetylamino-, methyl ester
biphenyl, N-hydroxy-4-acetylamino-
biphenyl, N-methoxy-4-acetylamino
bisabolol oxide A
bisabolol oxide B
bisabolol, α-
bisabolone oxide
bourbonene, β-
brefeldin A
camphene hydrate
campholene aldehyde, α-
capillin
carbimazole
carveol, *cis*-
carveol, *trans*-
carvone
chamazulene
chlorpheniramine
cineole, exo-2-hydroxy-
citric acid, acetyl-, tri-n-butyl ester
clonazepam
clonidine
cuminic aldehyde, p-
cymen-7-ol, p-
cymen-8-ol, p-
damascenone
dec-4-enoic acid, methyl ester
dihydrocarvone
dihydrocodeine
dillapiole
diosphenol
diosphenol, psi-
elemicin
ephedrine
ethylmorphine
eudesman-11-ol, 4β,5α-
eudesmane, 4αH-
eudesmol, α-
eudesmol, γ-
fluorene, N-hydroxy-2-acetylamino-
fluorene, N-hydroxy-3-acetylamino-
fluorene, N-mehtoxy-2-acetylamino-
fluorene-9-ol, 2-acetylamino-
Germacrene D
glibenclamide
guaifenesin
hotrienol
hydralazine
ibuprofen
indoleacetic acid, 4-chloro-, methyl ester
indomethacin
MDMA (ecstasy)
menth-2-en-1-ol, *cis*-p-
menth-2-en-1-ol, *trans*-p-
menthan-4-ol, p-
menthan-8-ol, p-
menthatriene, 1,3,8-p-
menthon-8-thiol, p-
methyl eugenol
methyprylone
miconazole
myrtanol
myrtanyl acetate
naphthalene, N-hydroxy-2-acetylamino-
naproxen
octadecyl acetate
octadiene-2,6-diol, 2,6-dimethyl-, 3,7-
octadiene-3,6-diol, 3,7-dimethyl-, 1,7-
phenacetin

Table 2 (continued)

phenacetin, 2-methoxy-
phenacetin, 3-methoxy-
phenacetin, N-hydroxy-
phenacetin, N-methoxy-
phenetidine, 2-hydroxy-
phenetidine, N-butyryl-
phenetidine, N-propionyl-2-methoxy-
pheniramine
phenyl-1-hexanone, 1-
phenylpropanolamine
pholcodine
pinocarveol
piperitol, *cis*-
piperitol, *trans*-
prazosin
propanamide, N-(4-chlorophenyl)-
propanamide, N-(4-methoxyphenyl)-
propiophenone, N-hydroxy-4-acetylamino-
quinine
radicicol
sabibene hydrate, *trans*-
selinene, α-
selinene, β-
selinene, δ-
seselin
spathulenol
sulindac
sulphanilamide, N1,N4-diacetyl-
sulphanilamide, N1-acetyl-
theophylline
thujone
verbenol
verbenone
viridiflorol
warfarin
zeatin
zierone
zingiberene

Table 2

Entries from the mass spectral library subsequently incorporated into the NIST/EPA/MSDC PC database.

5. REFERENCES

(Bold type indicates that the reference is included in full in Appendix B)

Adams, R.P. *Identification of Essential Oils by Ion Trap Mass Spectroscopy*, Academic Press, London, 1989

Aplin, R.T. and Hornby, G.M. "Application of mass spectrometry to the structural investigation of 9,19-cyclosterols and triterpenes" *Journal of the Chemical Society (B)* (1966), 1078-1079

Audier, H.E., Beugelmans, R. and Das, B.C. "Mass spectrometry of tetracyclic triterpenes: Part II. The lanostane group: the influence of the 9:19 cyclopropane ring" *Tetrahedron Letters* (1966), 36, 4341-4347

Baker, R. and Herbert, R.H. "Insect pheromones and related natural products" *Natural Products Report* 1 (1984), 299-318

Belman, S., Troll, W., Teebor, G. and Mukai, F. "The carcinogenic and mutagenic properties of N-hydroxyaminonaphthalenes" *Cancer Research* 28 (1968), 535-542

Bergstrom, G., Tengo, J., Reith, W. and Francke, W. "Multicomponent mandibular gland secretions in three species of Andrena bees (Hym., Apoidea)" *Zeischrift fur Naturforschung* 37c (1982), 1124-1129

Beroza, M. and Sarmiento, R. "Determination of the carbon skeleton and other structural features of organic compounds by gas chromatography" *Analytical Chemistry* 35 (1963), 1353-1357

Beroza, M. and Sarmiento, R. "Apparatus for reaction gas chromatography; instantaneous hydrogenation of unsaturated esters, alcohols, ethers, ketones and other compound types and determination of their separation factors" *Analytical Chemistry* 38 (1966), 1042-1047

Beynon, J.H. *Mass Spectrometry and its Applications to Organic Chemistry* Elsevier, Amsterdam, 1960

Beynon, J.H. and Cooks, R.G. "Ion kinetic energy spectrometry" *Research and Development* 22(11) (1971), 26-31

Beynon, J.H., Saunders, R.H. and Williams, A.E. *The Mass Spectra of Organic Molecules* Elsevier, Amsterdam, 1968

Blomquist, G.J., Howard, R.W., McDaniel, C.A., Remaley, S., Dwyer, L.A. and Nelson, D.R. "Application of methoxymercuration-demercuration followed by mass spectrometry as a convenient microanalytical technique for double-bond location in insect-derived alkenes" *Journal of Chemical Ecology* 6 (1980), 257-269

Boyd, R.K. and Beynon, J.H. "Scanning of sector mass spectrometers to observe the fragmentations of metastable ions" *Organic Mass Spectrometry* 12 (1977), 163-165

Budzikiewicz, H., Djerassi, C. and Williams, D.H. *Interpretation of Mass Spectra of Organic Compounds* Holden-Day Inc., San Francisco, 1964

Burlingame, A.L., Baillie, T.A. and Russell, D.H. "Mass spectrometry" *Analytical Chemistry* 64 (1992), 467R-502R

Burlingame, A.L., Millington, D.S., Norwood, D.L. and Russell, D.H. "Mass spectrometry" *Analytical Chemistry* 62 (1990), 268R-303R

Busch, K.L., Glish, G.L. and McLuckey, S.A. *Mass Spectrometry/Mass Spectrometry* VCH Publishers, New York, 1988

Cavill, G.W.K. and Ford, D.L. "The chemistry of ants" *Chemistry and Industry (London)* 1953, 351

Chapman, J.R. *Practical Organic Mass Spectrometry* John Wiley and Sons, New York, 1991

Chess, E.K. and Gross, M.L. "Determination of tetrachlorodibenzo-p-dioxins by mass spectrometric metastable decomposition monitoring" *Analytical Chemistry* 52 (1980), 2057-2061

Clark, B.C., Chamblee, T.S. and Iacobucci, G.A. "HPLC isolation of the sesquiterpene germacrene B from lime oil and its characterization as an important flavor impact constituent" *Journal of Agricultural and Food Chemistry*, 35 (1987), 514-518

Clarke, B.J. *Journal of the Institute of Brewing* 88 (1982), 296

Cooks, R.G. "Mixture analysis by mass spectrometry: MS/MS" *International Laboratory* January/February 1979, 79-94

Cramers, C.A., Scherpenzeel, G.J. and Leclerq, P.A. "Increased speed of analysis in directly coupled gas chromatography-mass spectrometry systems; capillary columns at sub-atmospheric outlet pressures" *Journal of Chromatography* 203 (1981), 207-216

Dandenau, R., Bente, P., Rooney, T. and Hiskes, R. "Flexible fused silica columns: an advance in high resolution chromatography" *American Laboratory* September 1979, 61-69

Dandenau, R. and Zerenner, E.H. "An investigation of glasses for capillary chromatography" *Journal of High Resolution Chromatography; Chromatography Communications* 2 (1979), 351-356

Davies, N.W. "Determination and optimization of flow rates in vacuum gas chromatography" *Analytical Chemistry* 56(13) (1984), 2618-2620

Davies, N.W. "Temperature programming and flow rates in capillary gas chromatography" *Analytical Chemistry* 56(13) (1984), 2600-2602

Davies, N.W. "Optimizing flow rates in capillary gas chromatography-mass spectrometry" *Journal of Chromatography* 325(1) (1985), 23-35

Davies, N.W. "Open split interfaces in capillary GC-MS: yield and quantitative aspects" *Journal of Chromatography* 450 (1988), 388-393

Davies, N.W. "Updating instrument control modes on a VG 7070F" N.W.Davies *Advances in Mass Spectrometry 11(A)*, edited by P.Longevialle, Heyden & Son Ltd., London, 1989, 178-179

Davies, N.W. "Gas chromatographic retention indices of monoterpenes and sesquiterpenes on methyl silicone and Carbowax 20M phases" *Journal of Chromatography* 503 (1990), 1-24

Davies, N.W. and Bignall, J.C. "Quantitative mixture analysis by linked sector selected metastable ion recording" presented at the Seventh Conference of the Australian and New Zealand Society for Mass Spectrometry, Sydney, 1981

Davies, N.W., Bignall, J.C. and Lincolne, R.W. "A rapid method for the generation of multiple constant

parent ion spectra" *Organic Mass Spectrometry* 17(9) (1982), 451

Davies, N.W., Bignall, J.C. and Roberts, M.S. "Direct quantitative determinations by multiple metastable peak monitoring 1. Warfarin in plasma" *Biomedical Mass Spectrometry* 10 (1983), 646-651

Davies, N.W., Lenk, W. and McLean, S. "Mass spectra of some N-arylacetylhydroxamic acids, acetamidophenols and their methyl derivatives" *Organic Mass Spectrometry* 17 (1982), 649-651

Davies, N.W. and Menary, R.C. "Essential oils of Tasmanian grown hops" *Journal of the Institute of Brewing* 88 (1982), 80-83

Davies, N.W. and Menary, R.C. "Tasmanian hop oils" *Journal of the Institute of Brewing* 89 (1983), 321

Davies, N.W. and Menary, R.C. "Volatile constituents of *Boronia megastigma* flowers" *Perfumer and Flavorist* 8(6) (1983), 3-8

Davies, N.W. and Madden, J.L. "Mandibular gland secretions of two parasitoid wasps (Hymenoptera: Ichneumonidae)" *Journal of Chemical Ecology* 11(8) (1985), 1115-1127

Davies, N.W., Miller, J.M., Naidu, R. and Sotheeswaran, S. "Triterpenoids in bud exudates of Fijian *Gardenia* Species (Rubiaceae)" *Phytochemistry* 31(1) (1992), 159-162

Davies, N.W., Veronese, M.E. and McLean, S. "Mass spectrometric determination of N-hydroxyphenacetin in urine using multiple metastable peak monitoring following thin layer chromatography" *Journal of Chromatography (Biomedical Applications)* 310 (1984), 179-187

Duffield, P.H., Birkett, D.J., Wade, D.N. and Duffield, A.M. "Quantitation of plasma warfarin levels by gas chromatography chemical ionization mass spectrometry" *Biomedical Mass Spectrometry* 6 (1979), 101-104

Durden, D.A. "Selected metastable ion monitoring using deuterium labelled internal standards: quantificaion of m- and p-hydroxymandelic acid in a single rat caudate nucleus" *29th Annual Conference on Mass Spectrometry and Allied Topics, Minneapolis, 1981 (American Society for Mass Spectrometry)* Abstracts, 127-128

Durden, D.A. "Selected metastable peak monitoring in mass spectrometry with stable-isotope-labelled internal standards and linked magnetic and electric sector fields" *Analytical Chemistry* 54 (1982), 666-670

Enzell, C.R., Appleton, R.A. and Wahlberg, I. "Terpenes and terpenoids" in *Biochemical Applications of Mass Spectrometry* edited by G.R. Waller, Wiley-Interscience, New York, 1972, 351-385

Ettre, L.S. "Viscosity of gases used as mobile phases in gas chromatography" *Chromatographia* 18 (1984), 243-248

Farnecombe, M.J., Mason, R.S., Jennings, K.R. and Scrivens, J. "Linked scanning and metastable ion mapping" *International Journal of Mass Spectometry and Ion Physics* 44 (1982), 91-107

Francke, W., Hindorf, G. and Reith, W. "Methyl-1,6-dioxaspiro[4.5]decanes as odors of *Paravespula vulgaris* (L.)" *Angewandte Chemie International Edition* 17 (1978), 862

Francke, W., Hindorf, G. and Reith, W. "Mass spectrometric fragmentation of alkyl-1,6-dioxaspiro[4.5]decanes" *Die Naturwissenschaften* 66 (1979), 619-620

Francke, W., Mackenroth, W., Schroder, W., Schulz, S., Tengo, J., Engels, E., Engels, W., Kittman, R. and Schneider, D. "Identification of cyclic enolethers from insects: alkyl dihydropyranes from bees and alkyl dihydro-4H-pyran-4-ones from a male moth" *Zeischrift fur Naturforschung* 40c (1985), 145-147

Francke, W., Reith, W. Bergstrom, G. and Tengo, J. "Spiroketals in the mandibular gland secretions of *Andrena* bees" *Die Naturwissenschaften* 67 (1980), 149-150

Gaskell, S.J, Finlay, E.M.H. and Millington, D.S. "The determination of testosterone in human blood plasma using multiple metastable peak monitoring" *Advances in Mass Spectrometry* 8(B) (1980), 1908-1910

Gaskell, S.J., Finlay, E.M.H. and Pike, A.W. "Analyses of steroids in saliva using highly selective mass spectrometric techniques" *Biomedical Mass Spectrometry* 7 (1980), 500-504

Gaskell, S.J., Finney, R.W. and Harper, M.E. "The determination of testosterone in hamster prostate by

gas chromatography mass spectrometry with selected metastable peak monitoring" *Biomedical Mass Spectrometry* 6 (1979), 113-116

Gaskell, S.J. and Millington, D.S. "Selected metastable peak monitoring: a new, specific technique in quantitative gas chromatography mass spectrometry" *Biomedical Mass Spectrometry* 5 (1978), 557

Gaskell, S.J. and Pike, A.W. "Qualitative and quantitative analyses of steroids by gas chromatography-mass spectrometry with selected metastable peak monitoring" *Advances in Mass Spectrometry* 8(A) (1980), 279-285

Giddings, J.C. *Dynamics of Chromatography. Part I. Principles and Theory* Marcel Dekker, New York, 1965

Gillette, J.R., Nelson, S.D., Mulder, G.J., Jollow, D.J., Mitchell, J.R., Pohl, L.R. and Hinson, J.A., "Formation of chemically reactive metabolites of phenacetin and acetaminophen" in *Biological Reactive Intermediates*, Volume II, edited by R.Snyder, D.V.Parke, J.J.Kocsis, D.J.Jollow, C.G.Gibson and C.M.Witmer, Plenum, New York, 1982, p. 931

Glish, G.L., Shaddock, V.M., Harmon, K. and Cooks, R.G. "Rapid analysis of complex mixtures by mass spectrometry/mass spectrometry" *Analytical Chemistry* 52 (1980), 165-167

Grob, K. (Jr.) and Grob, K. "Evaluation of capillary columns by separation number or plate number" *Journal of Chromatography* 207 (1981), 291-297

Guiochon, G. "Flow of gases in porous media: problems raised by the operation of gas chromatography columns" *Chromatographic Reviews* 8 (1966), 1-47

Harvey, D.J., Leuschner, J.T.A. and Paton, W.D.M. "Measurement of Δ1-tetrahydrocannabinol in plasma to the low picogram range by gas chromatography-mass spectrometry using metastable ion detection" *Journal of Chromatography* 202 (1980), 83-92

Hatch, F.W. and Parrish, M.E. "Vacuum gas chromatography using short glass capillary columns combined with mass spectrometry" *Analytical Chemistry* 50 (1978), 1164-1168

Heller, S.R. and Milne, G.W.A., editors, *EPA/NIH Mass Spectral Database*, U.S. Department of Commerce, 1978, 1980, 1982

Henneberg, D., Henrichs, U. and Schomburg, G. "Open split connection of glass capillary columns to mass spectrometers" *Chromatographia* 8 (1975), 449-451

Henyon, J., Maylin, G.A. and Thomson, B.A. "Determination of drugs in biological samples by thin-layer chromgatography tandem mass spectrometry" *Journal of Chromatography* 271 (1983), 107-124

Hermann, B.W., Freed, L.M., Thompson, M.Q., Phillips, R.J., Klein, K.J. and Snyder, W.D. "CGC using a programmable electronic pressure controller" *Journal of High Resolution Chromatography* 13 (1990), 361-366

Hirose, Y. "Mass spectra of sesquiterpenes" *Shitsuryo Bunseki* 15(1967), 162-175

Holland, L., Steckelmacher, W., and Yarwood, J. *Vacuum Manual*, E. and F.N. Spon, London, 1974

James, A.T. and Martin, A.J.P. "Gas liquid partition chromatography: a technique for the analysis of volatile materials" *The Analyst* 77 (1952), 915-932

Jennings, K.R. "Consecutive metastable transitions in a double-focussing mass spectrometer" *Chemical Communications* 1966, 283-284

Jennings, W.G. and Adam, S. "Gas chromatography: elution temperature, speed of analysis, and separation efficiency as influenced by rate of temperature programming and carrier gas velocity in open tubular glass capillary columns" *Analytical Biochemistry* 69 (1975), 61-69

Jennings, W.G. and Shibamoto, T. *Qualitative Analysis of Flavor and Fragrance Volatiles by Glass Capillary Column Gas Chromatography*, Academic Press, London, 1980

Jones, L.A., Kirby, S.L., Garganta, C.L., Gerig, T.M. and Mulik, J.D. "Optimization of separation number in gas chromatography with fused silica capillary columns under temperature programmed conditions" *Analytical Chemistry* 55 (1983), 1354-1360

Jones, L.A., Burton, C.D., Dean, T.A., Gerig, T.M. and Cook, J.R. "Effects of starting temperatures and temperature/pressure programming in optimization of gas chromatographic separation numbers" *Analytical Chemistry* 59 (1987), 1179-1186

Junk, G.A. "Gas chromatograph-mass spectrometer combinations and their applications" *International*

Journal of Mass Spectrometry and Ion Physics 8 (1972), 1-71

Kaiser, R. "New developments in gas chromatography from the 1961 literature" *Zeitschrift für Analytische Chemie* 189 (1961), 1-14

Karasek, F.W. and Clement, R.E. *Basic Gas Chromatography-Mass Spectrometry. Priciples and Techniques* Elsevier, New York, 1988

Kennett, B.H., Murray, K.E., Whitfield, F.B., Stanley, G., Bannister, P.A. and Shaw, K. *Mass Spectra of Organic Compounds*, Volume 6, CSIRO Division of Food Research, North Ryde, Sydney, 1977

Kennett, B.H., Murray, K.E., Whitfield, F.B., Stanley, G., Shipton, J. and Bannister, P.A. *Mass Spectra of Organic Compounds*, Volumes 1-5, CSIRO Division of Food Research, North Ryde, Sydney, 1977

Kennett, B.H., Whitfield, F.B. and Bannister, P.A. *Mass Spectra of Organic Compounds*, Volumes 9-10, CSIRO Division of Food Research, North Ryde, Sydney, 1982

Kennett, B.H., Whitfield, F.B., Shaw, K., Bannister, P.A. and Sugowdz, G. *Mass Spectra of Organic Compounds*, Volumes 7-8, CSIRO Division of Food Research, North Ryde, Sydney, 1980

Kiser, R.W., Sullivan, R.E. and Lupin, M.S. "Mass spectral metastable transitions determined by electric sector variation" *Analytical Chemistry* 41 (1969), 1958-1965

Klutch, A. and Bordun, M. "Chromatographic methods for the analysis of the metabolites of acetophenetidin (phenacetin)" *Journal of Pharmaceutical Science* 57 (1968), 524-527

Kondrat, R.W. and Cooks, R.G. "Direct analysis of mixtures by mass spectrometry" *Analytical Chemistry* 50 (1978) 81A-92A

Kondrat, R.W., McLuskey, G.A. and Cooks, R.G. "Multiple reaction monitoring in mass spectrometry/mass spectrometry for direct analysis of complex mixtures" *Analytical Chemistry* 50 (1978), 2107-2021

Kováts, E. sz. "Gas chromatographic characterization of organic compounds (I). Retention indexes of aliphatic halides, alcohols, aldehydes and ketones" *Helvetica Chimica Acta* 41 (1958), 1915-1932

Lacey, M.J. and McDonald, C.G. "A three-dimensional representation of metastable peaks from double focusing mass spectrometers" *Organic Mass Spectrometry* 12 (1977), 587-593

Lacey, M.J. and McDonald, C.G. "Three-dimensional representation of metastable peaks at high mass resolution" *Organic Mass Spectrometry* 13 (1978), 243-247

Lacey, M.J. and McDonald, C.G. "Constant neutral spectrum in mass spectrometry" *Analytical Chemistry* 51 (1979), 691-695

Lacey, M.J. and McDonald, C.G. "Interpreting metastable peaks from double focusiing mass spectrometers" *Organic Mass Spectrometry* 15 (1980), 484-485

Lassak, E.V. and Southwell, I.A. "Essential oil isolates from the Australian flora" *International Flavors and Food Additives* 1977, 126-132

Le Quere, J.-L. and Latrasse, A. "Composition of the essential oil of blackcurrant buds (*Ribes nigrum* L.) *Journal of Agricultural and Food Chemistry* 38 (1990), 3-10

Lias, S.G. and Stein, S.E. editors, *NIST/EPA/MSDC Mass Spectral Database, PC Version 3.0* U.S. Department of Commerce, 1990

Lias, S.G. and Stein, S.E. editors, *NIST/EPA/MSDC Mass Spectral Database, PC Version 4.0* U.S. Department of Commerce, 1992

Lipsky, S.R., McMurray, W.J., Hernandez, M., Purcell, J.E. and Billeb, K.A. "Fused silica glass capillary columns for gas chromatographic analyses" *Journal of Chromatographic Science* 18 (1980), 1-9

Macdonald, C.G. and Lacey, M.J. "Graphical aids and scanning modes for tandem mass spectrometry" *Organic Mass Spectrometry* 19 (1984), 55-62

Maier, J. "Chemical determination of hop varieties" (in German) *Hopfen-Rundschau*, 29 (1978), 258-263

Macklin, A.W. and Welch, R.M. "Phenacetin safety" *Science* 207 (1980), 129-131

McFadden, W.H. *Techniques of Combined Gas Chromatography/Mass Spectrometry* John Wiley and Sons, New York, 1973

McFadden, W.H. "Interfacing chromatography and mass spectrometry" *Journal of Chromatographic Science* 17 (1979), 2-16

McFadden, W.H., Teranishi, R., Black, D.R. and Day, J.C. "Use of capillary gas chromatography with a time-of-flight mass spectrometer" *Journal of Food Science* 28 (1963), 316-319

McLafferty, F.W. in *Determination of Organic Structures by Physical Methods* Vol. 2 edited by F.C. Nachod and W.D. Phillips, Academic Press, New York, 1962

McLafferty, F.W. *Interpretation of Mass Spectra* 3rd edition, University Science Books, Mill Valley, California, 1980

McLafferty, F.W. "Tandem mass spectrometry (MS/MS): a promising new analytical technique for specific component determination in complex mixtures" *Accounts of Chemical Research* 13 (1980), 33-39

McLafferty, F.W. "Tandem mass spectrometry in trace toxicant analysis" *Biomedical Mass Spectrometry* 8 (1981), 446-448

McLafferty, F.W. and Bockhoff, F.M. "Separation/identification system for complex mixtures using masss separation and mass spectral characterization" *Analytical Chemistry* 50 (1978), 69-76

McLafferty, F.W. and Turecek, F. *Interpretation of Mass Spectra* University Science Books, Mill Valley, California, 1993

McLean, S., Davies, N.W., Watson, H., Favretto, W.A. and Bignall, J.C. "N-hydroxyphenacetin - a new urinary metabolite of phenacetin in the rat" *Drug Metabolism and Disposition* 9 (1981), 255-260

McLean, S., Parsons, R.S., Chesterman, R.B., Dineen, R., Johnson, M.G. and Davies, N.W. "Drugs, alcohol and road accidents in Tasmania" *Medical Journal of Australia* 147 (1987), 6-11

McLuskey, G.A., Cooks, R.G. and Knevel, A.M. "Direct analysis of mushroom constituents by mass spectrometry" *Tetrahedron Letters* 46 (1978), 4471-4474

Mass Spectrometry Data Centre *Eight Peak Index of Mass Spectra*, Royal Society of Chemistry, Nottingham, 1983

Millington, D.S. and Smith, J.A. "Fragmentation patterns by fast linked electric and magnetic field scanning" *Organic Mass Spectrometry* 12 (1977), 264-265

Moshonas, M.G. and Lund, E.D. "The mass spectra of sesquiterpene hydrocarbons" *Flavour Industry* 1 (1970), 375-378

Neill, G.P., Davies, N.W. and McLean, S. "Automated screening procedure using gas chromatography-mass spectrometry for identification of drugs after their extraction from biological samples" *Journal of Chromatography (Biomedical Applications)* 565 (1991), 207-224

Panichanun, S. and Bick, I.R.C. "*Athrotaxis* alkaloids. Part II. Alkaloids of *A.Selaginoides* and *A. laxifolia*" *Tetrahedron* 40 (1984), 2685-2689

Penfold, A.R. "Preliminary note on the chemistry of concrete Otto of *Boronia megastigma* (Nees)" *Journal of the Royal Society of Western Australia* 14 (1927), 1-5

Ramaswami, S.K., Briscese, P., Gargiullo, R.J. and von Geldern, T. "Sesquiterpene hydrocarbons: from mass confusion to orderly line-up" in *Flavors and Fragrances: a World Perspective.* edited by B.M.Lawrence, B.D.Mookherjee and B.J.Willis, Proceedings of the 10th International Congress of Essential Oils, Washington, D.C., USA, 1986

Rose, K. "Simple and effective direct coupling for gas chromatography-mass spectrometry on the MS 50 mass spectrometer" *Journal of Chromatography* 259 (1983), 445-452

Schreier, P., Drawart, F. and Hunker, A. "Identification of volatile constituents from grapes" *Journal of Agricultural and Food Chemistry* 24 (1976), 331-336

Sellier, N. and Guiochon, G. "Influence of GC-MS coupling on the performances of a chromatographic system" *Journal of Chromatographic Science* 8 (1970), 147-150

Settlage, J. and Jaeger, H. "Advantages of fused silica capillary gas chromatographyfor GC/MS applications" *Journal of Chromatographic Science* 22 (1984), 192-197

Silverstein, R.M. "Chemical communication in insects: background and application" *Pure and Applied Chemistry* 54 (1982), 2473-2488

Southwell, I.A. "The constituents of *Rubus rosifolius*. the structure of rosifoliol, a biogenetically significant sesquiterpenoid" *Australian Journal of Chemistry* 31 (1978), 2527-2538

Southwell, I.A. "Essential oil isolates from the Australian flora. Part 2" *Flavor and Fragrance Journal* 2 (1987), 21-27

Stanley, G. and Kennet, B.H. "Reaction gas chromatography of microgram and sub-microgram samples using sealed glass capillaries" *Journal of Chromatography* 75 (1973), 304-307

Stenhagen, E., Abrahamsson, S, and McLafferty, F.W., editors. *Registry of Mass Spectral Data*, John Wiley and Sons, New York, 1974

Swigar, A.A. and Silverstein, R.M. *Monoterpenes - Infrared, Mass, ^{1}HNMR and ^{13}CNMR Spectra and Kováts' Indices*, Aldrich Chemical Co., Milwaukee, Wisconsin, 1981

Takaoka, D. and Hiroi, M. "Two acyclic monoterpene diols from *Cinnamomum camphora*" *Phytochemistry* 15 (1976), 330

Talapatra, B., Basak, A. and Talapatra, S.K. "Terpenoids & related compounds: Part XXII - schizandraflorin, a new tetracyclic triterpene dione from *Schizandra grandiflora* Hook. f. & Thom." *Indian Journal of Chemistry* 21B (1982), 76-78

ten Noever de Brauw, M.C., Bouwman, J., Tas, A.C. and La Vos, G.F. *Compilation of Mass Spectra of Volatile Compounds in Food*, Central Institute for Nutrition and Food Research, TNO, Zeist, The Netherlands, 1979, 1982, 1986.

Teranishi, R., Corse, J.W., McFadden, W.H., Black, D.E. and Morgan, A.I., Jr. "Volatiles from strawberries. 1. Mass spectral identifications of the more volatile components" *Journal of Food Science* 28 (1963) 478-483

Thorne, G.C. and Gaskell, S.J. "Dual metastable peak monitoring: application to the analysis of oestradiol-17β as the bis (*tert*-butyldimethylsilyl) ether" *Biomedical Mass Spectrometry* 12 (1985), 19-24

Tomer, K.B., Hemmerum, S. and Djerassi, C. "The structure of the high energy (M-ketene)$^{+\cdot}$ ions from acetanilide" *Tetrahedron Letters* (1973), 915-917

Trager, W.F., Lewis, R.J. and Garland, W.A. "Mass spectral analysis in the identification of human metabolites of warfarin" *Journal of Medicinal Chemistry* 13 (1970), 1196-1204

Tumlinson, J.H. "Insect pheromone systems" *Comments in Agricultural and Food Chemistry* 1 (1988), 115-146

Veronese, M.E. *Inter-Individual Differences in Drug Metabolism and Response* Ph.D. thesis, University of Tasmania, 1988

Veronese, M.E., McLean, S., D'Souza, C.A. and Davies, N.W. "Formation of reactive metabolites of phenacetin in humans and rats" *Xenobiotica* 15 (1985), 929-940

Vine, J. and Watson, T.R. "Incidence of drug and alcohol intake in road traffic accident victims" *Medical Journal of Australia* (1983), 1, 612-625

Waller, G.R. (editor) *Biochemical Applications of Mass Spectrometry* John Wiley and Sons, New York, 1972

Weast, R.C., (editor) *CRC Handbook of Chemistry and Physics*, CRC Press, Boca Raton, Florida, 65th edition, 1984

Weisburger, J.H. and Weisburger, E.K. "Biochemical formation and pharmacological, toxicological, and pathological properties of hydroxylamines and hydroxamic acids" *Pharmacological Reviews* 25 (1973), 1-66

Wetzel, E. and Kuster, T. "Construction of a gas chromatography-mass spectrometry interface using a fused silica transfer line" *Journal of Chromatography* 268 (1983), 177-185

Williams, P.J., Strauss, C.R. and Wilson, B. "New linalool derivatives in Muscat of Alexandria grapes and wines" *Phytochemistry* 19 (1980), 1137-1139

Wylie, P.L., Philips, R.J., Klein, K.J., Thompson, M.Q. and Hermann, B.W. "Improving splitless injection with electronic pressure programming" *Journal of High Resolution Chromatography* 14 (1991), 649-655

Wyllie, S.G. and Djerassi, C. "Mass spectrometry in structural and stereochemical problems. CXLVI. Mass spectrometric fragmentations typical of sterols with unsaturated side chains" *Journal of Organic Chemistry* 33 (1968), 305-313

Youssefi, M., Cooks, R.G. and McLaughlin, J.L. "Mapping of cocaine and cinnamoylcocaine in whole coca plant tissues by MIKES" *Journal of the American Chemical Society* 101 (12) (1979), 3400-3402

Zackett, D., Schoen, A.E., Kondrat, R.W. and Cooks, R.G. "Selected fragment scans of mass spectrometers in direct mixture analysis" *Journal of the American Chemical Society* 101 (1979), 6781-6783

APPENDIX A

ADDITIONAL PUBLICATIONS INVOLVING APPLICATIONS OF MASS SPECTROMETRY

"Variation in leaf oil of *Eucalyptus nitens* and *E.denticulata*" Haifeng Li, J.L.Madden, and N.W.Davies *Biochemical Systematics and Ecology* submitted for publication

"Identification and quantification of endogenous gibberellins in apical buds and the cambial zone of *Eucalyptus*" O.Hassan, B.G.Ridoutt, J.J.Ross, N.W.Davies and J.B.Reid *Physiologia Plantarum*, in press

"The metabolic fate of dietary terpenes from *Eucalyptus radiata* in the Common Ringtail possum (*Pseudocheirus peregrinus*)." S.McLean, W.K.Foley, N.W.Davies, S.Brandon, Li Duo and A.J.Blackman *Journal of Chemical Ecology* 19 (1993), 1625-1643

"An enantiospecific GC-MS procedure for the determination of ketoprofen and ibuprofen in synovial fluid and plasma; application to protein binding studies" D.S.Jack, R.H.Rumble, N.W.Davies and H.W.Francis *Journal of Chromatography (Biomedical Applications)* 584 (1992), 189-197

"Volatile and odorous compounds from the bryozoan *Biflustra perfragilis*" A.J.Blackman, N.W.Davies and C.E.Ralph *Biochemical Systematics and Ecology* 20(4) (1992), 339-342

"Hepatotoxic constituents in the rumen of *Brachiaria decumbens* intoxicated sheep" A.S.Abdullah, N.Lajis, J.B.Bremner, N.W.Davies, W.Mustapha and M.A.Rajon *Journal of Vetinerary and Human Toxicology*, 34(2) (1992), 154-155

"Internode length in *Lathyrus odoratus*. Effects of mutants *l* and *lb* on gibberellin metabolism and levels" J.J.Ross, N.W.Davies, J.B.Reid and I.C.Murfett *Physiologia Plantarum* 79 (1990), 453-458

"Internode length in *Lathyrus odoratus*. The involvement of gibberellins" J.J.Ross, J.B.Reid, N.W.Davies and I.C.Murfett *Physiologia Plantarum* 79 (1990), 448-452

"Distribution and metabolism of 1,2,4-trimethylbenzene in the rat" J.-Z.Huo, S.Aldous, K.Campbell and N.W.Davies *Xenobiotica* 19 (1989), 161-170

"Gas chromatographic quality control for oil of *Melaleuca alternifolia*, terpinene-4-ol type (Australian Tea Tree)" J.J.Brophy, N.W.Davies, I.A.Southwell, I.A.Stiff and L.Williams *Journal of Agricultural and Food Chemistry* 37 (1989), 1330-1335

"Drugs, alcohol and road accidents in Tasmania" S.McLean, R.S.Parsons, R.B.Chesterman, R.Dineen, M.G.Johnson and N.W.Davies *Medical Journal of Australia* 147 (1987), 6-11

"Formation of reactive metabolites of phenacetin in humans and rats" M.Veronese, S.McLean, C.A.D'Souza and N.W.Davies *Xenobiotica* 15 (1985), 929-940

"Hydrocarbon constituents of three Australian Dolichoderine ant species" J.J.Brophy, G.W.K.Cavill, N.W.Davies, T.D.Gilbert, R.P.Philp and W.Plant *Insect Biochemistry* 13(4) (1983), 381-389

"The analysis of nitrate esters by combined gas chromatography and electron capture negative ion mass spectrometry" J.C.Bignall, N.W.Davies, M.Power, M.S.Roberts, P.A.Cossum and G.W.Boyd, in, *Recent Developments in Mass Spectrometry in Biochemistry, Medicine and Environmental Research,* 7 Elsevier Scientific Publishing Co., Amsterdam (1981) 111-122

"N-hydroxyphenacetin - a new urinary metabolite of phenacetin in the rat" S.McLean, N.W.Davies, H.Watson, W.A.Favretto and J.C.Bignall *Drug Metabolism and Disposition* 9 (1981), 255-260

"Characterization of aggregation factors and associated compounds from the Argentine ant" G.W.K.Cavill, N.W.Davies and F.J.McDonald *Journal of Chemical Ecology* 6(2) (1980), 371-384

"An Argentine ant aggregation factor" G.W.K.Cavill, P.L.Robertson and N.W.Davies *Experientia* 35 (1979), 889-890

"Iridodials and nepetalactone in the defensive secretion of the coconut stick insect, *Graeffea crouani*" R.M.Smith, G.W.K.Cavill, J.J.Brophy and N.W.Davies *Journal of Chemical Ecology* 5(5) (1979), 727-735

APPENDIX B

PRINCIPAL PUBLICATIONS

Determination and Optimization of Flow Rates in Vacuum Capillary Gas Chromatography

Noel W. Davies

Central Science Laboratory, University of Tasmania, G.P.O. Box 252C, Hobart, Tasmania, Australia 7001

The direct insertion of capillary gas chromatography columns into mass spectrometer ion sources is a common method of coupling these instruments (*1–6*). This results in the pressure at the column outlet being effectively zero and the advantages of this such as increased speed of analysis over atmospheric outlet operation, total transfer of effluent to the ion source, and the relative ease of transfer of labile compounds have been well publicized. Cramers et al. (*7*) presented a detailed analysis of the various factors involved, including the gain in speed of analysis over atmospheric outlet for a given system and the potential loss in efficiency with vacuum outlet pressure.

In any capillary gas chromatographic analysis, the flow rate of carrier gas is a critical parameter for optimized performance. Average linear velocity ($\bar{v}$) is often the form in which this is expressed and relates to a particular carrier gas diameter, and outlet pressure. An increased average velocity will be required for optimum performance if outlet pressure is lowered (*6, 7*). However, the optimum volume flow rate, reduced to atmospheric pressure, remains independent of outlet pressure (*7*). Optimum average carrier gas velocity at atmospheric outlet pressure ($\bar{v}_{opt,atm}$) can be found from literature values, while in many situations the corresponding volume flow rate is also known. To obtain the optimum performance with vacuum outlet, $\bar{v}_{opt,atm}$ must be adjusted to the correct value for vacuum outlet ($\bar{v}_{opt,vac}$) or the volume flow must be measured. It is generally impracticable to measure flow in directly coupled gas chromatography/mass spectrometry, since the outlet of the source pump is the only available point for measurement, after isolation of all other pumps to ensure passage of total effluent. The erratic liberation of gas makes accurate measurement difficult, particularly for very low flow rates.

The discussion below shows how flow rate can be simply measured from readily accessible parameters, the air peak retention time ($t_{a,vac}$), the length of the column (L), and the carrier gas viscosity (η), without requiring column diameter or inlet pressure terms. Conversely, the air peak retention time required to give a particular flow rate can be predicted.

Alternatively, $\bar{v}_{opt,vac}$ and hence $t_{a,opt,vac}$, the optimum air peak time with zero outlet pressure, can be calculated from $\bar{v}_{opt,atm}$ after calculation or accurate measurement of the inlet pressure required for the latter.

Calculation of Flow Rates. Poiseuille's equation for viscous flow in long cylindrical columns can be written (*7*)

0003-2700/84/0356-2618$01.50/0

$$\bar{v} = \frac{3r^2P_o(P^2 - 1)^2}{32\eta L(P^3 - 1)} \quad (1)$$

where r is the column radius, P_0 is the outlet pressure, and $P = (P_i/P_o)$where P_i is inlet pressure. Since $\bar{v} = L/t_a$, where t_a is air peak retention time, rearrangement gives

$$t_a = \frac{32\eta L^2(P^3 - 1)}{3r^2P_o(P^2 - 1)^2}$$

$$= \frac{32\eta L^2\left(\frac{P_i^3 - P_o^3}{P_o^3}\right)}{3\left(\frac{d}{2}\right)^2 P_o\left(\frac{P_i^2 - P_o^2}{P_o^2}\right)^2}$$

$$= \frac{128\eta L^2(P_i^3 - P_o^3)}{3d^2(P_i^2 - P_o^2)^2} \quad (2)$$

where d is column diameter.

Now the flow rate as measured at the column outlet (Q), which unlike average flow rate (as defined by the ratio of the volume of the column to the air peak time t_a) incorporates a pressure term, can be determined from the product of the pressure drop across the column and the conductance (C_t) of the column (8).

$$C_t = \frac{\pi d^4(P_i + P_o)}{256\eta L}$$

$$Q = \frac{\pi d^4(P_i^2 - P_o^2)}{256\eta L} \quad (3)$$

$$P_i = \left(\frac{256\eta LQ}{\pi d^4} + P_o^2\right)^{1/2} \quad (4)$$

Substituting eq 4 in eq 2, for vacuum outlet pressure (P_o = 0), the time for the air peak ($t_{a,vac}$) can be found.

$$t_{a,vac} = \frac{128\eta L^2}{3d^2}\left(\frac{\pi d^4}{256\eta LQ}\right)^{1/2}$$

$$= \frac{8}{3}\left(\frac{\pi\eta L^3}{Q}\right)^{1/2} \quad (5)$$

Thus $t_{a,vac}$ can be predicted from a knowledge of Q, η, and L, is independent of d, and requires no knowledge of inlet pressure. Equation 5 also follows from Sellier and Guiochon (3) who found

$$t_{a,vac} = \frac{4\eta L^2}{3kP_i} \quad (6)$$

where k is the "column permeability" defined as $r^2/8$. When eq 4 is substituted in eq 6, eq 5 results.

Rearrangement of eq 5 gives the expression enabling direct calculation of flow rate

$$Q = \frac{64\pi\eta L^3}{9t_{a,vac}^2} \quad (7)$$

For a given gas at a fixed temperature this can be expressed as

$$Q = k\frac{L^3}{t_{a,vac}^2} \text{ mL atm min}^{-1} \quad (8)$$

where k is a constant. If L is in meters and $t_{a,vac}$ in seconds, some values for k allowing direct expression of the results in mL atm min^{-1} are as follows: helium, 20 °C, k = 0.2568; helium, 100 °C, k = 0.3017; hydrogen, 20 °C, k = 0.1156; hydrogen, 100 °C, k = 0.1360; nitrogen, 20 °C, k = 0.2311; nitrogen, 100 °C, k = 0.2752.

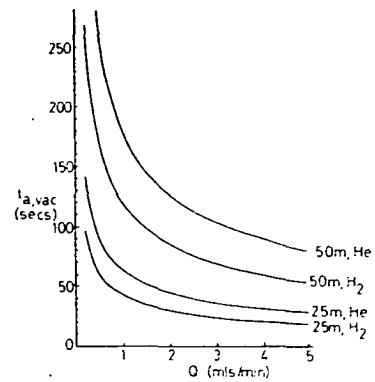

Figure 1. Plot of the air peak time required at vacuum outlet pressure ($t_{a,vac}$) to produce a given flow rate (Q), as would be measured at the column outlet at atmospheric pressure (i.e., milliliters at atmospheric pressure per minute), for 25-m and 50-m columns with hydrogen and helium at 20 °C. Column diameter has no bearing on this relationship.

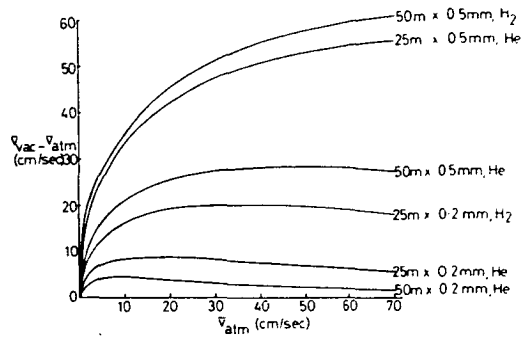

Figure 2. Plot of the additional average carrier gas velocity required at vacuum outlet pressure ($\bar{v}_{vac} - \bar{v}_{atm}$) to maintain the same flow rate, in atmospheric milliliters per minute, as a given average velocity at atmospheric outlet pressure ($\bar{v}_{atm}$). The results are for the column lengths, diameters, and carrier gases indicated at 20 °C.

Prediction of $t_{a,opt,vac}$ from $\bar{v}_{opt,atm}$. If the required flow is not known, but $\bar{v}_{opt,atm}$ for a similar diameter is known, from eq 2

$$\frac{128\eta_1 L_1\bar{v}_{opt,atm}}{3d^2} = \frac{(P_{i,opt,atm}^2 - P_{atm}^2)^2}{P_{i,opt,atm}^3 - P_{atm}^3} \quad (9)$$

where η_1 and L_1 are the viscosity of the gas and length of the column for which $\bar{v}_{opt,atm}$ is known, $P_{i,opt,atm}$ is the inlet pressure employed, and P_{atm} is atmospheric pressure.

From this, $P_{i,opt,atm}$ can be found by iteration, as the zero of the function of the form $x^4 - ax^3 - bx^2 + c = 0$.

From Cramers et al. (7), if $P_{i,opt,atm}$ for a given column is known

$$t_{a,opt,vac} = \frac{L_1}{\bar{v}_{opt,atm}}\frac{(P_{i,opt,atm}^2 - P_{atm}^2)^{3/2}}{(P_{i,opt,atm}^3 - P_{atm}^3)} \quad (10)$$

To transfer to a more general situation with a column with length L_2 at a different temperature ($\eta = \eta_2$), substituting eq 3 in eq 5 gives

$$t_{a,opt,vac} = \frac{128}{3d^2}\left(\frac{\eta_2 L_2^3 L_1\eta_1}{(P_{i,opt,atm}^2 - P_{atm}^2)}\right) \quad (11)$$

Figure 1 shows the relationship between flow rate and $t_{a,vac}$ for 25-m and 50-m columns with both hydrogen and helium, enabling ready estimation of one parameter from the other for these typical columns. Figure 2 illustrates the effect of column diameter, length, and carrier gas on the additional average velocity necessary to maintain the same flow rate at vacuum outlet pressure as that produced by a particular average velocity at atmospheric outlet ($\bar{v}_{atm}$). $t_{a,opt,vac}$ for each situation can thus be found readily from knowledge of $\bar{v}_{opt,atm}$. Taking the case of a 25 m × 0.5 mm column using helium, if $\bar{v}_{opt,atm}$ = 30 cm/s, the additional velocity required is 47 cm/s for a total of 77 cm/s. Hence $t_{a,opt,vac}$ = (25/0.77) = 32 s.

LITERATURE CITED

(1) Leferink, J. G.; Leclercq, P. A. *J. Chromatogr.* **1974**, *91*, 385–391.
(2) Vangaever, F.; Sandra, P.; Verzele, M. *Chromatographia* **1979**, *12*, 153–154.
(3) Sellier, N.; Guiochon, G. *J. Chromatogr. Sci.* **1970**, *8*, 147–150.
(4) Varadi, P. F.; Ettre, K. *Anal. Chem.* **1963**, *35*, 410–412.
(5) Giddings, J. C. *Anal. Chem.* **1962**, *34*, 314–319.
(6) Hatch, F. W.; Parrish, M. E. *Anal. Chem.* **1978**, *50*, 1164–1168.
(7) Cramers, C. A.; Scherpenzeel, G. J.; Leclercq, P. A. *J. Chromatogr.* **1981**, *203*, 207–216.
(8) Holland, L.; Steckelmacher, W.; Yarwood, J. "Vacuum Manual", E. & F. N. Spon: London, 1974; p 26.

RECEIVED for review April 4, 1984. Accepted June 18, 1984.

Reprinted from Analytical Chemistry, 1984, 56, 2600.

Temperature Programming and Flow Rates in Capillary Gas Chromatography

Sir: In a recent article in this journal, Jones et al. (*1*) discussed the combined effect of temperature program rate and carrier gas flow rate on the efficiency of capillary gas chromatographic separations. They employed a mathematical approach to infer optimum combination of flow rate and program rate values from a series of collected data from different compound classes at different temperature program and flow rates. There are several aspects of this article that require some comment.

In the first instance, the overall impression created by the article is that within each temperature-programmed run the carrier gas flow rate was held constant, due to the repeated

0003-2700/84/0356-2600$01.50/0

reference to a "flow rate", quoted to three decimal places, being used with a particular program rate. In their aim to find the best combination of the two for a particular column for a range of compound classes, there is no reference to the fact that the flow rate was itself dependent on temperature and subject to the normal variation associated with isobaric pressure-controlled columns. That this was so can be ascertained from the instrument described, a Hewlett-Packard 5880A, which has a flow controller situated upstream of the inlet splitter, while the column flow is controlled by a back-pressure regulator. While some hint of this may be gained from the reference in the Experimental Section to the value of "column-head pressures", if the authors were aware that flow rate was constantly falling with increased temperature, and falling more rapidly with faster program rates, it seems an oversight not to have included the effect of this in their mathematical treatment and discussion.

Assuming the quoted flow rates were measured at the initial temperature of 50 °C (viscosity of helium, 2.07×10^{-5} N s m^{-2}), from Poiseuille's law the flow rate at the final temperature of 250 °C (viscosity of helium, 2.85×10^{-5} N s m^{-2}) would be reduced, from the ratio of the viscosities, to some 72% of the initial value. Chromatographers generally do not find that this causes any practical difficulty in obtaining good resolution, since a range of the flow rates can be tolerated with only a small loss in efficiency, particularly on the high side of optimum. However, not only will there be an elution temperature for a given compound, increasing with increased program rate, but also an "elution flow rate", decreasing correspondingly with increased program rate. For the expression $TZ = a(\overline{CH} + b)$, where TZ is the separation number and $\overline{CH}$ the average carbon number of a pair of homologues (*1*), the actual data obtained from the regression equations for the series of homologues can still be plotted in three dimensions (TZ vs. program rate and flow rate), provided the flow rate axis is clearly marked as "initial flow rate". However, when a generalized relationship aimed at optimizing TZ in terms of both parameters is derived, account must be taken of the dependency of flow rate on temperature. There can be no theoretical combination of program rate and initial flow rate that will be an optimum for all compounds, since compounds eluting at higher temperatures will experience overall lower flow rates than those eluting at lower temperatures. Thus, an idealized flow rate/program rate combination that produces optimum performance under constant flow conditions for a specified compound will not necessarily be the same (based on initial flow rate) as when the column has isobaric pressure control and is subject to a gradual reduction in flow rate. These differences may or may not be significant, depending on the elution temperatures of the test compounds. The range of compounds used by Jones et al. may not show this effect to a significant degree, since flow rates may not have altered greatly during the analysis. From Table I in their article, elution temperatures of 118 and 172 °C for the C12 and C16 alkanes, respectively, are found (initial flow rate, 0.812 mL/min; program rate, 10 °C/min). These correspond to elution flow rates of 0.69 and 0.65 mL/min, respectively, a drop of some 8%, while the potential reduction between initial and final temperatures is 28%. The reduction in elution flow rates in the other compound classes is 12–14%. The gradual increase in peak widths at half height observed with increasing carbon number in this work may be due in part to the reduction in flow rate, in addition to any effect directly related to temperature.

A second important point is raised by the method of determining flow rates. Although not stated in the article, these were measured by dividing the volume of the column by the time taken for an unretarded component to elute (*2*), producing the "average flow rate". While there is argument in favor of this method, or of quoting average linear velocity, when column efficiency calculations are used (*3*, *4*), the method employed should be clearly stated. To many chromatographers "flow rate", when not further defined, means the flow rate at the column outlet that can be measured with a soap-bubble flow meter or similar device. Since the pressure in this context is constant, and usually atmospheric pressure, column outlet flow rate incorporates a pressure term, as flow rate also does in a strict physical sense. The units for average flow rate and column outlet flow rate are often both quoted as "mL/min", which strictly only applies to the former. Column outlet flow rate can be set experimentally to the appropriate value when installing a capillary column, while average flow rate cannot be used directly in this sense. Grob et al. (*5*), in their article on standardized quality tests for capillary columns, and on TZ numbers in particular, make no reference to flow rates as such but report the retention time of an unretarded component, enabling calculation of average velocity, average flow rate, or column outlet flow rate as required. Average flow rate is defined as

$$Q_{av} = (AL)/t \tag{1}$$

where A is the cross-sectional area of the column, L is the length, and t is the retention time of an unretarded component. To obtain the flow rate at the column outlet at atmospheric pressure (Q_{end}), rearranging from Zlatkis et al. (*3*)

$$Q_{end} = Q_{av}\frac{2(P_i^3 - 1)}{3(P_i^2 - 1)} \tag{2}$$

where P_i is the inlet pressure in atmospheres.

Thus, for the column quoted (12 m × 0.25 mm), the appropriate conversion can be made if P_i is known. The "column-head pressures" quoted (*1*) of 60, 70, and 80 kPa above atmospheric pressure, respectively, are in fact upstream of a trap and therefore are considerably higher than the actual column inlet pressure. P_i can be calculated from a rearrangement of Poiseuille's equation

$$\frac{(P_i^3 - P_o^3)}{(P_i^2 - P_o^2)^2} = \frac{3r^2}{32\eta L\bar{v}} \tag{3}$$

where P_o is the column outlet pressure, r the radius, η the viscosity of the carrier gas, and $\bar{v}$ the average linear gas velocity. This can be solved by iteration for P_i after determining $\bar{v}$ from Q_{av}/A. For the 0.649 mL/min average flow rate, $\bar{v}$ = 22 cm/s and P_i (total inlet pressure) is found to be 129.3 kPa, or some 28 kPa above atmospheric pressure. From eq 2, Q_{end} if found to be 0.74 mL atm/min at 50 °C. Table I summarizes the actual flow rates (Q_{av}) at the initial and final column temperatures and gives the corresponding Q_{end} values at the

Table I. Variation in Flow Rates with Temperature and Differences between Average and Column Outlet Flow Rates

Q_{av} (50 °C)[a]	$\bar{v}$ (50 °C)[b]	Q_{av} (250 °C)[c]	$\bar{v}$ (250 °C)[d]	Q_{end} (50 °C)[e]	Q_{end} (20 °C)[f]
0.649	22.0	0.47	16.0	0.74	0.79
0.812	27.6	0.59	20.0	0.96	1.02
0.982	33.3	0.71	24.1	1.20	1.28

[a] Flow rates as quoted in ref 1, equal to average flow rate at the initial column temperature, 50 °C. [b] Average velocity at initial column temperature. [c] Average flow rate at the final temperature, 250 °C. [d] Average velocity at the final temperature. [e] Column outlet flow rate at the initial temperature. [f] Column outlet flow rate at 20 °C necessary to approximately reproduce the described flow rates. Units for Q_{av} are mL/min, for Q_{end} mL atm/min, for average velocity ($\bar{v}$) cm/s.

initial temperature, as well as the Q_{end} at 20 °C which will approximate the required Q_{av} values when the column reaches the initial analytical temperature of 50 °C. Average velocities at both the initial and final temperatures for the three flow rates quoted are also included.

While in this case the difference between Q_{av} and Q_{end} is not substantial, for longer columns or higher flow rates where higher inlet pressure is employed, the difference can easily reach a factor of 2 or more, making it important that the type of flow rate is fully defined. The quoting of flow rates to three decimal places enables the average velocity and "dead time" to be calculated precisely where these are not given in the text, but it is unlikely that the actual column volume is known with this precision. A variation of only 1 μm between the quoted diameter of 0.25 mm and the actual effective diameter will make a difference of almost 1% in the average flow rate.

The conclusions reached by Jones et al. of flow rates of about 1 mL/min of helium (Q_{end} of 1.2 mL/min) and 2.5 deg/min program rate as being a general optimum are in agreement with our observations. It is somewhat misleading to refer to these as "high flow rates", however, particularly when they represent initial values that fall by 28% during the run. For the test column the initial average velocity corresponding to a 1 mL/min average flow rate is 34 cm/s, falling to 25 cm/s at 250 °C, which is within the range that might be expected from van Deemter plots at various isothermal temperatures.

LITERATURE CITED

(1) Jones, L. A.; Kirby, S. L.; Garganta, C. L.; Gerig, T. M.; Mulik, J. D.; *Anal. Chem.* **1983**, *55*, 1354–1360.
(2) Jones, L. A., personal communication.
(3) Zlatkis, A.; Fenimore, D. C.; Ettre, L. S.; Purcell, J. E. *J. Gas Chromatogr.* **1965** March, 75–81.
(4) Nygren, S.; Mattsson, P. E. *J. Chromatogr.* **1976**, *123*, 101–108.
(5) Grob, K., Jr.; Grob, G.; Grob, K. *J. Chromatogr.* **1978**, *156*, 1–20.

Noel W. Davies

Central Science Laboratory
University of Tasmania
P.O. Box 252 C
Hobart, Tasmania 7001, Australia

RECEIVED for review January 30, 1984. Accepted July 2, 1984.

Journal of Chromatography, 325 (1985) 23–35
Elsevier Science Publishers B.V., Amsterdam — Printed in The Netherlands

CHROM. 17 640

OPTIMIZING FLOW-RATES IN CAPILLARY GAS CHROMATOGRAPHY–MASS SPECTROMETRY

N. W. DAVIES
Central Science Laboratory, University of Tasmania, P.O. Box 252C, Hobart, Tasmania 7001 (Australia)
(First received December 17th, 1984; revised manuscript received February 11th, 1985)

SUMMARY

The effects of the type of gas chromatograph–mass spectrometer interface and the type of flow regulation on flow-rate requirements for optimum efficiency for both isothermal and temperature programmed analyses on capillary columns are examined. Equations and figures are presented which enable rapid selection of optimum parameters such as inlet pressure, average velocity and flow-rate for various situations.

INTRODUCTION

The flow-rate of carrier gas is an important parameter in obtaining the maximum separation efficiency in capillary gas chromatographic (GC) analyses. Column efficiency is generally measured in terms of either the number of effective theoretical plates or the Trenzzahl number, a measure of the degree of separation of a pair of homologues[1,2]. A general review of gas flow in GC was presented by Guiochon[3], and aspects relating to programmed temperature GC were discussed by Harris and Habgood[4].

While the measured flow-rate at the column outlet can be used as a guide when installing capillary columns, the average carrier gas velocity is the parameter more directly related to column performance. For operation with atmospheric outlet pressure, such as is the case in most capillary GC, the optimum average velocity is relatively constant for different column lengths and internal diameters, depending principally on the type of carrier gas used. For columns between 0.2 and 0.5 mm I.D., typical quoted values are 25–30 cm/sec for helium and 45–50 cm/sec for hydrogen[2,5,6].

Jennings and Adam[7] discussed the effects of the rate of temperature programming and carrier gas velocity on the speed of analysis and separation efficiency in capillary gas chromatography. Jones *et al.*[8] discussed an approach to optimizing performance in temperature programmed analyses in terms of both flow-rate and program rate. This article, however, did not note the direct relationship between column temperature and flow-rate that comes as a consequence of the type of flow regulation employed[9].

0021-9673/85/$03.30

Sellier and Guiochon[10] discussed the influence of the type of gas chromatography–mass spectrometry (GC–MS) coupling on column performance. Due to a limited pumping capacity they were not able to operate at the optimum flow-rate when using direct coupling, and this combined with the use of a very long capillary column led them to erroneously infer that column efficiency at a given average velocity was not affected by the column outlet pressure. Hatch and Parrish[6] subsequently showed that significantly higher average velocities were required when using direct coupling with its associated zero effective outlet pressure, and Cramers *et al.*[5] in a detailed analysis proved that it is the volume flow-rate that needs to remain the same for a given column to maintain optimum efficiency with variations in outlet pressure.

The following discussion reviews the effects on flow-rate requirements of the three principal forms of capillary GC–MS interface: direct coupling, open split and capillary leak. Equations and figures are presented enabling rapid determination of parameters such as optimum average velocity, dead time, flow-rate and inlet pressure for various situations. The effects on actual flow-rates of changes in column temperature with the two principal forms of flow regulation are examined in conjunction with the type of GC–MS interface employed.

EFFECT OF INTERFACE TYPE

Direct coupling

Cramers *et al.*[5] showed that column length and diameter had a very significant effect on the optimum average velocity when using directly coupled columns. Direct coupling in this context refers to situations in which the column is inserted right into the ion source, as well as when it is connected via a section of relatively high conductance tubing such that the column outlet pressure is still effectively zero. They showed that the optimum flow-rate from atmospheric outlet pressure studies can be used directly with vacuum outlet pressure to obtain the optimum efficiency. Optimum flow-rate for a particular temperature can be found from the following expression:

$$Q = \frac{\pi d^4 (P_i^2 - P_0^2)}{256 \eta L} \tag{1}$$

using the optimum value for $P_i = P_{i,opt,atm}$, which in turn can be found from an iterative solution to Poiseuille's equation[11]:

$$\frac{(P_i^2 - P_0^2)^2}{(P_i^3 - P_0^3)} = \frac{128 \eta L \bar{v}}{3d^2} \tag{2}$$

using $\bar{v} = \bar{v}_{opt,atm}$. Fig. 1 shows the result of this calculation for different column lengths for hydrogen (using $\bar{v}_{opt,atm}$ = 50 cm/sec) and helium (using $\bar{v}_{opt,atm}$ = 25 cm/sec) for three different diameter columns at 20°C. Where Q_{opt} is known, the flow-rate for directly coupled columns can be simply measured using the expression[11]:

$$Q = \frac{64 \pi \eta L^3}{9 t_a^2} \tag{3}$$

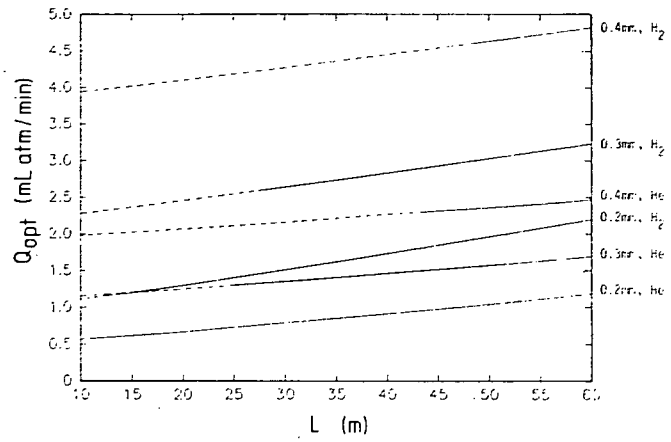

Fig. 1. Optimum flow-rates in ml/min at atmospheric pressure against column length for the internal column diameters and carrier gases indicated at 20°C. Dotted regions represent column lengths that will require sub-atmospheric inlet pressure when direct coupling is used. Values of 25 cm/sec for helium and 50 cm/sec for hydrogen as being the optimum average velocities with atmospheric outlet pressure operation have been used as the basis for calculations.

or alternatively, simply predict the optimum dead time, $t_a = t_{a,opt,vac}$ from the rearrangement of eqn. 3:

$$t_{a,opt,vac} = \left(\frac{64\pi\eta L^3}{9Q_{opt}}\right)^{\frac{1}{2}} \tag{4}$$

The conversion factor for ml atm/min to S.I. units of m^3 Pa/sec is $1.6885 \cdot 10^{-3}$.

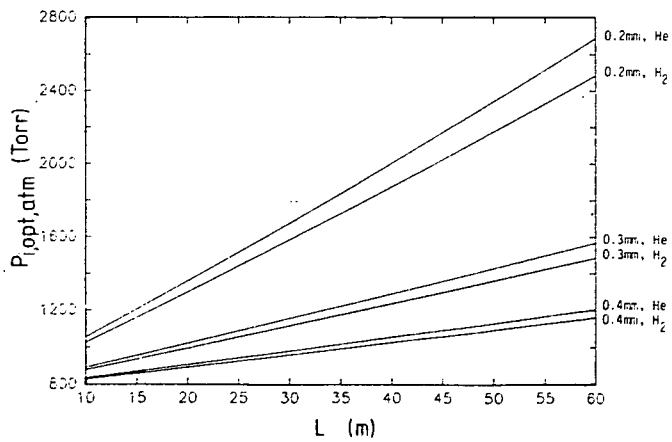

Fig. 2. Column inlet pressures required with atmospheric outlet pressure to generate the optimum flow-rates at 20°C in Fig. 1 for the lengths, internal diameters and carrier gases indicated.

The average velocity required with directly coupled columns is related to the optimum average velocity at atmospheric outlet pressure by the expression[5]:

$$\bar{v}_{opt,vac} = \bar{v}_{opt,atm} \cdot \frac{(P^3_{i,opt,atm} - P^3_{atm})}{(P^2_{i,opt,atm} - P^2_{atm})^{3/2}} \quad (5)$$

Figs. 3–5 illustrate the various parameters relating specifically to directly coupled columns versus column length for 3 different diameters and hydrogen and helium carrier gases at 20°C. Figs. 1 and 2 were obtained from eqns. 1 and 2 using ten different values for column length and constructing a curve of best fit. Fig. 4 was obtained from eqn. 5 for the same points, and Fig. 5 was obtained from $t_a = L/\bar{v}$. Fig. 3 was obtained from a rearrangement of eqn. 1, substituting $P_0 = 0$ and $Q = Q_{opt}$:

$$P_i = \left(\frac{256\eta LQ}{\pi d^4} + P_0^2\right)^{\frac{1}{2}} \quad (6)$$

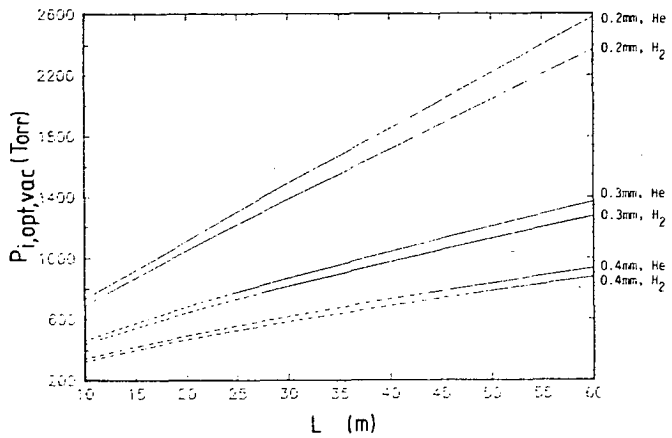

Fig. 3. Column inlet pressures required with vacuum outlet pressure (direct coupling) to generate the optimum flow-rates at 20°C in Fig. 1 for the lengths, internal diameters and carrier gases indicated. Dotted regions represent column lengths that will require sub-atmospheric inlet pressure.

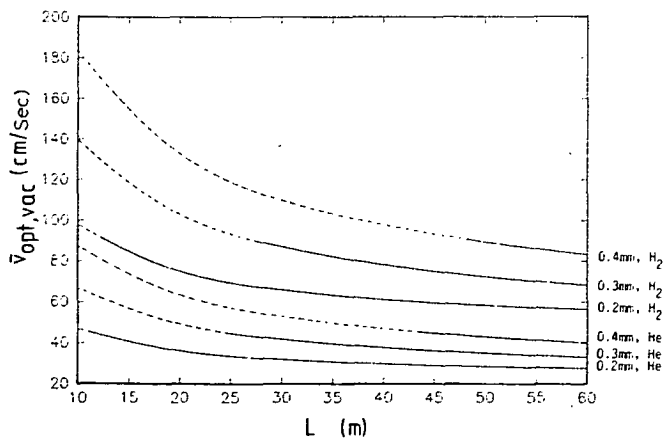

Fig. 4. Average carrier gas velocities required with vacuum outlet pressure (direct coupling) to generate the optimum flow-rates at 20°C in Fig. 1 for the lengths, diameters and carrier gases indicated. Dotted regions represent column lengths that will require sub-atmospheric inlet pressure.

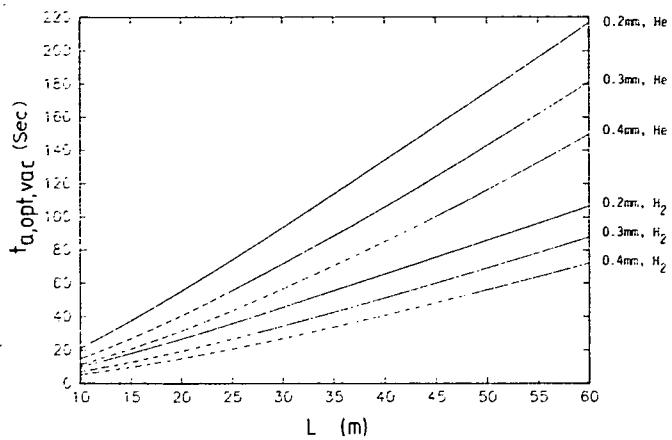

Fig. 5. Dead time required with vacuum outlet pressure (direct coupling) to generate the optimum flow-rates at 20°C in Fig. 1 for the lengths, internal diameters and carrier gases indicated. Dotted regions represent column lengths that will require sub-atmospheric inlet pressure.

The dotted region in each figure represents the column lengths for which sub-atmospheric inlet pressures would be required. Figs. 3–5 relate only to directly coupled columns with zero effective outlet pressure, while the dotted region in Fig. 1 refers to directly coupled columns as well, although the values for Q_{opt} are independent of the type of interface. While sub-atmospheric inlet pressures can be achieved readily enough, this naturally precludes the use of inlet splitting for injection. Column lengths and diameters can thus be quickly chosen by refering to the figures such that this situation does not arise.

Open split

In this interface, the pressure at the column outlet is maintained near 1 atmosphere, and hence the optimum average velocity will not differ from the values quoted for atmospheric outlet pressure.

Capillary leak

A third common type of interface incorporates a length of fine capillary tubing or other form of constriction between the end of the column and the mass spectrometer. This provides a substantial pressure drop so that a column is not exposed directly to the vacuum of the mass spectrometer, and yet all the sample is delivered to the ion source. This will result in atmospheric pressure at the column outlet for a specific flow-rate for each carrier gas, such that no change from normal atmospheric outlet operation is required. Even over the relatively wide range of flow-rates required to accommodate short, narrow bore columns up to long, wide bore columns, such as 0.5 to 3.0 ml atm/min for helium (Fig. 1), the difference in column outlet pressure remains less than a factor of 2 and the theoretical increase required in average velocity to maintain flow-rates is less than 30%.

For example an interface constructed of a 12-cm length of 0.1 mm internal diameter fused-silica tubing results in approximately 1 atmosphere outlet pressure when the optimum flow-rate (based on $\bar{v}_{opt,atm}$ = 25 cm/sec) of 2.5 ml atm/min of

helium is used for a 60 m × 0.4 mm column. A 20 m × 0.2 mm column with the optimum flow-rate of 0.7 ml atm/min of helium results in a calculated outlet pressure of around 400 Torr when used with same interface. The required inlet pressure can be found from eqn. 6, and from eqn. 2 the average velocity will need to be 31 cm/sec. This is an increase of only 25% over the atmospheric outlet pressure value, and almost within the normal quoted range.

Generally the differences in column outlet pressure in these cases can be ignored, and the normal atmospheric outlet pressure optimum average velocities can be used with little or no observable change in separation efficiency.

To calculate the length of a piece of capillary necessary to give atmospheric outlet pressure when constructing a capillary leak interface the following expression can be used:

$$L = \frac{\pi d^4 P_{atm}^2}{256 \eta Q_{opt}} \tag{7}$$

where L and d are the length and diameter of the interface tubing.

EFFECT OF TEMPERATURE PROGRAMMING

The following discussion points out the various changes that occur in flow-rates and average velocities as a consequence of changing column temperature after a flow-rate has been set with either constant pressure drop or "flow control". The influence that the type of GC–MS interface has on these changes is examined.

The theoretical optimum average velocity, $\bar{v}_{opt}$, increases slightly as temperature rises, due to the dependence, in the Van Deemter equation, of $\bar{v}_{opt}$ on the diffusion coefficient in the gas, and to some extent, liquid phases[3]. For the purposes of this discussion $\bar{v}_{opt}$ is not considered as varying with temperature, and also any changes in the column dimensions with increased temperature are ignored.

Isobaric pressure control

"Isobaric" refers to those systems in which the inlet pressure is set to a fixed value and hence a constant pressure drop is maintained throughout a temperature programmed analysis[1,2]. In these cases, the average carrier gas velocity and flow-rate at the column outlet, Q, will fall such that a value at a higher temperature will be related to a value at a lower temperature by the factor η_1/η_2, where η_1 and η_2 are carrier gas viscosities at the lower and higher temperatures respectively. This follows directly from Poiseuille's equation for average carrier gas velocity:

$$\bar{v} = \frac{(P_i^2 - P_0^2)^2 3d^2}{(P_i^3 - P_0^3)\ 128\eta L} \tag{8}$$

and from eqn. 1 describing flow-rate. This effect is illustrated in Fig. 6a. The flow-rate that would be measured at room temperature outside the column oven must be adjusted for the temperature difference:

$$Q_{end} = \frac{\eta_1 T_r}{\eta_2 T_2} \cdot Q_1 \tag{9}$$

where Q_1 is the flow-rate at the temperature corresponding to η_1, and Q_{end} is the measured flow-rate at room temperature corresponding to a column temperature T_2 with a carrier gas viscosity η_2.

Fig. 6b shows the effect of column temperature on Q_{end} relative to the value at 20°C.

With isobaric pressure control, there is no difference in the relative effects of direct coupling or open split interfaces, and the column length, diameter, flow-rate and carrier gas also have no effect on these relationships.

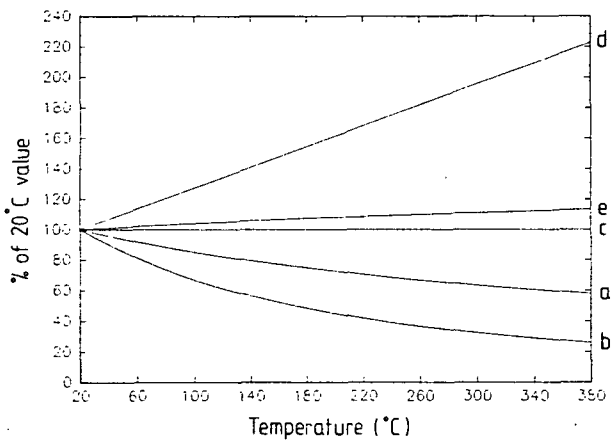

Fig. 6. Effects of temperature programming on various parameters after flow-rate has been set for different flow control and GC–MS interface combinations. The vertical axis shows the values as a percentage of any initial value at 20°C. (a) Q,Q_{av} and $\bar{v}$ with isobaric pressure control and any interface. (b) Q_{end} with isobaric pressure control and any interface. (c) Q_{end} with mass flow control and any interface. (d) Q with mass flow control and any interface. (e) Q_{av} and $\bar{v}$ with mass flow control and direct coupling.

For example a 25 m × 0.2 mm column programmed from 20°C to 200°C with an initial average velocity of 25 cm/sec using helium has $Q = Q_{end} = 0.73$ ml atm/min at 20°C from eqns. 1 and 2. The average flow-rate, as defined by the ratio of column volume to dead time is 0.47 ml/min. At 200°C the average velocity will be:

$$\bar{v} = \frac{(1.941 \cdot 10^{-5})}{(2.672 \cdot 10^{-5})} \cdot 25 \text{ cm/sec}$$

$$= 18.2 \text{ cm/sec}$$

$Q = 0.53$ ml atm/min, $Q_{end} = (293/473) \cdot 0.53 = 0.33$ ml atm/min, $Q_{av} = 0.34$ ml/min.

Flow controller

When flow-rate is regulated by a flow controller, a constant rate is maintained

through the controller regardless of any changes downstream such as in temperature or by installing a different column (Fig. 6c). However, the parameter that remains constant is Q_{end}, and hence changes to the actual flow-rate through the column occur whenever there is a change in temperature[3]. The flow-rate through the column will be:

$$Q = \frac{T_c}{T_r} \cdot Q_{end} \tag{10}$$

Thus in the example above the 0.73 ml atm/min becomes 1.00 ml atm/min at 200°C. Fig. 6d illustrates the effect on Q of changing column temperature with a flow controller in the line.

More relevant to the column performance, however, is the average velocity or average flow-rate. This effect will depend on the type of interface employed.

Atmospheric outlet pressure (open split, capillary leak interfaces). Average flow-rate, Q_{av}, can be found from Q from the following expression[13]:

$$Q_{av} = Q \cdot \left[\frac{3\left(\frac{P_i}{P_0}\right)^2 - 1}{2\left(\frac{P_i}{P_0}\right)^3 - 1} \right]$$

$$= Q \cdot \frac{3(P_i^2 - P_0^2)\,P_0}{2(P_i^3 - P_0^3)} \tag{11}$$

At a flow-rate Q_1 at room temperature with $P_i = P_1$, the average flow-rate $Q_{av,1}$ will be

$$Q_{av,1} = Q_1 \cdot \frac{3(P_1^2 - P_{atm}^2)P_{atm}}{2(P_1^3 - P_{atm}^3)}$$

At a column temperature T_c the flow-rate will be $Q_2 = Q_1 \cdot T_c/T_r$ with an inlet pressure P_2 when a flow controller exists in the line. The new average flow-rate $Q_{av,2}$ is now

$$Q_{av,2} = Q_1 \cdot \frac{T_c}{T_r} \cdot \frac{3(P_2^2 - P_{atm}^2)\,P_{atm}}{2(P_2^3 - P_{atm}^3)}$$

and the ratio is therefore

$$\frac{Q_{av,2}}{Q_{av,1}} = \frac{T_c(P_2^2 - P_{atm}^2)\,(P_1^3 - P_{atm}^3)}{T_r(P_2^3 - P_{atm}^3)\,(P_1^2 - P_{atm}^2)} \tag{12}$$

P_1 and P_2 can be calculated from eqn. 6 using the appropriate values for flow-rate and viscosity. Taking the example of the 25 m × 0.2 mm column using helium as

the carrier gas, programming from 20°C to 200°C with an initial average velocity of 25 cm/sec, corresponding to an initial flow-rate of 0.73 ml atm/min, from eqn. 6, P_1 = 1514 Torr, and P_2 at 200°C = 3319 Torr. From eqn. 12

$$\frac{Q_{av,2}}{Q_{av,1}} = \frac{473}{293} \cdot 0.769$$
$$= 1.24$$

The factor increase in average velocity will be the same as this, since $\bar{v} = Q_{av}/A$. The percentage increases thus clearly depends on the actual flow-rate, the column length and column diameter, as P_i is related to all these. The lower the initial inlet pressure, the larger the percentage increase in average velocity with increasing temperature.

Fig. 7 shows the percentage increase in $\bar{v}$ and Q_{av} with temperature for several situations relative to an initial value at 20°C. These are all much larger increases than the theoretical increase in $\bar{v}_{opt}$ with increasing temperature.

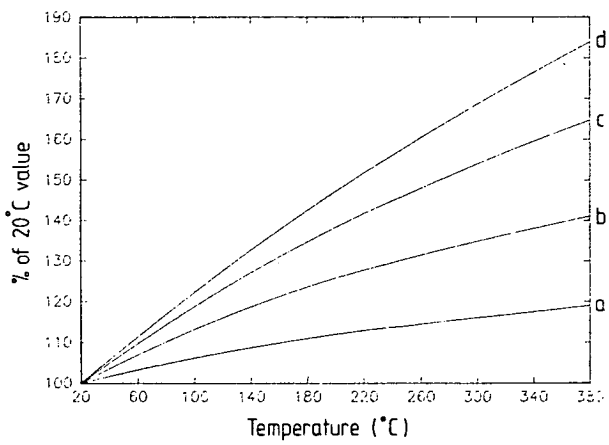

Fig. 7. Effects of temperature programming on Q_{av} and $\bar{v}$ after flow-rate has been set with a mass flow controller and with atmospheric outlet pressure. The vertical axis shows the values as a percentage of the specific initial values at 20°C for the columns indicated. (a) 50 m × 0.2 mm with hydrogen as carrier gas, initial $\bar{v}$ = 50 cm/sec, initial Q_{av} = 0.94 ml/min, Q_{end} = 2.0 ml atm/min. (b) 25 m × 0.2 mm with hydrogen as carrier gas, initial $\bar{v}$ = 50 cm/sec, initial Q_{av} = 0.94 ml/min, Q_{end} = 1.4 ml atm/min. (c) 25 m × 0.3 mm with hydrogen as carrier gas, initial $\bar{v}$ = 50 cm/sec, initial Q_{av} = 2.12 ml/min, Q_{end} = 2.5 ml atm/min. (d) 25 m × 0.5 mm with helium as carrier gas, initial $\bar{v}$ = 30 cm/sec, initial Q_{av} = 3.53 ml/min, Q_{end} = 4.0 ml atm/min.

Vacuum outlet pressure (direct coupling). As P_0 approaches zero in eqns. 11 and 12, the increase in average flow-rate can be seen to approach

$$\frac{Q_{av,2}}{Q_{av,1}} = \frac{T_c P_1}{T_r P_2} \tag{13}$$

However, this ratio can be found more simply without the use of inlet pressure terms. Since $\bar{v} = L/t_a$, substituting this and $K = 64\pi L/9$ in eqn. 3 gives

$$Q_1 = K\eta_1 \bar{v}_1^2$$

and

$$Q_2 = K\eta_2\bar{v}_2^2$$

where $\bar{v}_1$ and $\bar{v}_2$ are the average velocities corresponding to Q_1 and Q_2, respectively. Since $Q_2 = Q_1 \cdot T_c/T_r$

$$\bar{v}_1 = \left(\frac{Q_1}{K\eta_1}\right)^{\frac{1}{2}}$$

$$\bar{v}_2 = \left(\frac{Q_1 T_c}{K\eta_2 T_r}\right)^{\frac{1}{2}}$$

Hence

$$\frac{\bar{v}_2}{\bar{v}_1} = \left(\frac{\eta_1 T_c}{\eta_2 T_r}\right)^{\frac{1}{2}} \tag{14}$$

In the example from above, a 25 m × 0.2 mm column programmed from 20°C to 200°C with helium directly coupled to a mass spectrometer will have an increase in velocity of

$$\frac{\bar{v}_2}{\bar{v}_1} = \left(\frac{1.941 \cdot 10^{-5} \cdot 473}{2.672 \cdot 10^{-5} \cdot 293}\right)^{\frac{1}{2}} = 1.083$$

This figure is again independent of flow-rate, column length, diameter and carrier gas. Fig. 6e illustrates the percentage increase in average velocity and average flow-rate when using directly coupled columns and a flow controller. It can be seen that only slight increases are encountered in this situation.

It should be noted that the changes in flow-rates with column temperature described represent the equilibrium state. This is approximated by relatively slow program rates, but at faster program rates the changes will be somewhat less than those specified due to the time taken for equilibrium to be reached.

EFFECTS OF HIGHER ISOTHERMAL TEMPERATURES

Figs. 1–5 presented optimum values of various parameters that correspond to flow-rates at 20°C that yield average velocities of 25 cm/sec and 50 cm/sec, respectively for helium and hydrogen with atmospheric outlet pressure. Higher temperature operation will change all these to some extent, with the degree of change depending on column length, diameter and carrier gas. Fig. 8 illustrates the changes for the specific example of a 25 m × 0.2 mm internal diameter column with helium as carrier gas. Higher values of Q will be necessary to maintain the same average velocities (Fig. 8a), which requires higher inlet pressures (Fig. 8b). The optimum flow-rate

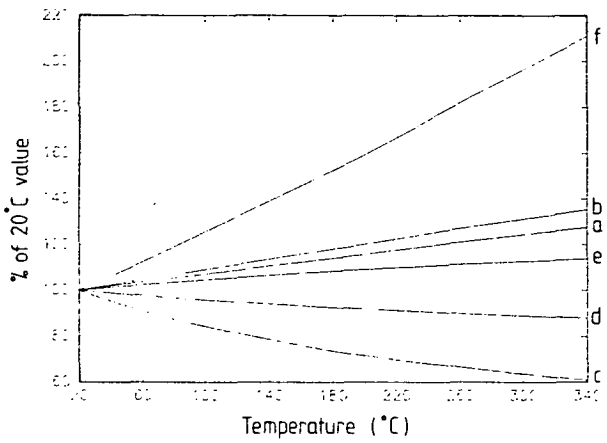

Fig. 8. Effects of increased isothermal temperature operation on optimum parameters for the specific case of a 25 m × 0.2 mm internal diameter column with helium as carrier gas. 25 cm/sec was used as the optimum average velocity for all temperatures with atmospheric outlet pressure. The vertical axis shows the values as a percentage of the specific initial values at 20°C. (a) Q_{opt}, initial value 0.73 ml atm/min; (b) $P_{i,opt,atm}$, initial value 1515 Torr; (c) $Q_{end,opt}$, initial value 0.73 ml atm/min; (d) $\bar{v}_{opt,vac}$, initial value 33.7 cm/sec; (e) $t_{a,opt,vac}$, initial value 74.2 sec; (f) Q_{end} set at 20°C and isobaric pressure control to give the optimum flow-rate at higher temperature, initial value 0.73 ml atm/min.

measured at room temperature (*e.g.* via a calibrated vacuum gauge) will fall (Fig. 8c). The optimum average velocity and dead time with vacuum outlet pressure will be the least affected (Fig. 8d and e). Fig. 8f illustrates the necessary increase in Q_{end} where this is set at room temperature with isobaric pressure control prior to establishing the column temperature.

PRACTICAL CONSIDERATIONS

The reduction in flow-rate and average velocity with rising temperature and isobaric flow control is a well known phenomenon. This can generally be compensated for in practice by setting flow-rates such that the optimum average velocity is achieved near the middle of the temperature range. *i.e.* set initial average velocity to $\bar{v}_{opt} \cdot (\eta_m/\eta_s)$ where η_m and η_s are the carrier gas viscosities at the middle and start of the temperature range, respectively. This then maintains the flow-rate closer to the optimum value at all times.

With flow control and vacuum outlet pressure, average velocity is maintained very close to the starting value. Where flow control is used with atmospheric outlet pressure operation, significant increases in average velocity can occur with increases in temperature, particularly where wider bore columns are used.

From Fig. 7d, a 25 m × 0.5 mm column with an initial average velocity of 30 cm/sec at 20°C with atmospheric outlet pressure results in 50 cm/sec at 300°C. In these cases close to optimum average velocities would be maintained again if the middle of the temperature range was chosen to set flow-rates. In the above example, 30 cm/sec is required at 160°C. From eqn. 2, P_i = 942 Torr; from eqn. 1 Q = 3.97 ml atm/min; Q_{end} = 2.68 ml atm/min. Since a flow controller is employed, the latter is the value that will remain constant throughout the run. Since Q at 20°C is 2.68 ml

atm/min, from eqn. 6 P_i at this temperature is 859 Torr, and the average velocity at 20°C will be, from eqn. 8, 21 cm/sec. A similar method yields an average velocity at 300°C of 43 cm/sec.

It can be seen from the above discussion the potential for significant discrepancy between actual and optimum flow-rates at higher temperatures during temperature programming unless the correct compromise flow-rate is set.

While average velocity can be determined and set accurately by the measurement of dead times, this can be time consuming where they are of the order of two or three minutes. The simplest method of assuring close to optimum flow-rates in capillary GC–MS systems which incorporate a backing pressure gauge is to calibrate the gauge against actual flow-rates at room temperature (in directly coupled systems eqn. 3 enables this to be simply done). The gauge is a measure of Q_{end}, and so actual flow-rates at the column temperature can be found by multiplying by T_c/T_r. Calcu-

TABLE I

FLOW-RATES CORRESPONDING TO AVERAGE VELOCITIES 25 cm/sec (FOR HELIUM) AND 50 cm/sec (FOR HYDROGEN), RESPECTIVELY, WITH AN OUTLET PRESSURE OF 1 atm FOR THE COLUMNS AND TEMPERATURES INDICATED

The optimum flow-rate values are independent of the type of interface used. A calibrated vacuum gauge should correspond approximately to $Q_{end,opt}$ at the midpoint of a temperature programmed analysis. With mass flow control this will be the value of Q_{end} for the whole analysis, while with isobaric pressure control the value of Q_{end} in the last column (*i.e.* set to this value with the column at room temperature) will result in the appropriate $Q_{end,opt}$ at the desired temperature.

Column	*Carrier gas*	*Temperature (°C)*	Q_{opt} *(ml atm/min)*	$Q_{end,opt}$ *(ml atm/min)*	$Q_{end,20°C}$ *(ml atm/min)*
25 m × 0.2 mm	H_2	100	1.50	1.18	1.76
	H_2	200	1.61	1.00	2.22
	H_2	300	1.72	0.88	2.71
	He	100	0.78	0.62	0.92
	He	200	0.84	0.52	1.16
	He	300	0.91	0.46	1.43
25 m × 0.3 mm	H_2	100	2.59	2.03	3.05
	H_2	200	2.67	1.66	3.69
	H_2	300	2.77	1.43	4.37
	He	100	1.35	1.06	1.59
	He	200	1.40	0.87	1.93
	He	300	1.46	0.75	2.30
50 m × 0.2 mm	H_2	100	2.17	1.70	2.55
	H_2	200	2.42	1.50	3.33
	H_2	300	2.68	1.37	4.23
	He	100	1.13	0.88	1.33
	He	200	1.27	0.79	1.74
	He	300	1.41	0.72	2.23
50 m × 0.3 mm	H_2	100	3.21	2.52	3.77
	H_2	200	3.43	2.12	4.73
	H_2	300	3.65	1.87	5.76
	He	100	1.67	1.31	1.96
	He	200	1.80	1.12	2.48
	He	300	1.92	0.98	3.03

lation of Q_{opt} at the midpoint of a temperature program, and hence $Q_{end,opt}$, enables flow-rates to be set correctly by the use of the backing pressure gauge. In the case of isobaric pressure control, the value of Q_{end} with the column at room temperature that will yield the appropriate $Q_{end,opt}$ at the midpoint of the temperature program is the relevant parameter when installing a column.

Table I summarizes some typical values of Q_{opt}, $Q_{end,opt}$ and Q_{end} set at 20°C with isobaric pressure control to yield the optimum flow-rate at the specified temperatures.

SYMBOLS

Q	flow-rate measured at atmospheric pressure and column temperature
d	internal column diameter
P_i	column inlet pressure
P_0	column outlet pressure
η	carrier gas viscosity
L	column length
$\bar{v}$	average carrier gas velocity
t_a	dead time, the retention time of an unretarded peak
$t_{a,opt,vac}$	optimum value of t_a with zero outlet pressure
Q_{opt}	optimum value of Q
$\bar{v}_{opt,vac}$	optimum value of $\bar{v}$ with zero outlet pressure
$\bar{v}_{opt,atm}$	optimum value of $\bar{v}$ with atmospheric outlet pressure
$P_{i,opt,atm}$	optimum value of P_i with atmospheric outlet pressure
$P_{i,opt,vac}$	optimum value of P_i with zero outlet pressure
P_{atm}	atmospheric pressure
T_r	room temperature in Kelvin
T_c	column temperature in Kelvin
Q_{end}	flow-rate measured at atmospheric pressure and room temperature
A	internal cross-sectional area of the column
Q_{av}	average flow-rate ($= AL/t_a$)
$Q_{end,opt}$	optimum value of Q_{end}
$\bar{v}_{opt}$	optimum value of $\bar{v}$

REFERENCES

1 R. E. Kaiser, *Z. Anal. Chem.*, 189 (1961) 1.
2 K. Grob, Jr. and K. Grob, *J. Chromatogr.*, 207 (1981) 291.
3 G. Guiochon, *Chromatogr. Rev.*, 8 (1966) 1.
4 W. E. Harris and H. W. Habgood, *Programmed Temperature GC*, Wiley, New York, 1966.
5 C. A. Cramers, G. J. Scherpenzeel and P. A. Leclerq, *J. Chromatogr.*, 203 (1981) 207.
6 F. W. Hatch and M. E. Parrish, *Anal. Chem.*, 50 (1978) 1164.
7 W. G. Jennings and S. Adam, *Anal. Biochem.*, 69 (1975) 61.
8 L. A. Jones, S. L. Kirby, C. L. Garganta, T. M. Gerig and J. D. Mulik, *Anal. Chem.*, 55 (1983) 1354.
9 N. W. Davies, *Anal. Chem.*, 56 (1984) 2600.
10 N. Sellier and G. Guiochon, *J. Chromatogr. Sci.*, 8 (1970) 147.
11 N. W. Davies, *Anal. Chem.*, 56 (1984) 2618.
12 A. Zlatkis, D. C. Fenimore, L. S. Ettre and J. E. Purcell, *J. Gas Chromatogr.*, March (1965) 75.
13 A. T. James and A. J. P. Martin, *Analyst (London)*, 77 (1942) 679.

Journal of Chromatography, 450 (1988) 388–393
Elsevier Science Publishers B.V., Amsterdam — Printed in The Netherlands

CHROM. 20 824

Note

Open split interfaces in capillary gas chromatography–mass spectrometry

Yield and quantitative aspects

N. W. DAVIES
Central Science Laboratory, University of Tasmania, P.O. Box 252C, Hobart, Tasmania 7001 (Australia)
(First received December 14th, 1987; revised manucript received June 9th, 1988)

One of the most common methods of coupling capillary gas chromatography (GC) columns to mass spectrometers is the open split interface first described by Henneberg *et al.*[1]. These devices usually employ a capillary restrictor tube which governs the amount of gas allowed into the mass spectrometer, with provision for venting any excess gas to atmosphere or a second detector. There is also usually provision for one or two "make-up" or "purge" gas lines to supplement column flow where necessary, to sweep dead volumes within the interface and to enable "cutting" of large GC peaks away from the mass spectrometer to avoid contamination[2–5]. Under these conditions the column exit is at atmospheric pressure and hence combined GC–mass spectrometry (MS) results can be directly compared with those from normal GC, since no change in retention times or resolution will have occurred for the same flow-rates. These interfaces also facilitate the rapid exchange of columns as the mass spectrometer is not directly exposed to atmospheric pressure, and enable columns requiring relatively high flow-rates to be used in conjunction with mass spectrometers of limited pumping capacity.

However, there are two related potential problems when open split interfaces are used in conjunction with isobaric pressure control of the GC column flow-rate and temperature programming, a combination found on several commercial instruments. The first is that if the interface is independently heated at a constant temperature, the "yield", defined as the proportion of any given compound that enters the mass spectrometer, depends on the elution temperature of the compound. This is evident since while the total flow-rate through the column will fall substantially as column temperature rises[6], the flow to the mass spectrometer will be fixed. As a consequence of this, it is possible for there to be insufficient gas at higher column temperatures if flow-rates are not established at the maximum operating column temperature, or appropriate allowances are not made. This results in an influx of air into the interface, which will be potentialy damaging to both the interface and the mass spectrometer.

Quantitative work based on standard curves of the analytes is not affected by the variation in yield provided the same temperature profile is used for standards and samples. Direct quantitative or semiquantitative comparisons of different peaks

0021-9673/88/$03.50

within a temperature programmed analysis will however require appropriate correction factors to be applied. Direct semiquantitative analysis of different compounds in a mixture by comparison of total ion currents is of course complicated by the different ionization cross sections of each compound. Nevertheless compounds in a homologous series such as alkanes will have a total ion current proportional to the total weight of sample and independent of the molecular weight of the individual species[7]. Useful semiquantitative data are then available from the mass spectrometer provided corrections for interface yield are made. If total ion current is indirectly determined by software from the summation of electron multiplier response for all ions in a given compound, then the dependence of the multiplier gain on ion size and structure further complicates direct comparisons. Notwithstanding the complications of total ion current, quantitative comparisons can be readily made using another detector monitoring the flow from the open split vent after appropriate corrections.

Operation in this mode also means that the yield to the mass spectrometer can only be maximized at the high temperature end of the analysis, causing losses in sensitivity by up to a factor of three for the earlier eluting components.

The following discussion presents the appropriate correction factors required to compensate for change in yield, and describes different methods for obtaining constant and maximum yield from an open split interface.

EXPERIMENTAL

The experimental results were obtained on an HP 5890A gas chromatograph with a 25 m × 0.32 mm I.D. fused-silica column installed, coupled to an HP 5970 mass selective detector with an open split interface. The interface was held at 270°C and the initial oven temperature (T_a) was 27°C. Flow-rates were measured at room temperature with a 1-ml soap bubble flow meter (Alltech) after the GC oven had equilibrated at the individual temperatures, with the average of three separate measurements being used in each case. The column flow-rate was measured only at 27°C (*i.e.* F_a), and the split vent flow-rate (F_{sa} and F_{sb}) at all indicated temperatures. F_m was determined from the difference between F_a and F_{sa} with no purge gas. F_p was determined from the difference between values of F_{sa} with the purge on and purge off.

RESULTS AND DISCUSSION

The schematic diagram shown in Fig. 1 illustrates an open split interface of the configuration described, with the flows used in the expressions below indicated. All flow-rates discussed are measured after equilibration with room temperature, so that the flux of gas can be compared fordifferent temperatures. Ignoring the very minor changes in column dimensions with increased temperature, the flow-rate F_b through the column at some elution temperature T_b (in Kelvin) will be[8]:

$$F_b = \frac{\eta_a T_a F_a}{\eta_b T_b} \tag{1}$$

where F_a is the original flow-rate at some temperature T_a, as measured after equilibration to room temperature, and η_a and η_b are the gas viscosities at T_a and T_b

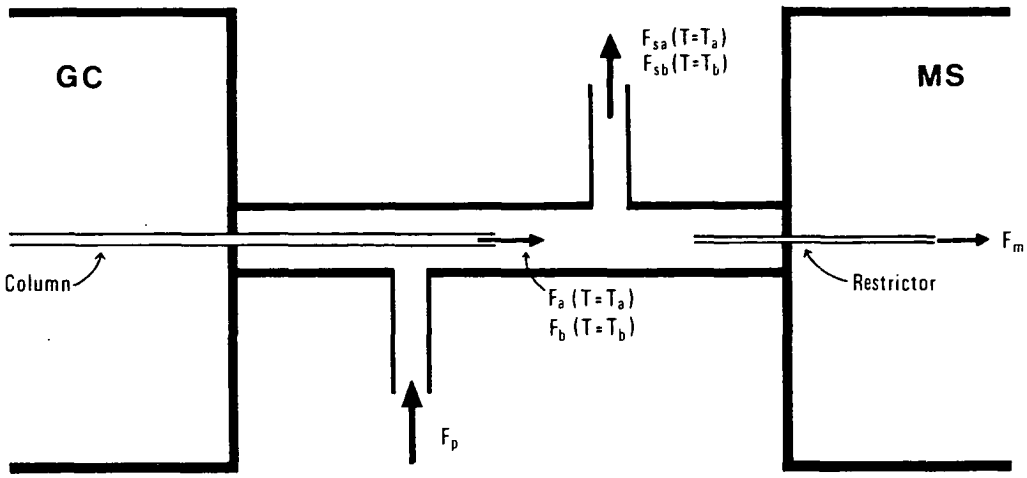

Fig. 1. Schematic diagram illustrating an independently heated open split interface with flows indicated.

respectively. The change in yield can be calculated from the following general case.

If the flow-rate going to the mass spectrometer is defined as F_m and the purge gas flow-rate is F_p, the initial percentage yield at T_a is

$$Y_a = \frac{100F_m}{F_p + F_a} \tag{2}$$

At temperature T_b the percentage yield becomes:

$$Y_b = \frac{100F_m}{F_p + \dfrac{\eta_a T_a F_a}{\eta_b T_b}} \tag{3}$$

Carrier gas viscosities can be calculated to within 1% for the normal temperature range of gas chromatography from the following relationship derived from empirical data[9]:

$$\eta = kT^{0.7} \cdot 10^{-7} \text{ kg m}^{-1} \text{ s}^{-1}$$

where T is the temperature in Kelvin and k is 3.60 for helium, 1.63 for hydrogen and 3.29 for nitrogen. Substitution in eqn. 3 gives:

$$Y_b = \frac{100F_m}{F_p + F_a(T_a/T_b)^{1.7}} \tag{4}$$

The ratio of the yields at T_b and T_a, which is the correction factor that integration results at each value of elution temperature T_b will have to be divided by for quantitative comparisons, is therefore:

$$Y_b/Y_a = \frac{F_p + F_a}{F_p + F_a(T_a/T_b)^{1.7}} \quad (5)$$

With no purge gas this reduces to:

$$Y_b/Y_a = (T_b/T_a)^{1.7} \quad (6)$$

As an illustration of the above effects, a change in temperature from 100 to 300°C results in slightly more than a doubling of the yield if no purge gas is employed. The same temperature change results in a 35% relative increase in yield when half the initial flow is from the purge line. The larger the proportion that the purge gas is of the total, the smaller the increase in yield.

Naturally if quantitative comparisons are made using a second detector monitoring the flow from the open split vent the correction will be opposite in direction. The ratio will be:

$$Y_{sb}/Y_{sa} = \frac{100 - Y_b}{100 - Y_a}$$

where Y_{sb} and Y_{sa} are the percentage of total flow going to the split vent at temperatures T_b and T_a respectively. Substitution of eqns. 2 and 4 and simplifying based on the fact that $F_p + F_a = F_{sa} + F_m$ where F_{sa} is the split vent flow-rate at oven temperature T_a, results in:

$$Y_{sb}/Y_{sa} = \frac{(F_p + F_a)[F_a(T_a/T_b)^{1.7} + F_{sa} - F_a]}{F_{sa}[F_p + F_a(T_a/T_b)^{1.7}]} \quad (7)$$

Integration results for each elution temperature T_b will need to be divided by this value for direct quantitative comparisons on a second detector.

Arithmetical yields of more than 100% in eqn. 4 correspond to an influx of air into the mass spectrometer. This situation is reached when

$$F_p + (T_a/T_b)^{1.7} F_a < F_m \quad (8)$$

Fig. 2 shows the comparison of calculated and experimental values for the yield ratios Y_b/Y_a and Y_{sb}/Y_{sa} for the examples listed. The discrepancy between experimental and calculated data ranged from −2.5 to +3.0% of the calculated yield ratio. During relatively rapid temperature programming the column may not be at equilibrium with the GC oven. Under these conditions there may be a somewhat greater discrepancy from calculated data than indicated here.

The yield will remain constant throughout a temperature programmed analysis only if the carrier gas is controlled by a mass flow controller, or if the interface is heated at the same rate as the GC column. The former method results in significant increases in average carrier gas velocity with increasing temperature[8], but would be suitable in many cases where it is desirable to maintain a constant and maximum yield. The latter method can be achieved either by independently heating the interface at the same rate

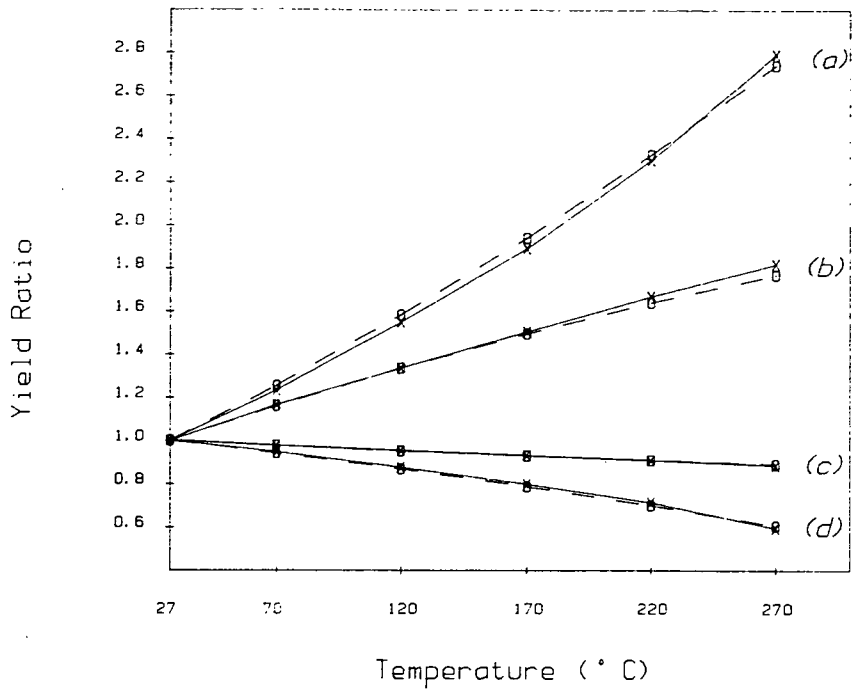

Fig. 2. Calculated data (○ – – – ○) and experimental data (× – – – ×) for yield ratios from an open split interface held at constant temperature during temperature programming of the GC oven, with isobaric control of flow-rates. (a) Y_b/Y_a, no purge gas, all values of Y_a. For experimental points F_a = 2.88 ml min, Y_a = 18.4%. (b) Y_b/Y_a, F_p = 1.30 ml/min, F_a = 2.83 ml/min, Y_a = 12.4%. (c) Y_{sb}/Y_{sa}, same conditions as for (b), Y_{sa} = 87.6%. (d) Y_{sb}/Y_{sa}, no purge gas, same conditions as for (a), Y_{sa} = 81.6%.

as the GC oven, or by incorporating the interface in the GC oven. The yield will be maintaned at a constant value in the absence of purge gas since both the column and restrictor flows will be reduced by the same factor. Provided that any purge gas added is also isobarically controlled original yields will still be maintained across a temperature range. If only the purge gas is controlled by a mass flow controller there will be a decrease in yield with rising temperature.

Incorporating the interface in the GC oven is the simpler alternative, but increases the dead volume of the system and goes against the normal practice of placing the interface as close as possible to the mass spectrometer. However, since the dead volume is all on the high vacuum side it is rapidly swept out and should not result in any detectable broadening due to diffusion. A piece of deactivated fused-silica or glass-lined tubing (50 cm in length) as the final connection to the mass spectrometer will take less than 0.2 s to sweep out with a flow of 1.5 ml/min of helium[10].

A second advantage of incorporating the interface in the GC oven is that it can be removed simply and rapidly, allowing the option of direct coupling if required.

A disadvantage of having the open split interface remote from the mass spectrometer could be in the transfer of relatively involatile compounds, such as those boiling above about 500°C. The best results for these appear to be when the column or the restrictor tube go directly into the ion source[11]. This is despite the fact that vapour pressure in equilibrium with a glass wall is higher than that with a liquid phase, and

hence interface temperatures can in theory be lower than the column temperatue[2]. The "Joule–Thompson" cooling effect upon expansion of gas from the restrictor tube does not explain this provided either helium or hydrogen are used as carrier gases, since both have a negative Joule–Thompson coefficient resulting in heating of the gas upon expansion.

The combination of type of flow control and method of interface heating therefore depends on the analytical requirements. If maximum yield is not essential and quantitative comparisons are not important, or the appropriate correction factors are applied, then isobaric pressure control of column flow and an open split interface that is held at constant temperature in association with temperature programmed analyses presents no problems. If it is desired to yield almost 100% of the GC effluent to the mass spectrometer over a wide temperature range, or to maintain a constant yield of effluent to the mass spectrometer, then the method of flow control or the method of heating the interface is relevant when an open split interface is employed.

REFERENCES

1 D. Henneberg, U. Henrichs and G. Schomburg, *Chromatographia*, 8 (1975) 449.
2 D. Henneberg, U. Henrichs and G. Schomburg, *J. Chromatogr.*, 112 (1975) 343.
3 H.-J. Stan and B. Abraham, *Anal Chem.*, 50 (1978) 2161.
4 D. Henneberg, U. Henrichs, H. Husmann and G. Schomburg, *J. Chromatogr.*, 167 (1978) 139.
5 E. Wetzel and Th. Kuster, *J. Chromatogr.*, 268 (1983) 177.
6 N. W. Davies, *Anal. Chem.*, 56 (1984) 2600.
7 G. F. Crable and N. D. Coggleshall, *Anal. Chem.*, 30 (1958) 310.
8 N. W. Davies, *J. Chromatogr.*, 325 (1985) 23.
9 R. C. Weast (Editor), *CRC Handbook of Chemistry and Physics*, CRC Press, Boca Raton, FL, 65th ed., 1984, p. F-43.
10 N. W. Davies, *Anal. Chem.*, 56 (1984) 2618.
11 N. W. Davies, unpublished results.

Journal of Chromatography, 565 (1991) 207–224
Biomedical Applications
Elsevier Science Publishers B.V., Amsterdam

CHROMBIO. 5725

Automated screening procedure using gas chromatography–mass spectrometry for identification of drugs after their extraction from biological samples

GLEN P. NEILL, NOEL W. DAVIES* and STUART McLEAN

School of Pharmacy and Central Science Laboratory, University of Tasmania, P.O. Box 252C, Hobart, Tasmania 7001 (Australia)*

(First received August 21st, 1990; revised manuscript received October 29th, 1990)

ABSTRACT

A novel analytical screening procedure has been developed, using computer-controlled gas chromatography–mass spectrometry (GC–MS), to detect 120 drugs of interest to road safety. This paper describes GC–MS methodology suitable for use on extracts of biological origin, while extraction procedures will be the subject of a future communication. The method was devised to identify drugs in extracts of blood samples, as part of an investigation into the involvement of drugs, other than alcohol, in road accidents. The method could be adapted to screen for other substances. The method depends on a "macro" program which was written to automate the search of GC–MS data for target drugs. The strategy used was to initially search for each drug in the database by monitoring for a single characteristic ion at the expected retention time. If a peak is found in this first mass chromatogram, a peak for a second characteristic ion is sought within 0.02 min of the first and, if found, the ratio of peak areas calculated. Probable drug identification is based on the simultaneous appearance of peaks for both characteristic ions at the expected retention time and in the correct ratio. If the ratio is outside acceptable limits, a suspected drug (requiring further investigation) is reported. The search macro can use either full mass spectra or, for enhanced sensitivity, data from selected ion monitoring (which requires switching between groups of ions during data acquisition). Quantitative data can be obtained in the usual way by the addition of internal standards.

INTRODUCTION

While the relationship between alcohol and road accidents has been well documented, little is known of the contribution of other drugs to road safety. A major difficulty has been the need to analyse a large number of blood samples, taken from road users involved in accidents, for the presence of drugs which could impair driving performance. A great variety of chemically dissimilar substances are used as medicines and social drugs and have the capacity to impair driving performance and the potential, therefore, to contribute to road accidents. This presents a considerable analytical challenge, which has been managed in previous studies by restricting the analytical screen to a relatively small number of drugs which are considered most likely to be involved in road accidents. Even so, batteries of analytical methods (radioimmunoassay, thin-layer chromatography, gas

0378-4347/91/$03.50

chromatography, high-performance liquid chromatography) have been used to screen for drugs in blood samples taken in road accident studies [1–4], as in many toxicological screens. These methods are often time-consuming and generally lack specificity, although drug findings can be confirmed by subsequent gas chromatography–mass spectrometry (GC–MS) [1,4].

Since many drugs contain nitrogen, GC with nitrogen–phosphorus detection (GC–NPD) can be used for initial screening [5], an approach taken in some previous road accident studies [6–8] and in other drug screening procedures [9–11]. GC–NPD provides a single analytical procedure which is sufficiently sensitive and selective to detect a large number of drugs. However, as drug detection is based only on retention time, searching complex chromatograms is laborious, and possible drug findings need to be confirmed by an additional analysis, such as GC–MS. Another problem, which we found in a previous study [8], was that even GC–NPD chromatograms of extracts of blood samples contained large numbers of extraneous peaks which eluted close to the retention times of drugs: these all required subsequent analysis by GC–MS although most proved negative. In addition, important non-nitrogenous drugs, especially tetrahydrocannabinol and its metabolites and anti-inflammatory agents, cannot be detected by NPD.

This report describes a GC–MS method of screening for 120 drugs of possible concern to road safety. Compared with previous methods, it has better specificity and sensitivity, and is faster in searching for the targeted drugs. In cases where the identification of a drug is critical, such as in forensic work and in analysis by selected ion monitoring (SIM), it may be necessary to confirm the drug finding by appropriate re-analysis to increase the number of ions used. Sample extraction procedures have not been investigated in this study, which instead focuses on the problem of the efficient identification of drugs in complex chromatograms, where there are many possible drugs present. The biomedical application of this method will be the subject of a separate paper.

EXPERIMENTAL

Materials

Water was purified by the Millipore-Q decontamination system (Millipore, Sydney, Australia). Organic solvent were HPLC grade (Waters Assoc., Division of Millipore, Sydney, Australia) except chloroform (nanograde, Mallinckrodt, Melbourne, Australia). All were found to be free from contaminants by GC analysis of a thousand-fold concentrated sample. Glassware was washed using Extran 300 detergent (BDH Chemicals, Melbourne, Australia), followed by a Milli-Q water wash and a methanol wash. After drying, all glassware was rinsed in dichloromethane prior to use. A list of drugs of interest to road safety was prepared, based on the drugs reported most frequently in road accident studies in Australia and other commonly used drugs with the potential to impair driving performance. Most reference drug standards were obtained from pharmaceutical

companies (see Acknowledgements). Benzoylecognine, 3,4-methylenedioxymethylamphetamine (MDMA) and 9-carboxy-11-nor-Δ^9-tetrahydrocannabinol were obtained from Alltech Assoc. (Deerfield, IL, U.S.A.) and tetrahydrocannabinol (THC) was a gift of the Research Triangle Institute (Research Triangle Park, NC, U.S.A.). *n*-Decane and *n*-triacontane were obtained from Sigma (St. Louis, MO, U.S.A.). Other chemicals were of analytical reagent grade.

Equipment

Samples for GC analysis (usually 1 ml) were placed in 1.5-ml crimp-top glass autosampler vials (Sun Brokers, Wilmington, NC, U.S.A.). Small volumes (less than 200 μl) were contained in smaller conical glass inserts (Microsun Insert, Sun Brokers). GC–MS analysis was performed on a Hewlett-Packard 5890 gas chromatograph and 5970 series mass-selective detector (Hewlett-Packard Australia, Melbourne, Australia). Automated injections were made with a Hewlett-Packard 7673A autosampler. Programming and data processing were carried out using a Hewlett-Packard 59970A workstation and Version 3.1.1 Pascal software. The injector was fitted with a wide-bore (4 mm) quartz liner, which contained a small plug of quartz wool in the centre. Free drugs and methylated derivatives were analysed on a 22 m × 0.32 mm I.D. fused-silica capillary column, coated with 0.52-μm cross-linked 5% phenyl methyl silicone gum (HP-5, Hewlett-Packard). Samples which had been treated with N-methyl-bis(trifluoroacetamide) (MBTFA; Pierce, Rockford, IL, U.S.A.) as a derivatising agent caused a loss of column performance when underivatised samples were analysed. Therefore, a separate column was used exclusively for analysis of samples treated with trifluoroacetylating reagent: this was a 12 m × 0.32 mm I.D. fused-silica column coated with 0.25-μm SE-30 gum (Econo-Cap, Alltech Assoc.). Each column was protected by a 20 cm length of the same type of column which was fitted as a pre-column, and changed when there was evidence of column activation. Separate analyses were performed for underivatised, methylated and trifluoroacetylated drugs. This reduced the total number of ions being monitored each time to a manageable size, as well as being consistent with conventional extraction procedures.

The following GC–MS conditions were used: injector temperature, 260°C; open-split interface temperature, 290°C; oven program, 40°C for 1 min, then increasing at 10°C/min to 290°C; carrier gas, helium, column head pressure, 105 kPa (22-m column) or 70 kPa (12-m column); column flow-rate at 40°C, 2.5 ml/min; sample size, 5μl; split ratio, 10:1.

Reference samples

To obtain reference GC and MS data, drug solutions (concentration 100 ng/μl) were prepared in chloroform and 1 ml was placed in a crimp-top autosampler vial. Hydrocarbon standards in chloroform (decane, 54 μg in 50 μl; triacontane, 26 μg in 100 μl) were added to the 1-ml sample to enable standardisation of GC retention times. Drugs which were obtained as salts were first dissolved in water

(1–2 mg in 1 ml), then the pH of the solution was adjusted with either 2 ml of 0.05 *M* sodium borate, pH 9.2 (for basic drugs) or 1 ml of 15% hydrochloric acid, pH 3 (for acidic drugs). The free drug was extracted with 1 ml of a mixture of dichloromethane–hexane–ethyl acetate (6:3:1) by vortex-mixing for 5 min and, after separation by centrifugation, the organic phase was transferred to a sample vial and concentrated to about 50 μl under nitrogen, then made to 1 ml with chloroform. An aliquot (usually 100 μl) was placed in a GC vial and made to 1 ml with chloroform, giving a final concentration of about 100 ng/μl. Drug solutions were stored at 4°C until analysed.

Derivatisation

Trifluoroacetyl derivatives were made of drugs with free hydroxyl, primary or secondary amino groups. This improved their chromatographic properties and enabled better resolution of peaks. The 1-ml drug solution in chloroform in the GC autosampler vial was concentrated to about 20 μl, 50 μl of MBTFA (Pierce) were added, and the vial was heated at 60°C for 30 min. Care was taken to keep the solvent dry and free from protic solvents to prevent cleavage of the trifluoroacetate derivatives. Then the sample was concentrated to about 20 μl under nitrogen and made to 1 ml with chloroform. Acidic drugs were similarly methylated with freshly prepared ethereal diazomethane (200 μl), except that the reaction was carried out at room temperature.

Extracts from tissue

Forensic samples were obtained from the Government Analyst (Hobart, Australia) as extracts of blood, urine or liver (TOXI-LAB Analytical Systems, Kansas City, MO, U.S.A.). This is similar to the extraction method described for reference samples. Extracts of biological samples were concentrated to 20–50 μl and placed in the small-volume inserts in the autosampler vials before GC–MS analysis. Blank plasma samples were similarly extracted to check on extraneous peaks and possible false positives.

GC–MS analysis

Database. Mass spectra and retention times of drugs were generated from the reference drug samples, which were analysed either individually or in simple mixtures. The "standard" retention times for decane (TC10 = 6.06 min) and triacontane (TC30 = 27.65 min) were chosen arbitrarily from an initial GC–MS run. Retention times from subsequent GC–MS analyses of reference drugs were corrected (TD, Table I), where necessary, by a transformation of the retention times of the two hydrocarbons to the standard times.

GC–MS. Full mass spectra were acquired by scanning over the mass range *m/z* 500 to 40 approximately once per second. For maximum sensitivity in analysing unknown samples, however, SIM is required. Because only twenty ions could be monitored at one time while there were 120 drugs to be searched for, the follow-

TABLE I

GC–MS DATA USED BY THE MACRO TO SCREEN FOR EACH DRUG

Compound[a]	Retention time TD (min)	ION1[b] *(m/z)*	ION2 *(m/z)*	Peak ratio (ION1/ION2)
Free drugs				
Benzaldehyde[c] (d)[d]	5.42	105.05	77.05	1:1
C10	6.07	71.05	–	–
Valproic acid	8.15	73.10	102.05	2:1
Amphetamine	8.17	91.05[e]	65.05	2:1
Methylamphetamine	9.08	58.05	91.05	15:1
Tranylcypromine	9.58	132.10	115.05	5:3
Ethosuximide	9.88	55.05	113.05	1:1
Ephedrine	12.12	58.05	77.05	10:1
MDMA	14.00	58.05	135.05	20:1
Clofibrate	14.25	128.00	169.05	5:1
Metronidazole	15.55	81.05	124.05	5:4
Tolbutamide (d)	15.61	91.05	171.00	5:2
Carbimazole	15.79	186.05	114.05	2:1
Paracetamol	16.15	109.05	151.05	5:2
Methyl phenidate	16.58	84.10	91.05	10:1
Pethidine	16.82	172.10[f]	247.15	1:1
Pheniramine	17.60	169.10	58.05	5:3
Caffeine	17.70	194.10	109.05	7:5
Alprenolol	17.78	72.10	249.15	20:1
Ketamine	18.00	180.05	209.10	5:1
Methylphenobarbitone	18.58	218.10	246.10	15:1
Captopril	18.82	70.05	198.10	10:1
Phenyltoloxamine	19.02	58.05	255.15	20:1
Phenobarbitone	19.21	204.10	232.10	10:1
Theophylline	19.23	180.05	95.00	2:1
Fenoprofen	19.30	242.10	197.10	1:1
Dexchlorpheniramine	19.68	203.05	58.05	1:1
Clonidine	20.52	229.00	171.95	2:1
Ranitidine	20.65	137.10	94.05	5:4
Diphenylpyraline	20.70	99.05	114.10	2:1
Diclofenac	20.90	214.05	242.05	5:4
Dextromethorphan	21.03	59.05	271.20	1:1
Methadone	21.10	72.10	294.20	50:1
Dextropropoxyphene	21.24	58.05	208.10	5:1
Procyclidine	21.41	84.10	204.15	20:1
Amitriptyline	21.59	58.05	275.20	50:1
Hyoscyamine	21.68	124.10	289.20	4:1
Cocaine	21.69	82.05	182.10	3:2
Mianserin	21.72	193.10	264.15	5:4
Procainamide	21.73	86.10	120.05	5:1
Nortriptyline	21.81	44.00	202.10	10:1
Trimipramine	21.82	58.05	249.15	5:1
Imipramine	21.88	234.15	280.20	5:2

(Continued on p. 212)

TABLE I (*continued*)

Compound[a]	Retention time TD (min)	ION1[b] (*m/z*)	ION2 (*m/z*)	Peak ratio (ION1/ION2)
Doxepin	21.92	58.05	277.15	50:1
Primidone	22.00	190.10	146.05	5:4
Desipramine	22.10	234.15	195.10	1:1
Benzhexol	22.13	98.10	218.15	20:1
Triprolidene	22.20	208.10	278.20	10:3
Promethazine	22.41	72.05	284.15	20:1
Trimeprazine	22.62	58.05	298.15	10:3
Benztropine	22.81	83.05	140.10	5:4
Carbamazepine	22.85	193.10	236.10	5:2
Phenytoin	22.86	180.05	252.10	5:3
Oxazepam	22.95	268.05	239.05	10:7
Hyoscine	23.09	94.05	138.10	3:1
Cyproheptadine	23.14	287.15	215.10	5:3
Pizotifen	23.23	295.15	96.00	5:4
Azatidine	23.36	246.15	290.20	6:5
Dothiepin	23.39	58.05	202.10	50:1
Codeine	23.45	299.15	162.10	2:1
Sulphamethoxazole	23.64	92.05	253.05	10:1
Dihydrocodeine	23.65	301.20	244.10	7:1
Lorazepam	23.69	239.05	274.00	1:1
Morphine	23.88	285.15	162.10	3:1
Diazepam	23.89	256.10	283.05	1:1
Δ^9-THC	23.95	299.20	314.20	5:4
Methdilazine	24.19	296.15	199.05	1:1
Disopyramide	24.31	195.05	212.05	5:3
Chlorpromazine	24.38	58.05	318.10	5:1
Desmethyldiazepam	24.47	242.05	269.05	1:1
Chlordiazepoxide	24.61	282.10	247.10	5:1
Oxycodone	24.93	315.15	230.10	5:2
Trimethoprim	25.00	290.15	259.10	5:2
Chloroquine	25.11	86.10	319.20	10:1
Haloperidol	25.29	224.10	237.10	5:4
Flunitrazepam	25.42	285.10	312.10	1:1
Metoclopramide	25.43	86.10	184.00	10:1
Trifluoperazine	25.49	407.15	267.05	1:1
Diamorphine	25.56	327.15	369.15	3:2
Nifedipine	25.82	329.10	284.15	1:1
Hydrochlorothiazide	25.94	268.95	228.00	4:1
Temazepam	26.00	271.05	300.05	10:1
Fentanyl	26.05	245.15	146.05	3:1
Nitrazepam	26.70	280.05	253.10	5:4
Sulindac	27.17	296.05	239.05	5:3
Quinine	27.20	136.10	189.10	13:1
Clonazepam	27.34	314.05	280.05	1:1
C30	27.65	71.05	–	–
Clomiphene	27.82	86.10	405.20	50:1

TABLE I (*continued*)

Compound[a]	Retention time TD (min)	ION1[b] (m/z)	ION2 (m/z)	Peak ratio (ION1/ION2)
Dextromoramide	27.97	100.10	265.15	5:4
Miconazole	28.23	159.00	334.95	5:1
Diltiazem	28.26	58.05	121.10	20:1
Prochlorperazine	28.38	373.15	272.05	3:1
Thioridazine	29.95	98.10	378.15	10:3
Verapamil	30.46	303.20	151.10	10:1
Pholcodine	30.92	114.10	100.10	10:7
Glibenclamide	35.17	169.05	287.10	5:1
Methylated drugs				
Valproic acid	6.65	87.10	116.10	10:3
Salicylic acid	9.98	120.05	92.05	10:7
Allopurinol (1)[g]	11.39	164.05	80.05	1:1
Ibuprofen	14.07	161.15	220.15	4:1
Allopurinol (2)[g]	15.06	164.05	136.05	10:1
Tolbutamide (d)	15.74	91.05	185.00	2:1
Captopril	16.86	70.05	231.10	10:1
Captopril (Me_2)	17.80	70.05	128.05	5:3
Diflunisal	17.97	232.05	264.05	2:1
Methylphenobarbitone	18.00	232.10	175.05	10:1
Phenobarbitone (Me_2)	18.00	232.10	175.05	10:1
Fenoprofen	18.36	197.10	256.10	5:4
Phenobarbitone	18.58	218.10	246.10	20:1
Naproxen	19.56	185.05	244.10	2:1
Chlorpropamide	19.73	111.00	175.00	1:1
Mefenamic acid	20.43	223.10	255.15	10:9
Tolbutamide (d)	20.51	91.05	155.00	5:4
Ketoprofen	20.74	209.10	105.05	5:4
Probenecid	21.16	270.10	135.05	5:3
Diclofenac	21.55	214.05	242.05	2:1
Benzoylecgonine	21.69	82.05	182.10	5:4
Phenytoin	21.87	180.05	266.10	10:9
Tolbutamide	22.09	91.05	129.00	10:9
Nitrazepam	24.32	294.10	248.10	5:4
Bendrofluazide (Me_2)	24.86	254.00	347.00	10:7
Clonazepam	25.11	329.05	294.10	10:7
Warfarin	25.14	279.10	322.10	5:1
Bendrofluazide	25.31	240.00	333.00	2:1
Enalaprilat	25.35	220.15	317.15	10:1
Enalaprilat (Me_2)	25.73	234.10	331.15	10:1
Nitrazepam (Me_2)	25.98	267.10	294.10	10:9
Chlorothiazide (Me_2)	26.47	323.95	245.00	3:2
Clonazepam	26.67	328.05	294.10	1:1
Frusemide (Me_2)	27.13	81.05	358.05	5:2
Chlorothiazide (Me_3)	27.13	308.95	337.00	5:4
Δ^9-THC acid metabolite	27.21	343.20	299.20	5:4
Indomethacin	27.40	139.00	371.10	5:2

(Continued on p. 214)

TABLE I (*continued*)

Compound[a]	Retention time TD (min)	ION1[b] (*m/z*)	ION2 (*m/z*)	Peak ratio (ION1/ION2)
Bumetanide (Me_2)	28.54	392.15	349.10	1:1
Bumetanide	29.23	318.10	378.15	1:1
Sulindac	30.70	233.05	354.10	5:3
Trifluoroacetylated drugs				
Amphetamine	7.54	140.05	118.05	5:4
Methylamphetamine	8.93	154.05	110.05	2:1
Tranylcypromine	9.48	116.05	69.00	10:3
Ephedrine	9.61	154.04	110.05	5:1
Metronidazole	10.81	141.00	221.05	5:4
Methoxyphenamine	11.00	154.05	148.05	2:1
Paracetamol	11.04	108.00	205.05	5:3
MDMA	12.97	154.10	289.10	5:3
Alprenolol (TFA_2)	14.50	266.05	308.05	10:7
Methylphenidate	14.65	180.05	150.05	10:1
Hydralazine (TFA_2 or TFA_3)	14.84	281.00	295.00	5:1
Oxprenolol (TFA_2)	15.25	266.05	308.05	10:7
Clonidine	15.50	290.05	199.00	5:1
Hyoscyamine	16.20	124.10	271.20	5:2
Metoprolol (TFA_2)	16.39	266.05	308.05	5:3
Propranolol (TFA_2)	17.24	266.05	308.05	10:7
Δ^9-THC	17.41	410.20	339.10	1:1
Hyoscine	17.52	94.05	399.15	5:1
Morphine (TFA_2)	18.29	364.10	477.10	5:2
Codeine	18.68	282.15	395.15	2:1
Metoclopramide	19.42	86.10	280.00	15:1
Nortriptyline	19.47	232.15	290.15	20:1
Desipramine	19.78	208.10	362.10	10:3
Dihydrocodeine	22.61	397.15	284.15	2:1
Pholcodine	24.35	100.10	114.10	10:9
Terfenadine (TFA_1 or TFA_2)	27.85	262.15	433.20	10:1

[a] Abbreviations: MDMA = 3,4-Methylenedioxymethylamphetamine; Δ^9-THC = Δ^9-tetrahydrocannabinol; Δ^9-THC acid metabolite = 9-carboxy-11-nor-Δ^9-tetrahydrocannabinol; Me_2 = dimethylated; Me_3 = trimethylated; TFA_2 = di(trifluoroacetylated); TFA_3 = tri(trifluoroacetylated).

[b] ION1 was the base peak, unless otherwise specified.

[c] Benzaldehyde was a decomposition product of ephedrine.

[d] (d) indicates a drug decomposition product.

[e] Base peak of amphetamine was *m/z* 44.

[f] Base peak of pethidine was *m/z* 71.

[g] Different positional isomers.

ing approach was taken. Two diagnostic ions (usually including the base peak) were chosen for each drug. An acquisition method file was created in which up to twenty ions were monitored during each of ten time periods (the maximum available with this instrument). Groups of ions were monitored during appropriate

A

```
NAME DRUGS
WRITELN 701, #10,#10,#10,#10
TAB HEADER, PRINTER:
WRITELN 701,'*************************************************************'
WRITELN 701, #10,#10,#10,#10
CH 4:5,71
GETS
A=X
IF Y<50000
    WRITELN701,'*************************************************************'
    WRITELN 701, "C10 AREA VERY LOW, CHECK THAT IDENTITY IS CORRECT"
    WRITELN 701,'*************************************************************'
    WRITELN 701, #10,#10,#10,#10
ENDIF
CH 25:30,71
GETS
B=X
IF Y<50000
    WRITELN 701,'*************************************************************'
    WRITELN 701, "C30 AREA VERY LOW, CHECK THAT IDENTITY IS CORRECT"
    WRITELN 701,'*************************************************************'
    WRITELN 701, #10,#10,#10,#10
ENDIF
TC10=6.06
TC30=27.65
P=1
.....(START OF REPEATING SECTION OF MACRO)
TD=DRUGTIME
TDCOR=(A+((TD-TC10)/(TC30-TC10)) * (B-A))
CH TDCOR-0.2:TDCOR+0.2, ION1
THRESH THRESH1, TDCOR-1
INT
THRESH THRESH1, -(TDCOR-1)
N=NPEAKS
IF NPEAKS>0
    CH TDCOR-0.2: TDCOR+0.2, ION2
    THRESH THRESH2, TDCOR-1
    INT
    THRESH THRESH2, -(TDCOR-1)
    NB=NPEAKS
    IF NPEAKS>0
        EX
        Z=1
        WHILE N>0
            PE Z
            RO -1
            P1=PEAK_AREA
            RT=RET_TIME
            EX
            Y=1
            M=NB
            WHILE M>0
                PE Y
                RO -1
                IF RT-RET_TIME<0.02
                    IF RT-RET_TIME>-0.02
                        P2=PEAK_AREA
                        ARATIO=P1/P2
                        IF ARATIO < MAXRATIO
                            IF ARATIO > MINRATIO
                                WRITELN 701, "PROBABLE DRUGNAME FOUND"
                                WRITELN 701, #10,#10,#10,#10
                                N=0
                                P=2
                            ENDIF
                        ENDIF
                        IF P=1
                            WRITELN 701, "*************************************************"
                            WRITELN 701, "IONS FOR DRUGNAME FOUND, RATIO SUSPECT"
                            WRITELN 701, "*************************************************"
                            WRITELN 701, #10,#10,#10,#10
                        ENDIF
                        MERGE
                        CLEAR 3
                        CLEAR Y
                        CLEAR Z
                        DR 3,X
                        SCR
                        WRITELN 701, #10,#10
                        IF P=2
                            TAB RESULTS, PRINTER:
                            WRITELN 701, #10,#10,#10
                            WRITELN 701, "*************************************************"
                            WRITELN 701, #10,#10,#10,#10
                            P=1
                        ENDIF
                    ENDIF
                    M=0
                ELSE
                    Y=Y+1
                    M=M-1
                ENDIF
            ENDWHILE
            Z=Z+1
            N=N-1
            EX
        ENDWHILE
    ENDIF
ENDIF
.....(END OF REPEATING SECTION OF MACRO)
QUIT
```

Fig. 1.

(*Continued on p. 216*)

B

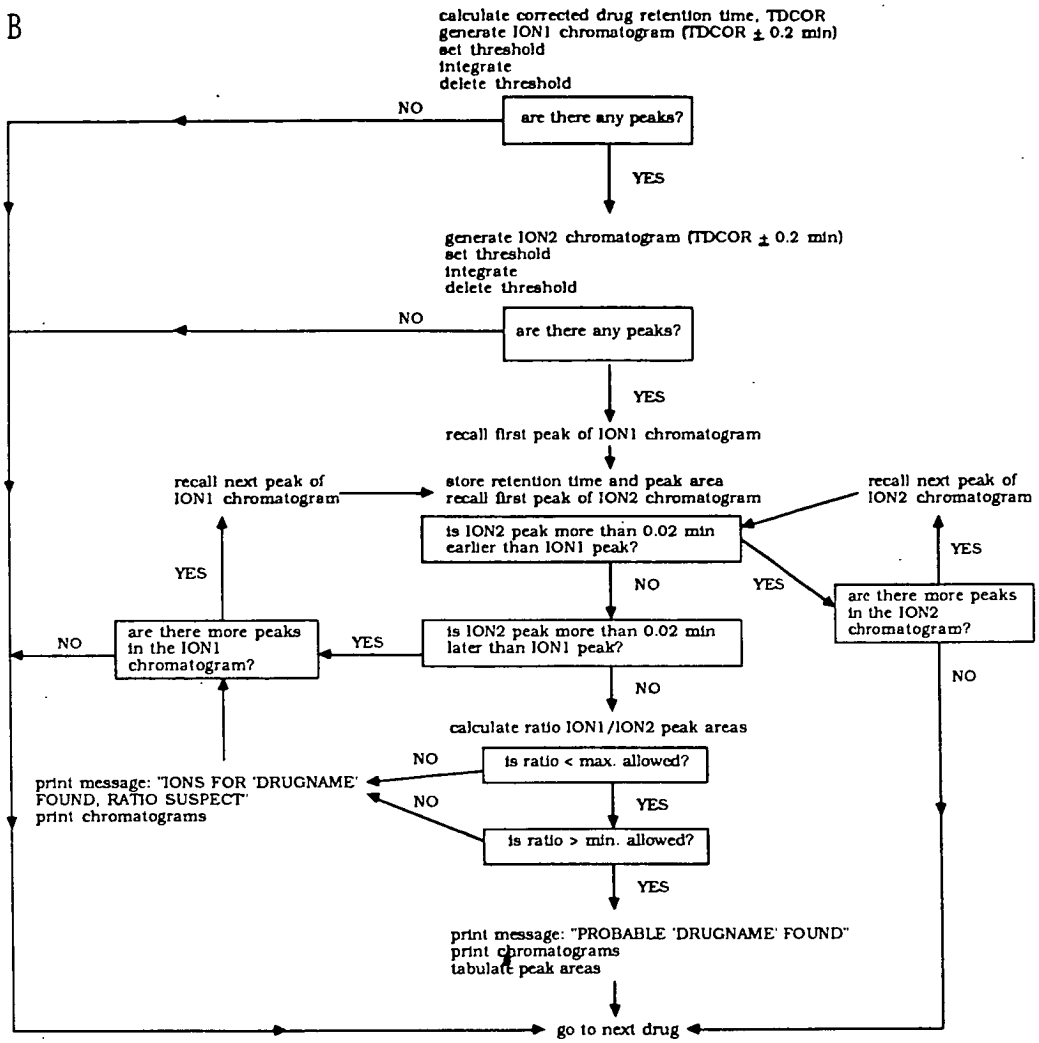

Fig. 1. (A) Listing of the macro program used to search the GC–MS acquisition file for drugs in the data base. The section between the two markers is repeated for each drug with appropriate names and values for the following variables: **DRUGTIME**, the standard drug retention time, based on retention times of 6.06 min for decane and 27.65 min for triacontane; **ION1**, the *m/z* value of the principal diagnostic ion; **THRESH1**, the integration threshold to use for ION1; **ION2**, the *m/z* value of the second diagnostic ion; **THRESH2**, the integration threshold to use for ION2; **MAXRATIO**, the maximum allowable ratio for the peak areas of ION1/ION2; **MINRATIO**, the minimum allowable ratio for the peak areas of ION1/ION2; **DRUGNAME**, the name of the target drug. (B) Flow diagram of the repeating section of the macro program.

time windows, based on the retention times of drugs of interest (Table I). This procedure enabled the maximum possible number of drugs to be included in the analytical screening procedure. Drugs which eluted close to the time when a different group of ions was monitored had to be included in both groups, to allow for changes in retention time. On the other hand, some ions were common to more than one drug, which improved efficiency (eleven drugs were monitored in one group).

Dwell time per ion was 30 ms. Masses of diagnostic ions were calculated to the nearest 0.05 mass units, based on ion structures. Where the empirical formula of the ion was not obvious, an estimate to the nearest 0.05 mass units was made. This level of accuracy was to enable interference from endogenous substances to be kept to a minimum, provided the maximum resolution of the mass spectrometer was used. For example, halogenated ions from drug molecules could be partially resolved from ions derived from lipids which had the same nominal mass, because of the lower mass defect of the halogenated ions.

Macro. Editing was automated by means of a "macro" built into the data editing portion of the sequencing software (Fig. 1A and B). This operated by checking a small time window (± 0.2 min) about the expected retention time of each drug for the principal diagnostic ion (ION1) and then, if successful, for the second ion (ION2). The macro program calculated the expected retention time (TDCOR) for each drug in the individual GC run based on a correction for any change in the retention times of decane and triacontane from the standard times. If both the primary (ION1) and secondary (ION2) ions for a drug were detected at the same time (within 0.02 min), the ratio of their peak areas (ION1/ION2) was compared with the expected ratio. Generous limits were allowed, because of the possible variability in relative ion abundances and the potential for interference from other substances in biological samples which could produce interfering ions at the same retention time. Thus if the expected ratio was 2, the limits could be > 1 to <4, although this must be decided for each drug and biological matrix depending on interferences.

In those cases when more than one peak was detected at the mass of ION1 or ION2 within the defined 0.4-min time window about the expected drug retention time, the macro checked all peaks until either a drug was found or all possibilities had been examined. Thus the retention time of the first possible ION1 peak was noted and the ION2 channel examined for the occurrence of a peak within 0.02 min of the retention time of the ION1 peak. If none was found, the next possible ION1 peak was considered and the ION2 channel again examined for a peak within 0.02 min of this second ION1 peak. This process continued until either a suitable pair of peaks was found or all options were exhausted. Results were only reported if there was a probable drug finding.

The macro consists principally of a repeating unit containing information on each drug: name, retention time, the two diagnostic ions with their thresholds for integration and the permissable range of ion ratios (Fig. 1A and B). The software does not allow this to be written as a single subroutine in which variables are substituted. The full macro for a hundred or so drugs is therefore quite long (160 KBytes), although each new drug can be readily added to it from a template of the repeating unit in which only the variables need to be changed.

Separate SIM data acquisition methods and macros were created for underivatised drugs, methylated drugs and trifluoroacetylated drugs. In practice, each biological sample would need to be split and subjected to three different

work-ups (for underivatised, methylated and trifluoroacetylated drugs), and these would then be analysed separately.

RESULTS AND DISCUSSION

The value of the macro is in the relatively rapid, automated searching of the acquisition file for a large number of possible drugs: while this can be done manually, it would be very time-consuming. The macro took about 5 s to check for each drug, provided that it found no peaks within the time window for the

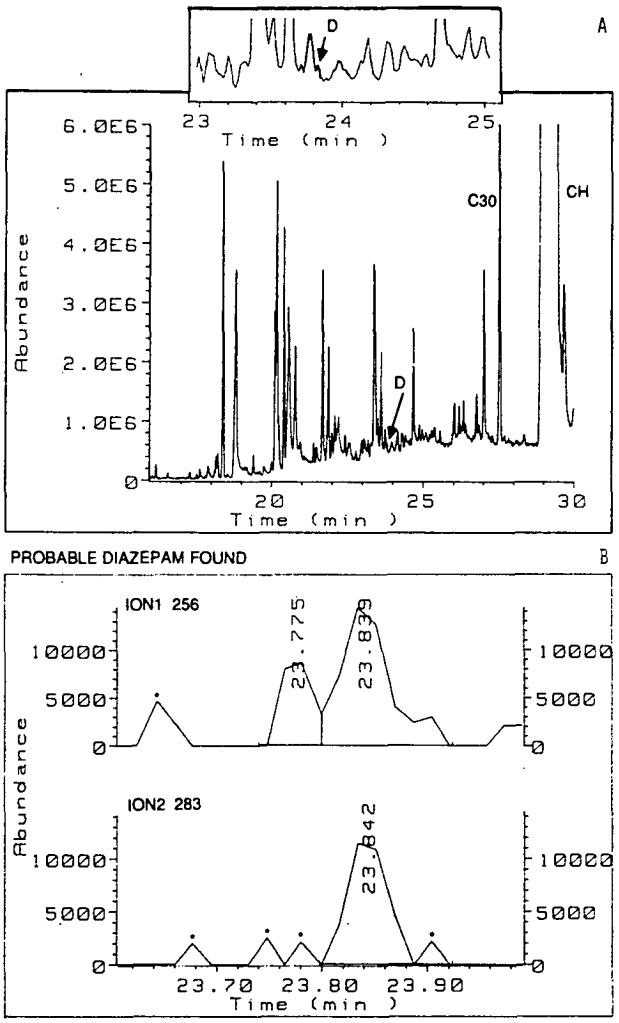

Fig. 2. (A) Portion of TIC chromatogram of an extract of a forensic blood sample. Arrow marks the position of diazepam peak, found in Fig. 2B. Inset: expansion of region from 23 to 25 min. CH is cholesterol. (B) Text and mass chromatograms for diagnostic ions for diazepam generated by the macro from the full scan acquisition data in (A), as part of a report of a probable diazepam finding (see text for details). The macro also tabulated retention times and peak areas for all integrated peaks. * = subthreshold peaks (not integrated).

principal diagnostic ion. Complex chromatograms with peaks for both ions present within the time window could take considerably longer. Automated editing time for biological samples could be up to 30 min per run, depending on the nature of the sample and the integration threshold levels used.

Fig. 2 illustrates the use of the macro in searching a complex chromatogram for target drugs. Fig. 2A shows a portion of a total ion current (TIC) chromatogram obtained by GC–MS analysis of a basic (pH 9) TOXI-LAB solvent extract of a forensic blood sample. Diazepam was present, but at a level giving only a very small peak, even when that region of the chromatogram was expanded

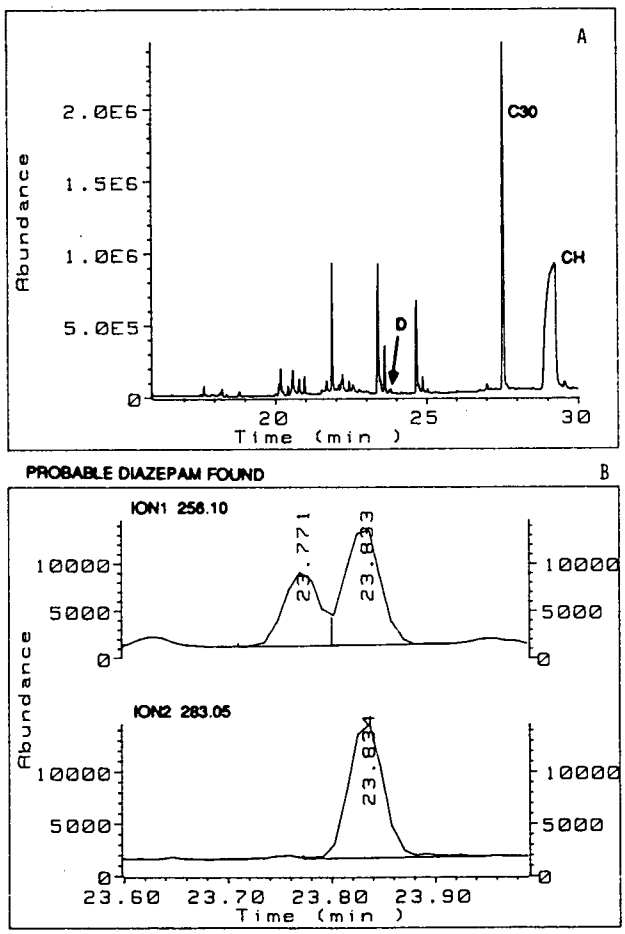

Fig. 3. (A) Portion of TIC chromatogram obtained by SIM re-analysis of the sample used in Fig. 2. The groups of ions monitored at different times are given in Table I. Arrow marks the position of diazepam peak, which is quite small even in SIM mode. (B) Text and mass fragmentograms generated by the macro from the SIM acquisition data in (A). Note that more accurate mass values were used for monitoring the diagnostic ions compared to full scan acquisition (Fig. 2B), and that there was less noise and smoother peak shapes.

(Fig. 2A insert). Fig. 2B shows the mass chromatograms generated by the macro from the full scan data in Fig. 2A. To search for diazepam, the macro first calculated the expected retention time of diazepam (TDCOR = 23.80 min in this run) by correcting for any changes in the retention times of C10 and C30, then examined the chromatogram of the first diagnostic ion for diazepam (ION1 = *m/z* 256) over the time interval within 0.2 min of TDCOR (*i.e.* 23.60–24.00 min). The first ION1 peak was below threshold, but the second (at 23.775 min) was not and this initiated a search in the ION2 (*m/z* 283) chromatogram for a peak occurring within 0.02 min of 23.775 min. No match was found, the second ION1 peak (23.839 min) was located, and this time paired with the ION2 peak at 23.842 min. The ratio of peak areas (ION1/ION2) was 1.39, within the set limits (0.5–2.0), and a report of a probable diazepam finding was printed, with the ION1 and ION2 chromatograms and a table of the areas of all integrated peaks. In this case, confirmation was obtained from a recognizable full spectrum of diazepam at the appropriate retention time, after careful background subtraction.

Fig. 3 shows the results from analysis of the same sample by SIM mode GC–MS. The TIC chromatogram (Fig. 3A) was produced by monitoring the ions listed in Table I for free drugs, sequentially in groups of up to twenty ions at a time. The diazepam peak was still quite small. Fig. 3B shows the mass fragmentograms generated by the macro as in Fig. 2B, except that in this case more accurate values for ION1 (*m/z* 256.10) and ION2 (*m/z* 283.05) were monitored during the SIM acquisition. Due to the inherently longer dwell times of SIM, and the more rapid sampling, there was less noise and smoother peak shapes than when the same nominal masses were acquired from full scans (Fig. 2B).

False positive findings could often be rejected by visual inspection of the mass chromatograms, as illustrated in Fig. 4. The SIM chromatogram of a basic extract (TOXI-LAB) of liver (a forensic sample) shows peaks near the retention times of diazepam and nordiazepam (Fig. 4A), and these drug findings were confirmed by the macro report. A probable finding of haloperidol was also reported by the macro, but inspection of the mass fragmentograms in Fig. 4C shows this to have been an error due to the threshold values having been set too low. The macro integrated an ION1 peak at 25.084 min and paired it with an ION2 peak at 25.075 min (peak ratio 0.54, limits 0.5–2.0), but inspection of the chromatogram (Fig. 4C) shows that neither was a real peak (compare Fig. 4B). The only possible ION1 and ION2 peaks in Fig. 4C did not occur within 0.02 min of each other and would not have led to a report of haloperidol.

It was more important to avoid false negative findings, which would result in drugs being missed altogether, than false positives, which could be detected by examination of the macro report or an additional GC–MS analysis. Interferences in one or both ion channels could cause the ION1/ION2 ratio to be outside the set limits, and this was reported as "IONS FOR **DRUGNAME** FOUND, RATIO SUSPECT", indicating the need for further investigation. This could be readily done for drugs which chromatographed in both free and derivatised forms

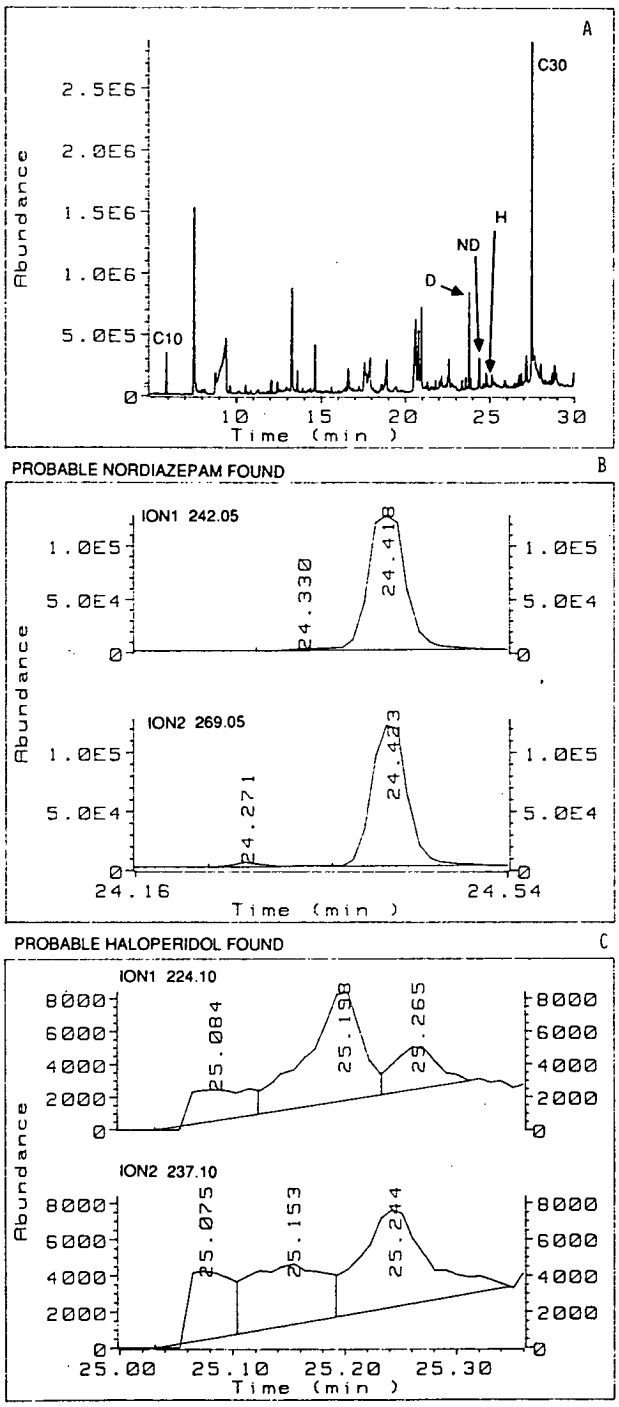

Fig. 4. (A) Portion of a SIM chromatogram of a chloroform extract of liver found to contain diazepam (D) and nordiazepam (ND). H indicates the retention time of haloperidol (see C). (B) Text and mass fragmentograms generated by the macro from the SIM data in (A), showing the identification of probable nordiazepam. (C) Text and mass fragmentogram generated by the macro from the SIM data in (A), showing identification of probable haloperidol. Visual inspection shows this to have been an error, due to integration of noise caused by thresholds being set too low. See text for discussion.

(Table I) by comparison with the macro report on the other analysis. Otherwise re-analysis was required, using specific acquisition methods to identify the particular drug.

Drugs could also be undetected because of deterioration of the chromatographic system, and this was avoided by routine monitoring of GC performance with a mixture of some of the drugs in the search database which were very sensitive to column activity (methylamphetamine, oxazepam and oxycodone). If peak shape indicated activity, the injection port accessories (quartz insert and quartz wool packing, septum and O-ring) were changed. If necessary, a new precolumn was fitted.

Some variability was found even in the corrected drug retention times. Note that the actual retention time of nordiazepam in Fig. 4B (24.42 min) was slightly later than the expected time (TDCOR = 24.35 min, at the centre of the mass chromatogram). The longer retention time was presumably due to the presence of biological molecules which modify the polarity of the liquid phase. This shows the need for the relatively wide limits (TDCOR ± 0.2 min) which were allowed on the search window used by the macro. For the same reason, drugs which eluted near the beginning or (more particularly) the end of a SIM ion group were also included in the adjacent group's acquisition file.

Warnings were also given if the areas of either of the hydrocarbon peaks were low (Fig. 1). This was to avoid the possibility of the wrong peak being assigned as the reference hydrocarbon. In addition, a small C10 peak could indicate a general loss of volatile substances, perhaps during a concentration step.

Caffeine was the only drug reported in blank plasma extracts since, although the SIM chromatogram contained many peaks (as in Fig. 3A), the other criteria in the macro prevented false drug identifications. The method has not yet been evaluated on plasma samples, but the simple solvent extraction procedure described in Experimental was successfully tested on a group of eighteen drugs added to blank plasma. The drugs found in spiked plasma samples included amphetamines, opiates, benzodiazepines, an antihistamine (azatedine), Δ^9-tetrahydrocannabinol and anticonvulsants. The concentrations added to plasma were relatively high (10 μg/ml) as the intention was to test the capacity of the macro to search complex chromatograms rather than the extraction procedure. Success in screening for drugs in biological samples is critically dependent on the efficiency of extraction procedures, and several methods have been described [1–12]. The signal-to-noise ratio is also of decisive importance in analysis of biological samples and becomes more of a problem with the low drug concentrations likely to be seen in practice. The measurement of low levels of drugs in biological samples may require changes to thresholds and even selection of different diagnostic ions, and this will be the subject of future work.

We were unable to analyse some drugs by GC, even as derivatives. Importantly, these included some of the β-blocking drugs: atenolol, labetalol, pindolol and timolol. However, alprenolol, metroprolol, oxprenolol and propranolol were

chromatographed as trifluoroacetyl derivatives (Table I). Leloux *et al.* [13] successfully analysed β-blockers by GC with on-column injection after double derivatisation (trimethylsilylation and trifluoroacetylation), but this was not used in our study.

This method was developed to provide a preliminary screen to detect drugs which could contribute to road accidents, using extracts of plasma suitable for GC analysis. In many cases the evidence of two diagnostic ions, in the correct ratio and occurring at the expected retention time of the drug, would be sufficient evidence for drug identification. Positive drug findings can be confirmed, when necessary, by additional analyses with specific acquisition methods designed to identify the particular drug. In SIM mode, up to twenty ions can be monitored per drug. The macro could be written to use a larger number of co-eluting characteristic ions for fewer target substances, which would increase certainty of identifications.

The Hewlett-Packard GC–MSD system is a widely used instrument, and the screening method described here could be readily adopted by other MSD users. It was not practical to use the quantitative report software supplied with the MSD for drug screening, because it gives full reports on peaks not found. This results in a very lengthy report when screening for over a hundred drugs. The method described in this article only reports on drug findings and is suitable for screening when most samples contain few, if any, of the target drugs. The macro could be applied to screening for other substances, such as metabolites used in clinical diagnosis [14,15], anabolic steroids and other doping agents [16,17] and possibly for pesticides or environmental pollutants.

Copies of the macro containing data on the drugs listed in Table I are available from the authors.

ACKNOWLEDGEMENTS

We are grateful to Kathryn Campbell, Government Analyst Laboratory (Hobart, Australia) for provision of forensic samples for analysis. We are also grateful to Dr. John Vine for helpful discussions. The following pharmaceutical companies are thanked for gifts of reference drugs: Alphapharm, Astra Pharmaceuticals, Bayer Australia, The Boots Co. (Australia), Ciba-Geigy Australia, Essex Laboratories, Faulding Pharmaceuticals, Glaxo Australia, Hoechst Australia, ICI Pharmaceuticals, IDT Australia, Janssen-Cilag, Lederle Laboratories, May & Baker Pharmaceuticals, Mercke Sharp & Dohme (Australia), Merrell Dow Pharmaceuticals Australia, Organon (Australia), Parke Davis, Pfizer, A. H. Robins, Sandoz Australia and Searle Australia. The project was supported by grants from Transport Tasmania and the Australian Research Council.

REFERENCES

1 D. J. Crouch, M. A. Peat, D. M. Chin and D. S. Finkle, *J. Forensic. Sci.*, 28 (1983) 945.
2 A. P. Mason and A. J. McBay, *J. Forensic. Sci.*, 29 (1984) 987.
3 P. Holmgren, E. Loch and J. Schuberth, *Forensic. Sci. Int.*, 27 (1985) 57.
4 S. H. Cosbey, *Forensic. Sci. Int.*, 32 (1986) 245.
5 W. O. Pierce, T. C. Lamoreaux, F. M. Urry, L. Kopjak and B. S. Finkle, *J. Anal. Toxicol.*, 2 (1978) 26.
6 A. W. Missen, *Chem. N.Z.*, 45 (1981) 61.
7 J. Vine and T. R. Watson, *Med. J. Aust.*, 1 (1983) 612.
8 S. McLean, R. S. Parsons, R. B. Chesterman, R. Dineen, M. G. Johnson and N. W. Davies, *Med. J. Aust.*, 147 (1987) 6.
9 B. J. Perrigo, H. W. Peel and D. J. Ballantyne, *J. Chromatogr.*, 341 (1985) 81.
10 A. Turcant, A. Premel-Cabic, A. Cailleux and P. Allain, *Clin. Chem.*, 34 (1988) 1492.
11 R. A. Cox, J. A. Crifasi, R. E. Dickey, S. C. Ketzler and G. L. Pschak, *J. Anal. Toxicol.*, 13 (1989) 224.
12 B. Ford, J. Vine and T. R. Watson, *J. Anal. Toxicol.*, 7 (1983) 116.
13 M. S. Leloux, E. G. DeJong and R. A. A. Maes, *J. Chromatogr.*, 488 (1989) 357.
14 E. Jellum, O. Thoresen, L. Horn, R. Seip, E. Nilsen, E. A. Kvittingen and O. Stokke, *J. Chromatogr.*, 468 (1989) 43.
15 A. G. Antoshechkin, A. B. Golovkin, L. A. Maximova and V. A. Bakharev, *J. Chromatogr.*, 489 (1989) 353.
16 A. K. Singh, M. Ashraf, K. Granley, U. Mishra, M. Madhusudana Rao and B. Gordon, *J. Chromatogr.*, 473 (1989) 215.
17 R. Massé, C. Ayotte and R. Dugal, *J. Chromatogr.*, 489 (1989) 23.

Direct Quantitative Determinations by Multiple Metastable Peak Monitoring

1—Warfarin in Plasma

Noel W. Davies,† John C. Bignall and Michael S. Roberts
Central Science Laboratory and School of Pharmacy, University of Tasmania, PO Box 252C, Hobart, Tasmania, Australia

A technique for the direct quantitative determination of plasma warfarin concentrations has been developed using multiple metastable peak monitoring on a double focusing mass spectrometer of normal geometry. The method uses a direct insertion probe and requires no sample purification or derivatization. Deuterated warfarin was added as an internal standard, and the first field free region metastable fragmentations for the loss of an acetyl radical from the molecular ion of both warfarin and internal standard were monitored. These independent daughter ions were focused by a simple combination of linking the magnetic and electric sectors, accelerating voltage switching and selected ion monitoring using standard instrumentation. Results were acquired and processed by normal selected ion monitoring software. Repeated determinations of plasma warfarin concentrations were made with plasma extracts representing approximately 4 μl of plasma, each sample taking two minutes to process by this technique.

INTRODUCTION

The anticoagulant drug warfarin (**1**) is used in the clinical management of thromboembolic disorders. Techniques such as spectrophotometry,[1] thin-layer chromatography (TLC),[2] high-performance liquid chromatography (HPLC),[3] gas chromatography[4] and gas chromatography chemical ionization (CI) mass spectrometry[5] have been used for the quantitative determination of warfarin. The therapeutic effect of warfarin and other coumarin anticoagulants is usually monitored from prothrombin times.[6] However, plasma warfarin assays are occasionally required to check patient compliance to therapy, to quantify covert anticoagulant ingestion, to monitor warfarin resistance and to study warfarin drug interactions.[6]

This paper reports the rapid and direct assay of warfarin from plasma extracts by the technique of multiple metastable peak monitoring. This involves the monitoring of specific metastable ion fragmentations in the first field free region of a normal geometry double focusing mass spectrometer, and is analogous to the monitoring of specific reactions in the second field free region of a reversed geometry instrument by the mass-analysed ion kinetic energy technique.[7] The focusing of first field free region metastable peaks for individual monitoring is normally achieved using accelerating voltage (V) adjustments, or the linked sector scan in which the ratio of magnetic field (B) to electric sector voltage (E) is held constant.[8] This technique has been applied to the determination of hormones and drugs in body fluids, in conjunction with gas chromatography, to provide better specificity over normal selected ion monitoring.[9–11] In these cases the internal standard undergoes the same reaction as the compound being determined, and is separated by gas chromatography. One report discusses the application of selected metastable peak monitoring to determinations directly from crude matrices, using a narrow sweep of metastable ions for better specificity as the sample contained chlorine, but without the use of an internal standard.[12] To quantify compounds by direct insertion with the use of an internal standard, it is clearly necessary to monitor more than one reaction. Different daughters from the same precursor can be readily focused by the B/E scan, but this does not allow much scope for the selection of internal standards. If deuterated internal standards are to be used, daughters from different precursors must be focused. This can be done by altering both B and E to appropriate values, and an instrumental modification to achieve this has been described.[13] This involves the use of a commercial linked scan unit and a 'metastable ratio amplifier' allowing the alternate selection of two B/E ratios, thus allowing sample and internal standard constant parent ion scans to be focused, respectively. Switching B to the appropriate value with the respective B/E ratio selected thus allows focusing of parents and first field-free region daughter ions from both the sample and internal standard. Another way in which independent reaction products can be focused is by combining a single B/E ratio and magnetic field switching with small accelerating voltage adjustments to change the precursors,[14] and this is the technique described in this paper. This involved no modifications to a standard commercial instrument. The number of independent reactions that can be monitored by this method depends on the number of channels in the selected ion monitoring mode and the number of preset accelerating voltage positions available.

Thus, while single or multiple metastable peak monitoring may be used in conjunction with gas chromatography or HPLC to provide a higher degree of specificity, multiple metastable peak monitoring may also be used with varying degrees of sample purification to the direct probe determination of compounds in mixtures. In this example no purification was required, and

† Author to whom correspondence should be addressed.

CCC-0306-042X/83/0010-0646 $03.00

this factor coupled with the absence of any chromatographic system enabled very rapid determinations. The multiple metastable peak mode can be selected and calibrated rapidly, making it well suited to an assay that is only infrequently required.

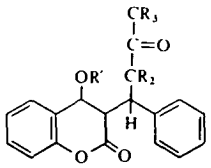

1 R = R′ = H
2 R = D, R′ = H
3 R = R′ = D

EXPERIMENTAL

Instrumentation

The instrument used was a Vacuum Generators 70/70F double focusing mass spectrometer, fitted with a multiple ion detection (MID) unit or a digital scan controller, a linked scan unit, three independent manually set accelerating voltage positions and a mode selection switch. The instrument was coupled to a Vacuum Generators 2235 Datasystem with selected ion recording software. No modifications to this standard instrumentation were required. The system was operated with the linked scan unit and selected ion facility (whether MID or digital scan controller) both switched in. The ion source was maintained at 180–220 °C, and was operated at 70 eV in the electron impact mode with a trap current of 200 μA. Accelerating voltage was nominally 4 kV for main beam ions, and was adjusted to appropriate values for desired precursors by reference to a four figure digital panel meter. The electric sector voltage was adjusted to transmit main beam ions at 4 kV accelerating voltage. Resolution was set to 1000 with 50% transmission on the slit preceding the electric sector. The datasystem was used to control magnetic field switching, and thus switched electric sector voltage as this was coupled via the linked scan unit.

Metastable peaks

The reaction chosen for monitoring was the loss of an acetyl radical from the molecular ion of warfarin i.e. m/z 308 → m/z 265, which from the full B/E scan was shown to produce the strongest daughter ion. m/z 265 is also the base peak in the normal electron impact (EI) mass spectrum of warfarin (see Fig. 1). In the case of the internal standard (**2**) this becomes m/z 313 → m/z 267, as two of the deuterium atoms remain after the loss of the acetyl group.

Setting up

The ion at m/z 314 in the mass spectrum of the standard reference compound perfluorotributylamine was used for initial determination of the B/E ratio, removing the need for the introduction of warfarin. This ion was selected with magnetic field controls, at a nominal

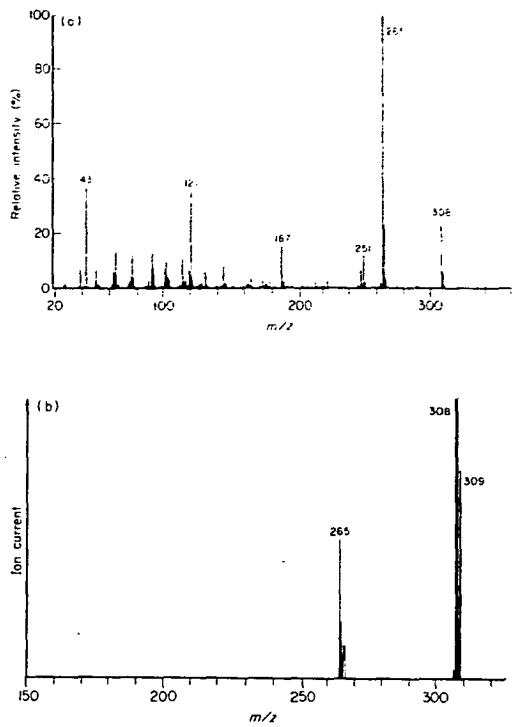

Figure 1. (a) Normal 70 eV electron impact mass spectrum of warfarin. (b) B/E Linked scan of warfarin from the molecular ion at m/z 308. The mass scale shows actual m/z values rather than apparent m/z values. The molecular ion is off scale, and is thirteen times the height of the first field free region m/z 265 daughter ion.

accelerating voltage of 4 kV (V1), and this magnetic field was then linked to the electric sector voltage so that when B was scanned the B/E ratio remained constant. This created a constant parent ion scan from m/z 314, transmitting only daughter ions formed in the first field free region. Using two of the independent potentiometers and switch positions on the accelerating voltage control unit, voltages $V2 = (308/314) \times V1 = 0.981\ V1$ and $V3 = (313/314) \times V1 = 0.997\ V1$ were accurately selected. This has the effect of bringing to focus at these positions the constant parent ion scans from m/z 308 and m/z 313, respectively, without the need to change the B/E ratio. The daughter ions formed at these voltages are nevertheless on the mass scale as initially determined by the selection of m/z 314. Hence these daughters follow the equation $m^* = \text{daughter mass}^2/\text{parent mass}$ where m^* is the apparent m/z value of the daughter ions and parent mass is 314.[14] Thus the two channels requested were $265^2/314 = 223.6$ and $267^2/314 = 227.0$. On the 70/70F in the linked scan mode the mass marker shows the actual mass of the daughter ions, so that these requested channels resulted in indicated values of 265 and 267, respectively. Two extra channels, at apparent m/z values 225.0 and 229.0 were also included to allow time for the accelerating voltage to be switched to the appropriate constant parent scan position. Dwell time per channel was 500 ms, which gave sufficient time to switch between the two preset

voltages in synchronization with the B/E switching to the genuine daughter channels. Although this may sound daunting, it was relatively simple as switching was required only every second, and the 500 ms dwell time in the extra channels meant that no great precision in timing was necessary. Clearly the automatic switching of the accelerating voltage in synchronization with the B/E switching would simplify the technique.

In this way the distillation off the direct insertion probe of compounds undergoing the unimolecular metastable fragmentations m/z 308 → m/z 265 and m/z 313 → m/z 267 could be monitored, and subsequently quantified by measurement of area of the ion current against time. The total time required for this setting-up procedure was approximately 5 min. Small quantities of both warfarin and internal standard were introduced prior to the acquisition of data to ensure the accurate centering of the respective channels.

Internal standard

The internal standard (**2**) was prepared by a previously described method,[5] using 50 mg warfarin sodium salt and 5 ml ^2H_2O. The product had an isotopic composition, as determined by direct insertion at an ion source temperature of 180 °C and corrected for ^{13}C isotope effects, of 0.4% $^2H_1$, 0.6% $^2H_2$, 4.6% $^2H_3$, 22.6% $^2H_4$, 53.9% $^2H_5$ (**2**) and 17.9% $^2H_6$ (**3**). A 2 μg μl^{-1} solution of the mixed isotope product in acetonitrile was prepared and stored at −20 °C. The isotopic composition of this solution was checked before each use to guard against back exchange.

The ion source temperature was maintained at a constant level throughout the acquisition of data from the samples and standard curve solutions, to ensure constant isotopic composition of the internal standard.[5]

In general, the number of deuterium atoms that should be present in the daughter ion to be monitored depends on the mass of the compound, the energy resolution of the instrument and the number of deuterium atoms in the parent compound. Thus for the Vacuum Generators 70/70F around mass 300 at least two deuteriums should remain in the daughter if the parent contains two or three deuteriums. This avoids interference from the ^{13}C sample daughter ion, which may be partially transmitted even when parents with two or three deuteriums atoms are requested for the reasons outlined below. For internal standards with four or more deuterium atoms, it should be possible to monitor daughters with only one deuterium.

Additional peaks

The $^2H_4$ product in the mixed isotopes will also contribute to some extent to the daughter at m/z 267, due to the relatively poor precursor resolution of the technique. The energy discrimination of the B/E scan results in the complete resolution of daughters of adjacent mass, but some ambiguity of assignment of precursors to daughters exists. This arises since daughters from adjacent precursors will be partially transmitted due to the energy spread of the daughter ions.[15] A consequence of the energy spread of the main beam is the inclusion of adjacent main beam peaks, as shown in Fig. 1(b) where m/z 307 and 309 are present in the spectrum. Instruments with higher energy resolution will have proportionally fewer of these main beam and first field free region additional peaks, and those transmitted will be of smaller relative intensity.

Sample preparation

Plasma samples (1 ml) from patients on regular but different warfarin regimes were acidified to pH 3.0 with 1M HCl. Internal standard solution (1 μl) was added and the plasma was extracted with 250 μl of chloroform. This was then centrifuged if necessary to separate the two phases. Aliquots (1 μl) of this extract were loaded onto the direct insertion probe for the monitoring of the two first field free region daughter ions.

Standard curve

To 1 ml aliquots of blank plasma, 0.5, 1, 2, 3 and 5 μg amounts of warfarin in acetone were added. Internal standard (1 μl) was added and extraction proceeded as for normal samples. A blank (internal standard only) was also included.

RESULTS

Figure 2(a) shows the result of monitoring the reaction m/z 308 → m/z 265 from a blank plasma extract (no internal standard), and clearly indicates the presence of this reaction to some extent in compounds other than warfarin. This could arise from molecular or fragment ions undergoing the identical reaction, or could arise from reactions from adjacent precursors giving rise to a daughter at m/z 265 for the reasons outlined above. Furthermore, metastable fragmentations from non field-free regions can also be detected by this procedure, as shown by a three dimensional approach to the representation of metastable peaks from a double focusing mass spectrometer.[16] Thus, daughter ions of m/z 265 arising from parents greater than m/z 308 during acceleration will create a ridge which will be a potential small source of background. Similarly, the ridge due to fragmentations within the electric sector from reactions where the ratio of (daughter mass)^2/(parent mass) is approximately the same as this ratio for the reaction under consideration will contribute to the background, when both parent and daughter masses are greater than those of the sample. For warfarin the ratio is $265^2/308 = 228.0$. The endogenous background can therefore be viewed as the sum of these various factors.

Figure 2(b) shows the result of monitoring the same reaction from plasma which had 1 μg ml^{-1} of added warfarin, representing typical therapeutic levels.[6,17] This is over 13 times the size of the blank, and clearly shows a distinct distillation profile off the probe. A pure warfarin sample exhibited the same profile.

Figure 2(c) shows the profile for the same reaction from a plasma sample which had internal standard added only. This also shows the warfarin profile, and arises from any $^2H_1$ and $^2H_2$ warfarin present in the internal

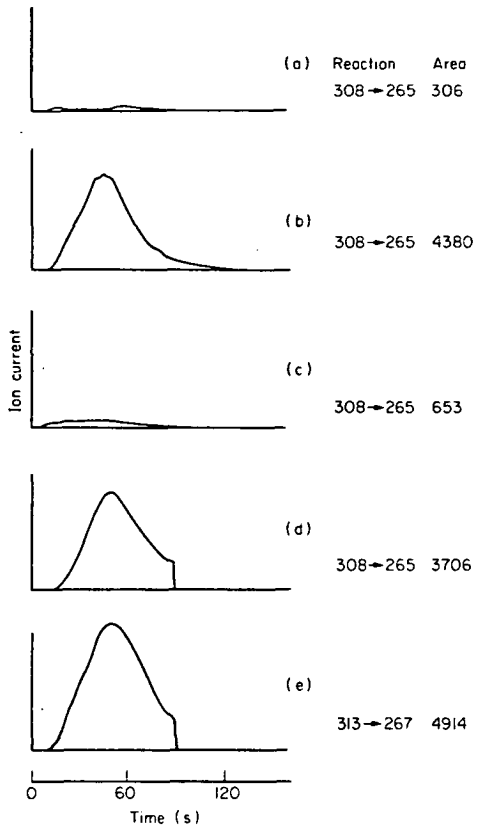

Figure 2. Each trace shows the metastable ion current versus time for the reaction indicated, with area in arbitrary units. The traces are drawn to the same scale and represent the material from 4 μl of plasma: (a) blank plasma; (b) plasma + 1 μg warfarin ml^{-1}; (c) plasma + internal standard only; (d) and (e) plasma from patient A.L., simultaneously acquired traces showing endogenous warfarin and internal standard.

standard, which will produce a proportion of daughters at m/z 265 partially transmitted at accelerating voltage V2. However, it would appear to have its main origin from fragmentations within the electric sector from the fully labelled ($^2H_5$) internal standard for the reasons outlined above, i.e. $267^2/313 = 227.8$ which is almost the same ratio as for normal warfarin, and hence fragmentations within the electric sector will be detected when monitoring the 308 → 265 reaction in the first field free region. This situation only arises due to the relative number of deuterium atoms in the parent and daughter ions, so that an internal standard can be designed so that the electric sector ridge from the internal standard does not intersect the sample first field free region daughter ion. The possibility of back exchange of the deuterium label also exists in this case where it has been synthesized by exchange, but a time course study of plasma with only deuterated warfarin added showed no measurable amount of ($^2H_0$)warfarin formed over 1 h.

For each determination it was not necessary to acquire the entire warfarin profile, as the internal standard would compensate for any material remaining on the probe. Therefore, to further speed up the assay data were normally only acquired until the levels had fallen to approximately 25% of the maximum value. The probe was then removed and the quartz tip flamed ready for the next sample.

Least squares linear regression analysis on the metastable peak ratios ((area m/z 380 → m/z 265)/(area m/z 313 → m/z 267)) obtained for the standard curve points versus warfarin concentration gave a line defined by $y = 0.11 + 0.63x$, with a correlation coefficient of 0.998. Repetitive determinations on the same plasma sample (1 μg ml^{-1}) gave an average ratio of 0.75, with a standard deviation of 0.05 (coefficient of variation 7.2%, $n = 5$).

Figure 2(d) shows the profile for the m/z 308 → m/z 265 reaction from the plasma of patient A.L., who was receiving a 7 mg oral dose of warfarin daily as part of normal therapy. Figure 2(e) shows the results from the internal standard channel for the same sample. Peak area ratio was therefore 3706/4914 = 0.75, which gave a value of 1.02 μg warfarin ml^{-1} plasma from the regression equation.

The results for patients on different warfarin regimes are summarized in Table 1, together with the prothrombin times for the same samples. Each concentration is the average of two determinations. The daily dose rates for each patient had been determined from previous prothrombin time data.

At the 0.5 μg ml^{-1} of plasma level, the amount of material loaded onto the probe corresponds to 2 ng warfarin. This gave a signal to noise ratio of 20:1, so that at normal levels sensitivity was more than adequate. However, the limitation to sensitivity is the background in the warfarin channel from the plasma and the internal standard for the reasons described, so that at a level of 0.2 μg ml^{-1} of warfarin in plasma, the signal is only twice that of a blank plasma with internal standard only. This then represents the approximate sensitivity limit of the assay. If the internal standard was changed by substituting deuterium at different sites (e.g. five deuterium atoms on the phenyl ring) then this background would be considerably lower, and hence the sensitivity of the assay will be increased.

The amount of plasma equivalent loaded onto the probe for each determination was 4 μl, and the amount of chloroform soluble (pH = 3) 'volatile' material (i.e.

Table 1. This shows the warfarin concentration in the plasma of five patients on continual warfarin therapy. Daily dose rates had been determined by monitoring of prothrombin time results. The natural differences in metabolic rate are reflected in the four-fold range of doses with less than two-fold range in warfarin concentrations

Patient	Concentrations of warfarin in plasma (μg ml^{-1})	Dose (mg)	Prothrombin time (min)
P.E.	0.55	5	2.2
M.A.	0.71	2	2.9
M.T.	0.59	2	3.5
S.E.	0.57	8	2.2
A.L.	1.02	7	1.7

with a boiling point less than or equal to 180 °C at 10^{-7} Torr such that it will vaporize in the ion source of the mass spectrometer) can be calculated from composition tables[18] to be on average about 20 μg. Since the majority of this is lipid material, an initial extraction at alkaline pH could be carried out if desired to remove this material,[5] and so reduce the quantity used to the order of single micrograms. Thus the amount of sample used in terms of ion source contamination likely to result is no more than would be used for normal probe spectra or individual gas chromatography mass spectrometry (GC/MS) runs, a factor which was critical to the success of the assay. Clearly if large quantities of plasma equivalent are used for each determination, this places an excessive amount of material into the ion source with subsequent increase in background levels. This generally will not interfere with the assay, but would prohibit subsequent acquisition of normal spectra and degrade instrument resolution. Where large quantities of plasma equivalent are required for sufficient sensitivity, some form of sample purification to reduce the amount of material being vaporized into the ion source would be required. Similarly where blank plasma shows an unacceptable degree of background for the reaction of interest, this may be overcome by selective purification of the sample prior to insertion.

DISCUSSION

The strength of the unimolecular first field free region metastable decompositions initially determines whether this technique can be used, and the ratio of the background for the chosen reaction to the endogenous level of the drug or metabolite in question ultimately decides the suitability of the assay. Collisional activation of ions in the first field free region to promote fragmentation, by the introduction of a collision gas, will generally increase the number and size of daughter ions. However, this will not necessarily result in any increase in specificity, as background from the plasma will also be increased.

It should be noted that several compounds could be monitored simultaneously by this method. The small changes in accelerating voltage used in any isotope dilution assay will not measurably decrease ion transmission. Nevertheless the same constraints applying to normal voltage switched selected ion monitoring exist, so that precursors covering a wide mass range cannot be covered by a single B/E ratio without a decrease in transmission. Very volatile compounds that have normally evaporated completely in a few seconds will require either faster magnet and accelerating voltage switching or a cooled probe to obtain sufficient sampling points for accurate quantification.

It is also necessary to guard against the possibility of interference from metabolites of the drug in question. If a metabolite is capable of producing an ion at the same mass as the parent drug, this fragment ion is likely to produce interfering daughters. This happens, for example, in the case of hydroxylated metabolites that lose an oxygen atom from their molecular ion, yielding an ion of the same mass as the parent drug. The analgesic phenacetin is an example in this class, so that to monitor the loss of ketene from the molecular ion at m/z 179 would also include the N-hydroxylated metabolite which yields a daughter at m/z 179 and a subsequent loss of ketene.[19] The various hydroxylated metabolites of warfarin do not produce an ion at m/z 308.[20] The ion at m/z 265 in these spectra comes from the ion at m/z 267, which in turn is derived from the molecular ion m/z 324, as well as m/z 306 and 281,[20] none of which interfere with either channel being monitored. The warfarin alcohol diastereoisomers resulting from the reduction of the ketone group produce the reaction m/z 310 → m/z 265,[20] which could produce a very minor interference peak when monitoring m/z 308 → m/z 265.

For the application to warfarin, this assay compares favorably with the gas chromatographic CI mass spectrometric assay[5] in sensitivity (similar values), time required per sample (2 min against 6 min) and specificity as judged by blank plasma traces. In addition, it avoids chromatographic 'active site' effects and loss of deuterium from the labelled compound. The main requirement for this type of assay is a double focusing mass spectrometer. While the method has been described for a magnetic/electric sector instrument of conventional geometry, it could be readily adapted to an instrument of reversed geometry using either first or second field free region metastable transitions, or to a multi-sector instrument of any type.

The major advantage of the method we describe over a previously published method of multiple metastable peak monitoring[13] is that no modifications to a standard commercial instrument were required. This does, however, involve a degree of manual operation not necessary in the other method. Furthermore, it is the application of a stable isotope dilution assay to the direct determination of a specific compound that is somewhat novel. While second field-free region metastable transitions in tandem mass spectrometers have been used for the direct determination of compounds in crude mixtures, using either full scans or selected reaction monitoring,[7,21] the use of first field-free region metastable transitions in conventional geometry double-focusing mass spectrometers has been largely applied to gas chromatographic mass spectrometric assays.

Providing the limitations of precursor resolution and 'ridge' effects from non field-free region transitions are recognized, this technique should be able to be applied to the qualitative and quantitative determinations of specific drugs and metabolites in body fluids. It is of particular value where conventional separation techniques are time consuming or the sample is labile. In the present study the technique provides a rapid method for the determination of plasma warfarin levels without the need for derivatization or chromatography of any form.

Acknowledgements

The authors wish to thank Dr D. Jupe and Ms R. Griffiths of the Haematology Department, Royal Hobart Hospital for seeking their assistance in determining plasma warfarin concentrations and for providing plasma samples and prothrombin results.

REFERENCES

1. P. G. Welling, K. P. Lees, U. Khanna and J. G. Wagner, *J. Pharm. Sci.* **59**, 1621 (1970).
2. R. J. Lewis and L. P. Ilnicki, *Clin. Res.* **17**, 332 (1969).
3. L. T. Wong, G. Solomonraj and B. H. Thomas, *J. Chromatogr.* **135**, 149 (1977).
4. K. K. Midha, I. J. McGilveray and J. K. Cooper, *J. Pharm. Sci.* **63**, 1725 (1974).
5. P. H. Duffield, D. J. Birkett, D. N. Wade and A. M. Duffield, *Biom. Mass Spectrom.* **6**, 101 (1979).
6. M. L'E. Orme and A. M. Breckenridge, in *Therapeutic Relevance of Drug Assays* edited by F. A. deWolff, H. Mattie and D. D. Breimer, p. 95. Leiden University Press (1980).
7. R. W. Kondrat, G. A. McLuskey and R. G. Cooks, *Anal. Chem.* **50**, 2017 (1978).
8. R. K. Boyd and J. H. Beynon, *Org. Mass Spectrom.* **17**, 451 (1977).
9. S. J. Gaskell, R. W. Finney and M. E. Harper, *Biomed. Mass Spectrom.* **6**, 113 (1979).
10. S. J. Gaskell and D. S. Millington, *Biomed. Mass Spectrom.* **5**, 557 (1978).
11. D. J. Harvey, J. T. A. Leuschner and W. D. M. Paton, *J. Chromatogr.* **202**, 83 (1980).
12. E. K. Chess and M. L. Gross, *Anal. Chem.* **52**, 2057 (1980).
13. D. A. Durden, *Anal. Chem.* **54**, 666 (1982).
14. N. W. Davies, J. C. Bignall and R. W. Lincolne, *Org. Mass Spectrom.* **17**, 451 (1982).
15. M. J. Lacey and C. G. McDonald, *Org. Mass Spectrom.* **14**, 465 (1979).
16. M. J. Lacey and C. G. McDonald, *Org. Mass Spectrom.* **12**, 587 (1977).
17. C. L. Winek, *Clin. Chem.* **22**, 832 (1976).
18. K. Diem and C. Lentner (Eds), *Scientific Tables*, seventh edition, J. R. Geigy S. A., Basle, Switzerland,
19. S. McLean, N. W. Davies, H. Watson, W. A. Favretto and J. C. Bignall, *Drug Metab. Dispos.* **9**, 255 (1981).
20. W. F. Trager, R. J. Lewis and W. A. Garland, *J. Med. Chem.* **13**, 1196 (1970).
21. F. W. McLafferty, *Acc. Chem. Res.* **13**, 33 (1980).

Received 15 November 1982

Journal of Chromatography, 310 (1984) 179—187
Biomedical Applications
Elsevier Science Publishers B.V., Amsterdam — Printed in The Netherlands

CHROMBIO. 2173

MASS SPECTROMETRIC DETERMINATION OF N-HYDROXYPHENACETIN IN URINE USING MULTIPLE METASTABLE PEAK MONITORING FOLLOWING THIN-LAYER CHROMATOGRAPHY

NOEL W. DAVIES, MAURICE E. VERONESE and STUART McLEAN*

School of Pharmacy and Central Science Laboratory, University of Tasmania, P.O. Box 252C, Hobart, Tasmania 7001 (Australia)

(First received January 26th, 1984; revised manuscript received April 4th, 1984)

SUMMARY

This work describes a method for the quantitative determination of the labile, toxic N-hydroxy metabolite of phenacetin in urine. A thin-layer chromatography step was used for the preliminary purification of extracts, and the specificity of the assay was based on the monitoring of specific metastable decompositions in a forward geometry double-focussing mass spectrometer, in a manner analogous to conventional tandem mass spectrometry. This precluded the need for a gas chromatographic separation, thus minimizing thermal decomposition which can occur with these compounds, as well as enabling very rapid analyses.

INTRODUCTION

The toxicity of the antipyretic—analgesic drug, phenacetin, is considered to be at least partly mediated by its N-hydroxy metabolite [1]. The formation of N-hydroxyphenacetin (NHP), and its biochemical reactivity, have been studied extensively in vitro, but little is known of the extent of N-hydroxylation of phenacetin in vivo. The problem has been to measure NHP, which is only formed in small amounts from phenacetin, in the presence of other phenacetin metabolites and endogenous interfering substances in urine. A variety of assays have been reported for NHP and similar N-arylacetylhydroxamic acids. At first, colorimetric methods were used for urinary analysis [2], but these lack specificity [3]. NHP and other N-arylacetylhydroxamic acids formed in biochemical reactions in vitro have been assayed by high-performance liquid chromatography (HPLC) [4, 5], gas chromatography—mass spectrometry (GC—MS) [6], and thin-layer chromatography (TLC) using radiolabelled phenacetin [7]. We have previously reported the assay of urinary NHP by GC

0378-4347/84/$03.00

of its methylated derivative, N-methoxyphenacetin (NMP), using flame-ionization detection [8]. However, as mentioned in that report [8], NMP can undergo decomposition under GC conditions, so we sought a more reliable assay of NHP.

This paper describes the determination of NHP, as NMP, using TLC to separate NMP from most interfering substances, followed by specific detection by MS using metastable peak monitoring. This MS technique deserves some introductory remarks.

Increasing use is being made of mass spectrometers with more than one analysing region to act as specific and sensitive detectors for target compounds in relatively impure samples. Much of this work has been carried out with reversed geometry [9, 10] or tandem quadrupole [11, 12] instruments. In these cases, the two sectors are used sequentially, the first to isolate an ion of interest and the second to examine its metastable or collisionally induced decomposition products (MS—MS). Full daughter ion spectra [13, 14] or selected daughter ion monitoring [15—17] have been used. Double-focussing mass spectrometers of normal geometry have also been used, in which the metastable or collisionally induced decompositions occur in the first field-free region, just after the ion source. This was used originally to increase the specificity of GC—MS [18, 19], and more recently has been applied to direct probe analyses [20, 21]. Although the sectors are not used sequentially in normal geometry instruments, since the products of specific decompositions are being monitored, it nevertheless constitutes a form of MS—MS.

EXPERIMENTAL

Materials

NHP was prepared and characterised as previously described [8]. As internal standard, the deuterated analogue of N-hydroxyphenacetin was synthesized from 4-nitro[2,3,5,6-$^2H_4$]phenol (KOR Isotopes, Cambridge, MA, U.S.A.). The deuterated 4-nitrophenol was first ethylated, using ethyl iodide–potassium carbonate in acetone, after the method of Vogel [22]. The resulting 4-nitro-[$^2H_4$]phenetole was reduced and selectively acetylated to give N-hydroxy-[2,3,5,6-$^2H_4$]phenacetin (DNHP), by the method used for the synthesis of unlabelled NHP [8]. DNHP was identical to NHP in m.p. (104°C) and TLC mobility, and on reduction with titanous chloride it yielded a single product which co-chromatographed with phenacetin on TLC [8]. The mass spectrum of DNHP was similar to that of NHP [23] except the major fragments were four a.m.u. higher. The isotopic purity was 98% $^2H_4$.

N-Butyryl-4-aminobenzoic acid (4-BABA) was prepared by reacting 4-aminobenzoic acid with butyric anhydride, and was recrystallized from 95% ethanol, m.p. 228—231°C. 4-BABA ran as a single substance on TLC, and its methylated derivative, N-butyryl-4-aminomethyl benzoate (4-BAMB), behaved as one compound on TLC and GC. The mass spectrum of 4-BAMB was consistent with its structure.

Diazomethane was made in small quantities, fresh as required, from *p*-tosylsulphonylmethylnitrosamide [22], and was used as the ethereal solution. Other chemicals and solvents were of analytical grade.

Extract of *Helix pomatia* (β-glucuronidase plus arylsulphatase) was obtained from Boehringer (Mannheim, F.R.G.).

Apparatus

Glass TLC plates (20 × 20 cm) were coated with silica gel (0.25-mm thick) containing a fluorescent marker (Sigma type GF, size 10—40 μm; St. Louis, MO, U.S.A.). The mass spectrometer was a Vacuum Generators (U.K.) 70/70F double-focussing instrument, with a digital scan controller, linked-scan unit, mode switch, 8-channel M.I.D. unit and 2035 data system with magnet switching selected ion software. The instrument was operated in the electron impact mode at 70 eV and 4 kV main beam accelerating voltage.

Extraction and methylation

Urine was collected from subjects who had taken a dose of phenacetin (10 mg/kg in two gelatin capsules), and samples were kept at −20°C until analysed. The analysis was commenced on the day of collection, since the glucuronide conjugate of NHP is known to be unstable in aqueous solution [24].

Calibration curves were obtained by addition of known amounts of NHP (in methanol) to urine from an undosed subject.

A 2-ml aliquot of urine was placed in a 30-ml stoppered centrifuge tube, 200 μl of 1.10 *M* acetate buffer, pH 5.2 were added and the final solution was adjusted to pH 5.2, if necessary, with 5 *M* hydrochloric acid. To this were added 100 μl extract of *Helix pomatia* and 25 μl of methanol containing the internal standard. The internal standard was originally 25 μg of 4-BABA, but eventually 5 μg of DNHP were used when DNHP became available. The mixture was incubated overnight (17 h) at 37°C to hydrolyse conjugated NHP.

The tubes were then cooled in ice, the hydrolysate adjusted to pH 1.0 with 5 *M* hydrochloric acid (200 μl) and extracted with 15 ml methylene chloride by vortexing for 30 sec. The phases were separated by centrifugation (1200 *g*, 5 min), and freezing (dry ice—acetone), and the methylene chloride decanted into a 50-ml round bottomed flask. The extract was taken to dryness on a rotary evaporator (40°C), the residue redissolved in 2 ml methanol, and cooled in ice. Methylation was achieved with 2 ml ethereal diazomethane (1 h, on ice) and the reaction mixture again evaporated to dryness.

Thin-layer chromatography

The residue in the flask was redissolved in 200 μl methylene chloride and applied as a 5-cm strip to a silica gel TLC plate, which was developed twice with chloroform. A band which moved with reference NMP (R_F 0.26) was scraped off and eluted by vortexing for 30 sec with 10 ml methanol. After sedimenting the silica gel by centrifugation (1200 *g*, 5 min) the methanol was transferred by Pasteur pipette to a 50-ml round bottom flask, and the solvent removed with a rotary evaporator. The residue was redissolved in 200 μl methylene chloride and transferred to a conical-tipped tube ready for analysis.

Mass spectrometry

The daughter ions chosen for monitoring NMP and DNMP were *m/z* 135

and 139, respectively (see Results). The two metastable peaks were alternately brought to focus by a combination of linked magnetic field/electric sector (B/E) and accelerating voltage switching, through a modification of a previously described method [21].

At a resolution of 1000, the ion at *m/z* 214 in the mass spectrum of perfluorotributylamine was selected as the starting point of a theoretical B/E linked scan (i.e. the magnetic field which transmitted *m/z* 214 was linked to the electric sector voltage). B/E scans from *m/z* 209 and 213 could then be easily focussed by small accelerating voltage adjustments [25]. Accelerating voltages $V_1 = (209/214) \times V_0$ and $V_2 = (213/214) \times V_0$, where V_0 was the accelerating voltage at which the main beam was being transmitted, were entered into two channels of the M.I.D. unit, the output of which was routed directly to the accelerating voltage programmed power supply, bypassing the normal electric sector coupling. The appropriate constant parent ion scans were then focussed when the respective channel was selected.

Two genuine daughter ion channels were entered, at *m/z* 85.16 ($= 135^2/214$) (channel 2), and *m/z* 90.28 ($= 139^2/214$) (channel 4) into the magnetic selected ion software, along with two additional channels at *m/z* 82.66 ($= 133^2/214$) (channel 1) and *m/z* 87.70 ($= 137^2/214$) (channel 3), with the linked scan unit remaining on. These channels resulted in *m/z* 133, 135, 137 and 139 daughter ions being selected, and to be shown as such on the mass indicator of the 70/70.

A small sample of standard NMP and DNMP was loaded onto the direct insertion probe, and using a small sweep of the B/E scan over 1 mass unit each genuine daughter channel was accurately centred with the appropriate M.I.D. channel selected. The collector slit was then opened to give flat topped peaks.

The accelerating voltage was cycled to switch during daughter channels 1 and 3 so that the appropriate voltage was selected when genuine daughter channels 2 and 4 were selected. Dwell time was 1 sec for each accelerating voltage channel, and 500 msec, including reset time, for each daughter ion channel, with a full cycle resulting every 2 sec. For synchronization, the accelerating voltage cycle was started and the magnet switching was then initiated at the appropriate instant to result in V_1 being selected during channel 1 and V_2 during channel 3.

To avoid a very rapid distillation of NMP from the probe, a relatively cool (120°C) source temperature was used. This resulted in the distillation maximizing at about 20 sec after insertion of the probe, providing 20 sampling points.

A 1-μl aliquot of the sample was loaded on to the direct insertion probe and the results of the 209 → 135 and 213 → 139 decompositions were acquired in the manner described, being displayed as intensity versus time. The area of each was measured on the data system and the ratio calculated for determination of unknown concentrations.

RESULTS AND DISCUSSION

Thin-layer chromatography

Preliminary experiments showed that the extracted hydrolysate contained

too many interfering substances for NHP to be determined by direct insertion MS—MS, as we had previously found it to be too impure for GC analysis [8]. TLC was used to separate NHP from most of these interfering compounds.

Methylation of NHP gave a stable derivative for TLC. NHP itself tails badly on silica gel [8], possibly because of chelation to trace metals [4]. Hinson and Mitchell [7] found it necessary to add non-radioactive NHP to minimize adsorption losses of [^{3}H]NHP during their TLC assay.

Recovery from urine

Blank urine was spiked with NHP to examine the effect of pH on the extraction of NHP into methylene chloride. In this experiment 4-methylacetanilide was used to standardize the GC assay [8]. Recovery of NHP was better at pH 1 (95%) than at pH 3 or 5 (65%).

The methylation reaction mixture was analysed at various times up to 24 h to check on the completeness of NHP conversion to NMP. The reaction was 90% complete in 30 min, and no further NMP was formed after 1 h.

Optimal conditions for hydrolysis of conjugated NHP were found by treating urine from a subject dosed with phenacetin with different amounts of enzyme and various incubation times. It was found that 0.1 ml extract *Helix pomatia* per 2 ml urine gave the highest recovery of NHP, as well as most phenolic metabolites of phenacetin (to be reported elsewhere). An exception was 2-hydroxyphenacetin (2HP), whose recovery, and therefore hydrolysis, was maximal with 0.04 ml enzyme mixture. Incremental additions of enzyme (0.02 ml) resulted in a progressive decline in 2HP recovery, and a concomittant increase in NHP found. It seems likely that this reciprocal relationship is due to two competing reactions: the rearrangement of NHP-glucuronide to 2HP-glucuronide [24] and the enzymatic hydrolysis of the NHP-glucuronide. More enzyme, and therefore a faster hydrolysis, leaves less time for the rearrangement to occur. Lacking an NHP-glucuronide standard, we were unable to check on the extent of residual isomerization under conditions giving maximum recovery of NHP.

Using 0.1 ml enzyme, hydrolysis was found to be complete after incubation for 17 h (overnight).

Mean overall recovery was 63%, estimated from the NMP/DNMP ratio found when 5 μg NHP were added to urine and 5 μg DNHP added at the methylation step.

Mass spectrometry

Fig. 1 shows the normal 70-eV mass spectrum of NMP, with that of DNMP, in which all the major ions are shifted by 4 a.m.u. A full B/E linked scan from the molecular ion (*m/z* 209) of NMP, to find the direct daughter ions from the first field-free region, gave a spectrum with *m/z* 179 (2.5%), 178 (5%), 167 (100%), 166 (10%), and 135 (18%) as the only significant peaks. The ions at *m/z* 167 and 166 corresponded to the loss of ketene and an acetyl radical respectively, and were also found to occur in the normal and B/E spectra of the isomeric ring methoxylated compounds, 2- and 3-methoxyphenacetin [23]. Therefore these daughter ions were not suitable for monitoring NMP in the presence of isomeric phenolic metabolites of phenacetin. However, the

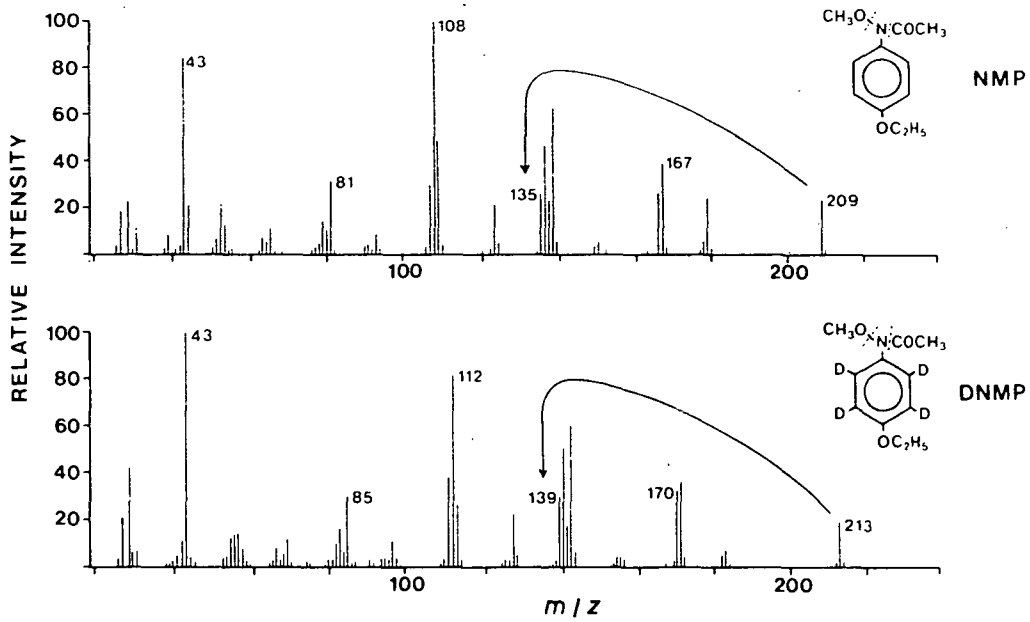

Fig. 1. Electron impact mass spectra of NMP and DNMP, with arrows showing the metastable reactions monitored for quantitative analysis. Broken lines show the sites of cleavage in these reactions.

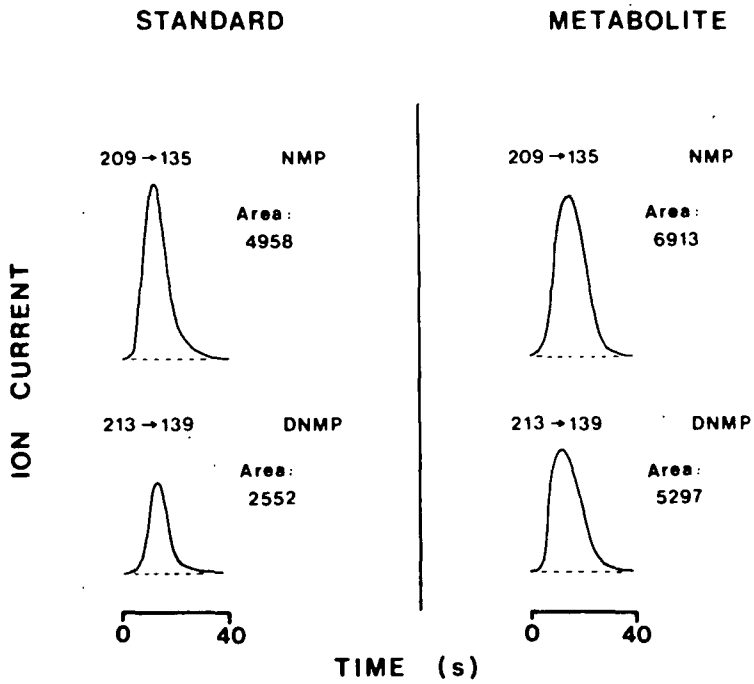

Fig. 2. Ion traces obtained during metastable peak monitoring of NMP and DNMP. The left side shows a calibration standard, in which 10 μg NHP was added to 2 ml blank urine. The right side shows analysis of urine following a dose of phenacetin; 6.7 μg NHP was found per 2 ml urine.

daughter ions at *m/z* 179, 178 and 135 were not found to be present in the normal or B/E spectra of the ring-substituted compounds, making them suitable candidates for a specific assay. Due to the relative size, and specificity of the loss, the ion at *m/z* 135 was chosen as being the most suitable. This ion was found from the high-resolution studies of the main beam *m/z* 135 ion to be C_8H_9NO, corresponding to the loss of the elements of the acetyl and methoxy groups by an undetermined mechanism. Thus the decompositions monitored were 209 → 135 for NMP, and 213 → 139 for DNMP, as indicated in Figs. 1 and 2.

An extract of hydrolysed urine from an undosed subject, without any preliminary purification, was monitored for these decompositions to determine the extent, if any, of interference from compounds other than NMP. This indicated there was some interference from other 209 → 135 decompositions, or additional reactions which could be focussed under the conditions employed [21]. Although the interference did not display the distillation profile of NMP from the direct insertion probe, it would nevertheless have made accurate quantification difficult. Hence a preliminary purification was necessary, and the TLC procedure was employed. An examination of the extract of a TLC scrape at the R_F of NMP from an undosed subject indicated virtually no detectable signal in either channel being monitored.

Calibration curve

Addition of NHP (1—20 μg) and DNHP (5 μg) to 2 ml blank urine gave a good linear relationship using either peak heights or peak areas (ratio NMP/DNMP versus amount NHP added). Peak areas gave a slope of 0.191, *y*-intercept 0.03, and correlation coefficient 0.9983. Peak heights gave a slope of 0.186, *y*-intercept 0.055, and correlation coefficient 0.9994. Repeated measurements on the same sample gave an instrumental coefficient of variation (C.V.) of 1.94% (n = 8). Replicate assays using eight lots of 2 ml urine from one urine collection sample from a subject who had taken phenacetin gave a C.V. of 9.2% (by peak area) and 7.2% (by peak height).

The selectivity of the assay depends on two separation steps: (1) TLC and (2) the selection of specific daughter ions produced from the molecular ions of NMP and DNMP in the first field-free region of the mass spectrometer. Thus NHP can be assayed in the presence of many other metabolites of phenacetin which are mostly formed in far greater amounts.

In early experiments, before DNHP was available, 4-BABA was used successfully as an internal standard. In this case the metastable reaction monitored was 221 → 151 (the molecular ion losing C_4H_6O). There was no interference from blank urine, and the calibration curve was linear (slope 0.0098, *y*-intercept 0.0018, correlation coefficient 0.9993). The only unsatisfactory aspect of 4-BAMB was that it distilled off the probe much more slowly than NMP, which considerably prolonged the MS analysis time. DNMP, having the same distillation profile as NMP, enabled much faster analyses, and is the ideal internal standard.

Formation of NHP from phenacetin in man

Fig. 3 shows the urinary excretion of NHP by a male subject following a

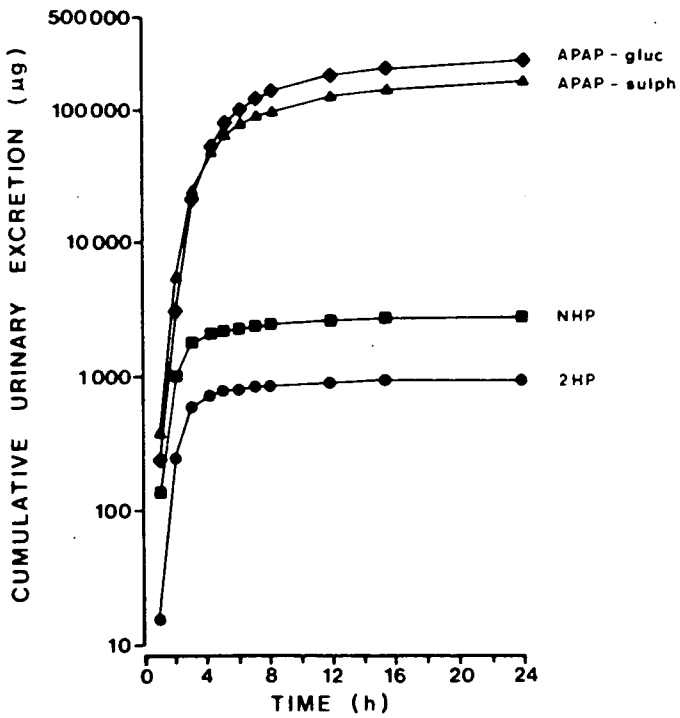

Fig. 3. Cumulative urinary excretion of NHP and some other phenacetin metabolites, following an oral dose of 10 mg/kg phenacetin in a male subject. APAP-gluc (♦) is paracetamol glucuronide and APAP-sulph (▲) is paracetamol sulphate. These two major metabolites of phenacetin are included for comparison with NHP (■) and 2HP (●), and their HPLC determination will be described in a separate communication.

dose of phenacetin (10 mg/kg, orally in two gelatin capsules). The presence of NHP in urine was separately confirmed by GC—MS, as previously described [8]. The total amount of NHP excreted in 24 h corresponded to 0.40% of the dose of phenacetin. This is comparable with the finding of 0.28% NHP after 900 mg phenacetin, in which NHP was determined by its ability to chelate copper and extract it into water [2]. However, in view of the complex metabolism of phenacetin, we believe that our structurally specific assay is preferable.

The assay is sensitive to less than 0.5 µg NHP per ml urine, which appears quite adequate for metabolic studies involving urine analysis.

ACKNOWLEDGEMENTS

We are grateful to Mrs. Heather Galloway for technical assistance and for drawing the figures, and to Miss Helen Lawler for typing the manuscript. We are particularly grateful to Mr. M. Power for the modification of the mass spectrometer electric sector coupling.

REFERENCES

1 J.R. Gillette, S.D. Nelson, G.J. Mulder, D.J. Jollow, J.R. Mitchell, L.R. Pohl and J.A. Hinson, in R. Snyder, D.V. Parke, J.J. Kocsis, D.J. Jollow, C.G. Gibson and C.M. Witmer (Editors), Biological Reactive Intermediates - II, Plenum, New York, 1982, p. 931.

2 S. Belman, W. Troll, G. Teebor and F. Mukai, Cancer Res., 28 (1968) 535.
3 J.H. Weisburger and E.K. Weisburger, Pharmacol. Rev., 25 (1973) 2.
4 M.D. Corbett and B.R. Chipko, Anal. Biochem., 98 (1979) 169.
5 J.A. Hinson, L.R. Pohl and J.R. Gillette, Anal. Biochem., 101 (1980) 462.
6 I.M. Kapetanovic, J.S. Dutcher and J.M. Strong, Anal. Chem., 49 (1977) 1843.
7 J.A. Hinson and J.R. Mitchell, Drug Metab. Dispos., 4 (1976) 430.
8 S. McLean, N.W. Davies, H. Watson, W.A. Favretto and J.C. Bignall, Drug Metab. Dispos., 9 (1981) 255.
9 R.W. Kondrat and R.G. Cooks, Anal. Chem., 50 (1978) 81A.
10 F.W. McLafferty, Acc. Chem. Res., 13 (1980) 34.
11 R.A. Yost and C.G. Enke, Anal. Chem., 51 (1979) 1251A.
12 R.A. Yost, H.O. Brotherton and R.J. Perchalski, Int. J. Mass Spectrom. Ion Phys., 48 (1983) 77.
13 G.A. McLuskey, R.G. Cooks and A.M. Knevel, Tetrahedron Lett., 46 (1978) 4471.
14 J. Henion, G.A. Maylin and B.A. Thomson, J. Chromatogr., 271 (1983) 107.
15 R.W. Kondrat, G.A. McLuskey and R.G. Cooks, Anal. Chem., 50 (1978) 2017.
16 M. Youssefi, R.G. Cooks and J.L. McLaughlin, J. Amer. Chem. Soc., 101 (1979) 3400.
17 P. Prome, C. Lacave, J. Roussel and J.C. Prome, Biomed. Mass Spectrom., 9 (1982) 527.
18 S.J. Gaskell and D.S. Millington, Biomed. Mass Spectrom., 5 (1978) 557.
19 S.J. Gaskell, R.W. Finney and M.E. Harper, Biomed. Mass Spectrom., 6 (1979) 113.
20 E.K. Chess and M.L. Gross, Anal. Chem., 52 (1980) 2057.
21 N.W. Davies, J.C. Bignall and M.S. Roberts, Biomed. Mass Spectrom. , 10 (1983) 646.
22 A.I. Vogel, Practical Organic Chemistry, Longmans, London, 1956.
23 N.W. Davies, W. Lenk and S. McLean, Org. Mass Spectrom., 17 (1982) 649.
24 G.J. Mulder, J.A. Hinson and J.R. Gillette, Biochem. Pharmacol., 27 (1978) 1641.
25 N.W. Davies, J.C. Bignall and R.W. Lincolne, Org. Mass Spectrom., 17 (1982) 451.

Updating Instrument Control Modes on a VG 7070F

N W Davis
Central Science Laboratory, University of Tasmania, PO Box 252C, Hobart, Tasmania, Australia

INTRODUCTION

The normal operational modes on a VG 7070F double focussing mass spectrometer can be updated by relatively simple modifications to allow independent control of the magnetic sector field (B), the electric sector field (E) and the accelerating voltage (V). This enables multiple reaction monitoring of metastable or collisionally induced decompositions in the first field free region (1st FFR) for added specificity when targeting specific compounds by qualitative or quantitative mass spectrometry or gas chromatography-mass spectrometry (GCMS). The acquisition of data for ion current surfaces (Lacey and McDonald, 1977) is also made simpler and more flexible.

METHODS

Where a "DIGMID" unit is present, this makes an ideal source of accurately controlled 0 to 10V input for stepping either E or V between magnetic sector scans for mapping ion current surfaces. The only modification required is to the cable connections. Use of 'continuum' mode during data acquisition gives up to 4000 data points per scan. Where a DIGMID and digital scan controller are both present then multiple reaction monitoring is also possible simply with changes to cable connections. If only one multichannel variable voltage supply is present, an independent unit will be required. Due to the relatively slow magnet response, rapid cycling between different decompositions can best be achieved by synchronized independent control of E and V, with fixed B. For this case, with any main beam ion m_a focussed with $B = B_o$, $E = E_o$ and $V = V_o$, a 1st FFR decomposition m_b --> m_c can be focussed with $B = B_o$, $E = (m_a/m_c)E_o$ and $V = (m_a m_b/m_c^2)V_o$. Figure 1a illustrates the normal mode of operation for an instrument equipped with a digital scan controller. Figure 1b shows the necessary modifications to enable steps of V between scans of B for mapping of ion current surfaces. This same configuration, using two or more channels on the independent voltage source (in this case the DIGMID) and on the normal selected ion mode, enables multiple reaction monitoring with changes to B and V or E and V.Suitable choice of dwell times enables synchronization to be maintained for the length of GCMS analyses. Mapping by control of E and B is possible by connecting the independent input to the electric sector power supply, while providing fixed accelerating voltage from the decoupled ('manual') position of the accelerating voltage power supply.

178

RESULTS

Figure 2 shows a portion of the cross section through the ion current surface for camphor, obtained at $\rho = 0.722$, where $\rho = (V_0/V)(E/E_0)$, with the configuration shown in Figure 1b. This is the result of five averaged scans at 10 s/decade. Figure 3 shows the results of GCMS multiple reaction monitoring for the 1st FFR metastable decompositions 386 --> 371 for the trimethylsilyl (TMS) derivative of Δ^1-tetrahydrocannabinol (THC) (Harvey *et al* 1980), the active constituent of cannabis, and 389 --> 374 for 5'-$^2H_3$ - THC (internal standard) for a blood sample containing 2.5 ng/ml of THC and (nominally) 10 ng/ml of the internal standard. This was achieved by independent control of E and V with a cycle time of 1 second. Chromatography was on a 25m x 0.32mm x 0.52μ HP-1 column directly coupled to the ion source and temperature programmed from 60° to 280° at 30°/minute.

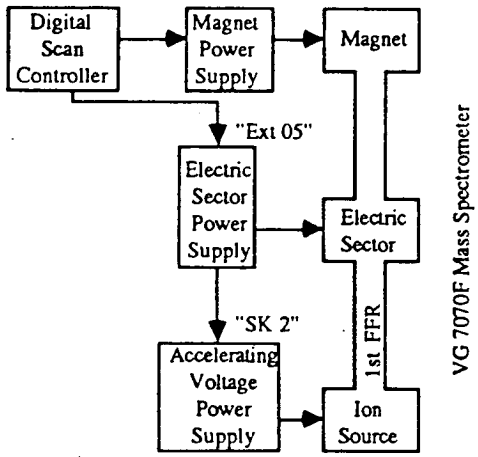

Figure 1a

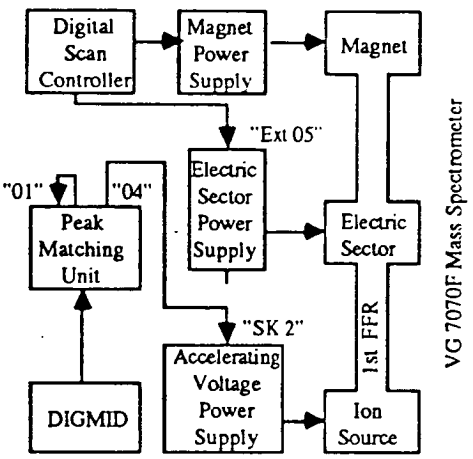

Figure 1b

Figure 1. Schematic diagram of normal and modified connections

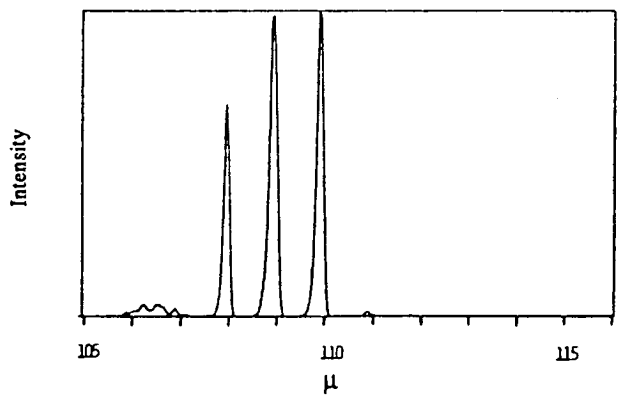

Figure 2 Cross section of the ion current surface for camphor. $\mu = (E_0/E)m_B$ where m_B is the mass of a singly charged main beam ion transmitted with $V = V_0$ and $E = E_0$. This corresponds to the normal calibrated mass scale with accelerating voltage adjustments to ρ.

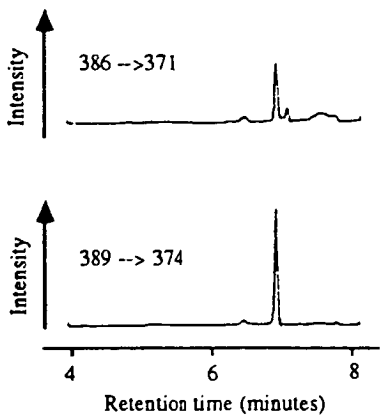

Figure 3. Multiple reaction monitoring GCMS for THC and deuterated internal standard from blood.

D.J. Harvey, J.T.A. Leuschner and W.D.M. Paton. J. Chromatogr. 202, 83 (1980).
M.J. Lacey and C.G. McDonald. Org. Mass Spectrom. 12, 587 (1977)

Dear Sir

A Rapid Method for the Generation of Multiple Constant Parent Ion Spectra

Linked scans of the magnetic field (B) and the electric sector voltage (E) at constant accelerating voltage (V) to produce spectra containing only ions originating in the 1st field free region (FFR) of double focusing mass spectrometers are well known.[1,2] Three-dimensional representation by various techniques using more than one scanning mode has been shown to provide the maximum amount of information about metastable peaks for cases where sample size is not limiting.[3-5] Computer techniques now also allow for automatic switching to linked scans during normal magnet scans, using previously entered calibration files for each desired daughter or precursor.[6]

We would like to point out a simplified procedure for the acquisition of all desired constant parent ion spectra for a given sample, based on the linked scan at constant B/E. Normally, individual scans would be carried out for each parent ion using different B/E ratios for each, at constant accelerating voltage. This necessitates changes in the initial magnetic field and electric sector voltage to be selected manually, and also results in a new mass scale. This can be time-consuming and wasteful where sample size is limited. A much faster way of generating constant parent ion spectra for all required parents is to set up on the initial precursor (P_1), at B_1, E_1 and V_1 in the normal manner, and then for each subsequent precursor P_n change the accelerating voltage to P_nV_1/P_1 and scan at constant B/E using the same ratio as set up for P_1 ($=B_1/E_1$). This generates a B/E scan from each precursor without the need to change the B/E ratio, and at the same time maintains the correct mass scale for all scans.[5] This mass scale is normally already adjusted for the apparent mass of the 1st FFR daughters ($=D^2/P$ where D is the m/z value of the daughters formed in the ion source), so that ions appear at their actual m/z values.

While it is not desirable to lower accelerating voltage in general, in practice a moderate lowering of voltage results in an acceptable loss in transmission. If parents less than $0.8\,P_1$ are required, then V may need to be changed back to V_1 and a new B/E ratio entered.

A justification of the above considerations can be seen from the following. If two parents P_1 (at B_1, E_1 and V_1) and P_2 give rise to daughters D_1 and D_2 respectively, since $m/z = B^2R^2/2V$ where R is the radius of curvature of the magnet, main beam daughters are transmitted at magnetic fields of $B_1(D_1/P_1)^{1/2}$ and $B_1(D_2/P_1)^{1/2}$, while 1st FFR daughters will be transmitted at D_1B_1/P_1 and $D_2B_1/(P_1P_2)^{1/2}$ respectively. In the normal linked scan at constant B/E from P_1 at constant V, 1st FFR D_1 ions would require an electric sector voltage of D_1E_1/P_1 and all daughters would be transmitted at a B/E ratio of B_1/E_1. Similarly, a normal linked scan at constant B/E from P_2 at V_1 would produce 1st FFR D_2 ions at $B = D_2B_1/(P_1P_2)^{1/2}$ and $E = D_2E_1/P_2$, and a B/E ratio of $P_2B_1/E_1(P_1P_2)^{1/2}$.

The same 1st FFR ions will be transmitted at different accelerating voltage, provided the ratios E/V and B^2/V remain constant, as m/z is proportional to both. Hence, the new values are $x^{1/2}B_n$, xE_n and xV_n, where B_n, E_n and V_n are the original values for D_2, and x is the factor by which V is to be changed. If the B/E ratio is to be the same as for P_1 daughters, substitution gives

$$\frac{x^{1/2}D_2B_1P_2}{x(P_1P_2)^{1/2}D_2E_1} = B_1/E_1$$

$$x^{1/2} = P_2/(P_1P_2)^{1/2}$$

$$x = P_2/P_1$$

The new values then become D_2B_1/P_1, D_2E_1/P_1 and P_2V_1/P_1. Thus, all constant parent scans can be generated at the same B/E ratio. The mass scale as set up for P_1 is still correct since D_2B_1/P_1 is the magnetic field required, before accelerating voltage was changed, to focus any D_2 ions arising from P_1. Similarly, main beam P_2 ions are also placed on the correct mass scale.

This procedure facilitates the rapid acquisition of all constant parent scans for a given sample, with only a few seconds required to manually adjust the accelerating voltage to the calculated positions between successive scans. A further advantage is that an ion from a reference compound such as heptacosatributylamine, slightly lower than the highest precursor required, can be used for the initial setting up of the B/E ratio, and the accelerating voltage increased to bring in P_1 before successive reduction for subsequent precursors. Thus, any valuable sample is not required prior to the actual acquisition of the data.

There are also analytical applications for this method using selected metastable ion monitoring for the analysis of mixtures, either in conjunction with gas chromatography mass spectrometry or as direct mixture analysis.[7-9] In this case an internal standard could be employed with rapid switching between daughters from the sample and the standard. The linked scan at constant B/E would be linked to accelerating voltage as well as to a peak switching unit, thus enabling any daughter from any parent to be readily focused. Furthermore, computer acquisition of normal linked scan data would be facilitated by using the same mass scale for different constant parent scans, thus requiring at most only a few calibration files to cover the entire mass range.

Yours

NOEL W. DAVIES, JOHN C. BIGNALL and ROSS W. LINCOLNE
Central Science Laboratory,
University of Tasmania,
P.O. Box 252C,
Hobart,
Tasmania,
Australia 7001

November 1981

References

1. R. K. Boyd and J. H. Beynon, *Org. Mass Spectrom.* **12**, 163 (1977).
2. D. S. Millington and J. A. Smith, *Org. Mass Spectrom.* **12**, 264 (1977).
3. M. J. Lacey and C. G. Macdonald, *Org. Mass Spectrom.* **12**, 587 (1977).
4. M. J. Lacey and C. G. Macdonald, *Org. Mass Spectrom.* **13**, 243 (1978).
5. M. J. Lacey and C. G. Macdonald, *Org. Mass Spectrom.* **14**, 465 (1979).
6. W. F. Haddon, *Anal. Chem.* **51**, 983 (1979).
7. F. W. McLafferty and F. M. Bockoff, *Anal. Chem.* **50**, 69 (1978).
8. S. J. Gaskell and D. S. Millington, *Biomed. Mass Spectrom.* **5**, 557 (1978).
9. D. A. Durden, Paper MPB2, American Society for Mass Spectrometry, 29th Annual Conference on Mass Spectrometry and Allied Topics, Minneapolis, Minnesota (1981).

Dear Sir

Distinction Between Epimeric 3-Hydroxy Steroids by Mass Analysed Ion Kinetic Energy Spectrometry

Steroids have been extensively studied by conventional mass spectrometry,[1] and it is known that the stereochemistry of the A/B ring junction and the orientation of a hydroxy substituent at the ring system may influence the peak pattern of the mass spectra.[2] Recently, Larka *et al.*[3] have shown that epimers of certain steroidal hydrocarbons and ketones can be distinguished by differences in the kinetic energy released during $CH_3^{\cdot}$ loss from the molecular ions. Usually, the value of $T_{0.5}$ is larger for the 5α-isomer. During the course of an extended study of steric effects in the mass analysed ion kinetic energy (MIKE) spectra of stereoisomeric cyclic alcohols[4] we also investigated the fragmentations of metastable molecular ions of some stereoisomeric 3-hydroxy steroids after 70 eV electron impact ionization in the 2nd field free region of a VG ZAB 2F mass spectrometer. For all the compounds investigated loss of $CH_3^{\cdot}$ and H_2O, respectively, from metastable molecular ions was observed. The values of the kinetic energy T released during these fragmentations are given in Table 1. It is clearly seen that the correlation observed by

Journal of Chemical Ecology, Vol. 11, No. 8, 1985

MANDIBULAR GLAND SECRETIONS OF TWO PARASITOID WASPS (HYMENOPTERA: ICHNEUMONIDAE)

N. W. DAVIES[1] and J. L. MADDEN[2]

[1]*Central Science Laboratory*
[2]*Faculty of Agricultural Science*
University of Tasmania
P.O. Box 252C
Hobart, Tasmania 7001 Australia

(Received August 20, 1984; accepted December 19, 1984)

Abstract—Males of *Rhyssa persuasoria* and *Megarhyssa nortoni nortoni* exhibit marked aggregation behavior prior to and during the emergence of females from host trees, and this has been linked with the secretion of an odorous liquid from the mandibular glands. The volatile components of these secretions were examined by combined gas chromatography–mass spectrometry. While both species contained 6-methylhept-5-en-2-one, *M. nortoni nortoni* was characterized by a series of alkyl spiroacetals and *R. persuasoria* contained 3-hydroxy-3-methylbutan-2-one. The same spiroacetals have previously been isolated from the mandibular glands of other Hymenoptera and have been directly associated with aggregation behavior in some species. The chemical and behavioral aspects of the two species are discussed.

Key Words—Mandibular secretions, parasitoids, aggregation pheromones, spiroacetals, 6-methylhept-5-en-2-one, 3-hydroxy-3-methylbutan-2-one, *Rhyssa, Megarhyssa*, Hymenoptera, Ichneumonidae.

INTRODUCTION

The parasitoids *Megarhyssa nortoni nortoni* Cresson (hereafter referred to as *M. nortoni*) and *Rhyssa persuasoria* L. (Hymenoptera: Ichneumonidae) were introduced into Australia as natural enemies of the wood wasp, *Sirex noctilio* F., an exotic pest of radiata pine (*Pinus radiata* D Don) (Taylor, 1967). Both species attack mature larvae of *S. noctilio* within the wood of infested trees to emerge, in general, 12 months later.

Males of both species aggregate at sites of potential emergence or at sites

0098-0331/85/0800-1115$04.50/0

which are otherwise attractive. The aggregation response is initiated by volatiles produced by the symbiotic fungus of *S. noctilio, Amylosterum areolatum* (Madden, 1968). Localized generation of fungal volatiles is presumably stimulated by moisture changes associated with adult eclosion, since injection of water into fine drill holes made in dry, fungus-infested logs will promote aggregation at such sites after 24–48 hr (Madden, unpublished results).

The aggregation behavior of male *M. nortoni* is similar to that described for several other *Megarhyssa* species (Heatwole et al., 1963; Crankshaw and Matthews, 1981), and the group is typically compact with arching of the abdomen so that the distal abdominal segments make contact with the bark substrate at the point of interest discerned by the antennae. Aggregations of *R. persuasoria* are less compact and males are incapable of arching their abdomens, although curvature of the abdomen may be observed.

In laboratory studies with *M. nortoni* males, presentation of the fungus on agar or water extracts of insect frass is sufficient to initiate individual interest followed by, through 4-min exposure periods, accelerated recruitment of males to the sites. This second response is a function of the number of males making contact with each other (Madden, unpublished results). In this situation mutual antagonism occurs between individuals, in which opening of the mandibles is observed. Furthermore, the rapid drumming of the antennae at the sites of emerging insects elicits a like response in the emergent. In the majority of cases, the space between the mandibles is observed to be occupied by a liquid.

Depending on the species of the emergent, a number of outcomes may occur: (1) If the emergent is a nonparasitoid, e.g., *S. noctilio*, the male aggregation of either parasitoid is retained and males will mount the emergent and display precopulatory movements. (2) If the emergent parasitoid species is a conspecific, of either sex, precopulatory activity is enhanced and mounting occurs. (3) If the emergent parasitoid species is dissimilar, the males' precopulatory activity, which may include males mounting males, will subside and the aggregation will disperse.

The odor of each species is characteristically different and, in preliminary experiments, it was found that it could be released if the insects were grasped or shaken. In addition, mandibular opening with the appearance of liquid could be elicited by swift decapitation. The odor source was clearly localized in the head, as crop and stomach contents and thorax and abdomen possessed no such odor.

It would appear that this secretion plays an important role in the complex species recognition, aggregation formation, and defensive behavior of the two species. This paper reports the chemical identity of the major volatile compounds occurring in the mandibular secretion of male and female *R. persuasoria* and *M. nortoni*. Compound classes encountered include spiroacetals, ketones, alcohols, and esters.

METHODS AND MATERIALS

Insect Material. Insects were collected as they emerged from infested logs in an insectary, were kept in polystyrene pots, provided with water and honey, and held at 10°C between tests. They were then available for bioassy or chemical examinations as required.

Three main approaches were used in the study of the volatiles. These were the direct collection of the secretions from stimulated individuals, examination of extracts of dissected mandibular glands to confirm the origin of the secretion, and the examination of extracts of excised heads. Males and females were treated separately.

Collection of Secretions. The mandibular secretions were collected in the following manner. Individual insects were grasped at the thorax between thumb and forefinger, an action which resulted in the opening of the mandibles and the appearance of the secretion in variable amounts. The tip of a 1-μl microcapillary tube (Microcaps, Drummond Scientific Co., Broomall, Pa.) was placed between the extended mandibles resulting in the uptake of the liquid. The microcap was either immediately dropped into, or its contents flushed into, a vial of pentane. Maximum yield per collection ranged from 0.25 μl to 0.80 μl for *R. persuasoria* and *M. nortoni*, respectively. In general greater quantities were obtained from females and *M. nortoni*. Insects were returned to a new container, stored at 10°C, and could be processed daily for up to 14 days.

Gland Material. Mandibles and associated glands, gland reservoirs, and muscles were dissected from parasitoids that had been killed by short exposure to −20°C prior to analysis. Ten to fourteen mandibles for each species and sex were prepared. In another approach, insects were decapitated, antennae removed, and the heads stored in pentane.

Extraction. The frozen gland material and heads were crushed and left in pentane overnight. The gland extract was filtered and used without further work-up after evaporation to minimum volume. The head extracts were washed with 5% sodium bicarbonate solution to remove fatty acids, dried over $MgSO_4$, and evaporated to a minimum volume prior to injection.

Bioassay. The response of male parasitoids to live females contained in perforated vials, excised female heads, and mandibular secretion was evaluated. In paired comparisons, presentation of a test subject to 25 males of one species was alternated with a similar presentation to 25 males of the second species through 10 presentations for each of the three species treatments. The number of males that visited or revisited and drummed the test site with their antennae during a 2-min exposure was recorded to evaluate the response to each treatment.

Gas Chromatography-Mass Spectrometry. A Pye 204 gas chromatograph was employed, directly coupled to a VG 70/70F mass spectrometer with 2035

data system. The mass spectrometer was normally operated in the electron impact mode at 70 eV, 4 KV accelerating volts, and a source temperature of 200°C. Scans from *m/z* 350–20 were stored every 1.6 sec. Chemical ionization analyses were carried out with isobutane as the reagent gas at a pressure of approximately 1 torr in the ion chamber. Accurate masses were determined at a resolution of 1000 by means of perfluorokerosene as an internal reference with peak times relative to the reference peak times being used. The gas chromatography was carried out on 50-m × 0.2-mm fused silica OV-101 or 25-m × 0.2-mm BP1 (bonded-phase equivalent of OV-101, SGE Pty. Ltd) with the column passing through into the ion source. The carrier gas was hydrogen, with a flow rate at 70°C of 1.8 ml atm/min (Davies, 1984). Injections were splitless at 250°C, and a typical column temperature program was 70–250° at 4°/min.

The mandibular secretions inside microcapillaries were sealed inside larger capillaries (2 cm × 1 mm) and injected with a capillary crusher, a modification of a previously described device (Stanley and Kennett, 1973).

Hydrogenations were carried out in sealed Reacti-vials (Pierce) using Adams catalyst. Methylations were carried out with ethereal diazomethane. Trimethylsilylation was carried out with BSTFA (Pierce), and methoxime derivatives were prepared with methoxylamine hydrochloride (2% in pyridine).

Identifications were based on GC retention indices, mass spectra, chemical modification of functional groups and, where possible, by comparison with authentic standards.

RESULTS

The mandibular gland secretion is presumably produced by the glandular mass of cells that envelop the mandibular gland reservoir (Figure 1). The volumetric capacity per reservoir was approximately 2.0 and 1.4 μl for average-size female and male *M. nortoni,* respectively, and 1.5 and 1.0 μl for average-size female and male *R. persuasoria.* The ducts from the reservoir pass through the mandible to open on the inner margin at the base of the mandible.

The secretions showed the presence of several volatile components, with that of *M. nortoni* being considerably more complex than that of *R. persuasoria.* Figure 2 shows the chromatogram obtained from the secretion of a single *M. nortoni* female. Peak 1 was found to be pentan-2-one, and peak 2 to be 6-methylhept-5-en-2-one. This latter compound was also readily identified in the secretion of *R. persuasoria. M. nortoni,* however, also produced a series of compounds (peaks 3–6, Figure 2), the mass spectra of which did not match any compound in the available mass spectral data bases.

Three of these compounds (peaks 3, 4, and 6) were found to have a molecular weight of 184 and prominent fragment ions at *m/z* 112 and 115, while the molecular weight of the other (peak 5) was 168. Peak 5 was not consistently

FIG. 1. Excised mandibles and associated glands and tissue from a *M. nortoni* male. Photographed in 70% ethanol. Scale represents 1 mm.

found and appeared to diminish rapidly on storage, indicating an unstable structure. The molecular weight 184 compounds were found from accurate mass determinations to be $C_{11}H_{20}O_2$ (found, 184.149; calculated for $C_{11}H_{20}O_2$, 184.146). Using bulked material from whole heads, compounds 3, 4, and 6 failed to hydrogenate or form any methyl ester, methoxime, or trimethylsilyl deriva-

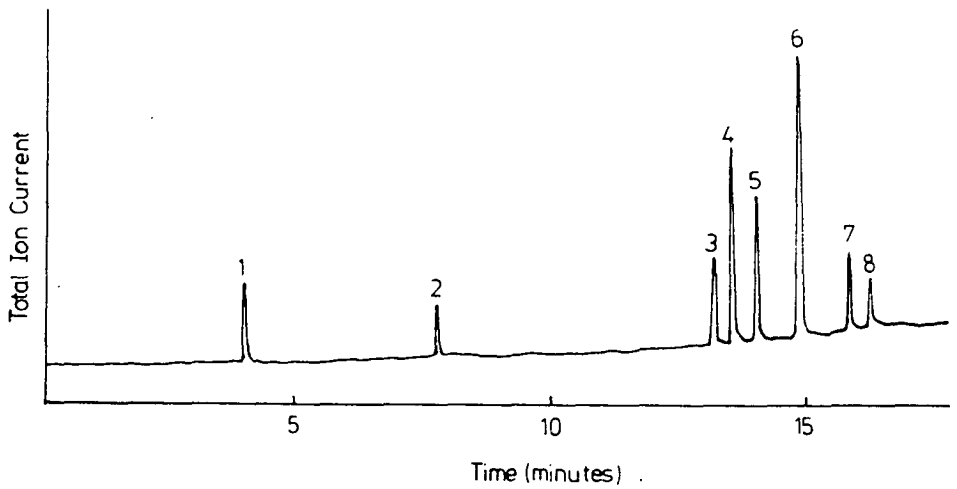

FIG. 2. Chromatogram of the volatile components in the mandibular gland secretion of a single *M. nortoni* female. GC column was 50 m OV-101, fused silica, programed from 70° to 200°C at 4°/min. Peak numbers are referred to in the text and Table 1.

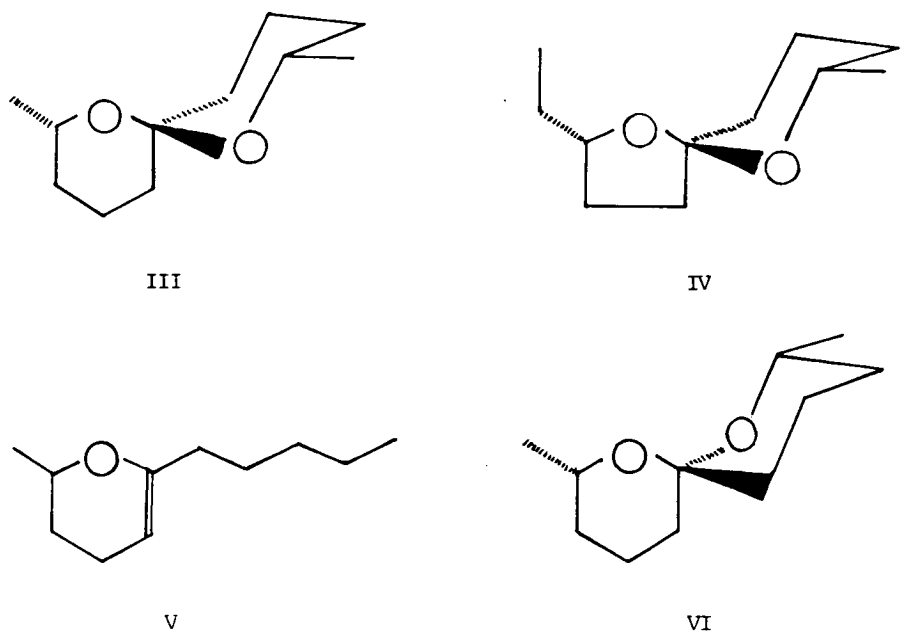

FIG. 3. Structures of characteristic *M. nortoni* compounds, with numerals corresponding to peak numbers in Figure 2. III: *E*, *E*-2,8-dimethyl-1,7-dioxaspiro[5.5]undecane; IV: *E*,*E*-2-ethyl-7-methyl-1,6-dioxaspiro[4.5]decane; V: 2-methyl-6-pentyl-3,4-dihydro-2H-pyran; VI: *Z*,*E*-2,8-dimethyl-1,7-dioxaspiro[5.5]undecane.

tive, indicating that there were no double bonds present and that the oxygens were not present as acid, ketone, or alcohol groups. Saponification with ethanolic potassium hydroxide also effected no change, indicating that no ester function was present.

The two degrees of unsaturation, therefore, had to be accounted for by ring systems, with the oxygens in the ring, suggesting a cyclic acetal could account for the structure. An examination of the literature for known acetals of the same formula showed that the mass spectra of compounds 3, 4 and 6 did in fact match closely a series of previously reported spiroacetals (Francke et al., 1978, 1979, 1980a) from the mandibular glands of bees and wasps. Close comparison of mass spectra and gas chromatographic retention indices with those of authentic samples run under identical conditions confirmed the identities, and enabled stereoisomers to be assigned. Peak 3 was shown to be *E*,*E*-2,8-dimethyl-1,7-dioxaspiro[5.5]undecane, peak 4 to be *E*,*E*-2-ethyl-7-methyl-1,6-dioxaspiro-[4.5]decane, and peak 6 to be *Z*,*E*-2,8-dimethyl-1,7-dioxaspiro[5.5]undecane. (Figure 3)

The two stereoisomers of the synthetic dimethyl-1,7-dioxaspiro[5.5]-undecanes are well separated on nonpolar stationary phases and can be distinguished as well by their mass spectra which show significant differences (Francke

et al., 1980a). The two synthetic dimethyl-1,6-dioxaspiro[4.5] decanes (*E,E* and *Z,E* isomers) were much closer in relative retention time and had virtually identical mass spectra. Only the *E,E* and *Z,E* steroisomers of the 1,7-dioxaspiro[5.5]undecanes would appear to be thermodynamically stable (Francke et al., 1980b; Mori and Tanida, 1981). The chirality of the spiroacetals was not determined.

Peak 5 was shown to correspond to $C_{11}H_{20}O$ (found, 168.147; calculated for $C_{11}H_{20}O$, 168.151), and it appeared that it could be related to an unknown previously reported in association with the same spiroacetals (Bergström et al., 1982) which was subsequently shown to be the biogenetically related 2-methyl-6-pentyl-3,4-dihydro-2H-pyran (Francke, 1984; Francke et al., 1985). Peak 5 had a mass spectrum with *m/z* 168 (23%), 125 (42), 112 (100), 97 (30), 84 (16), 83 (31), 70 (25), 58 (15), 55 (61), and 41 (36). Comparison of this spectrum with that of the above dihydropyran (Francke, personal communication) confirmed that the spectra were very similar, and an authentic sample run under the same conditions confirmed the assignment based on an identical retention index and mass spectrum.

Peaks 7 and 8 in Figure 2 were found to be undecan-2-one and undecan-2-ol, respectively. Methyl oleate was observed as a major component in the *M. nortoni* secretion. A major peak in the *R. persuasoria* secretion gave a mass spectrum with *m/z* 31 (42%), 39 (17), 41 (28), 43 (49), 59 (100) and 87 (5). After chemical ionization mass spectrometry to obtain a molecular weight, and subsequent comparison of GC and MS data with an authentic sample, this was found to be 3-hydroxy-3-methylbutan-2-one.

The components identified in the two secretions are summarized in Table 1. Analysis of excised mandibular gland extracts confirmed that the volatiles in the secretion did in fact originate from this gland. In addition to the compounds listed, several other peaks were observed at longer retention times in *M. nortoni* which have yet to be identified. The gland and head extracts of *M. nortoni* were also found to contain normal fatty acids such as palmitoleic, palmitic, oleic, linoleic, and stearic acids and a range of cuticle wax hydrocarbons including *n*-heneicosane, *n*-tricosane, *n*-pentacosane, *n*-heptacosane, as well as a C-25 alkene, while *R. persuasoria* contained the same range of fatty acids with a number of branched-chain alkanes in addition to the *n*-alkanes.

Whole females, excised female heads, and female secretions were used in bioassays to determine the degree of attraction to conspecific males and the degree of interspecific attraction. Table 2 summarizes these results. In each comparison, a significant preference for males to respond to females of the same species, their excised heads, and in particular their mandibular secretions was apparent. Excised heads were the least effective in eliciting activity by males, followed by live females, and then mandibular secretion which was the most active and specific.

TABLE 1. PRINCIPAL COMPONENTS FOUND IN MANDIBULAR SECRETIONS[a]

Peak no.	Compound	*M. nortoni*		*R. persuasoria*	
		Male	Female	Male	Female
1	Pentan-2-one	+	+		
	3-Hydroxy-3-methylbutan-2-one			++	++
2	6-Methylhept-5-en-2-one	+	+	++	++
3	*E*, *E*-2,8-Dimethyl-1,7-dioxaspiro[5.5]undecane	+	+		
4	*E*, *E*-2-Ethyl-7-methyl-1,6-dioxaspiro[4.5]decane	++	++		
5	2-Methyl-6-pentyl-3,4-dihydro-2H-pyran		++		
6	*Z*, *E*-2,8-dimethyl-1,7-dioxaspiro[5.5]undecane	+++	+++		
7	Undecan-2-one	+	+		
8	Undecan-2-ol	+	+		
	Methyl oleate	+++	+++		

[a]Key: + = minor component, ++ = medium component, +++ = major component.

TABLE 2. RESPONSE OF MALE PARASITOIDS TO LIVE FEMALES, EXCISED HEADS, AND MANDIBULAR SECRETIONS OF FEMALE PARASITOIDS[a]

	Treatment					
	Excised heads		Live females		Mandibular secretion	
	R. persuasoria	*M. nortoni*	*R. persuasoria*	*M. nortoni*	*R. persuasoria*	*M. nortoni*
Male *R. persuasoria*	14	1	39	8	78	16
Male *M. nortoni*	1	9	25	59	50	156
χ^2	15.4		34.16		89.77	
Significance	$P < 0.001$		$P < 0.001$		$P < 0.001$	

[a]Key response was the number of visits made by males, from 25 of each species, to the presentation point over two minutes.

DISCUSSION

Males of both parasitoid species aggregate at potential emergence sites by a common stimulus of fungal origin (Madden, 1968; Madden and Coutts, 1979). Male *M. nortoni,* the larger of the two species, excludes *R. persuasoria* where they compete for a common site, and this exclusion is complemented by the release of repellent mandibular secretions from a compact aggregation. *R. persuasoria* males will then stand outside the aggregation and may reform if the emerging insect results in the dispersal of *M. nortoni.*

It has been demonstrated that the mandibular glands produce distinctly different compounds which confer species identification. In *M. nortoni* these compounds include a number of closely related spiroacetals, while in *R. persuasoria* the species-specific compound would appear to be 3-hydroxy-3-methylbutan-2-one. 6-Methylhept-5-en-2-one may act as a repellent and alarm pheromone. After the first report of this compound in ants (Cavill and Ford, 1953), it has been confirmed to be associated with alarm and defense in numerous species of ants (Regnier and Law, 1968; Blum, 1978), as well as in secretions of *Andrena* bees (Tengo and Bergstrom, 1976), other parasitic bees (Hefetz et al., 1982) and some beetles, such as the Douglas-fir beetle (*Dendroctonus pseudotsugae* Hopkins) (Ryker et al., 1979). The species-specific compounds may act to synergize the repellent effect of the secretion while masking or potentiating its effect on the precopulatory activity of conspecifics.

Compound 4 was first found together with the *Z,E* isomer in three vespine wasp species (Francke et al., 1978), while compounds 3 and 6 were first reported in the mandibular secretions of *Andrena* bees (Francke et al., 1980a) together with the two former spiroacetals. The spiroacetals represent a class of compounds increasingly being identified as having pheromone activity. The first isolation of them from insects would appear to be 'chalcogran' (2-ethyl-1,6-dioxaspiro[4.4]nonane), an aggregation pheromone of the beetle, *Pityogenes chalcographus* (Francke et al., 1977). Cyclic acetals such as brevicomin (Silverstein et al., 1968) have, of course, been known for some time as insect pheromones, again principally as attraction or aggregation pheromones. Since the first reported spiroacetal, a range of these compounds has been found in bees (Francke et al., 1981; Tengö et al., 1982; Bergström et al., 1982), wasps (Francke et al., 1979) and the olive fly (Baker et al., 1980). The ring systems include dioxaspiro[4.4]nonanes, -[4.5]decanes, -[5.5]undecanes, -[4.6]undecanes, and -[5.6]dodecanes. The alkyl substituents range from methyl to butyl, with over 20 skeletons identified, excluding stereoisomers. These are almost always based on an odd carbon number and unbranched skeletons, as are the three found in *M. nortoni.* In these reports and the other references to spiroacetals, the function assigned has generally been that of attraction to members of the same species.

Undecan-2-one and undecan-2-ol, which are biosynthetically related to the spiroacetals found in *M. nortoni* were also found in association with the spiroacetals in *Andrena* bees (Bergström et al., 1982). These two compounds are widespread among the Hymenoptera. There appear to be few reports of normal fatty acid methyl esters appearing in insects generally. Methyl oleate was found along with the methyl esters of other fatty acids in extracts of the Argentine ant, *Iridomyrmex humilis* (Cavill et al., 1980). 3-Hydroxy-3-methylbutan-2-one has only been isolated once before from an insect source (Francke et al., 1974), as an attractant for the ambrosia beetle, *Xyloterus domesticus*. Pentan-2-one has not been commonly found in insects, but has been detected in cockroach secretions (Brossut, 1978), beetles (Moore and Brown, 1979), and bumblebees (Cederberg, 1977), again in mandibular secretions.

Although no mixed species aggregations were observed in the present study, the phenomenon is common among *Megarhyssa* species (Heatwole et al., 1963; Crankshaw and Matthews, 1981) and could be due to the presence of similar spiroacetals in other members of the genus, with final recognition only occurring when the emergent insect releases its secretion. In contrast, *R. persuasoria* is predominantly allopatric with respect to other *Rhyssa* species (Kirk, 1975).

Male aggregations have also been observed in the ichneumonid *Certonotus tasmaniensis* (Turner) which is an indigenous species which has adapted to attack *S. noctilio* in radiata pine. This species also has a characteristic odor. Cephalic secretions are not confined solely to the Ichneumonidae, as myrtenol and methyl oleate were found to be the major volatiles in the mandibular secretion of *Schletterarius cinctipes* (Cresson) of the family Stephanidae. (Davies and Madden, unpublished results).

It is, therefore, apparent that mandibular secretions occur within the parasitic Hymenoptera, acting to facilitate species recognition in mating behavior and the possible exclusion of competing species during oviposition.

Acknowledgments—The authors thank Prof. W. Franke for his helpful correspondence and generous donations of synthetic samples, including *Z,E-* and *E,E*-2-8-dimethyl-1,7-dioxaspiro[5.5]undecane, *Z,E-* and *E,E*-2-ethyl-7-methyl-1,6-dioxaspiro[4.5]decane, 2-methyl-6-pentyl-3,4-dihydro-2H-pyran, and 3-hydroxy-3-methylbutanone. The authors also thank Dr. J.J. Brophy for helpful discussions, Prof. G.W.K. Cavill for a sample of 6-methylhept-5-en-2-one, and Mr. K.L. Taylor and Dr. H. Elliott for the supply of insects.

REFERENCES

BAKER, R., HERBERT, R., HOWSE, P.E., JONES, O.T., FRANCKE, W., and REITH, W. 1980. Identification and synthesis of the major sex pheromone of the olive fly (*Dacus oleae*). *J. Chem. Soc. Chem. Commun.* 1980:52–53.

BERGSTRÖM, G., TENGÖ, J., REITH, W., and FRANCKE, W. 1982. Multicomponent mandibular gland secretions in three species of *Andrena* bees (Hym. Apoidea). *Z. Naturforsch.* 37c:1124–1129.

BLUM, M.S. 1978. Biochemical defenses in insects, pp. 466–573, *in* M. Rockstein (ed.). Biochemistry of Insects. Academic Press, New York.

BROSSUT, R. 1978. Gregariousness in cockroaches and in *Eublaberus* in particular. *In* R. J. Ritter (ed.) Chem. Ecol: Odour Commun. Anim., Proc. Adv. Res. Inst. Elsevier, Amsterdam, pp. 237-246.

CAVILL, G.W.K., and FORD, D.L. 1953. The chemistry of ants. *Chem. Ind. (London)* 351.

CAVILL, G.W.K., DAVIES, N.W., and MCDONALD, F.J. 1980. Characterization of aggregation factors and associated compounds from the Argentine ant (*Iridomyrmex humilis*). J. Chem. Ecol. 6:371-384.

CEDERBERG, B. 1977. Chemical basis for defense in bumblebees. *Proc. Int. Congr. Int. Union Study Soc Insects, 8th*, Centre Agric. Publications, Wageningen, Netherlands. p. 77.

CRANKSHAW, O.S., and MATTHEWS, R.W. 1981. Sexual behavior among parasitic *Megarhyssa* (Hymenoptera: Ichneumonidae). *Behav. Ecol Sociobiol* 9:1-7.

DAVIES, N.W. 1984. Determination and optimization of flow rates in vacuum capillary gas chromatography. *Anal. Chem.* 56:2618-2620.

FRANCKE, W. 1984. Acetogenins in systems of chemical communication. *Nova Acta Regiae Soc. Sci. Ups. C* 3:119-126.

FRANCKE, W., HEEMANN, V., and HEYNS, K. 1974. Volatile substances from ambrosia beetles. I. *Z. Naturforsch.* 29c:243-245.

FRANCKE, W., HEEMANN, V., GERKEN, B., RENWICK, J.A.A., and Vité, J. 1977. 2-Ethyl-1,6-dioxaspiro-[4.4]nonane, principal aggregation pheromone of *Pityogenes chalcographus* (L.) *Naturwissenschaften* 64:590-591.

FRANCKE, W., HINDORF, G., and REITH, W. 1978. Alkyl-1,6-dioxaspiro-[4.5]decanes—a new class of pheromones. *Agnew. Chem. Int. Ed.* 17:862.

FRANCKE, W., HINDORF, G., and REITH, W. 1979. Mass spectrometric fragmentations of alkyl-1,6-dioxaspiro[4.5]decanes. *Naturwissenschaften* 66:619-620.

FRANCKE, W., REITH, W., BERGSTRÖM, G., and TENGÖ, J. 1980a. Spiroketals in the mandibular glands of *Andrena* Bees. *Naturwissenschaften* 67:149-150.

FRANCKE, W., REITH, W., and SINNWELL, V. 1980b. Determination of relative configurations of spiroacetals by [^{1}H]- and [^{13}C]NMR spectroscopy. *Chem. Ber.* 113:2686-2693.

FRANCKE, W., REITH, W., BERGSTRÖM, G., and TENGÖ, J. 1981. Pheromone bouquet of the mandibular glands in *Andrena haemorrhoa* (Hym. Apoidea). *Z. Naturforsch.* 36c:928-932.

FRANCKE, W., MACKENROTH, W., SCHRÖDER, W., SCHULZ, S., TENGÖ, J., ENGELS, E., ENGELS, W., KITTMAN, R., and SCHNEIDER, D. 1985. Indentification of cyclic emolethers from insects: Alkyldihydropyranes from bees and alkyldihydro-4H-pyran-4-ones from a male moth. *Z. Naturforsch.* 40C: 145-147.

HEATWOLE, H., DAVIS, D.M., and WENNER, A.M. 1963. The behavior of *Megarhyssa*, a genus of parasitic hymenopterans (Ichneumonidae: Ephialtinae). *Z. Tierpsychol.* 19:652-664.

HEFETZ, A., EICKWORT, G.C., BLUM, M.S., CANE, J., and BOHART, G.E. 1982. A comparative study of the exocrine products of cleptoparasitic bees (*Holcopasites*) and their hosts (*Calliopsis*) (Hymenoptera: Anthophoridae, Andrenidae). *J. Chem. Ecol.* 8:1389-1397.

KIRK, A.A. 1975. Siricid woodwasps and their associated parasitoids in southeastern United States. *J. G. Entomol.* 9:141-144.

MADDEN, J.L. 1968. Behavioral responses of parasites to the symbiotic fungus associates with *Sirex nocitilio* F. Nature 218:189-190.

MADDEN, J.L., and COUTTS, M.P. 1979. The role of fungi in the biology and ecology of woodwasps, pp. 165-174. *in* L.R. Batra (ed.). Insect-Fungus Symbiosis. Allanheld, Osmun, and Co., Montclair, New Jersey.

MOORE, B.P., and BROWN, W.V. 1979. Chemical composition of the defensive secretion in *Dyschirius bonelli* (Coleoptera: Carabidae: Scaratinae) and its taxonomic significance. *J. Aust. Entomol. Soc.* 18:123-125.

MORI, K., and TANIDA, K. 1981. Synthesis of three stereoisomeric forms of 2,8-dimethyl-1,7-dioxaspiro[5.5]undecane, the main component of the cephalic secretion of *Andrena wilkella*. *Heterocycles* 15(2):1171-1174.

REGNIER, F.E., and LAW, J.H. 1968. Insect pheromones. *J. Lipid Res.* 9:541-551.

RYKER, L.C., LIBBEY, L.M., and RUDINSKY, J.A. 1979. Comparison of volatile compounds and stridulation emitted by the Douglas-fir beetle from Idaho and western Oregon populations. *Environ. Entomol.* 8:789-798.

SILVERSTEIN, R.M., BROWNLEE, R.G., BELLAS, T.E., WOOD, D.L., and BROWNE, L.E. 1968. Brevicomin. Principal sex attractant in the frass of the female western pine beetle. *Science* 159:889-891.

STANLEY, G., and KENNETT, B.H. 1973. Reaction gas chromatography of microgram and submicrogram samples using sealed glass capillaries. *J. Chromatogr.* 75:304-307.

TAYLOR, K.L. 1967. The introduction, culture, liberation, and recovery of parasites of *Sirex noctilio* in Tasmania, 1962-1967. Division of Entomology Technical Paper 8, C.S.I.R.O., Canberra.

TENGÖ, J., and BERGSTRÖM, G. 1976. Comparative analyses of lemon-smelling secretions from heads of *Andrena* F. (Hymenoptera, Apoidea) bees. *Comp. Biochem. Physiol.* 55B:179-188.

TENGÖ, J., BERGSTRÖM, G., BORG-KARLSON, A.K. GROTH, I., and FRANCKE, W. 1982. Volatile compounds from cephalic secretions of females in two cleptoparasite bee genera, *Epeolus* (Hym. Anthrophoridae) and *Coelioxys* (Hym. Megachilidae). *Z. Naturforsch.* 37c:376-380.

Journal of Chromatography, 503 (1990) 1–24
Elsevier Science Publishers B.V., Amsterdam — Printed in The Netherlands

CHROM 22 151

Review

Gas chromatographic retention indices of monoterpenes and sesquiterpenes on methyl silicone and Carbowax 20M phases

N. W. DAVIES
Central Science Laboratory, University of Tasmania P.O. Box 252C, Hobart, Tasmania 7001 (Australia)
(Received November 3rd, 1989)

CONTENTS

INTRODUCTION

The separation and identification of monoterpenes and sesquiterpenes in plant essential oils and other natural and synthetic sources relies heavily on gas chromatography. In some cases gas chromatography may be the sole means of identification, in which case at least two columns of substantially different polarity are required for any confidence in assignments based on direct comparison of retention times with standards or precise knowledge of Kováts' retention indices[1]. Even where combined gas chromatography–mass spectrometry is used for the analysis, assignments often cannot be made on the basis of mass spectrometric data only. As has been noted by Jennings and Shibamoto[2], many terpenes have essentially identical mass spectra. This can be due to the initial similarity of structures, or due to various fragmentations and rearrangements after ionization. Hence some knowledge of retention characteristics is often required to complement mass spectral data.

Much of the relevant literature is concerned with retention data on the many different types of stationary phase that have been used for terpene separations. However, most work now is carried out on capillary columns with "standard" dimethyl polysiloxane (methyl silicone) non-polar and Carbowax 20M polar phases. Indices on these phases have been reported in the literature over many years, but no single source to data has provided a comprehensive summary. Jennings and Shibamoto[2] have published a substantial set of retention indices for flavour and fragrance compounds on these phases, including some 150 terpenes. Andersen and

0021-9673/90/$03.50

co-workers[3–8] have provided a significant amount of information on sesquiterpene hydrocarbons. A general discussion on the use of retention indices in essential oil analyses has been presented by Shibamoto[9].

The following tables list Kováts' retention indices for some 400 monoterpenes and sesquiterpenes (including some hydrogenation products) on either or both of these two types of stationary phase from various literature sources. Carbowax 20M (CW20M) phases include DB-Wax, BP20, PEG 20M and HP20, while methyl silicone phases include SE-30, SF-96, OV-1, OV-101, BP1, CPSIL5CB, SP2100, DB1 and HP1. There will be slight differences between the McReynold's constants on these various "equivalent" phases. The age of a column and amount of use it has had also have a slight influence on polarity of the liquid phase.

The dependence of retention index on temperature has been extensively described, including specific reference to terpenes[10–13]. In the temperature programmed mode variables such as carrier gas flow-rate and programme rate affect the measurement, since they determine the temperature range that the sample is exposed to prior to elution. Several articles have described the relationships between isothermal and temperature programmed retention indices[14–18].

Temperature has a relatively small effect on Kováts' indices of terpenes on methyl silicone phases, but can have quite marked effects on the indices on CW20M. Differences of over 50 units can readily occur in indices determined under widely different conditions on CW20M. Multiple entries occur in the tables for many compounds to enable comparisons between different references and to give an indication of the dependence of the retention index on temperature. Some indices have been specifically excluded from the tables where there is a clear discrepancy between different sources.

This summary is primarily intended as a guide to aid the analysis of essential oils and related natural and synthetic products by gas chromatography combined with mass spectrometry or other spectroscopic detection. Data on the majority of commonly occurring monoterpenes and sesquiterpenes are listed here, as well as data on some that are relatively obscure. The tables are listed in alphabetical order, and also in order of reported Kováts' indices on CW20M and methyl silicone phases. These naturally do not represent elution sequences since the data include indices obtained under various isothermal and temperature programmed conditions, as well as multiple entries. Where possible generally accepted common names have been used. Isomer identification symbols (α, β, γ, δ, ε, *cis*, *trans*, *p*, *epi*, etc.) have been added at the end of the parent compound name.

2. KOVÁTS' RETENTION INDICES

The Kováts' retention indices are listed in Tables 1–3.

TABLE 1

ALPHABETICAL LIST OF REPORTED KOVÁTS' INDICES OF MONOTERPENES AND SESQUITERPENES ON CW20M AND METHYL SILICONE PHASES

I = Kováts' index; *T* = isothermal temperature (°C) at which the index was determined, or "prog" if the index was determined using temperature programming.

Compound	*CW20M*			*Methyl silicone*		
	I	*T*	*Ref.*	*I*	*T*	*Ref.*
Aequilobene	1702	150	4	1483	170	4
Agarofuran α-	1907	prog	19			
Alaskene α-	1763	165	5			
Alaskene β-	1738	165	5			
Alloaromadendrene	1660	130	20	1475	150	20
	1662	prog	2	1478	prog	2
	1683	prog	21[a]			
Allo-ocimene *cis*-	1373	70	13	1132	110	13
Allo-ocimene *trans*-	1392	70	13	1120	110	13
Amorphene α-	1691	prog	22	1451	prog	22
	1724	165	3	1492	170	3
Anastreptene	1568	150	4	1391	170	4
Aromadendrene	1650	prog	21[a]			
Ascaridole				1278	110	23
Ascaridole epoxide				1215	110	23
Barbatene α-	1627	150	4	1440	170	4
Barbatene β-	1690	150	4	1473	170	4
Bergamotene α-	1590	prog	24	1436	prog	24
Bergamotene *trans*-β-	1586	prog	22	1427	prog	22
Bicycloelemene	1482	prog	24			
Bicyclogermacrene	1744	prog	22	1490	prog	22
	1738	130	20			
	1768	prog	21[a]			
Bisabolane a	1492	130	25	1448	150	25
Bisabolane b	1510	130	25	1458	150	25
Bisabolene α-	1766	165	3	1505	170	3
Bisabolene *cis*-α-	1740	prog	22	1496	prog	22
Bisabolene β-	1745	165	3	1496	130	3
Bisabolol α-	2022	160	26	1595	175	26
Bisabolol β-				1666	175	27
Borneol	1698	prog	2	1164	prog	2
	1735	prog	21[a]	1154	110	23
				1177	175	27
Bornyl acetate	1599	135	28	1278	135	28
	1615	150	29			
Bornyl benzoate				1749	prog	2
Bornyl butyrate	1760	prog	2	1473	prog	2
Bornyl formate	1610	prog	2	1239	prog	2
Bornyl isopentanoate	1774	prog	2	1512	prog	2
Bourbonene β-	1586	165	3	1386	130	3
	1546	prog	2	1406	prog	2
	1526	prog	22			
Bulnesene α-	1729	prog	22	1502	prog	22
Cadalene	2203	prog	30	1646	prog	22
Cadina-1,4-diene	1786	prog	22	1518	prog	22

(Continued on p. 4)

TABLE I *(continued)*

Compound	*CW20M*			*Methyl silicone*		
	I	*T*	*Ref.*	*I*	*T*	*Ref.*
Cadinene δ-	1784	165	3	1504	130	3
	1761	prog	2	1524	prog	2
	1785	prog	21[a]			
Cadinene γ-	1792	165	3	1507	130	3
	1766	prog	2	1227	prog	2
Cadinol α-	2224	prog	24			
Cadinol δ-	2150	prog	31			
Cadinol T-	2136	prog	31			
Calacorene α-	1926	165	6			
	1916	prog	22			
Calamenene	1837	prog	22	1502	prog	22
	1839	150	4	1524	170	4
	1842	prog	2	1518	prog	2
Camphane	1021	65	32	953	100	32
Camphene	1066	75	5	952	100	5
	1078	75	28	956	100	28
	1083	prog	2	954	prog	2
Camphor	1518	prog	2	1136	prog	2
				1126	110	23
Carane *cis*-	1064	65	32	986	100	32
Carene 3-	1141	75	5	1009	100	5
	1156	75	28	1013	100	28
Carvacrol	2159	prog	2	1297	prog	2
Carveol *cis*-	1820	prog	2	1215	120	23
				1222	prog	2
Carveol *trans*-	1790	prog	2	1209	prog	2
				1200	120	23
Carveyl acetate *cis*-	1795	150	29			
Carveyl acetate *trans*-	1759	150	29			
Carvomenthone				1181	110	23
Carvomenthyl acetate	1641	150	29			
Carvone	1715	prog	2	1228	prog	2
				1223	125	23
Carvone oxide	1805	prog	2	1261	prog	2
Carvyl propionate	1833	prog	2	1440	prog	2
Caryolan-1-ol	2019	prog	31			
Caryophyllane *a*	1522	130	25	1425	150	25
Caryophyllane *b*	1533	130	25	1432	150	25
Caryophyllane *c*	1555	130	25	1450	150	25
Caryophyllane *d*	1562	130	25	1450	150	25
Caryophyllene	1617	prog	2	1428	prog	2
	1618	130	20	1436	150	20
	1655	165	3	1417	130	3
Caryophyllene alcohol	2033	prog	31	1559	prog	24
Caryophyllene oxide	2000	prog	24	1576	prog	24
	1966	prog	31			
Cedrane 8βH-	1617	130	25	1458	150	25
Cedrane 8αH-	1627	130	25	1465	150	25
Cedrene epoxide α-	1961	prog	2	1585	prog	2
Cedrene α-	1640	165	3	1414	130	3
	1578	prog	22	1411	prog	22
	1600	prog	2	1436	prog	2

TABLE 1 *(continued)*

Compound	*CW20M*			*Methyl silicone*		
	I	*T*	*Ref.*	*I*	*T*	*Ref.*
Cedrene β-	1670	165	3	1421	130	3
	1633	prog	2	1446	prog	2
	1605	prog	22			
Cedrol	2100	prog	2	1609	prog	2
				1616	175	27
Chamigrene α-	1765	150	4	1523	170	4
Chamigrene β-	1737	150	4	1550	170	4
Chrysanthenone				1100	100	23
Cineole 1,4-	1185	prog	2	1010	prog	2
				1000	80	23
Cineole 1,8-	1223	70	20	1025	100	20
	1228	prog	2	1017	prog	2
Citronellal	1465	prog	2	1137	prog	2
	1491	135	28	1143	135	28
				1146	160	33
Citronellic acid				1300	125	23
Citronellol β-	1722	prog	2	1215	prog	2
	1765	150	34	1216	100	23
				1224	175	27
Citronellol α-	1760	150	34			
Citronellyl acetate	1645	prog	2	1335	prog	2
	1662	135	28	1335	135	28
	1671	150	29	1335	140	23
Citronellyl butyrate	1786	prog	2	1511	prog	2
	1811	150	29			
Citronellyl ethyl acetal	1626	prog	2	1423	prog	2
Citronellyl formate	1600	prog	2	1261	prog	2
	1638	150	29			
Citronellyl isobutyrate	1705	prog	2	1469	prog	2
	1739	150	29			
Citronellyl pentanoate	1880	prog	2	1608	prog	2
Citronellyl propionate	1700	prog	2	1427	prog	2
	1738	150	29			
Clovane	1621	175	35			
Clovene	1601	175	35			
Copaene α-	1551	165	3	1378	130	3
	1493	prog	22	1369	prog	22
	1519	prog	2	1398	prog	2
Copaene β-	1626	prog	2	1445	prog	2
Cubebene α-	1481	130	20	1362	150	20
	1458	prog	22	1381	prog	22
Cubebene β-	1560	130	20	1400	150	20
	1541	prog	22	1381	prog	22
Cubenol *epi*-	2037	prog	30			
Cuparene	1811	130	20	1506	150	20
	1838	150	4	1516	170	4
	1831	prog	22			
Curcumene α- (ar-)	1777	prog	22			
	1787	165	3	1475	130	3
Curcumene β-	1756	165	3	1510	170	3

(Continued on p. 6)

TABLE 1 *(continued)*

Compound	*CW20M*			*Methyl silicone*		
	I	*T*	*Ref.*	*I*	*T*	*Ref.*
Cyclocitral α-				1100	110	23
Cyclocitral β-				1200	125	23
Cyclosativene	1549	165	3	1400	170	3
Cymene *p*-	1250	75	5	1016	100	5
	1272	prog	2	1020	prog	2
	1275	70	20	1018	100	20
Cymene-7-ol *p*-				1270	115	23
Cymene-8-ol *p*-	1846	prog	24	1167	115	23
Cymenene				1277	100	23
Cyperene	1606	165	3	1398	130	3
	1535	prog	22	1398	prog	22
Damascenone	1801	prog	31			
Dihydrocurcumene	1696	130	25	1448	150	25
Dihydroagarofuran β-	1737	prog	19			
Dihydrocarveol	1713	prog	2	1188	prog	2
Dihydrocarvone	1600	prog	2	1183	prog	2
Dihydrocarvyl acetate	1670	prog	2	1319	prog	2
	1700	150	29			
Dihydrogeraniol	1759	150	34			
Dihydrohumulene	1655	175	35			
Dihydrolinalool 1.2-	1512	prog	2	1122	prog	2
	1537	150	34			
Dihydrolinalool 6.7-	1449	150	34			
Dihydromyrcenol 6.10-	1438	prog	2	1063	prog	2
	1473	150	34	1056	80	23
Dihydromyrcenyl acetate	1431	prog	2	1202	prog	2
Dihydronerol	1725	150	34			
Dihydroterpinyl acetate	1561	prog	2	1282	prog	2
Dimethyl-1.6-octadiene 3.7-				946	90	23
Dimethyloctane 2.6-	922	65	32	938	100	32
Dimethyl-2-octene 2.6-				966	80	23
Drimenol	2525	prog	19			
Elemane	1460	130	25	1403	150	25
Elemene β-	1608	130	20	1400	150	20
	1591	prog	22			
Elemene δ-	1469	prog	22	1381	prog	22
Elemene γ-	1642	prog	22	1425	prog	22
Elemol	2078	prog	24	1540	prog	24
Eudesmane 4αH.5αH-	1636	130	25	1497	150	25
Eudesmane 4βH.5αH-	1582	130	25	1405	150	25
Eudesmol α-	2237	prog	19			
	2249	prog	21[a]			
Eudesmol β-	2248	prog	19			
	2258	prog	21[a]			
Eudesmol γ-	2182	prog	19			
Eudesmol 7-*epi*-α-	2244	prog	19			
Eudesmol 10-*epi*-γ-	2121	prog	19			
Farnesene *cis,cis*-α-	1697	prog	22			
Farnesene *cis,trans*-α-	1727	prog	22			
Farnesene *trans,cis*-α-	1722	prog	22			

TABLE 1 *(continued)*

Compound	*CW20M*			*Methyl silicone*		
	I	*T*	*Ref.*	*I*	*T*	*Ref.*
Farnesene *trans,trans-α-*	1756	130	20	1501	150	20
	1735	prog	22	1494	prog	22
Farnesene *cis-β-*	1636	prog	22			
Farnesene *trans-β-*	1671	130	20	1426	150	20
	1668	165	3	1449	170	4
	1668	prog	22	1448	prog	36
Farnesol *trans,trans-*				1745	175	27
Farnesyl acetate	2225	200	28	1787	200	28
Fenchene α-	1071	70	13	957	110	13
Fenchene *β-*	1057	70	13	949	110	13
Fenchol	1574	prog	2	1110	prog	2
	1580	135	28	1125	135	28
Fenchone	1410	prog	2	1080	prog	2
				1077	105	23
Fenchyl acetate	1473	prog	2	1220	prog	2
Geranial	1730	prog	2	1252	prog	2
				1260	120	23
Geranic acid				1347	140	23
Geraniol	1842	150	34	1234	175	27
	1797	prog	2	1243	prog	2
				1237	120	23
Geranyl acetate	1754	135	28	1363	135	28
Geranyl butyrate	1872	prog	2	1532	prog	2
	1904	150	29			
Geranyl formate	1684	prog	2	1282	prog	2
	1717	150	29			
Geranyl isobutyrate	1795	prog	2	1493	prog	2
	1821	150	29			
Geranyl isopentanoate	1895	prog	2	1593	prog	2
Geranyl pentanoate	1960	prog	2	1632	prog	2
Geranyl propionate	1834	150	29			
Germacrane *b*	1572	130	25	1477	150	25
Germacrane *c*	1585	130	25	1482	150	25
Germacrane *d*	1593	130	25	1489	150	25
Germacrene D	1712	prog	22	1468	prog	22
	1718	130	20	1488	150	20
Globulol	2104	prog	21[a]			
Grandisol				1200	110	23
Guaiene α-	1651	prog	22	1454	prog	22
Guaiene *β-*	1667	prog	22	1482	prog	22
Guaiene *δ-*	1729	prog	22	1502	prog	22
Gurjunene α-	1591	165	3	1413	130	3
	1529	prog	22	1400	prog	22
Gurjunene *β-* (calarene)	1656	165	3	1435	130	3
	1593	prog	22			
Helmiscapene α-	1683	150	4	1467	170	4
Helmiscapene *β-*	1686	150	4	1466	170	4
Himachalene ar-	1873	150	4	1542	170	4
Himachalene α-	1704	165	3	1444	130	3
	1649	prog	22	1442	prog	22
Himachalene *β-*	1736	150	4	1517	170	4
	1718	prog	22	1494	prog	22

(Continued on p. 8)

TABLE I *(continued)*

Compound	*CW20M*			*Methyl silicone*		
	I	*T*	*Ref.*	*I*	*T*	*Ref.*
Himachalene γ-	1723	150	4	1499	170	4
Hop ether	1360	prog	31			
Humuladienone	1952	prog	31			
Humulane	1609	175	35			
Humulene	1672	prog	22	1437	prog	22
	1707	prog	21[a]	1465	prog	2
	1719	165	3	1447	130	3
Humulene epoxide I	1972	prog	31			
Humulene epoxide II	2011	prog	31			
Humulenol II	2234	prog	31			
Humulol	2124	prog	31			
Ipsdienol				1128	100	23
Ipsenol				1087	90	23
Iridomyrmecin				1400	135	23
Isoborneol	1660	prog	2	1157	prog	2
				1149	110	23
Isobornyl acetate	1584	prog	2	1279	prog	2
	1623	150	29			
Isobornyl formate	1596	prog	2	1228	prog	2
Isobornyl propionate	1676	prog	2	1376	prog	2
Isocamphane *trans-*	1056	65	32	975	100	32
Isocamphane *cis-*	1065	65	32	980	100	32
Isogeraniol *cis-*	1812	150	2			
Isogeraniol *trans-*	1812	150	2			
Isogeraniol γ-	1800	150	2			
Isogeranyl acetate γ-	1726	150	29			
Isoiridomyrmecin				1422	150	23
Isomenthol	1667	130	20	1182	130	20
				1174	100	23
Isomenthone	1528	130	20	1156	130	20
	1468	prog	39	1151	prog	39
Isomenthyl acetate	1579	130	20	1283	130	20
	1599	150	29			
Isopinocampheol				1170	115	23
Isopinocamphone				1157	110	23
Isopulegol	1574	prog	2	1145	prog	2
				1133	110	23
Isopulegyl acetate	1585	prog	2	1258	prog	2
	1608	150	29			
Isosativene	1639	165	3	1441	170	3
Junenol	2028	prog	31			
Karahana ether	1368	prog	31			
Lavandulol	1662	prog	2	1154	prog	2
	1707	150	34	1153	110	23
Lavandulyl acetate	1597	prog	2	1274	prog	2
	1609	150	29			
Limonene	1187	75	5	1025	100	5
	1206	prog	2	1030	prog	2
	1210	70	20	1024	100	20
Limonene epoxide *cis-*				1119	100	23
Limonene epoxide *trans-*				1122	100	23

TABLE I *(continued)*

Compound	*CW20M*			*Methyl silicone*		
	I	*T*	*Ref.*	*I*	*T*	*Ref.*
Linalool	1506	prog	2	1092	prog	2
	1533	135	28	1097	135	28
	1555	150	34	1086	90	23
Linalool oxide *cis-* (furan)	1423	prog	2[b]	1068	prog	2[b]
	1461	prog	30[b]			
Linalool oxide *trans-* (furan)	1451	prog	2[b]	1082	prog	2[b]
	1432	prog	30[b]			
Linalool oxide I (pyran)				1063	100	23
Linalool oxide II (pyran)				1077	100	23
Linalyl acetate	1538	prog	2	1246	prog	2
	1569	150	29	1240	130	23
Linalyl butyrate	1680	prog	2	1420	prog	2
	1698	150	29			
Linalyl formate	1570	prog	2	1206	prog	2
Linalyl isobutyrate	1597	prog	2	1366	prog	2
	1622	150	29			
Linalyl isopentanoate	1698	prog	2	1461	prog	2
Linalyl 2-methylbutyrate	1695	prog	2	1450	prog	2
Linalyl pentanoate	1765	prog	2	1500	prog	2
Linalyl propionate	1596	prog	2	1324	prog	2
	1624	150	29			
Longicyclene	1554	165	3	1371	130	3
Longifolane 7αH-	1627	130	25	1460	150	25
Longifolane 7βH-	1633	130	25	1467	150	25
Longifolene	1574	prog	22	1398	prog	22
	1643	165	3	1404	130	3
Longipinene α-	1541	165	37	1359	130	3
Longipinene β-	1612	150	4	1432	170	4
Mentha-2,8-dien-1-ol *cis-p-*				1120	95	23
Menthane *trans-p-*	1022	65	32	981	100	32
Menthane *cis-p*	1045	65	32	995	100	32
Menthan-1-ol *p-*				1156	160	33
Menthan-2-ol *p-*				1205	160	33
Menthan-7-ol *cis-p-*	1823	120	12			
Menthan-7-ol *trans-p-*	1800	120	12			
Menthan-8-ol *p-*				1162	160	33
Menthan-9-ol *cis-p-*	1806	120	12			
Menthan-9-ol *trans-p-*	1777	120	12			
Menthan-8-yl acetate *cis-p-*	1598	150	29			
Menthan-8-yl acetate *trans-p-*	1623	150	29			
Menth-1-ene *p-*				985	160	33
Menth-4(8)-ene *p-*				998	160	33
Menth-1-en-9-ol *p-*	1904	120	12			
Menth-1(7)-en-9-ol *p-*	1881	120	12			
Menth-2-en-1-ol *cis-p-*	1560	prog	38[c]	1111	prog	38[c]
	1662	prog	21[a,c]			
Menth-2-en-1-ol *trans-p-*	1628	prog	38[c]	1128	prog	38[c]
	1597	prog	21[a,c]			
Menth-2-en-7-ol *cis-p-*	1839	120	12			
Menth-2-en-7-ol *trans-p-*	1842	120	12			
Menth-3-en-9-ol *p-*	1736	120	12			

(Continued on p. 10)

TABLE 1 *(continued)*

Compound	*CW20M*			*Methyl silicone*		
	I	*T*	*Ref.*	*I*	*T*	*Ref.*
Menth-8-en-1-ol *p*-				1156	160	33
Menth-8-en-2-ol *p*-				1208	160	33
Menthofuran	1503	130	20	1147	130	20
	1460	prog	39	1155	prog	39
Menthol	1612	prog	2	1171	prog	2
	1640	130	20	1168	130	20
	1600	prog	39	1171	prog	39
Menthone	1478	prog	2	1143	prog	2
	1518	130	20	1158	130	20
	1444	prog	39	1142	prog	39
Menthyl acetate	1600	150	29			
	1541	prog	39	1281	prog	39
Muurolene α-	1753	165	3	1495	130	3
	1727	prog	22			
	1730	prog	2	1500	prog	2
Muurolene γ-	1695	130	20	1486	150	20
	1725	165	3	1486	150	20
	1692	prog	22			
Muurolene ε-	1714	165	3	1445	130	3
Myrcene	1156	prog	2	986	prog	2
	1166	75	28	988	100	28
	1168	70	20	984	100	20
Myrcene-8-ol	1919	150	34			
Myrcenol	1585	prog	2	1103	prog	2
	1631	150	34			
Myrcenyl acetate	1574	prog	2	1247	prog	2
	1595	150	29			
Myrcenyl propionate	1625	prog	2	1327	prog	2
Myrtanol *cis*-				1245	120	23
Myrtenal				1173	120	23
Myrtenol				1281	120	23
Myrtenyl acetate	1720	150	29			
Neocarvomenthyl acetate	1604	150	29			
Neoisocarvomenthyl acetate	1672	150	29			
Neoisomenthol	1634	130	20	1180	130	20
Neoisomenthyl acetate	1602	130	20	1297	130	20
	1623	150	29			
Neomenthol	1559	prog	39	1159	prog	39
				1159	120	23
Neomenthyl acetate	1569	150	29			
Neral	1680	prog	2	1227	prog	2
				1220	120	23
Nerol	1757	prog	2	1218	prog	2
	1808	150	34	1218	120	23
Nerolic acid				1316	140	23
Nerolidol *cis*-	1961	prog	2	1524	prog	2
				1540	175	27
Nerolidol *trans*-	2000	prog	2	1553	prog	2
	2044	prog	19			
Neryl acetate	1699	prog	2	1345	prog	2
	1735	150	29	1343	135	23

TABLE 1 *(continued)*

Compound	*CW20M*			*Methyl silicone*		
	I	*T*	*Ref.*	*I*	*T*	*Ref.*
Neryl butyrate	1868	150	29			
Neryl formate	1663	prog	2	1267	prog	2
	1700	150	29			
Neryl isobutyrate	1764	prog	2	1474	prog	2
	1790	150	29			
Neryl isopentanoate	1864	prog	2	1574	prog	2
Neryl propionate	1771	prog	2	1436	prog	2
	1794	150	29			
Nootkatone	2250	prog	2	1802	prog	2
Norbornyl acetate	1476	prog	2	1112	prog	2
Ocimene *cis*-β-	1238	70	20	1027	100	20
	1228	prog	2	1025	prog	2
				1027	90	23
Ocimene *trans*-β-	1257	70	20	1042	100	20
	1250	prog	2	1038	prog	2
Ocimenol *cis*-	1660	150	34			
Ocimenol *trans*-	1685	150	34			
Patchoulene β-	1488	prog	22	1378	prog	22
Perilla aldehyde				1253	120	23
Perillyl acetate	1791	150	29			
Perillyl alcohol				1281	115	23
Phellandrene α-	1177	prog	2	1002	prog	2
	1173	70	13	1007	110	13
				1000	90	23
Phellandrene β-	1216	prog	2	1025	prog	2
	1213	70	13	1032	110	13
Phellandrol	1896	120	12			
Pinane *cis*-	1075	prog	2	987	prog	2
	1061	65	32	977	80	23
				1002	160	33
Pinane *trans*-	1062	prog	2	981	prog	2
	1049	65	32	973	100	32
Pinene α-	1036	75	28	942	100	28
	1038	70	20	939	100	20
				942	prog	2
Pinene oxide α-				1100	112	23
Pinene β-	1120	70	20	978	100	20
	1120	75	28	983	100	28
	1124	prog	2	981	prog	2
Pinocamphone				1152	110	23
Pinocarveol *trans*-				1132	110	23
Pinocarveyl acetate *trans*-	1682	150	29			
Pinonic acid *cis*-				1427	165	23
Piperitenone				1315	125	23
Piperitenone oxide	1997	prog	21[a]			
Piperitone	1739	prog	2	1247	prog	2
				1231	125	23
Pulegone	1662	prog	2	1230	prog	2
Pyrovetivene α-	1817	165	3	1522	170	3
Rose oxide *cis*-	1354	prog	2	1087	prog	2
				1100	95	23

(Continued on p. 12)

TABLE 1 *(continued)*

Compound	*CW20M*			*Methyl silicone*		
	I	*T*	*Ref.*	*I*	*T*	*Ref.*
Rose oxide *trans*-	1370	prog	2	1100	prog	2
				1114	95	23
Sabinene	1130	70	20	972	100	20
	1130	prog	2	976	prog	2
Sabinene hydrate *cis*-				1092	prog	38
Sabinene hydrate *trans*-	1463	prog	38	1060	prog	38
Sabinol (*cis*-)	1683	prog	2	1135	prog	2
				1130	115	23
Sabinyl acetate (*cis*-)	1651	prog	2	1262	prog	2
	1677	150	29			
Safranal				1167	120	23
Santalene *epi*-β-	1638	prog	22	1437	prog	22
Santalene α-	1574	prog	22	1412	prog	22
Santalene β-	1653	prog	22	1450	prog	22
Santalol α-				1660	175	27
Sativene	1595	165	3	1421	170	3
Scapanene	1664	150	4	1465	170	4
Selina-3,7(11)-diene	1791	prog	19			
Selina-4(14), 7(11)-diene	1816	165	3			
Selina-4(14), 7-diene	1694	165	3	1476	170	3
Selina-4,11-diene	1702	150	4			
Selinene α-	1751	150	4	1513	170	3
	1729	prog	22	1484	prog	22
	1759	prog	21[a]			
Selinene β-	1767	165	3	1506	170	3
	1727	prog	22	1477	prog	22
	1756	prog	21[a]			
Selinene δ-	1728	165	3			
Selinene 7-*epi*-α-	1775	prog	19			
Selinene 10-*epi*-α-	1803	165	37			
Sesquiphellandrene β-	1776	prog	22	1512	prog	22
Seychellene	1669	prog	22			
Shisool				1248	130	23
Sibirene	1594	150	4	1427	170	4
Sinuene	1646	150	4	1451	170	4
Spathulenol	2153	prog	21[a]			
Tagetone *cis*-				1136	110	23
Tagetone *trans*-				1125	110	23
Terpinene α-	1189	70	20	1016	100	20
	1188	70	13	1018	110	13
Terpinene γ-	1247	75	28	1056	100	28
	1251	prog	2	1057	prog	2
Terpinene-1-ol	1576	prog	24			
Terpinene-4-ol	1601	135	28	1129	135	28
	1628	prog	2	1175	prog	2
	1637	prog	21[a]	1170	115	23
				1160	175	27
Terpinene-4-yl acetate	1640	150	29	1282	120	23
Terpineol α-	1731	prog	21[a]	1185	prog	2
	1685	135	28	1178	135	28
				1205	160	33
Terpineol β-	1616	prog	2	1137	prog	2
Terpineol δ-	1655	prog	2	1160	prog	2

TABLE 1 *(continued)*

Compound	*CW20M*			*Methyl silicone*		
	I	*T*	*Ref.*	*I*	*T*	*Ref.*
Terpinolene	1279	75	28	1074	100	28
	1289	70	20	1081	100	20
	1287	prog	2			
Terpinyl acetate	1687	prog	2	1333	prog	2
	1722	150	29	1337	140	23
Terpinyl acetate *cis*-β-	1622	150	29			
Terpinyl butyrate	1828	prog	2	1514	prog	2
Terpinyl formate	1666	prog	2	1333	prog	2
Terpinyl isobutyrate	1748	prog	2	1467	prog	2
Terpinyl isopentanoate	1858	prog	2	1565	prog	2
Terpinyl pentanoate	1928	prog	2	1614	prog	2
Terpinyl propionate	1747	prog	2	1426	prog	2
Tetrahydrogeraniol	1626	prog	2	1185	prog	2
	1675	150	34			
Tetrahydrogeranyl acetate	1582	150	29			
Tetrahydrohumulene	1653	175	35			
Tetrahydrolavandulol	1600	150	34			
Tetrahydrolinalool	1397	prog	2	1087	prog	2
	1431	150	34	1088	90	23
Tetrahydrolinalyl acetate	1422	150	29			
Tetrahydromyrcenol	1414	prog	2	1090	prog	34
	1449	150	34			
Tetrahydrothujopsane *a*	1668	130	25	1496	150	25
Tetrahydrothujopsane *b*	1678	130	25	1508	150	25
Thuj-2-en-4-ol *cis*-	1551	100	40	1053	140	40
Thuj-2-en-4-ol *trans*-	1468	100	40	1035	140	40
Thujene α-	1038	70	20	931	100	20
	1023	70	13	935	110	13
				938	prog	2
Thujone α-				1100	110	23
Thujopsene	1626	prog	22	1425	prog	22
	1660	prog	2	1451	prog	2
	1684	165	3	1430	130	3
Thujyl acetate	1626	150	29			
Thymol				1270	130	23
Tricyclene	1009	75	5	928	100	5
Undulatene	1812	150	4	1557	170	4
Valencane (nootkatane)	1624	130	25	1493	150	25
Valencene	1722	prog	22	1482	prog	22
	1751	prog	34	1487	prog	2
	1760	165	3	1457	130	3
Valerianol	2231	prog	19			
Verbenol *cis*-				1165	100	23
Verbenol *trans*-				1140	120	23
Verbenone	1733	prog	2	1195	prog	2
				1185	110	23
Vetivenene β-	1885	165	3	1563	170	3
	1868	prog	22	1544	prog	22
Viridiflorene	1697	prog	22	1484	prog	22
Viridiflorol	2103	180	20	1588	150	20
	2112	prog	21[a]			

(Continued on p. 14)

TABLE 1 *(continued)*

Compound	*CW20M*			*Methyl silicone*		
	I	*T*	*Ref.*	*I*	*T*	*Ref.*
Ylangene α-	1539	165	3	1396	170	3
	1491	prog	22	1368	prog	22
Zingiberene	1728	prog	22	1486	prog	22
	1738	165	3	1480	170	3
Zizaene	1706	165	3	1482	170	3
Zonarene	1781	165	8			

[a] Indices reported from this laboratory were determined on a 50 m × 0.33 mm I.D. BP20 column with a 0.5-μm film thickness (S.G.E.), temperature programmed from 100 to 220°C at 3°C/min with helium as carrier gas.

[b] Refs. 2 and 30 have conflicting orders of elution for *cis*- and *trans*-linalool oxides.

[c] Refs. 21 and 38 have conflicting orders of elution for *cis*- and *trans*-*p*-menth-2-en-1-ols.

TABLE 2
KOVÁTS' INDICES LISTED IN ORDER ON CW20M

Column headings and footnotes as for Table 1.

Compound	*I*	*T*	*Ref.*	*Compound*	*I*	*T*	*Ref.*
Dimethyloctane 2,6-	922	65	32	Myrcene	1156	prog	2
Tricyclene	1009	75	5	Myrcene	1166	75	28
Camphane	1021	65	32	Myrcene	1168	70	20
Menthane *trans-p-*	1022	65	32	Phellandrene α-	1173	70	13
Thujene α-	1023	70	13	Phellandrene α-	1177	prog	2
Pinene α-	1036	75	28	Cineole 1,4-	1185	prog	2
Pinene α-	1038	70	20	Limonene	1187	75	5
Thujene α-	1038	70	20	Terpinene α-	1188	70	13
Menthane *cis-p-*	1045	65	32	Terpinene α-	1189	70	20
Pinane *trans-*	1049	65	32	Limonene	1206	prog	2
Isocamphane *trans-*	1056	65	32	Limonene	1210	70	20
Fenchene β-	1057	70	13	Phellandrene β-	1213	70	13
Pinane *cis-*	1061	65	32	Phellandrene β-	1216	prog	2
Pinane *trans-*	1062	prog	2	Cineole 1,8-	1223	70	20
Carane *cis-*	1064	65	32	Cineole 1,8-	1228	prog	2
Isocamphane *cis-*	1065	65	32	Ocimene *cis-β-*	1228	prog	2
Camphene	1066	75	5	Ocimene *cis-β-*	1238	70	20
Fenchene α-	1071	70	13	Terpinene γ-	1247	75	28
Pinane *cis-*	1075	prog	2	Cymene *p-*	1250	75	5
Camphene	1078	75	28	Ocimene *trans-β-*	1250	prog	2
Camphene	1083	prog	2	Terpinene γ-	1251	prog	2
Pinene β-	1120	70	20	Ocimene *trans-β-*	1257	70	20
Pinene β-	1120	75	28	Cymene *p-*	1272	prog	2
Pinene β-	1124	prog	2	Cymene *p-*	1275	70	20
Sabinene	1130	70	20	Terpinolene	1279	75	28
Sabinene	1130	prog	2	Terpinolene	1287	prog	2
Carene 3-	1141	75	5	Terpinolene	1289	70	20
Carene 3-	1156	75	28	Rose oxide *cis-*	1354	prog	2

TABLE 2 *(continued)*

Compound	*I*	*T*	*Ref.*	*Compound*	*I*	*T*	*Ref.*
Hop ether	1360	prog	31	Linalyl acetate	1538	prog	2
Karahana ether	1368	prog	31	Ylangene α-	1539	165	3
Rose oxide *trans-*	1370	prog	2	Cubebene β-	1541	prog	22
Allo-ocimene *cis-*	1373	70	13	Longipinene α-	1541	165	37
Allo-ocimene *trans-*	1392	70	13	Menthyl acetate	1541	prog	39
Tetrahydrolinalool	1397	prog	2	Bourbonene β-	1546	prog	2
Fenchone	1410	prog	2	Cyclosativene	1549	165	3
Tetrahydromyrcenol	1414	prog	2	Copaene α-	1551	165	3
Tetrahydrolinalyl acetate	1422	150	29	Thuj-2-en-4-ol *cis-*	1551	100	40
Linalool oxide *cis-* (furan)	1423	prog	2[b]	Longicyclene	1554	165	3
Dihydromyrcenyl acetate	1431	prog	2	Caryophyllane *c*	1555	130	25
Tetrahydrolinalool	1431	150	34	Linalool	1555	150	34
Linalool oxide *trans-* (furan)	1432	prog	30[b]	Neomenthol	1559	prog	39
Dihydromyrcenol 6,10-	1438	prog	2	Cubebene β-	1560	130	20
Menthone	1444	prog	39	Menth-2-en-1-ol *cis-p-*	1560	prog	38[c]
Dihydrolinalool 6,7-	1449	150	34	Dihydroterpinyl acetate	1561	prog	2
Tetrahydromyrcenol	1449	150	34	Caryophyllane *d*	1562	130	25
Linalool oxide *trans-* (furan)	1451	prog	2[b]	Anastreptene	1568	150	4
Cubebene α-	1458	prog	22	Linalyl acetate	1569	150	29
Elemane	1460	130	25	Neomenthyl acetate	1569	150	29
Menthofuran	1460	prog	39	Linalyl formate	1570	prog	2
Linalool oxide *cis-* (furan)	1461	prog	30[b]	Germacrane *b*	1572	130	25
Sabinene hydrate *trans-*	1463	prog	38	Fenchol	1574	prog	2
Citronellal	1465	prog	2	Isopulegol	1574	prog	2
Isomenthone	1468	prog	39	Longifolene	1574	prog	22
Thuj-2-en-4-ol *trans-*	1468	100	40	Myrcenyl acetate	1574	prog	2
Elemene δ-	1469	prog	22	Santalene α-	1574	prog	22
Dihydromyrcenol 6,10-	1473	150	34	Terpinene-1-ol	1576	prog	24
Fenchyl acetate	1473	prog	2	Cedrene α-	1578	prog	22
Norbornyl acetate	1476	prog	2	Isomenthyl acetate	1579	130	20
Menthone	1478	prog	2	Fenchol	1580	135	28
Cubebene α-	1481	130	20	Eudesmane 4βH, 5αH-	1582	130	25
Bicycloelemene	1482	prog	24	Tetrahydrogeranyl acetate	1582	150	29
Patchoulene β-	1488	prog	22	Isobornyl acetate	1584	prog	2
Citronellal	1491	135	28	Germacrane *c*	1585	130	25
Ylangene α-	1491	prog	22	Isopulegyl acetate	1585	prog	2
Bisabolane *a*	1492	130	25	Myrcenol	1585	prog	2
Copaene α-	1493	prog	22	Bergamotene *trans-*β-	1586	prog	22
Menthofuran	1503	130	20	Bourbonene β-	1586	165	3
Linalool	1506	prog	2	Bergamotene α-	1590	prog	24
Bisabolane *b*	1510	130	25	Elemene β-	1591	prog	22
Dihydrolinalool 1,2-	1512	prog	2	Gurjunene α-	1591	165	3
Camphor	1518	prog	2	Germacrane *d*	1593	130	25
Menthone	1518	130	20	Gurjunene β- (calarene)	1593	prog	22
Copaene α-	1519	prog	2	Sibirene	1594	150	4
Caryophyllane *a*	1522	130	25	Myrcenyl acetate	1595	150	29
Bourbonene β-	1526	prog	22	Sativene	1595	165	3
Isomenthone	1528	130	20	Isobornyl formate	1596	prog	2
Gurjunene α-	1529	prog	22	Linalyl propionate	1596	prog	2
Caryophyllane *b*	1533	130	25	Lavandulyl acetate	1597	prog	2
Linalool	1533	135	28	Linalyl isobutyrate	1597	prog	2
Cyperene	1535	prog	22	Menth-2-en-1-ol *trans-p-*	1597	prog	21[a,c]
Dihydrolinalool 1,2-	1537	150	34	Menthan-8-yl acetate *cis-p-*	1598	150	29

(Continued on p. 16)

TABLE 2 *(continued)*

Compound	*I*	*T*	*Ref.*	*Compound*	*I*	*T*	*Ref.*
Bornyl acetate	1599	135	28	Santalene *epi-β-*	1638	prog	22
Isomenthyl acetate	1599	150	29	Isosativene	1639	165	3
Cedrene α-	1600	prog	2	Cedrene α-	1640	165	3
Citronellyl formate	1600	prog	2	Menthol	1640	130	20
Dihydrocarvone	1600	prog	2	Terpinene-4-yl acetate	1640	150	29
Menthol	1600	prog	39	Carvomenthyl acetate	1641	150	29
Menthyl acetate	1600	150	29	Elemene γ-	1642	prog	22
Tetrahydrolavandulol	1600	150	34	Longifolene	1643	165	3
Clovene	1601	175	35	Citronellyl acetate	1645	prog	2
Terpinene-4-ol	1601	135	28	Sinuene	1646	150	4
Neoisomenthyl acetate	1602	130	20	Himachalene α-	1649	prog	22
Neocarvomenthyl acetate	1604	150	29	Aromadendrene	1650	prog	21[a]
Cedrene β-	1605	prog	22	Guaiene α-	1651	prog	22
Cyperene	1606	165	3	Sabinyl acetate (*cis*-)	1651	prog	2
Elemene β-	1608	130	20	Santalene β-	1653	prog	22
Isopulegyl acetate	1608	150	29	Tetrahydrohumulene	1653	175	35
Humulane	1609	175	35	Caryophyllene	1655	165	3
Lavandulyl acetate	1609	150	29	Dihydrohumulene	1655	175	35
Bornyl formate	1610	prog	2	Terpineol δ-	1655	prog	2
Longipinene β-	1612	150	4	Gurjunene β- (calarene)	1656	165	3
Menthol	1612	prog	2	Alloaromadendrene	1660	130	20
Bornyl acetate	1615	150	29	Isoborneol	1660	prog	2
Terpineol β-	1616	prog	2	Ocimenol *cis*-	1660	150	34
Caryophyllene	1617	prog	2	Thujopsene	1660	prog	2
Cedrane 8βH-	1617	130	25	Alloaromadendrene	1662	prog	2
Caryophyllene	1618	130	20	Citronellyl acetate	1662	135	28
Clovane	1621	175	35	Lavandulol	1662	prog	2
Linalyl isobutyrate	1622	150	29	Menth-2-en-1-ol *cis-p-*	1662	prog	21[a,c]
Terpinyl acetate *cis-β-*	1622	150	29	Pulegone	1662	prog	2
Isobornyl acetate	1623	150	29	Neryl formate	1663	prog	2
Menthan-8-yl acetate				Scapanene	1664	150	4
trans-p-	1623	150	29	Terpinyl formate	1666	prog	2
Neoisomenthyl acetate	1623	150	29	Guaiene β-	1667	prog	22
Linalyl propionate	1624	150	29	Isomenthol	1667	130	20
Valencane (nootkatane)	1624	130	25	Farnesene *trans-β-*	1668	165	3
Myrcenyl propionate	1625	prog	2	Farnesene *trans-β-*	1668	prog	22
Citronellyl ethyl acetal	1626	prog	2	Tetrahydrothujopsane *a*	1668	130	25
Copaene β-	1626	prog	2	Seychellene	1669	prog	22
Tetrahydrogeraniol	1626	prog	2	Cedrene β-	1670	165	3
Thujopsene	1626	prog	22	Dihydrocarvyl acetate	1670	prog	2
Thujyl acetate	1626	150	29	Citronellyl acetate	1671	150	29
Barbatene α-	1627	150	4	Farnesene *trans-β-*	1671	130	20
Cedrane 8αH-	1627	130	25	Humulene	1672	prog	22
Longifolane 7αH-	1627	130	25	Neoisocarvomenthyl acetate	1672	150	29
Menth-2-en-1-ol *trans-p-*	1628	prog	38[c]	Tetrahydrogeraniol	1675	150	34
Terpinene-4-ol	1628	prog	2	Isobornyl propionate	1676	prog	2
Myrcenol	1631	150	34	Sabinyl acetate (*cis*-)	1677	150	29
Cedrene β-	1633	prog	2	Tetrahydrothujopsane *b*	1678	130	25
Longifolane 7βH-	1633	130	25	Linalyl butyrate	1680	prog	2
Neoisomenthol	1634	130	20	Neral	1680	prog	2
Eudesmane 4αH, 5αH-	1636	130	25	Pinocarveyl acetate *trans*-	1682	150	29
Farnesene *cis-β-*	1636	prog	22	Alloaromadendrene	1683	prog	21[a]
Citronellyl formate	1638	150	29	Helmiscapene α-	1683	150	4

TABLE 2 *(continued)*

Compound	*I*	*T*	*Ref.*	*Compound*	*I*	*T*	*Ref.*
Sabinol (*cis*-)	1683	prog	2	Bulnesene α-	1729	prog	22
Geranyl formate	1684	prog	2	Guaiene δ-	1729	prog	22
Thujopsene	1684	165	3	Selinene α-	1729	prog	22
Ocimenol *trans*-	1685	150	34	Geranial	1730	prog	2
Terpineol α-	1685	135	28	Muurolene α-	1730	prog	2
Helmiscapene β-	1686	150	4	Verbenone	1733	prog	2
Terpinyl acetate	1687	prog	2	Borneol	1735	prog	21[a]
Barbatene β-	1690	150	4	Farnesene *trans,trans*-α-	1735	prog	22
Amorphene α-	1691	prog	22	Neryl acetate	1735	150	29
Muurolene γ-	1692	prog	22	Himachalene β-	1736	150	4
Selina-4(14), 7-diene	1694	165	3	Menth-3-en-9-ol *p*-	1736	120	12
Linalyl 2-methylbutyrate	1695	prog	2	Chamigrene β-	1737	150	4
Muurolene γ-	1695	130	20	Dihydroagarofuran β-	1737	prog	19
Dihydrocurcumene	1696	130	25	Alaskene β-	1738	165	5
Farnesene *cis,cis*-α-	1697	prog	22	Bicyclogermacrene	1738	130	20
Viridiflorene	1697	prog	22	Citronellyl propionate	1738	150	29
Borneol	1698	prog	2	Zingiberene	1738	165	3
Linalyl butyrate	1698	150	29	Citronellyl isobutyrate	1739	150	29
Linalyl isopentanoate	1698	prog	2	Piperitone	1739	prog	2
Neryl acetate	1699	prog	2	Bisabolene *cis*-α-	1740	prog	22
Citronellyl propionate	1700	prog	2	Bicyclogermacrene	1744	prog	22
Dihydrocarvyl acetate	1700	150	29	Bisabolene β-	1745	165	3
Neryl formate	1700	150	29	Terpinyl propionate	1747	prog	2
Aequilobene	1702	150	4	Terpinyl isobutyrate	1748	prog	2
Selina-4-,11-diene	1702	150	4	Selinene α-	1751	150	4
Himachalene α-	1704	165	3	Valencene	1751	prog	34
Citronellyl isobutyrate	1705	prog	2	Muurolene α-	1753	165	3
Zizaene	1706	165	3	Geranyl acetate	1754	135	28
Humulene	1707	prog	21[a]	Curcumene β-	1756	165	3
Lavandulol	1707	150	34	Farnesene *trans,trans*-α-	1756	130	20
Germacrene D	1712	prog	22	Selinene β-	1756	prog	21[a]
Dihydrocarveol	1713	prog	2	Nerol	1757	prog	2
Muurolene ε-	1714	165	3	Carveyl acetate *trans*-	1759	150	29
Carvone	1715	prog	2	Dihydrogeraniol	1759	150	34
Geranyl formate	1717	150	29	Selinene α-	1759	prog	21[a]
Germacrene D	1718	130	20	Bornyl butyrate	1760	prog	2
Himachalene β-	1718	prog	22	Citronellol α-	1760	150	34
Humulene	1719	165	3	Valencene	1760	165	3
Myrtenyl acetate	1720	150	29	Cadinene δ-	1761	prog	2
Citronellol (β-)	1722	prog	2	Alaskene α-	1763	165	5
Farnesene *trans,cis*-α-	1722	prog	22	Neryl isobutyrate	1764	prog	2
Terpinyl acetate	1722	150	29	Chamigrene α-	1765	150	4
Valencene	1722	prog	22	Citronellol (β-)	1765	150	34
Himachalene γ-	1723	150	4	Linalyl pentanoate	1765	prog	2
Amorphene α-	1724	165	3	Bisabolene	1766	165	3
Dihydronerol	1725	150	34	Cadinene γ-	1766	prog	2
Muurolene γ-	1725	165	3	Selinene β-	1767	165	3
Isogeranyl acetate γ-	1726	150	29	Bicyclogermacrene	1768	prog	21[a]
Farnesene *cis,trans*-α-	1727	prog	22	Neryl propionate	1771	prog	2
Muurolene α-	1727	prog	22	Bornyl isopentanoate	1774	prog	2
Selinene β-	1727	prog	22	Selinene 7-*epi*-α-	1775	prog	19
Selinene δ-	1728	165	3	Sesquiphellandrene β-	1776	prog	22
Zingiberene	1728	prog	22	Curcumene α- (ar-)	1777	prog	22

(Continued on p. 18)

TABLE 2 *(continued)*

Compound	*I*	*T*	*Ref.*	*Compound*	*I*	*T*	*Ref.*
Menthan-9-ol *trans-p-*	1777	120	12	Citronellyl pentanoate	1880	prog	2
Zonarene	1781	165	8	Menth-1(7)-en-9-ol *p-*	1881	120	12
Cadinene *δ-*	1784	165	3	Vetivenene *β-*	1885	165	3
Cadinene *δ-*	1785	prog	21[a]	Geranyl isopentanoate	1895	prog	2
Cadina-1,4-diene	1786	prog	22	Phellandrol	1896	120	12
Citronellyl butyrate	1786	prog	2	Geranyl butyrate	1904	150	29
Curcumene *α-* (ar-)	1787	165	3	Menth-1-en-9-ol *p-*	1904	120	12
Carveol *trans-*	1790	prog	2	Agarofuran *α-*	1907	prog	19
Neryl isobutyrate	1790	150	29	Calacorene *α-*	1916	prog	22
Perillyl acetate	1791	150	29	Myrcene-8-ol	1919	150	34
Selina-3,7(11)-diene	1791	prog	19	Calacorene *α-*	1926	165	6
Cadinene *γ-*	1792	165	3	Terpinyl pentanoate	1928	prog	2
Neryl propionate	1794	150	29	Humuladienone	1952	prog	31
Carveyl acetate *cis-*	1795	150	29	Geranyl pentanoate	1960	prog	2
Geranyl isobutyrate	1795	prog	2	Cedrene epoxide *α-*	1961	prog	2
Geraniol	1797	prog	2	Nerolidol *cis-*	1961	prog	2
Isogeraniol *γ-*	1800	150	2	Caryophyllene oxide	1966	prog	31
Menthan-7-ol *trans-p-*	1800	120	12	Humulene epoxide I	1972	prog	31
Damascenone	1801	prog	31	Caryophyllene oxide	2000	prog	24
Selinene 10-epi-*α-*	1803	165	37	Nerolidol *trans-*	2000	prog	2
Carvone oxide	1805	prog	2	Humulene epoxide II	2011	prog	31
Menthan-9-ol *cis-p-*	1806	120	12	Caryolan-1-ol	2019	prog	31
Nerol	1808	150	34	Bisabolol *α-*	2022	160	26
Citronellyl butyrate	1811	150	29	Junenol	2028	prog	31
Cuparene	1811	130	20	Caryophyllene alcohol	2033	prog	31
Isogeraniol *cis-*	1812	150	2	Cubenol *epi-*	2037	prog	30
Isogeraniol *trans-*	1812	150	2	Nerolidol *trans-*	2044	prog	19
Undulatene	1812	150	4	Elemol	2078	prog	24
Selina-4(14),7(11)-diene	1816	165	3	Cedrol	2100	prog	2
Pyrovetivene *α-*	1817	165	3	Viridiflorol	2103	180	20
Carveol *cis-*	1820	prog	2	Globulol	2104	prog	21[a]
Geranyl isobutyrate	1821	150	29	Viridiflorol	2112	prog	21[a]
Menthan-7-ol *cis-p-*	1823	120	12	Eudesmol 10-*epi-γ-*	2121	prog	19
Terpinyl butyrate	1828	prog	2	Humulol	2124	prog	31
Cuparene	1831	prog	22	Cadinol T-	2136	prog	31
Carvyl propionate	1833	prog	2	Cadinol *δ-*	2150	prog	31
Geranyl propionate	1834	150	29	Spathulenol	2153	prog	21[a]
Calamenene	1837	prog	22	Carvacrol	2159	prog	2
Cuparene	1838	150	4	Eudesmol *γ-*	2182	prog	19
Calamenene	1839	150	4	Cadalene	2203	prog	30
Menth-2-en-7-ol *cis-p-*	1839	120	12	Cadinol *α-*	2224	prog	24
Calamenene	1842	prog	2	Farnesyl acetate	2225	200	28
Geraniol	1842	150	34	Valerianol	2231	prog	19
Menth-2-en-7-ol *trans-p-*	1842	120	12	Humulenol II	2234	prog	31
Cymene-8-ol *p-*	1846	prog	24	Eudesmol *α-*	2237	prog	19
Terpinyl isopentanoate	1858	prog	2	Eudesmol 7-*epi-α-*	2244	prog	19
Neryl isopentanoate	1864	prog	2	Eudesmol *α-*	2248	prog	19
Neryl butyrate	1868	150	29	Eudesmol *α-*	2249	prog	21[a]
Vetivenene *β-*	1868	prog	22	Nootkatone	2250	prog	2
Geranyl butyrate	1872	prog	2	Eudesmol *β-*	2258	prog	21[a]
Himachalene ar-	1873	150	4	Drimenol	2525	prog	19

TABLE 3

KOVÁTS' INDICES LISTED IN ORDER ON METHYL SILICONE

Column headings and footnotes as for Table 1.

Compound	*I*	*T*	*Ref.*	*Compound*	*I*	*T*	*Ref.*
Tricyclene	928	100	5	Cineole 1,8-	1025	100	20
Thujene α-	931	100	20	Limonene	1025	100	5
Thujene α-	935	110	13	Ocimene *cis*-β-	1025	prog	2
Dimethyloctane 2,6-	938	100	32	Phellandrene β-	1025	prog	2
Thujene α-	938	prog	2	Ocimene *cis*-β-	1027	100	20
Pinene α-	939	100	20	Ocimene *cis*-β-	1027	90	23
Pinene α-	942	100	28	Limonene	1030	prog	2
Pinene α-	942	prog	2	Phellandrene β-	1032	110	13
Dimethyl-1,6-octadiene 3,7-	946	90	23	Thuj-2-en-4-ol *trans*-	1035	140	40
Fenchene β-	949	110	13	Ocimene *trans*-β-	1038	prog	2
Camphene	952	100	5	Ocimene *trans*-β-	1042	100	20
Camphane	953	100	32	Thuj-2-en-4-ol *cis*-	1053	140	40
Camphene	954	prog	2	Dihydromyrcenol 6,10-	1056	80	23
Camphene	956	100	28	Terpinene γ-	1056	100	28
Fenchene α-	957	110	13	Terpinene γ-	1057	prog	2
Dimethyl-2-octene 2,6-	966	80	23	Sabinene hydrate *trans*-	1060	prog	38
Sabinene	972	100	20	Dihydromyrcenol 6,10-	1063	prog	2
Pinane *trans*-	973	100	32	Linalool oxide I (pyran)	1063	100	23
Isocamphane *trans*-	975	100	32	Linalool oxide *cis*- (furan)	1068	prog	2[b]
Sabinene	976	prog	2	Terpinolene	1074	100	28
Pinane *cis*-	977	80	23	Fenchone	1077	105	23
Pinene β-	978	100	20	Linalool oxide II (pyran)	1077	100	23
Isocamphane *cis*-	980	100	32	Fenchone	1080	prog	2
Menthane *trans*-*p*-	981	100	32	Terpinolene	1081	100	20
Pinane *trans*-	981	prog	2	Linalool oxide *trans*- (furan)	1082	prog	2[b]
Pinene β-	981	prog	2	Linalool	1086	90	23
Pinene β-	983	100	28	Ipsenol	1087	90	23
Myrcene	984	100	20	Rose oxide *cis*-	1087	prog	2
Menth-1-ene *p*-	985	160	33	Tetrahydrolinalool	1087	prog	2
Carane *cis*-	986	100	32	Tetrahydrolinalool	1088	90	23
Myrcene	986	prog	2	Tetrahydromyrcenol	1090	prog	34
Pinane *cis*-	987	prog	2	Linalool	1092	prog	2
Myrcene	988	100	28	Sabinene hydrate *cis*-	1092	prog	38
Menthane *cis*-*p*	995	100	32	Linalool	1097	135	28
Menth-4(8)-ene-*p*-	998	160	33	Chrysanthenone	1100	100	23
Cineole 1,4-	1000	80	23	Cyclocitral α-	1100	110	23
Phellandrene α-	1000	90	23	Pinene oxide α-	1100	112	23
Phellandrene α-	1002	prog	2	Rose oxide *cis*-	1100	95	23
Pinane *cis*-	1002	160	33	Rose oxide *trans*-	1100	prog	2
Phellandrene α-	1007	110	13	Thujone α-	1100	110	23
Carene 3-	1009	100	5	Myrcenol	1103	prog	2
Cineole 1,4-	1010	prog	2	Fenchol	1110	prog	2
Carene 3-	1013	100	28	Menth-2-en-1-ol *cis*-*p*-	1111	prog	38[c]
Cymene *p*-	1016	100	5	Norbornyl acetate	1112	prog	2
Terpinene α-	1016	100	20	Rose oxide *trans*-	1114	95	23
Cineole 1,8-	1017	prog	2	Limonene epoxide *cis*-	1119	100	23
Cymene *p*-	1018	100	20	Allo-ocimene *trans*-	1120	110	13
Terpinene α-	1018	110	13	Mentha-2,8-dien-1-ol *cis*-*p*-	1120	95	23
Cymene *p*-	1020	prog	2	Dihydrolinalool 1,2-	1122	prog	2
Limonene	1024	100	20	Limonene epoxide *trans*-	1122	100	23

(Continued on p. 20)

TABLE 3 *(continued)*

Compound	*I*	*T*	*Ref.*	*Compound*	*I*	*T*	*Ref.*
Fenchol	1125	135	28	Borneol	1177	175	27
Tagetone *trans-*	1125	110	23	Terpineol α-	1178	135	28
Camphor	1126	110	23	Neoisomenthol	1180	130	20
Ipsdienol	1128	100	23	Carvomenthone	1181	110	23
Menth-2-en-1-ol *trans-p-*	1128	prog	38[c]	Isomenthol	1182	130	20
Terpinene-4-ol	1129	135	28	Dihydrocarvone	1183	prog	2
Sabinol (*cis-*)	1130	115	23	Terpineol α-	1185	prog	2
Allo-ocimene *cis-*	1132	110	13	Tetrahydrogeraniol	1185	prog	2
Pinocarveol *trans-*	1132	110	23	Verbenone	1185	110	23
Isopulegol	1133	110	23	Dihydrocarveol	1188	prog	2
Sabinol (*cis-*)	1135	prog	2	Verbenone	1195	prog	2
Camphor	1136	prog	2	Carveol *trans-*	1200	120	23
Tagetone *cis-*	1136	110	23	Cyclocitral β-	1200	125	23
Citronellal	1137	prog	2	Grandisol	1200	110	23
Terpineol β-	1137	prog	2	Dihydromyrcenyl acetate	1202	prog	2
Verbenol *trans-*	1140	120	23	Menthan-2-ol *p-*	1205	160	33
Menthone	1142	prog	39	Terpineol α-	1205	160	33
Citronellal	1143	135	28	Linalyl formate	1206	prog	2
Menthone	1143	prog	2	Menth-8-en-2-ol *p-*	1208	160	33
Isopulegol	1145	prog	2	Carveol *trans-*	1209	prog	2
Citronellal	1146	160	33	Ascaridole epoxide	1215	110	23
Menthofuran	1147	130	20	Carveol *cis-*	1215	120	23
Isoborneol	1149	110	23	Citronellol (β-)	1215	prog	2
Isomenthone	1151	prog	39	Citronellol (β-)	1216	100	23
Pinocamphone	1152	110	23	Nerol	1218	prog	2
Lavandulol	1153	110	23	Nerol	1218	120	23
Borneol	1154	110	23	Fenchyl acetate	1220	prog	2
Lavandulol	1154	prog	2	Neral	1220	120	23
Menthofuran	1155	prog	39	Carveol *cis-*	1222	prog	2
Isomenthone	1156	130	20	Carvone	1223	125	23
Menth-8-en-1-ol *p-*	1156	160	33	Citronellol (β-)	1224	175	27
Menthan-1-ol *p-*	1156	160	33	Cadinene γ-	1227	prog	2
Isoborneol	1157	prog	2	Neral	1227	prog	2
Isopinocamphone	1157	110	23	Carvone	1228	prog	2
Menthone	1158	130	20	Isobornyl formate	1228	prog	2
Neomenthol	1159	prog	39	Pulegone	1230	prog	2
Neomenthol	1159	120	23	Piperitone	1231	125	23
Terpinene-4-ol	1160	175	27	Geraniol	1234	175	27
Terpineol δ-	1160	prog	2	Geraniol	1237	120	23
Menthan-8-ol *p-*	1162	160	33	Bornyl formate	1239	prog	2
Borneol	1164	prog	2	Linalyl acetate	1240	130	23
Verbenol *cis-*	1165	100	23	Geraniol	1243	prog	2
Cymene-8-ol *p-*	1167	115	23	Myrtanol *cis-*	1245	120	23
Safranal	1167	120	23	Linalyl acetate	1246	prog	2
Menthol	1168	130	20	Myrcenyl acetate	1247	prog	2
Isopinocampheol	1170	115	23	Piperitone	1247	prog	2
Terpinene-4-ol	1170	115	23	Shisool	1248	130	23
Menthol	1171	prog	2	Geranial	1252	prog	2
Menthol	1171	prog	39	Perilla aldehyde	1253	120	23
Menthol	1173	175	27	Isopulegyl acetate	1258	prog	2
Myrtenal	1173	120	23	Geranial	1260	120	23
Isomenthol	1174	100	23	Carvone oxide	1261	prog	2
Terpinene-4-ol	1175	prog	2	Citronellyl formate	1261	prog	2

TABLE 3 *(continued)*

Compound	*I*	*T*	*Ref.*	*Compound*	*I*	*T*	*Ref.*
Sabinyl acetate (*cis*-)	1262	prog	2	Cubebene *β*-	1400	150	20
Neryl formate	1267	prog	2	Cyclosativene	1400	170	3
Cymene-7-ol *p*-	1270	115	23	Elemene *β*-	1400	150	20
Thymol	1270	130	23	Gurjenene α-	1400	prog	22
Lavandulyl acetate	1274	prog	2	Iridomyrmecin	1400	135	23
Cymenene	1277	100	23	Elemane	1403	150	25
Ascaridole	1278	110	23	Longifolene	1404	130	3
Bornyl acetate	1278	135	28	Eudesmane 4*β*H,5αH-	1405	150	25
Isobornyl acetate	1279	prog	2	Bourbonene *β*-	1406	prog	2
Menthyl acetate	1281	prog	39	Cedrene α-	1411	prog	22
Myrtenol	1281	120	23	Santalene α-	1412	prog	22
Perillyl alcohol	1281	115	23	Gurjunene α-	1413	130	3
Dihydroterpinyl acetate	1282	prog	2	Cedrene α-	1414	130	3
Geranyl formate	1282	prog	2	Caryophyllene	1417	130	3
Terpinene-4-yl acetate	1282	120	23	Linalyl butyrate	1420	prog	2
Isomenthyl acetate	1283	130	20	Cedrene *β*-	1421	130	3
Carvacrol	1297	prog	2	Sativene	1421	170	3
Neoisomenthyl acetate	1297	130	20	Isoiridomyrmecin	1422	150	23
Citronellic acid	1300	125	23	Citronellyl ethyl acetal	1423	prog	2
Piperitenone	1315	125	23	Caryophyllane *a*	1425	150	25
Nerolic acid	1316	140	23	Elemene γ-	1425	prog	22
Dihydrocarvyl acetate	1319	prog	2	Thujopsene	1425	prog	22
Linalyl propionate	1324	prog	2	Farnesene *trans*-*β*-	1426	150	20
Myrcenyl propionate	1327	prog	2	Terpinyl propionate	1426	prog	2
Terpinyl acetate	1333	prog	2	Bergamotene *trans*-*β*-	1427	prog	22
Terpinyl formate	1333	prog	2	Citronellyl propionate	1427	prog	2
Citronellyl acetate	1335	prog	2	Pinonic acid *cis*-	1427	165	23
Citronellyl acetate	1335	135	28	Sibirene	1427	170	4
Citronellyl acetate	1335	140	23	Caryophyllene	1428	prog	2
Terpinyl acetate	1337	140	23	Thujopsene	1430	130	3
Neryl acetate	1343	135	23	Caryophyllane *b*	1432	150	25
Neryl acetate	1345	prog	2	Longipinene *β*-	1432	170	4
Geranic acid	1347	140	23	Gurjunene *β*- (calarene)	1435	130	3
Longipinene α-	1359	130	3	Bergamotene α-	1436	prog	24
Cubebene α-	1362	150	20	Caryophyllene	1436	150	20
Geranyl acetate	1363	135	28	Cedrene α-	1436	prog	2
Linalyl isobutyrate	1366	prog	2	Neryl propionate	1436	prog	2
Ylangene α-	1368	prog	22	Humulene	1437	prog	22
Copaene α-	1369	prog	22	Santalene *epi*-*β*-	1437	prog	22
Longicyclene	1371	130	3	Barbatene α-	1440	170	4
Isobornyl propionate	1376	prog	2	Carvyl propionate	1440	prog	2
Copaene α-	1378	130	3	Isosativene	1441	170	3
Patchoulene *β*-	1378	prog	22	Himachalene α-	1442	prog	22
Cubebene α-	1381	prog	22	Himachalene α-	1444	130	3
Cubebene *β*-	1381	prog	22	Copaene *β*-	1445	prog	2
Elemene *δ*-	1381	prog	22	Muurolene ε-	1445	130	3
Bourbonene *β*-	1386	130	3	Cedrene *β*-	1446	prog	2
Anastreptene	1391	170	4	Humulene	1447	130	3
Ylangene α-	1396	170	3	Bisabolane *a*	1448	150	25
Copaene α-	1398	prog	2	Dihydrocurcumene	1448	150	25
Cyperene	1398	130	3	Farnesene trans-*β*-	1448	prog	36
Cyperene	1398	prog	22	Farnesene trans-*β*-	1449	170	4
Longifolene	1398	prog	22	Caryophyllane *c*	1450	150	25

(Continued on p. 22)

TABLE 3 *(continued)*

Compound	*I*	*T*	*Ref.*	*Compound*	*I*	*T*	*Ref.*
Caryophyllane *d*	1450	150	25	Linalyl pentanoate	1500	prog	2
Linalyl 2-methylbutyrate	1450	prog	2	Muurolene α-	1500	prog	2
Santalene β-	1450	prog	22	Farnesene *trans,trans*-α-	1501	150	20
Amorphene α-	1451	prog	22	Bulnesene α-	1502	prog	22
Sinuene	1451	170	4	Calamenene	1502	prog	22
Thujopsene	1451	prog	2	Guaiene δ-	1502	prog	22
Guaiene α-	1454	prog	22	Cadinene δ-	1504	130	3
Valencene	1457	130	3	Bisabolene	1505	170	3
Bisabolane *b*	1458	150	25	Cuparene	1506	150	20
Cedrane 8βH-	1458	150	25	Selinene β-	1506	170	3
Longifolane 7αH-	1460	150	25	Cadinene γ-	1507	130	3
Linalyl isopentanoate	1461	prog	2	Tetrahydrothujopsane *b*	1508	150	25
Cedrane 8αH-	1465	150	25	Curcumene β-	1510	170	3
Humulene	1465	prog	2	Citronellyl butyrate	1511	prog	2
Scapanene	1465	170	4	Bornyl isopentanoate	1512	prog	2
Helmiscapene β-	1466	170	4	Sesquiphellandrene β-	1512	prog	22
Helmiscapene α-	1467	170	4	Selinene α-	1513	170	3
Longifolane 7βH-	1467	150	25	Terpinyl butyrate	1514	prog	2
Terpinyl isobutyrate	1467	prog	2	Cuparene	1516	170	4
Germacrene D	1468	prog	22	Himachalene β-	1517	170	4
Citronellyl isobutyrate	1469	prog	2	Cadina-1,4-diene	1518	prog	22
Barbatene β-	1473	170	4	Calamenene	1518	prog	2
Bornyl butyrate	1473	prog	2	Pyrovetivene α-	1522	170	3
Neryl isobutyrate	1474	prog	2	Chamigrene α	1523	170	4
Alloaromadendrene	1475	150	20	Cadinene δ-	1524	prog	2
Curcumene α- (ar-)	1475	130	3	Calamenene	1524	170	4
Selina-4(14),7-diene	1476	170	3	Nerolidol *cis*-	1524	prog	2
Germacrane *b*	1477	150	25	Geranyl butyrate	1532	prog	2
Selinene β-	1477	prog	22	Elemol	1540	prog	24
Alloaromadendrene	1478	prog	2	Nerolidol *cis*-	1540	175	27
Zingiberene	1480	170	3	Himachalene ar-	1542	170	4
Germacrane *c*	1482	150	25	Vetivenene β-	1544	prog	22
Guaiene β-	1482	prog	22	Chamigrene β-	1550	170	4
Valencene	1482	prog	22	Nerolidol *trans*-	1553	prog	2
Zizaene	1482	170	3	Undulatene	1557	170	4
Aequilobene	1483	170	4	Caryophyllene alcohol	1559	prog	24
Selinene α-	1484	prog	22	Vetivenene β-	1563	170	3
Viridiflorene	1484	prog	22	Terpinyl isopentanoate	1565	prog	2
Muurolene γ-	1486	150	20	Neryl isopentanoate	1574	prog	2
Zingiberene	1486	prog	22	Caryophyllene oxide	1576	prog	24
Valencene	1487	prog	2	Cedrene epoxide α-	1585	prog	2
Germacrene D	1488	150	20	Viridiflorol	1588	150	20
Germacrane *d*	1489	150	25	Geranyl isopentanoate	1593	prog	2
Bicyclogermacrene	1490	prog	22	Citronellyl pentanoate	1608	prog	2
Amorphene α-	1492	170	3	Cedrol	1609	prog	2
Geranyl isobutyrate	1493	prog	2	Terpinyl pentanoate	1614	prog	2
Valencane (nootkatane)	1493	150	25	Cedrol	1616	175	27
Farnesene *trans,trans*-α-	1494	prog	22	Geranyl pentanoate	1632	prog	2
Himachalene β-	1494	prog	22	Cadalene	1646	prog	22
Muurolene α-	1495	130	3	Santalol α-	1660	175	27
Bisabolene *cis*-α-	1496	prog	22	Bisabolol β-	1666	175	27
Bisabolene β-	1496	130	3	Farnesol *trans,trans*-	1745	175	27
Tetrahydrothujopsane *a*	1496	150	25	Bornyl benzoate	1749	prog	2
Eudesmane 4αH,5αH-	1497	150	25	Farnesyl acetate	1787	200	28
Himachalene γ-	1499	170	4	Nootkatone	1802	prog	2

3. ACKNOWLEDGEMENTS

Drs. J. Brophy and M. Ridd are thanked for their comments and provision of some of the references.

4. SUMMARY

Gas chromatographic retention indices (Kováts' indices) are a valuable aid in the identification of monoterpenes and sesquiterpenes in essential oils and related natural and synthetic products. Some 900 Kováts' indices of 400 individual compounds on methyl silicone (dimethyl polysiloxane) and/or Carbowax 20M liquid phases are summarized from the general literature.

REFERENCES

1 E. sz. Kováts, *Helv. Chim. Acta*, 41 (1958) 1915.
2 W. Jennings and T. Shibamoto, *Qualitative Analysis of Flavor and Fragrance Volatiles by Glass Capillary Column Gas Chromatography*, Academic Press, New York, 1980.
3 N. H. Andersen and M. S. Falcone, *J. Chromatogr.*, 44 (1969) 52.
4 N. H. Andersen, P. Bissonette, C.-B. Liu, B. Shunk, Y. Ohta, C.-L. W. Tseng, B. Moore and S. Huneck, *Phytochemistry*, 16 (1977) 1731.
5 N. H. Andersen and D. D. Syrdal, *Phytochemistry*, 9 (1970) 1325.
6 N. H. Andersen, Y. Ohta, C.-B. Liu, C. M. Kramer, K. Allison and S. Huneck, *Phytochemistry*, 16 (1977) 1727.
7 N. H. Andersen, C. R. Costin, C. M. Kramer Jr., Y. Ohta and S. Huneck, *Phytochemistry*, 12 (1973) 2709.
8 N. H. Andersen, D. D. Syrdal, B. M. Lawrence, S. J. Terhune and J. W. Hogg, *Phytochemistry*, 12 (1973) 827.
9 T. Shibamoto, in P. Sandra and C. Bicchi (Editors), *Capillary Gas Chromatography in Essential Oil Analysis*, Hüthig, Heidelberg, 1987, p. 259.
10 P. N. Breckler and T. J. Betts, *J. Chromatogr.*, 53 (1970) 163.
11 J. Karlsen and H. Siwon, *J. Chromatogr.*, 110 (1975) 187.
12 J. Albaiges and X. Guardino, *J. High Resolut. Chromatogr. Chromatogr. Commun.*, 8 (1985) 301.
13 T. Saeed, G. Redant and P. Sandra, *J. High Resolut. Chromatogr. Chromatogr. Commumn.*, 2 (1979) 75.
14 H. W. Habgood and W. E. Harris, *Anal. Chem.*, 32 (1960) 450.
15 H. van den Dool and P. D. Kratz, *J. Chromatogr.*, 11 (1963) 463.
16 G. Guiochon, *Anal. Chem.*, 36 (1964) 661.
17 R. B. Watts and R. G. O. Kekwick, *J. Chromatogr.*, 88 (1974) 165.
18 Y. Guan, J. Kiraly and J. A. Rijks, *J. Chromatogr.*, 472 (1989) 129.
19 T. A. van Beek, R. Kleis, M. A. Posthumus and A. van Veldhuizen, *Phytochemistry*, 28 (1989) 1909.
20 T. M. Malingre and H. Maarse, *Phytochemistry*, 13 (1974) 1531.
21 N. W. Davies, unpublished results.
22 S. K. Ramaswami, P. Briscese, R. J. Gargiullo and T. von Geldern, in B. M. Lawrence, B. D. Mookherjee and B. J. Willis (Editors), *Flavors and Fragrances: A World Perspective (Proceedings of the 10th International Congress of Essential Oils, Flavors and Fragrances, Washington, DC, 1986)*, (*Developments in Food Science*, Vol. 18), Elsevier, Amsterdam, 1988, p. 951.
23 A. A. Swigar and R. M. Silverstein, *Monoterpenes*, Aldrich, Milwaukee, WI, 1981.
24 Analytical Methods Committee, *Analyst (London)*, 109 (1984) 1343.
25 H. Maarse, *J. Chromatogr.*, 106 (1975) 369.
26 P. A. Hedin, A. C. Thompson and R. C. Gueldner, *Phytochemistry*, 10 (1971) 1693.
27 P. A. Hedin, R. C. Gueldner and A. C. Thompson, *Anal. Chem.*, 42 (1970) 403.
28 T. Sakai, H. Maarse, R. E. Kepner, W. G. Jennings and W. M. Longhurst, *J. Agric. Food Chem.*, 15 (1967) 1070.
29 R. Ter Heide, *Z. Anal. Chem.*, 236 (1968) 215.
30 R. Tressl, L. Friese, F. Fendesack and H. Köppler, *J. Agric. Food Chem.*, 26 (1978) 1426.

31 R. Tressl, L. Friese, F. Fendesack and H. Köppler, *J. Agric. Food Chem.*, 26 (1978) 1422.
32 R. E. Kepner and H. Maarse, *J. Chromatogr.*, 66 (1972) 229.
33 P. A. Hedin, A. C. Thompson and R. C. Gueldner, *Anal. Chem.*, 44 (1972) 1254.
34 R. Ter Heide, *J. Chromatogr.*, 129 (1976) 143.
35 R. U. Luisetti and R. A. Yunes, *J. Chromatogr. Sci.*, 9 (1971) 624.
36 L. Schreyen, P. Dirinck, P. Sandra and N. Schamp, *J. Agric. Food Chem.*, 27 (1979) 872.
37 Y. Ohta, *Tetrahedron*, 33 (1977) 617.
38 Analytical Methods Committee, *Analyst (London)*, 113 (1988) 1125.
39 T. Shibamoto, in *Applications of Glass Capillary Gas Chromatography*, Marcel Dekker, New York, 1981.
40 M. Novak, *Phytochemistry*, 24 (1985) 858.

ESSENTIAL OILS OF TASMANIAN GROWN HOPS*

By N. W. Davies

(*Central Science Laboratory, University of Tasmania, GPO Box 252C, Hobart, Tasmania, Australia, 7001*)

and R. C. Menary

(*Department of Agricultural Science, University of Tasmania*)

Received 2 June 1981

The hop varieties Northern Brewer, Brewers' Gold, Bullion, Cluster, Pride of Ringwood and the new variety 'B23' were grown in Tasmania and their essential oils analysed, primarily by combined gas chromatography/mass spectrometry. The results for those varieties previously studied were similar to the published reports, while Pride of Ringwood and B23 are reported for the first time. In particular, the selinadiene content of the six oils was examined. High levels of α- and β-selinenes were recorded in Pride of Ringwood. Mass spectral data for these two selinadienes is presented in full to facilitate future identification. An attempt is made to clarify some of the confusion in the area of sesquiterpene hydrocarbons in hops.

Key words: *hops, essential oils, sesquiterpenes, selinadienes.*

Introduction

The numerous commercial varieties of hops (*Humulus lupulus*) exhibit large qualitative and quantitative differences in the composition of their essential oils. Several commercial varieties were grown to confirm the integrity of varietal oil composition, and to report for the first time on the Australian high α-acid cultivar 'Pride of Ringwood', upon which the Australian hop industry is largely based, and on the as yet experimental variety 'B23'. The other varieties studied included Bullion, Brewers' Gold, Cluster and Northern Brewer. The interrelationship between oil composition and 'aroma' and 'non-aroma' hop types is discussed.

Experimental

The cultivars were grown in individual experimental plots within a commercial garden. A sample of the dried cones (approximately 100 g) of each variety was steam distilled in a British Pharmacopaeia still, the oil collected and dried over anhydrous sodium sulphate.

Analyses were carried out by combined gas chromatography/mass spectrometry (GC/MS) using a Pye 204 Gas Chromatograph directly coupled via a glass-lined steel tube to a VG70/70 mass spectrometer. Support Coated Open Tubular (SCOT) columns, with either Carbowax 20 M (CW20M) or SP2100 liquid phases, were used, with a Helium flow rate of 2 ml per min. The mass spectrometer was operated at an ionising energy of 70eV, a 4Kv accelerating voltage, and an ion source temperature of 200°C. The range m/z 300 to 20 was scanned exponentially downward at 1 s/decade, resulting in a full mass spectrum every 2 s. The data was stored in VG2000 datasystem. Spectra were enhanced by background subtraction, and generation of reconstructed spectra and gas chromatograms[3] where necessary to help resolve partially resolved components. Gas chromatograms were represented by Total Ion Current (TIC) change with time.

Quantities were determined on separate runs using a Pye 104 Gas Chromatograph coupled to a Flame Ionisation Detector and a Pye Unicam DP88 Computer Integrator.

Preparative gas chromatography was carried out on a Pye 104 with a 10% SE30 on Chromosorb W/AW (80–100 mesh) packed column (8 mm × 2 m).

Hydrogenations were carried out in 1 ml sealed vials under a hydrogen atmosphere, with P_2O catalyst.

*A brief presentation of some of this work was made at VIIIth International Congress on Essential Oils, Cannes, 1980.

β-Selinene (Fig. 1, (I)) was isolated by preparative gas chromatography from celery oil, and α-selinene (Fig. 1, (II)) was isolated from Brazilian rosewood oil. δ-Selinene (selina-4,6-diene) was synthesised from β-eudesmol.[20]

Spectra of selina-4(14), 7(11)diene (Fig. 1, (III)), selina-3, 7(11)-diene (Fig. 1, (IV)) and Germacrene B (Fig. 1,, (V)) were obtained from Sunshine hop oil.

Identification of components was based on reported Kovats' Indices (I_K's)[12] (*e.g.* for sesquiterpene hydrocarbons see references 1 and 2), mass spectra[4,21] and where possible by comparison with authentic compounds.

Results

The yield of oil from the various cultivars is summarized in Table I. The percentage of oil recorded for each cultivar is similar to those recorded in the literature.[11,14]

Chromatograms for Northern Brewer, 'Pride of Ringwood' and 'B23' are shown in Fig. 2. A detailed table of components and quantities is presented in Table II. Numbers on peaks in Fig. 2 correspond to the components in the table.

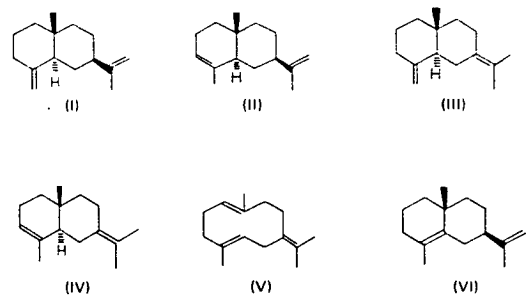

Fig. 1. Structural formulae.

TABLE I. Yield of Essential Oil for the Different Varieties as Percentage of Dry Matter.

Variety	Yield (% DM)
Brewers' Gold	1·4
Bullion	3·5
Cluster	1·3
Northern Brewer	2·2
Pride of Ringwood	2·4
B23	1·8

TABLE II. Essential Oil Composition of the Hop Varieties Studied. Figures are Percentages of Total Oil.

Peak	Compound	Bullion	Cluster	Brewers' Gold	Northern Brewer	Pride of Ringwood	B23
1	α-pinene	0·04	tr*	tr	tr	tr	tr
2	isobutyl isobutyrate	0·18	0·66	0·34	0·58	0·20	tr
3	β-pinene	1·3	1·47	1·20	0·97	1·80	0·28
4	myrcene	51	57	52	52	60	53
5	2-methylbutylpropionate	0·80	0·28	0·40	0·25	0·20	0·08
6	2-methylbutylisobutyrate	4·09	4·20	1·71	2·20	3·31	0·34
7	methyl 6-methylhexanoate	0·43	0·31	0·20	0·31	0·10	tr
8	ocimene	0·36	0·17	0·35	0·10	0·10	tr
9	methyl n-heptanoate	0·26	0·30	0·23	0·71	0·41	0·20
10	unknown	0·04	0·24	0·07	tr	0·05	tr
11	unknown	0·06	0·07	0·11	tr	0·11	tr
12	methyl 4-methylhex-2-enoate	0·04	0·12	0·08	0·25	0·40	0·31
13	methyl 6-methylheptanoate	0·49	0·75	0·22	0·31	0·71	0·26
14	2-nonanone	0·20	0·55	tr	0·52	0·20	0·08
15	methyl n-octanoate	0·38	0·94	0·22	0·68	1·25	0·35
16	unknown	0·12	0·26	0·07	0·23	tr	0·06
17	3 (4-methyl-3-pentenyl) furan	0·23	0·12	tr	0·36	—	tr
18	methyl nonanoate (branched)	0·08	0·14	—	—	tr	—
19	methyl nonanoate (branched)	0·12	0·04	tr	tr	tr	—
20	2-decanone	0·14	tr	tr	0·18	0·15	0·15
21	methyl n-nonanoate	0·13	0·25	0·10	0·37	0·50	0·15
22	methyl nonenoate isomer	tr	0·14	tr	tr	0·17	tr
23	linalool	0·27	0·08	0·27	0·21	0·15	tr
24	9-methyl decan-2-one	0·12	0·09	tr	0·11	0·15	0·30
25	methyl 8-methylnonanoate	0·10	0·17	tr	0·08	0·25	0·21
26	caryophyllene	6·20	2·30	8·60	7·00	4·20	6·60
27	2-undecanone	0·61	0·62	0·53	0·82	1·50	1·00
28	methyl n-decanoate	0·31	1·21	0·25	0·43	0·30	0·31
29	undecen-2-one isomer	—	—	tr	—	tr	tr
30	methyl dec-4-enoate	1·31	3·13	0·50	1·01	5·62	1·02
31	humulene	18·20	7·80	21·10	20·2	0·50	20·9
32	selina-4, 11-diene	—	—	—	—	0·90	—
33	germacrene D	0·36	—	0·23	0·20	—	—
34	methyl decadienoate isomer	tr	—	tr	0·13	0·36	0·38
35	unknown	—	1·20	—	—	—	—
36	methyl decadienoate isomer	0·49	2·40	1·21	1·05	1·26	0·81
37	β-selinene	0·15	0·13	0·30	0·35	6·07	3·40
38	α-selinene	0·15	0·17	0·32	0·45	7·01	4·69
39	2-dodecanone	tr	0·20	tr	tr	tr	tr
40	unknown	—	—	—	—	tr	tr
41	γ-cadinene	tr	—	—	—	0·40	0·10
42	δ-cadinene	0·98	0·14	1·01	0·51	0·60	0·97
43	unknown	0·47	tr	tr	tr	—	tr
44	unknown	—	—	—	—	0·41	—
45	2-tridecanone (branched)	tr	0·07	tr	tr	tr	tr
46	calamenene	0·20	—	0·16	tr	0·10	tr
47	2-tridecanone	tr	0·23	tr	0·32	0·34	0·40
48	methyl dodecenoate isomer	—	0·66	tr	tr	0·17	tr
49	unknown	0·57	0·30	0·17	0·11	0·08	0·07
50	unknown	—	tr	0·75	—	0·10	—
51	tridecene-2-one isomer	0·23	—	tr	—	—	—
52	methyl dodecadienoate isomer	0·36	0·19	0·10	0·32	0·18	0·09
53	unknown	—	—	—	tr	0·06	—
54	unknown	0·17	tr	—	tr	0·09	tr
55	unknown	0·19	tr	0·11	0·13	0·11	tr
56	caryophyllene epoxide	0·64	0·54	0·52	0·64	0·18	0·17
57	unknown	—	0·12	—	tr	0·10	—
58	humulene epoxide I	tr	0·13	0·10	0·15	—	tr
59	humulene epoxide II	1·20	0·68	1·23	1·86	—	0·40
60	unknown sesquiterpene	0·12	tr	tr	0·20	0·18	tr
61	2-pentadecanone	0·08	tr	tr	0·15	0·08	tr
62	pentadecene-2-one isomer	0·07	tr	—	tr	0·18	tr
63	pentadecadienone isomer	0·23	0·16	—	0·26	1·24	0·24
64	unknown sesquiterpene	tr	tr	tr	tr	0·20	tr

*tr = trace (< 0·04%)

The varieties Brewers' Gold, Bullion, Cluster and Northern Brewer show little difference to previous reports for the same varieties grown in the northern hemisphere.[4,18]

The poorly resolved region of peaks 37 and 38 (Fig. 2 (b)) was clearly resolved on a SCOT SP2100 column (see Fig. 3). For purposes of quantitation this column also resolved some of the methyl esters and ketones unresolved on CW20M.) These major peaks in Pride of Ringwood were initially difficult to identify, due to errors for the entry for β-selinene (Fig. 1, (I)) in the mass spectral atlases,[9,21] and for α-selinene (Fig. 1, (II)) in the literature.[17] The mass spectra (Fig. 4) were consistent with partial spectra from other literature references[10,19] and also with authentic samples of each sesquiterpene. The initial evidence for both being selinadienes was based on isolated samples both producing eudesmane upon hydrogenation.

Peak 32 which had M^+ 204 (60%) and base m/z 189, has been tentatively identified as selina-4,11-diene (Fig. 1, (VI)), on the basis of its Kovat's Index and eudesmane skeleton on hydrogenation, and appears to be previously unreported from hops. δ-Selinene, which has a similar Kovat's Index[2] was excluded by comparison with a synthetic sample.

No selina-4(14),7(11)-diene (Fig. 1, (III)), selina-3,7(11)-

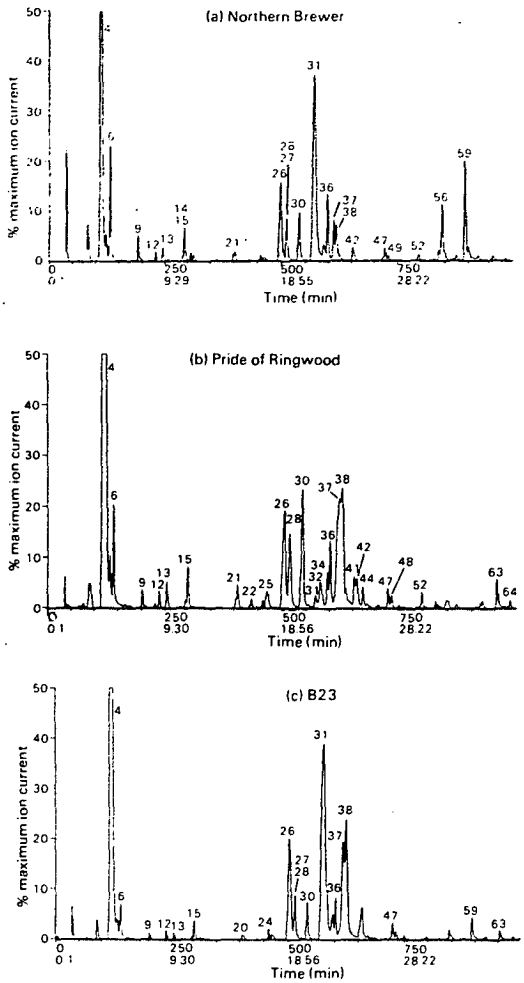

Fig. 2. Gas chromatograms (total ion currents) of three of the hop varieties. The column was a 30 m × 0·5 mm glass SCOT CW20 M, programmed from 80°–200°C at 4°C/min. Injector and detector temperature was 200°C. Numbered peaks correspond to the components listed in Table II. Carrier gas was helium at 2 ml/min. The top number on the bottom axis represents scan number, and the lower number represents time in minutes from the injection.

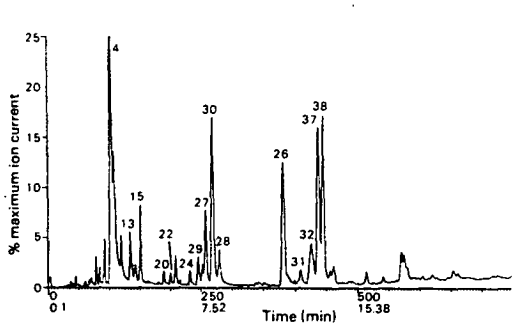

Fig. 3. Gas chromatogram of Pride of Ringwood. The column was a 30 m × 0·5 mm glass SCOT SP2100, programmed from 120°–230°C at 4°C/min. Carrier gas was helium at 2 ml/min.

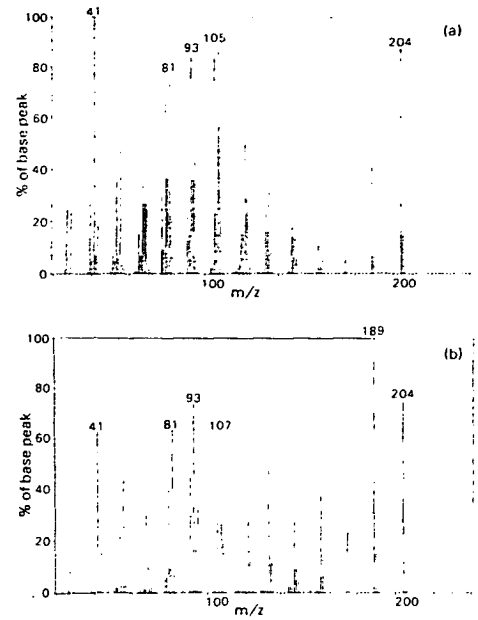

Fig. 4. (a). Electron impact mass spectrum of β-selinene. Source operated at 70 eV, 200°C.
(b). Electron impact mass spectrum of α-selinene. Source operated at 70 eV, 200°C.

diene (Fig. 1, (IV)) or Germacrene B (Fig. 1, (V)), characteristic of varieties such as Sunshine, Hersbruck Gebirg and Tasmanian White Vine,[8] was found in these six varieties.

The most obvious differences between Pride of Ringwood and the varieties Northern Brewer, Brewers' Gold, Bullion and Cluster is the extremely low humulene content, and the relatively large levels of α- and β-selinenes. In addition, the combined ketones and esters represent a significantly larger total percentage in Pride of Ringwood than in any of the other varieties. The new variety B23 maintains a high humulene level, with levels of α- and β-selinene somewhat higher than the four previously reported varieties.

Discussion

The close agreement of the results for Brewers' Gold, Bullion, Cluster and Northern Brewer with previously published data[4,18] supports the work of Likens & Vickersen[15] who showed that soil, climatic and even disease influences had almost no effect on the oil composition of hop varieties, and so the results for 'Pride' and 'B23' are solely representative varietal differences.

In all cases myrcene is by far the major component in the fresh oils. Myrcene is considered a less desirable component in the so-called 'aroma' varieties,[7] although autoxidation of myrcene,[6] as well as of the hop resins,[5] is thought to be partly responsible for flavour and aroma in finished beer. Myrcene tends to be highest in high α-acid (and consequently 'non-aroma') varieties.[13] 'Aroma' varieties generally have a high level of humulene and correspondingly lower myrcene levels.[16] Pride of Ringwood is consistent with the 'non-aroma' stereotype, in that it is an acknowledged high α-acid variety and has a myrcene level of 60% and humulene of only 0·5%.

To what extent the selinadienes contribute to (or detract from) the final aroma of the finished beer is not clear. Recognised 'aroma' hops have not been reported with significant levels of selinadienes. However, the German

literature cites components designated as 'Posthumulene 1' and 'Posthumulene 2', which are particularly large in the 'aroma' variety 'Hersbrucker Spat'.[16] This variety was not available for comparative analysis, but it would seem that these correspond to sesquiterpene hydrocarbons—probably from among the group of selinadienes, cadinenes or α-muurolene on the basis of comparison of reports of these 'posthumulene' components in Northern Brewer.[7] Until these two components are correlated with the known sesquiterpenes comparison between varieties will remain difficult.

The variety B23, which maintains a high level of α-acids (≃ 10%)[22] is somewhat unusual in that it also has a humulene content of 21% of the oil, and may prove to be a useful hop for both bittering and aroma, and is high yielding under Tasmanian conditions.

Acknowledgements.—The authors gratefully acknowledge the technical assistance given by Mrs A., McEldowney, fresh hop samples supplied by Mr P. Versluys of Australian Hop Marketers Pty Ltd, Sunshine hop oil from Dr C. Green, Wye College, and funding assistance from Australian Hop Marketers Pty Ltd, and the Reserve Bank of Australia Rural Credits Development Fund.

REFERENCES

1. Andersen, N. H., Bissonette, P., Lui, C.-B., Shunk, B., Ohta, Y., Tseng, C.-L.W., Moore, A. & Huneck, S., *Phytochemistry*, 1977, **16**, 1731.
2. Andersen, N. H. & Falcone, M. S., *Journal of Chromatography*, 1969, **44**, 52.
3. Biller, J. E. & Biemann, K., *Analytical Letters*, 1974, **7**, 515.
4. Buttery, R. G. & Ling, L. C. *Journal of Agricultural and Food Chemistry*, 1967, **15**, 531.
5. De Mets, M., & Verzeele, M., *Journal of the Institute of Brewing*, 1968, **74**, 74.
6. Dieckman, R. H. & Palamand, S. R., *Journal of Agricultural and Food Chemistry*, 1974, **22**, 498.
7. Forster, I. A., *Brewing and Distilling International*, 1977, **7**, 28.
8. Hartley, R. D. & Fawcett, C. H., *Phytochemistry*, 1969, **8**, 1793.
9. Heller, S. R. & Milne, G. W. A. (Editors). *EPA/NIH Mass Spectral Data Base, U.S. Department of Commerce*, 1978.
10. Hirose, Y., *Shitsuryo Bunseki*, 1967, **15**, 162.
11. Howard, G. A., *Journal of the Institute of Brewing*, 1970, **76**, 381.
12. Kovats, E., *Helvetica Chimica Acta*, 1915, **41**, 195
13. Krauss, G., *Monatsschrift für Brauerei*, 1978, **31**, 396.
14. Likens, S. T., *Master Brewers Association of the Americas Diamond Jubilee Convention*.
15. Likens, S. T. & Nickerson, G. B., *Journal of Agricultural and Food Chemistry*, 1967, **15**, 525.
16. Maier, J., *Hopfen-Rundschau*, 1978, **29**, 258.
17. Moshonas, M. G. & Lund, E. D., *Flavour Industry*, 1970, **1**, 375.
18. Naya, Y. & Kotake, M., *Bulletin of the Chemical Society of Japan*, 1972, **45**, 2887.
19. Schreier, P., Drawert, F. & Junker, A., *Journal of Agricutural and Food Chemistry*, 1976, **24**, 331.
20. Southwell, I. A., *Australian Journal of Chemistry*, 1978, **31**, 2527.
21. Stenhagen, E., Abrahamsson, S. & McLafferty, F. W. (Editors), *Registry of Mass Spectral Data*, John Wiley and Sons, 1974.
22. Versluys, P., *Personal communication*.

Volatile Constituents of Boronia Megastigma Flowers

By N. W. Davies, Central Science Laboratory, and R. C. Menary, Faculty of Agricultural Science, University of Tasmania, Hobart, Tasmania, Australia

The concrete obtained from the flowers of *Boronia megastigma* (Nees) by solvent extraction has been employed on a small scale for many years in the production of cosmetics, and is finding increased usage in both the perfume and flavour industries. However, little attention has been paid to the chemical nature of the components responsible for the characteristic Boronia fragrance. Beta-ionone (1) was identified in Boronia by Penfold,[1] the first report of this important odour substance as a natural product. Naves and Parry did further chemical analyses and confirmed the work of Penfold, as well as identifying other components principally from the involatile portion of the concrete.[2] A brief summary of the botany and physicochemical properties of Boronia concretes is presented by Guenther.[3]

In a preliminary communication some twenty constituents of Boronia concretes were reported.[4] The variability within a seed population was discussed, along with horticultural aspects of Boronia production. This paper presents a much more detailed analysis of the volatile components of Boronia, including the identification of several relatively major components. In all, over 150 compounds were detected by gas chromatography, of which some 50% have been identified.

Experimental

The plants used were from plots in southern Tasmania, which were originally planted for the cut flower market. The flowers were harvested with hand combs, and the concretes were obtained by mixing for twelve hours with petroleum ether (B.P. 40-60°). Individual plant harvests were extracted separately in many cases to determine the type and degree of variation within the population. The bulk of the solvent was removed under reduced pressure at room temperature, with residual levels of about 1% remaining.

Initial analyses were carried out by combined GC/MS, using SCOT or fused silica OV101 capillary columns in a Pye 204 GC directly coupled to a V.G. 70/70F mass spectrometer and V.G. 2035 datasystem, Preparative gas chromatography was carried out on a Pye 104 GC fitted with a 10% SE30 2m x 8mm glass column using glass capillary traps. Quantitative data was obtained from separate analytical runs on the Pye 104 with Flame Ionization Detector and Perkin-Elmer Sigma 10 Data Station. Raman spectra were recorded on a Cary 82 Laser Raman Spectrometer. Empirical formulae of unknowns were determined by high resolution mass spectrometry.

Vol. 8, December 1983/January 1984 0272-2666/83/0006-0301$02.00/00—

Boronia

Table I

1 alpha-thujene	40 dihydroactinidiolide
2 alpha-pinene	41 n-pentadecane
3 camphene	42 isoamyl salicylate
4 myrcene	43 'sesquicineole'
5 beta-pinene	44 dodecyl acetate
6 octanal	45 methyl jasmonate
7 limonene	46 methyl jasmonate isomer
8 delta-3-carene	47 iso-heptadecane
9 ocimene	48 (Z)-heptadec-8-ene
10 nonanal	49 n-heptadecane
11 linalool	50 methyl-p-hydroxy cinnamate
12 methyl octanoate	51 tetradecenyl acetate
13 camphor	52 tetradecyl acetate
14 octanoic acid	53 n-nonadecane
15 2,6-dimethyl-3,7-octadiene-2,6-diol	54 methyl palmitate
16 ethyl octanoate	55 ethyl palmitate
17 menthone	56 iso-heneicosane
18 undecanal	57 n-heneicosane
19 methyl nonanoate	58 methyl oleate
20 nerol	59 methyl stearate
21 methyl naphthalene	60 ethyl stearate
22 nonanoic acid	61 n-docosane
23 bornyl acetate	62 iso-tricosane
24 ethyl nonanoate	63 n-tricosane
25 decyl acetate	64 n-tetracosane
26 acyclic monoterpene	65 iso-pentacosane
27 methyl decanoate	66 n-pentacosane
28 benzyl pentanoate	67 n-hexacosane
29 decanoic acid	68 iso-heptacosane
30 ethyl decanoate	69 n-heptacosane
31 alpha-ionone	70 n-octacosane
32 dihydro-beta-ionone	71 iso-nonacosane
33 5,6-epoxy ionone	72 n-nonacosane
34 phenylethyl pentanoate	73 n-triacontane
35 tetrahydroionone	74 iso-hentriacontane
36 caryophyllene	75 n-hentriacontane
37 dodecanol	76 iso-tritriacontane
38 beta-ionone	77 n-tritriacontane
39 humulene	

This table shows the components identified so far from Boronia megastigma concretes. The numbers refer to peaks in the chromatograms on OV101 columns, as indicated for several components in figures 1, 2 and 3. Not all components listed in this table were necessarily present in the clones illustrated in the figures.

Fractions for further detailed chemical study were obtained by chromatography on silica gel H, eluting with chloroform. Hydrogenations were carried out in solution at room temperature with palladium on charcoal as catalyst, or else using the method of Stanley et al.[5] in sealed capillaries before crushing in the injection port of the GC. Hydrogenolyses were carried out by the latter method. Double bond positions were determined by the methoxymercuration technique.[6]

An initial 'volatile' fraction was defined as that portion of the concrete eluting up to the retention time of n-eicosane. Quantitative data is quoted as percentage of this fraction. The percentage of the whole concrete that this fraction represented was determined by adding a known weight of internal standard to a known weight of concrete, and relating the total F.I.D. peak area up to n-eicosane to the area of the internal standard.

Initial identification of most components was based on reference mass spectra coupled with GC retention indices. Compounds not readily identified by this means were subjected to the microchemical techniques and additional mass spectrometric measurements outlined above.

Results

Figure 1 shows the Total Ion Current (TIC) trace for a typical Boronia flower extract from a single plant. The components are summarized in Table I, in which the numbers refer to the peaks marked in figures 1, 2 and 3. The higher boiling end of the chromatogram is now shown, and was determined from independent high temperature GC-MS analyses.

Figure 2 shows the TIC trace of a series of clones in which a component not generally present in other clones (peak 43) represents one of the major volatiles. This compound is a previ-

Allured Publishing Corporation
P.O. Box 318
Wheaton, IL 60189, U.S.A.
(312) 653-2155
TWX 910-252-2133

Perfumer & Flavorist is published bi-monthly by Allured Publishing Corporation, also publishers of *Cosmetics & Toiletries, Flavor and Fragrance Materials, Essential Oils, and Cosmetic Bench Reference.*

Stanley E. Allured, Publisher

Jean E. Allured, Assistant Publisher

Nancy Allured, Advertising

Janet Ludwig, Advertising Production

Betty Lou Allured, *Circulation*

Subscriptions U.S.A. $45.00 one year surface rate, single copy, $9.00; Canada $50.00 one year surface rate; Other countries $60.00 except Central and South America $65.00 one year shipped by air, single copy, $12.00. Copyright 1983. Second Class postage paid at Wheaton, Illinois and at additional mailing offices. Postmaster: send Form 3579 to *Perfumer & Flavorist*, P.O. Box 318, Wheaton, Illinois 60189.

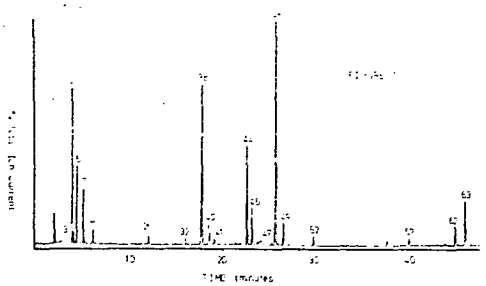

Figure 1. Total Ion Current (TIC) trace versus retention time for a GC-MS analysis of a Boronia megastigma floral concrete for a typical individual clone. Peak numbers refer to compounds listed in Table I. The GC column was a 50m x 0.2mm fused silica OV101 capillary, temperature programmed from 100° to 300°C at 3° per minute. Hydrogen was used as carrier gas at a flow rate of 1.4mls per minute. Samples were injected at 300°C with a split ratio of 10:1, with the column connected directly to the mass spectrometer resulting in sub-ambient outlet pressure. The mass spectrometer was repetitively scanned every two seconds from m/z 500 to m/z 20, and the results stored in the datasystem.

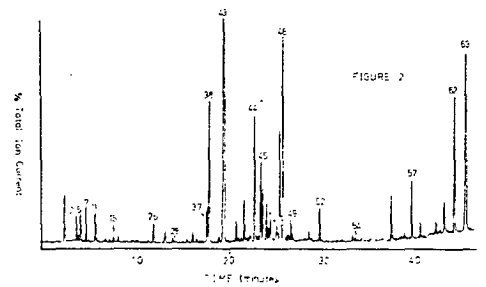

Figure 2. TIC trace versus retention time for a concrete characterised by the presence of a major component, given the trivial name 'sesquicineole,' not found in the majority of clones. Conditions were as for figure 1.

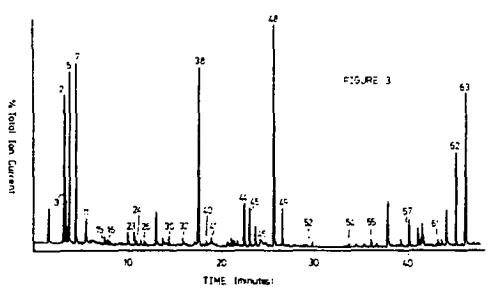

Figure 3. TIC trace versus retention time for concrete from a clone characterised by the presence of a series of ethyl esters in addition to the normal major constituents. Conditions were as for figure 1.

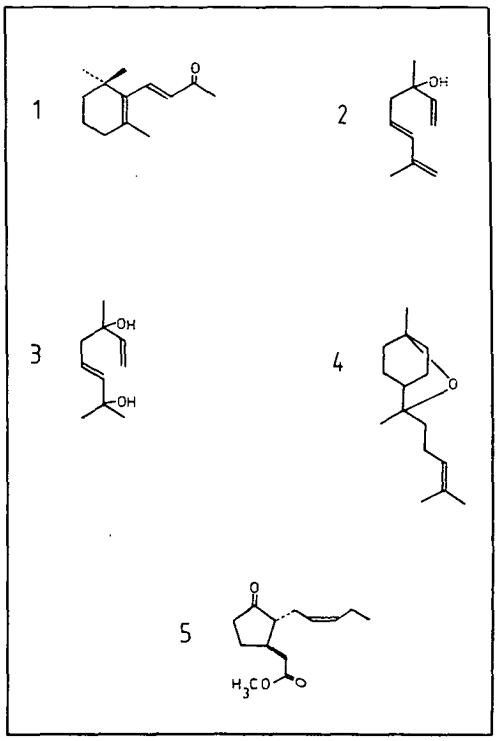

ously unreported natural product, and has been given the trivial name 'sesquicineole' from a partial structural elucidation (see below).

Figure 3 shows the TIC trace for a clone typical of a series characterised by the presence of a number of ethyl esters (peaks 16, 24, 30 and 55) in addition to the normal major components. In general there was a high degree of variability between individual concretes, especially among the minor components. Beta-ionone, dodecyl acetate, methyl jasmonate and (Z)-heptadec-8-ene were always present as relatively major components, as were the wax hydrocarbons from heneicosane to tritriacontane. The monoterpene hydrocarbons alpha-pinene, beta-pinene and limonene, on the other hand, showed very large differences in proportions, being virtually absent in some clones.

Quantitative data for several representative compounds are presented in Table II. The percentages quoted are for the 1982 harvest, and represent the proportion of the total peak area of the initial 'volatile' fraction up to n-eicosane. A sample of bulked 1981 concrete was vacuum distilled to remove this portion of the concrete (100°C, 0.02 Torr), and a 14% reduction in weight

was recorded. The same result was obtained using internal standard GC technique, implying FID response factors had little overall effect.

By far the majority of the typical Boronia fragrance was found in the latter portion of the 'volatile' fraction (b.p. 40°-100°C, 0.02 Torr), corresponding to the region on the chromatogram starting around peak 15 and going through to peak 52 (as elution order on a non-polar stationary phase is approximately proportional to boiling point).

Table II

Compound	Clone		
	1	2	3
alpha-pinene	2.3	4.4	11.0
beta-pinene	1.5	4.6	15.0
limonene	1.0	2.2	2.7
linalool	0.9	1.7	1.5
peak 26	0.8	1.5	1.3
ethyl decanoate	-	-	2.0
beta-ionone	22.5	11.9	21.1
'sesquicineole'	-	19.3	-
dodecyl acetate	11.1	7.2	5.6
methyl jasmonate	7.2	4.3	3.4
(Z)-heptadec-8-ene	31.2	19.7	24.1
% volatiles to C20	16.0	25.9	19.2

This table shows the relative proportions, as percentages of total FID peak area, of representative compounds from the clones shown in figures 1 to 3 from the 1982 harvest. Only compounds up to the retention time of n-eicosane have been included in determining total peak area. The total percentage that this fraction represents of the concretes is shown on the bottom line.

Peaks 15 and 26–Hotrienol Related Compounds

The mass spectrum of peak 15 showed m/z 82(100%), 71(77), 43(58), 67(42), 55(16) and 59(8), and was similar in some respects to that of hotrienol (2) (m/z 71(100%), 82(68), 43(50), 67(31) and 55(14)). However, a pure sample of hotrienol eluted just after linalool and well before peak 15 on OV101. The difference in retention times could not readily be explained by geometric or positional isomers of hotrienol. A 'stereoisomer' of hotrienol was reported recently as a major component responsible for the aroma of ripe baelfruit,[7] but in view of the retention time and mass spectral differences reported between this compound and hotrienol, it seems that this compound is more likely to be one of the hydrated forms of hotrienol first found in ho-leaf oil.[8] These are 2,6-dimethyl-3,7-octadiene-2,6-diol and 3,7-dimethyl-1,7-octadiene-3,6-diol, and the data presented would appear to indicate the 'unknown' is the former isomer.[7] These hydrated forms were also considered for peak 15, and it was found that 2,6-dimethyl-3,7-octadiene-2,6-diol (3) was indistinguishable in mass spectrum and retention time from the Boronia compound, thus confirming its identity. This diol is a known linalool oxidation product[9] and is related to the furanoid linalool oxides by cyclization.

Peak 26 gave a mass spectrum with m/z 71(100%), 43(86), 82(77), and 67(59) which also was very similar to that of hotrienol. This component eluted well after both diols on OV101. On Carbowax 20M stationary phase this component elutes before 2,6-dimethyl-3,7-octadiene-2,6-diol, implying a less polar nature than the diol and may possibly represent an ester of the diol.

Peak 43–'Sesquicineole'

As shown in figure 2, some clones were characterized by a large component which was not present in the majority of clones. The mass spectrum of this component showed M^+ 222 (1%) (found, C15 H26 O1), m/z 43 (95%), 69 (27%), 95 (25%), 109 (27%) and 139 (100%). This compound on hydrogenation gave a product with M^+ 224 (0.2%), m/z 43 (98%), 95 (45%), 139 (100%) and 209 (2%), indicating the presence of one double bond in the original compound. The ion at m/z 139 was found to be C9 H15 O from high resolution mass spectrometry, thus containing two degrees of unsaturation but no carbon-carbon double bonds as it was unaltered in the hydrogenated product. This evidence suggested an oxygenated sesquiterpene, with a cyclic C9 H15 O nucleus, and a C6 H11 side chain with one double bond. The compound failed to form any oxime, 2,4-dinitrophenylhydrazone or trimethylsilyl derivatives, indicating that the oxygen function was not present as a carbonyl group or as an alcohol. Thus the oxygen would appear to be present as an ether linkage, and to maintain an intact sesquiterpene skeleton this must be a cyclic ether.

One of the degrees of unsaturation is then accounted for by the cyclic ether function, while the other must be a cyclic carbon system.

Hydrogenolysis of this compound yielded mixed bisabolane isomers as the major product (M^+ 210, base m/z 97). The hydrogenolysis of terpene cyclohexane cyclic ethers (e.g., 1,8-cineole) has been studied,[10] and it was found that they produce a mixture of the stereoisomeric saturated compounds, and the fully aromatic compound (cis- and trans-p-menthane and p-cymene from

1,8-cineole), with the aromatic compound predominating at higher reaction temperatures. However, when cineole was run under the same experimental conditions as peak 43, the only significant products were the mixed p-menthanes. Thus the production of bisabolane is consistent with the expected hydrogenolysis product of a cyclic ether with the bisabolane carbon skeleton.

The stability of the ion at m/z 139 could be accounted for if one of the ether linkage points was carbon atom 8, in which case alpha cleavage would be favoured with the production of a C9 H15 O ion. The other linkage point could be at carbons 1,2,3,4,7 or 9. From biosynthetic considerations, the most likely positions would be carbons 1 (analagous to 1,8-cineole) or 2 (analagous to dihydropinol). The former is closely related to the known alpha-bisabolol, from which it could be obtained biosynthetically, and would appear the more likely position. Thus with the double bond in the normal position in the side chain of bisabolene compounds, a tentative structure for this compound is 1,3-dimethyl-3(4-methyl)-pent- 4-enyl-2-oxabicyclo(2.2.2)-octane (4). The early retention time of this substance is consistent with this structure, analagous to the early retention time of 1,8-cineole relative to other oxygenated monoterpenes.

The related components marked on figure 2 also showed a base peak m/z 139, and would therefore appear to represent other components with the same C9 H15 O nucleus.

Peaks 45 and 46-Methyl Jasmonates

These two components were both found to match the mass spectrum of methyl jasmonate (5). Initial evidence was based on high resolution mass spectrometry of the molecular ion (found C13 H20 O3) and major fragment ions 83 (found C5 H7 O), 151 (C10 H15 O1) and 156 (C8 H12 O3). This suggested the compounds could be substituted cyclopentanones, with a C5 H9 side chain on the carbon adjacent to the carbonyl to give a McLafferty rearrangement at m/z 156, and also a CH2COOCH3 side chain. Other minor peaks in the mass spectrum (m/z 59, 74) also supported the methyl ester function being present. Hydrogenation yielded a product C13 H22 O3, with an ion at m/z 153 instead of m/z 151, indicating the double bond to be in the C5 H9 portion.

The only known natural product that was consistent with this data was methyl jasmonate, first reported in jasmine concrete.[11] Peak 45 was found to match the mass spectrum and retention time of methyl jasmonate from an Egyptian Jasmine absolute, confirming this identification. Peak 46 would appear to be a stereoisomer about the cyclopentanone ring (i.e., cis substitution rather than trans), or else the trans geometric isomer about the double bond. A very small peak was also observed in the Egyptian Jasmine absolute with the same retention index and mass spectrum as the second methyl jasmonate isomer. In Boronia this peak is occasionally larger than the first isomer.

Methyl jasmonate has only been reported as a component of a few other species in addition to jasmine, but is widely used in the perfume industry as a synthetic product. It has only a subtle odour of its own, but is considered to enhance the odours of other substances.

Peak 48-(Z)-Heptadec-8-ene

This alkene is often the major volatile in the concretes. Methoxymercuration/demercuration yielded a mixture of 8- and 9-methoxy heptadecanes, which indicated the double bond was between carbons 8 and 9. The cis geometry was determined from a Raman spectrum of the purified product, which showed an absorption at 1657 cm^{-1}, characteristic of cis double bonds, and the absence of absorption in the 1665-1676 cm^{-1} for a trans double bond. This alkene could be obtained biosynthetically by the simple decarboxylation of the common oleic acid. Nevertheless simple long chain alkenes are seldom reported as components of floral concretes or essential oils. (Z)-Heptadece-8-ene has been previously reported as a major volatile of *Yucca gloriosa* flowers[12] and in neroli oil.[13]

Discussion

It is clear from the study of extracts of individual Boronia plants that a considerable amount of chemical variation occurs within the population. This ranges from differences in percentages of common components, to the presence or absence of relatively minor components (which may nevertheless be extremely important to the overall aroma), to the occurrence of major peaks in some clones not normally found among the rest of the population. A considerable variation was also observed in the yield of 'volatiles' from the concrete, as distinct from the total yield of concrete. (These aspects will be discussed elsewhere in a paper on the horticultural aspects of *Boronia megastigma*.) All these factors are important in the selection of the most suitable clones for large scale vegetative propagation.

From vacuum distillation studies, and several GC runs in which the effluent was split and

aromas assessed as they eluted from the column, it is clear that the important aroma components are found from peak 15 through to peak 52. The monoterpene hydrocarbons appear to have very little favourable effect. (Z)-Heptadec-8-ene, although a major component of all concretes, would not seem to have an important role in the overall aroma impression. Of the compounds identified, the most important would seem therefore to be the ionones and related epoxides and dihydro compounds; the esters including fatty acid methyl and ethyl esters and acetates of decyl, dodecyl and tetradecyl alcohols; dihydroactinidiolide; methyl jasmonate isomers. 'Sesquicineole' would also appear to markedly modify the aroma.

The occurrence of the long chain acetates in the Boronia flowers parallels the reports of these substances as insect pheromones. The acetates with 12 to 18 carbons in the alcohol residue in particular, with or without double bonds, are typical of the sex pheromones of female moths. Dodecyl acetate has been found as a component in several dozen moth pheromones, for example, that of the cotton bollworm.[14] In its native habitat of western Australia, *Boronia megastigma* is known to be pollinated by a single species of night-flying moth, so it is tempting to suggest that this is an instance of the Boronia producing specific sex attractants for the pollinating insect, rather than general chemical attractants. This view is supported by the failure of Boronia to set seed outside of western Australia, and the observation that dodecyl and tetradecyl acetates are concentrated in the stigma of the flower,[15] ensuring good 'pollination' by incoming moths.

Again, however, alkyl acetates are not commonly reported as major components of essential oils or floral concretes. Bulgarian rose concrete has been shown to contain tetradecyl acetates,[16] along with a small number of other oils of flower or leaf origin. Dodecyl acetate was reported as a component in *Cestrum diurnum* flower oil[17] and subsequently in a few other oils. It is nevertheless used as a synthetic product in the fragrance industry.[18]

The petal waxes clearly contribute the bulk of the weight of the concrete from Boronia flowers, and the C17 to C33 saturated branched and linear hydrocarbons represent the proportion of these waxes amenable to GC analysis. The major involatile compounds of the concrete were beyond the scope of this study.

Great care should be used in the storage and handling of Boronia concretes, due to the relative ease with which some of the components can be altered. Dihydroactinidiolide, a known breakdown product of beta-ionone, was observed to increase slowly with time at the expense of beta-ionone in small samples stored under air. A 24 hour exposure of a concrete in solution to daylight caused radical changes in composition, including the almost complete disappearance of beta-ionone and heptadec-8-ene, and the occurrence of several new components derived from these.

Acknowledgements

The authors would like to thank Mrs. A. McEldowney for technical assistance in the preparation of concretes and analytical gas chromatography, and Mr. J. Bignall for the Raman spectrum, Dr. P. Williams of the Australian Wine Research Institute is thanked for samples of trans-hotrienol, 2,6-dimethyl-3,7-octadien-2,6-diol and 3,7-dimethyl-1,7-octadien-3,6-diol.

References

Address correspondence to Mr. N. W. Davies, Central Science Laboratory, The University of Tasmania, P.O. Box 252 C, Hobart, Tasmania 7001, Australia.

1. A. R. Penfold, J.Roy. Soc. W.A., 14, pp. 1-5, 1927
2. Y. R. Naves and G. R. Parry, Perf. & Ess. Oil Record, 38, pp 129-131, 139, 1947
3. E. Guenther, The Essential Oils, Vol. III, p. 364, D. Van Nostrand Co. Inc., 1949
4. G. W. Leggett and R. C. Menary, Proceedings VIIIth International Congress of Essential Oils, Cannes, 1980, pp 132-137, (pub. 1982, Fedarom, Grasse)
5. G. Stanley and B. H. Kennett, J.Chromatog., 75, pp 304-307, 1973
6. P. Abley, F. J. McQuillin, D. E. Minnikin, K. Kusamran, K. Maskeus, and N. Polger, Chem Comm., pp 348-349, 1970
7. Y. Tokitomo, Y. Shimono, A. Kobayishi and T. Yamanishi, Agr. Biol. Chem., 46, pp 1873-1877, 1982
8. D. Takaoka and M. Hiroi, Phytochemistry, 15, 330, 1976
9. T. Matsuura and Y. Butsugan, J. Chem. Soc. Japan, 89, 513, 1968
10. R. E. Kepner and H. Maarse, J. Chromatogr., 66, 229-237, 1972
11. E. Demole, E. Lederer and D. Mercier, Helv. Chim. Acta, 45, pp 675-685, 1962
12. C. P. Wang and H. Kameoka, Nippon Nogei Kagaku aishi, 51, pp 649-653, 1977
13. B. Corbier and P. Teisseire, Recherches, 19, pp 289-290, 1974
14. B. F. Nesbitt, B. R. A. Cole, R. Lester and R. G. Poppi, J. Insect Physiol., 21, pp 1091-1096, 1975
15. S. R. Wilson, Honours Thesis, University of Tasmania, 1982
16. I. Watanabe, T. Yanai and S. Tomogami, Proceedings VIIth International Congress of Essential Oils, Japan, 1977, pp 461-466 (pub. 1979, Japan Flavour Fragrance Manufacturers Association)
17. R. P. Collins and A. F. Halim, Flavour Ind., 3, pp 159-160, 1972
18. D. L. J. Opdyke, Food Cosmet. Toxicol., 14 (Suppl.), pp 667-668, 1976

Phytochemistry, Vol. 31, No. 1, pp. 159–162, 1992
Printed in Great Britain.

0031-9422/92 $5.00 + 0.00

TRITERPENOIDS IN BUD EXUDATES OF FIJIAN *GARDENIA* SPECIES

NOEL W. DAVIES, JOHN M. MILLER,* RAGINA NAIDU* and SUBRAMANIAM SOTHEESWARAN*†

Central Science Laboratory, University of Tasmania, Hobart, Australia; *School of Pure and Applied Sciences, University of the South Pacific, Suva, Fiji

(*Received in revised form* 5 *June* 1991)

Key Word Index—*Gardenia* species; Rubiaceae; bud exudates; triterpenoids.

Abstract—Five out of the nine bud exudates of Fijian *Gardenia* species examined contained triterpenoids. Three new triterpenoids have been characterized. They are: 9,19-cyclolanostane-3,24-dione; 9,19-cyclolanost-24-ene-3,23-dione; 4-nor-9,19-cyclolanost-24-ene-3,23-dione.

INTRODUCTION

The genus *Gardenia* consists of more than 80 species spread among the tropical forests of certain regions of the world, including Fiji. Nine *Gardenia* species are recorded in Fiji. In the Fijian traditional system of medicine the indigenous Fijians have used the bud exudates of *Gardenia* species as dental masticants [1]. The most interesting use of the *Gardenia* bud exudates appears to be in the control of insects [2–4]. Chemical constituents of the bud exudates are reported to be mainly flavanoids [2–4] except for one report which showed the presence of *p*-coumaric esters of straight chain aliphatic alcohols [5]. We have recently [6] completed our phytochemical investigation of bud exudates of all *Gardenia* species indigenous to Fiji. Five out of the nine species studied [6] contained triterpenoids and we report the characterization of several triterpenoids, including three new triterpenoids: 9,19-cyclolanostane-3,24-dione (**2**); 9,19-cyclolanost-24-ene-3,23-dione (**3**); and 4-nor-9,19-cyclolanost-24-ene-3,23-dione (**4**).

RESULTS AND DISCUSSION

The bud exudates of the nine *Gardenia* species collected in different locations in Fiji were separately extracted with chloroform–methanol. The syrup obtained on concentration of the extract in each case, was extracted with *n*-hexane, chloroform, ethyl acetate and methanol. The chloroform and ethyl acetate extracts of all the syrups contained mainly flavonoids [6], whereas the *n*-hexane extracts of the bud exudates of five *Gardenia* species (Table 1) contained terpenoids.

Cycloartenone (**1**) was found in the bud exudates of four (Table 1) *Gardenia* species. Mass spectral data of **1** was useful in its structural identification, and key fragment ions are given. The mass spectral fragmentation mechanisms of cycloartane triterpenes have been extensively studied with a view to enabling structural assignments [7–9]. The base peak was observed at *m/z* 69 due to the ion $(Me)_2C=CHCH_2^+$. The presence of the cluster of ions at *m/z* 339, 340 and 341 in the mass spectrum of **1** was taken as evidence for the C-24 double bond [10] and hence the structure of **1** has been identified as cycloartenone (**1**). The identity of **1** was further confirmed by comparison with an authentic sample of cycloartenone (co-TLC, ^1H and ^{13}C NMR). The presence of key diagnostic ions and additional characteristic ions enabled the initial structural assignment in most of the triterpenoids where the cycloartane skeleton was present. This is discussed separately for each triterpenoid characterized. A second triterpenoid, 9,19-cyclolanostane-3,24-dione (**2**), co-occurred with cycloartenone (**1**) in all of the four species (Table 1). Compound **2** could not be readily separated from two other minor triterpenoids, **3** and **4**, in the hexane extracts of three species (Table 1). GC-MS analysis was used to separate and characterize compound **2**. The mass spectrum of compound **2** showed ions at *m/z* 440, 354, 313, 302, 203, 175, 127, 95, 71 and 43. The base peak was at *m/z* 43 and was due to the ion, Me_2CH^+. The molecular ion was at *m/z* 440 ($C_{30}H_{48}O_2$). These data are in agreement with the cycloartan-3-one frame work. The extra oxygen function was located on the side chain of **2** from its mass spectral fragmentation pattern. The presence of the McLafferty rearrangement product at *m/z* 354 indicated the presence of a carbonyl group in the side chain of **2** at C-24. This was further confirmed by the presence of the fragment ions at *m/z* 71, 127 and 302. From these data, **2** is 9,19-cyclolanostane-3,24-dione, which is a new cycloartane derivative.

Triterpenoids **3** and **4** were minor constituents. The GC-MS analysis showed that **3** is another new triterpenoid and it has been identified as 9,19-cyclolanost-24-ene-3,23-dione. The key ions in the mass spectrum of **3** which were useful in obtaining the structure were at *m/z* 438 $[M]^+$, ($C_{30}H_{46}O_2$), 340, 125, 98 and 83 (base peak). The molecular ion at *m/z* 438 showed that **3** is a dehydro derivative of **2**. The fragment ion at *m/z* 125 for $C_8H_{13}O$ indicated that the unsaturation and the carbonyl group are located in the side chain of compound **3**. Further evidence for this was forthcoming from the presence of the ions at *m/z* 83 (base peak) for C_5H_7O and at *m/z* 55 for $C_4H_7^+$. The ions at *m/z* 98 and 340 resulted from a McLafferty rearrangement involving the hydrogen and carbonyl in the side chain of **3**. The ^1H NMR spectrum of

†Author to whom correspondence should be addressed.

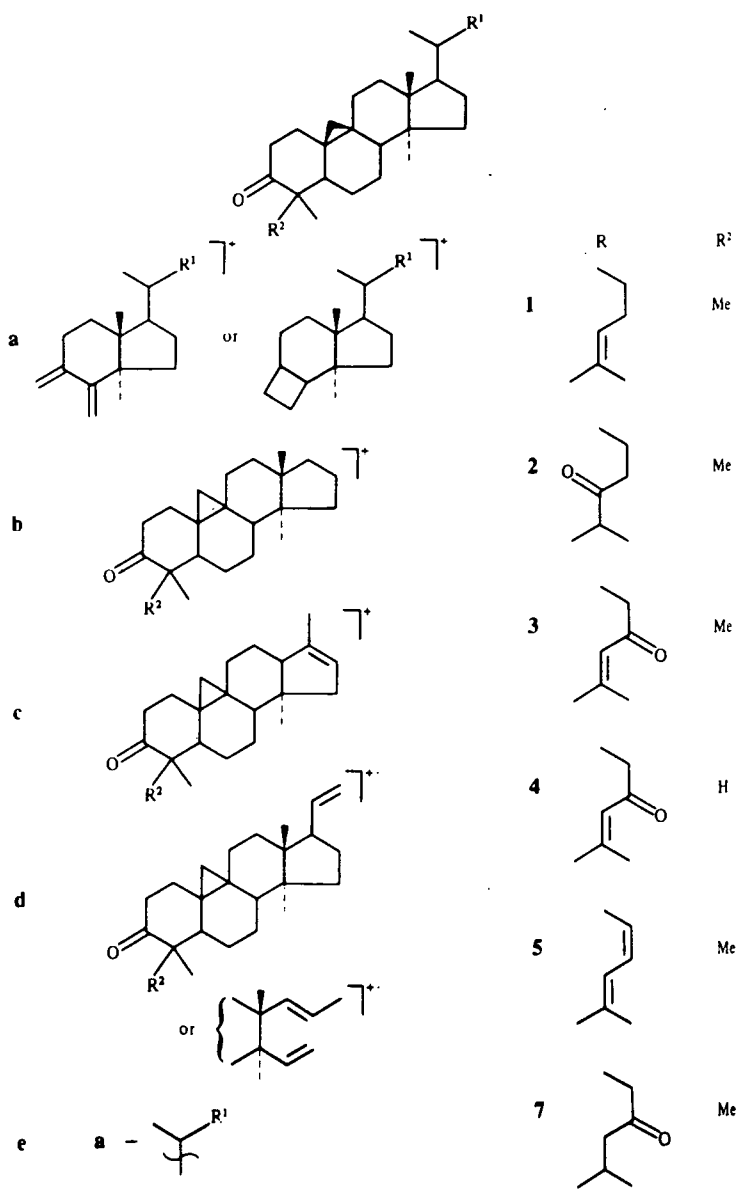

Table 1. Distribution of terpenoids from the bud exudates of Fijian *Gardenia** species

Species	% Yield of triterpenoids									
	1	**2**	**3**	**4**	**5**	**6**	**7**	**8**	**9**	**10**
Gardenia storckii	2.6	1.6	1.7	0.5	0.9	—	—	—	—	—
Gardenia gordonii	2.9	1.3	1.5	0.7	0.4	—	—	—	—	—
Gardenia hillii (Labasa)	1.2	0.2	0.8	0.1	0.4	—	—	—	—	—
Gardenia hillii (Bua)	1.7	0.8	0.6	0.1	0.3	—	—	—	—	—
Gardenia taitensis	—	—	—	—	—	0.4	0.05	0.1	0.1	—
Gardenia grievei	0.07	0.03	—	—	—	—	—	—	—	0.01

*No triterpenoids were isolated from the other *Gardenia* species.
†Yield per cent reported with respect to the bud exudate.

3 showed a prominent signal at δ_H 6.07 due to the olefinic proton adjacent to the carbonyl group. The GC-MS analysis of the mixture containing 2 and 3 showed that a minor compound, but with a significant peak in GC-MS with $[M]^+$ at *m/z* 424 ($C_{29}H_{44}O_2$), *m/z* 326, 147, 125, 83, is in fact the 4-nor-homologue of compound 3. The ^{13}C NMR signals at δ201 (singlet) (C=O at C-23), 154 (singlet) (C=C at C-25), 124 (doublet) (C=C at C-24) for 3 and its 4-nor-homologue were in agreement with the structures assigned for these compounds. The 4-nor-homologue of 3 is also a new natural product 4. The distribution of 1–4 in the *Gardenia* bud exudates is given in Table 1. Three species, *G. storckii*, *G. gordonii*, and *G. hillii*, contained all the four triterpenoids. *Gardenia grievei* contained only two triterpenoids. 1 and 2.

Another triterpenoid which was present in three out of the five species (Table 1) was identified as a cycloartadienone (5). It was separated from cycloartenone (1) by GC and a GC-MS study showed 5 to have a $[M]^+$ at *m/z* 422 ($C_{30}H_{46}O$). The mass spectral fragmentations of 5 were similar to those of 1 with the base peak at *m/z* 69 (C_5H_9) suggesting the presence of a Me_2C=C group. The fragment ion at *m/z* 109 for 5 showed the presence of two olefinic double bonds in its side chain. The presence of two C=C bonds were confirmed by catalytic hydrogenation over Pd-C. The reduced product had $[M]^+$ at *m/z* 426 ($C_{30}H_{50}O$) with fragment ions at *m/z* 313, 288, 113 and 95.

The triterpenoid composition of the bud exudates of *G. taitensis* was different from the other *Gardenia* species discussed above. Four triterpenoids were isolated from *G. taitensis* and one has been characterized as 9,19-cyclolanostane- 3,23-dione (7). Three other terpenoids, 6, 8 and 9, could not be characterized due to lack of materials.

Compound 7 could not be separated easily by chromatographic methods from 8. However, GC-MS analysis was useful in elucidating the structure of 7 which had a $[M]^+$ at *m/z* 440 ($C_{30}H_{48}O_2$) and was isomeric with 2. The presence of the fragment ions at *m/z* 355, 340, 313, 311, 302, 127 and 57 in the mass spectrum of compound 7 was the key to identifying 7 as 9,19-cyclolanostane-3,23-dione. Two species of *Gardenia hillii* collected in different locations in Fiji gave similar triterpenoid profiles (Tables 1 and 2).

EXPERIMENTAL

Gardenia species were collected in Fiji during 1986–1988. Voucher specimens for all the shrubs and trees sampled and a map indicating the place of collection are deposited in the South Pacific Herbarium, Suva, Fiji. Selected duplicate vouchers are deposited in the Bernie Bishop Museum, Honolulu, Hawaii (BISH) and Rancho Santa Ana Botanic Garden, Claremont, California (RSA-POM). The bud exudates were dissolved in $CHCl_3$–MeOH. The residue on evaporation was extracted with *n*-hexane to give fractions containing terpenoids. Out of the 9 species studied [6], only the *Gardenia* species listed in Table 1 contained terpenoids in their bud exudates. The distribution of terpenoids is also given in Table 1. The bud exudates of three species, *G. storckii*, *G. gordonii*, and *G. hillii* gave two main terpenoid fractions when separated by VLC (silica gel) [11]. These have been labelled as terpenoid fractions A and B (Table 2). The GC-MS determinations were carried out on a HP-MSD, using a 25 m × 0.32 mm HP-5 column (0.52 μm film), with an SGE on-column injector, and temp. programming from 30 to 240° at 30° min^{-1}, then to 300° at 10° min^{-1} using He as carrier gas. The HR ^1H and ^{13}C NMR spectra were recorded at ambient temp. at 250 and 300 MHz, respectively, using TMS as int. ref.

Table 2. Terpenoid fractions from Fijian *Gardenia* species

Species	Terpenoid fraction	% Yield
G. gordonii	A	3.9
	B	3.4
G. hillii	A	2.0
(collected from Labasa)	B	1.8
G. hillii	A	1.9
(collected from Bua)	B	1.5
G. storckii	A	3.5
	B	2.9
G. taitensis	6	0.4
	7 and 8	0.6
	8 and 9	0.7
G. grievei	C	0.1
	D	0.2

The terpenoid fraction *A* showed a distinct pink spot on silica gel TLC (60% $CHCl_3$–*n*-hexane) when sprayed with ceric sulphate reagent. This fr. was purified further by prep. TLC on silica gel and using 60% $CHCl_3$–*n*-hexane as eluting solvent. On GC analysis this fraction was found to contain cycloartenone (1) and cycloartadienone (5) in GLC peak ratio of 74%:26%.

Terpenoid fraction A. Cycloartenone (1). GC-IR (gas phase) cm^{-1}: 1720 max (C=O). ^1H NMR ($CDCl_3$): δ0.8-1.8 (–CH_2–, Me), 2.3 (–CH_2–CO–), 4.7, (–CH=). ^{13}C NMR ($CDCl_3$): δ216.52 (C=O), 130.79 (C-25), 125.08 (*d*, C-24), 52.16 (*d*, C-17), 50.11 (C-4), 48.60 (C-14), 48.30 (*d*, C-5), 47.78 (*d*, C-8), 45.19 (C-13), 37.36 (*t*, C-2) 36.20 (*t*, C-22), 35.75 (*d*, C-20), 35.45 (*t*, C-15), 33.30 (*t*, C-1) 32.66 (*t*, C-12), 29.45 (*t*, C-19), 28.03 (*t*, C-7), 26.60 (*t*, C-16), 25.83 (C-10), 25.75 (*t*, C-11), 25.63 (*q*, C-27), 24.81 (*t*, C-23), 22.096 (*q*, C-30), 21.39 (*t*, C-6), 20.96 (C-9), 20.66 (*q*, C-29), 19.18 (*q*, C-18), 18.11 (*q*, C-28), 17.98 (*q*, C-21), 17.54 (*q*, C-26). MS *m/z* (rel. int.): 424 (18) $[M]^+$, 409 (24), 340 (17), 313 (20), 311 (22), 286 (24), 271 (20), 205 (18), 147 (20), 111 (187), 95 (57), 69 (100). HR-MS: 424.370 $[M]^+$ ($C_{30}H_{48}O$ requires 424.3705), 340.278 ($C_{24}H_{36}O$ requires 340.2766), 313.250 ($C_{22}H_{33}O$ requires 313.2530), 286.265 ($C_{21}H_{34}$ requires 286.2660). Cycloartadienone (5): GC-IR (gas phase): 1720 cm^{-1} (–C=O). MS *m/z* (rel. int.): 422 (26) $[M]^+$ ($C_{30}H_{46}O$), 313 (18), 311 (25), 259 (20), 121 (68), 111 (12), 94 (42), 69 (100). HR-MS: *m/z* 422.358 ($C_{30}H_{46}O$ requires 422.3548).

Reduced fraction A. MS *m/z* (rel. int.): 426 (15) $[M]^+$ ($C_{30}H_{50}O$), 313 (17), 288 (10), 109 (30), 95 (28).

Terpenoid fraction B (Table 2). The terpenoid fraction B was purified on prep. on TLC (silica gel). GC-MS analysis showed that this fraction contained three compounds in the GC ratio indicated in parentheses. 9,19-cyclolanostane-3,24-dione (2) (40): 9,19-cyclolanost-24-ene-3,23-dione (3) (30): 4-nor-homologue of 3 (4) (19). ^1H NMR ($CDCl_3$): δ0.78–2.00 (CH_2 and Me). 2.21 (MeC=), 2.31 (CH_2CO), 6.07 (=CHCO). 2: MS (rel. int.): *m/z* 440 (18) $[M]^+$ ($C_{30}H_{48}O_2$), 354 (24), 313 (45), 302 (21), 203 (24), 175 (38), 127 (40), 95 (64), 71 (60), 43 (100). HR-MS: *m/z* 440.363 $[M]^+$ ($C_{30}H_{48}O_2$ requires 440.3654), 354.290 ($C_{25}H_{38}O$ requires 354.2922), 302.262 ($C_{21}H_{34}O$ requires 302.2609), 127.112 ($C_8H_{15}O$ requires 127.1123), 71.051 (C_4H_7O requires 71.0497). 3: MS *m/z* (rel. int.): 438 (10) $[M]^+$ ($C_{30}H_{46}O_2$), 340 (45), 125 (75), 98 (46), 83 (100), HR-MS: *m/z* 438.351 $[M]^+$ ($C_{30}H_{46}O_2$ requires

438.3497), 340.275 ($C_{24}H_{36}O$ requires 340.2766), 125.098 ($C_8H_{13}O$ requires 125.0966), 98.073 ($C_6H_{10}O$ requires 98.0731) 83.049 (C_5H_7O requires 83.0497). **4**: MS *m/z* (rel. int.): 424 (10) $[M]^+$ ($C_{29}H_{44}O_2$), 326 (39), 147 (71), 125 (86), 83 (100). HR-MS: *m/z* 424.334 $[M]^+$ ($C_{29}H_{44}O_2$ requires 424.3341), 326.259 ($C_{23}H_{34}O$ requires 326.2609).

The fractions of the bud exudates of *G. taitensis* containing terpenes on GC-MS analyses showed that they were chemically different to those of the bud exudates of the three Gardenia species discussed above (Table 1). The terpenoids and their GC peak ratios (in parentheses) are given below: 9,19-Cycloanostane-3,23-dione (**7**) (25%): Three yet unidentified triterpenoids (**6**, **8** and **9**) (75%). *GC-MS of the triterpenoids of the bud exudates of G. taitensis.* **6**: *m/z* (rel. int.): 424 (100) $[M]^+$ ($C_{30}H_{48}O$), 409 (5), 218 (100), 189 (15). **7** *m/z* (rel. int.): 440 (14) $[M]^+$ ($C_{30}H_{48}O_2$), 355 (17), 340 (78), 313 (12), 311 (15), 302 (28), 175 (22), 127 (60), 85 (65), 57 (42). **8** *m/z* (rel. int.): 424 (22) $[M]^+$ ($C_{30}H_{48}O$), 355 (40), 340 (50), 298 (60), 221 (100), 205 (75), 147 (58), 111 (55), 85 (78), 55 (90). **9** *m/z* (rel. int.): 438 (10) $[M]^+$ ($C_{30}H_{46}O_2$), 353 (16), 338 (34), 323 (15), 202 (26), 147 (100), 121 (77), 85 (22), 57 (48).

Two triterpenoid fractions C and D (Table 2) were obtained from the bud exudates of *Gardenia grievei*. GC-MS analyses showed that the terpenoid fraction c contained cycloartenone (**1**) and a triterpenoid (**10**). The terpenoid fraction D was mainly 9,19-cyclolanostane-3,24-dione (**2**) mp. 175–177°. *GC-MS of* **10** (*mp* 183–185°). *m/z* (rel. int.): 424 (16) $[M]^+$ ($C_{30}H_{48}O$), 409 (52), 339 (2), 271 (20), 257 (100), 137 (38), 95 (36), 55 (30). ^1H NMR ($CDCl_3$, 250 MHz) of **10**: δ0.6–1.58 (CH_2 and CH_3, 2.69 (CH_2CO), 5.11 (=CH).

Acknowledgements—The authors thank the Australia and Pacific Science Foundation for a research grant. Drs M. I. Burgar and M. Ridd are thanked for the provision of some NMR data and for the GC-IR data.

REFERENCES

1. Weiner, M. A. (1978) *The Secrets of Fijian Medicine*. Government Publications, Fiji.
2. Chatterjee, A., Saha, S. K. and Bhattacharya, S. (1980) *Indian J. Chem.* **5**, 421.
3. Chhabra, S. C., Gupta, S. R. and Sharma, N. D. (1977) *Phytochemistry* **7**, 1109.
4. Gunatilaka, A. A. L., Sirimanne, S. R., Sotheeswaran, S. and Nakanishi, T. (1979) *J. Chem. Res.* (M) 2637.
5. Durga, K., Gupta, S. R. and Sharma, N. D. (1979) *Indian J. Chem.* **2**, 181.
6. Miller, J. M., Naidu, R., Sotheeswaran, S., Davies, N., Bokel, M. and Kraus W. (1989) *Proc. Pacifichem* '89. Honolulu, Hawaii.
7. Audier, H. E., Beugelmans, R. and Das, B. C. (1966) *Tetrahedron Letters* 4341.
8. Wyllie, S. G. and Djerassi, C. (1968) *J. Org. Chem.* **33**, 305.
9. Aplin, R. T. and Hornby, G. M. (1966) *J. Chem. Soc.*, (B) 1078.
10. Budzikiewicz, H., Wilson, J. M. and Djerassi, C. (1963) *J. Am. Chem. Soc.* **85**, 3688.
11. Coll. J. C., Liyanage, N., Stokie, G. J., Van Altena, I., Nemosin, J. N. E., Sternhell, S. and Kazlauskas, R. (1978) *Aust. J. Chem.* **31**, 157.

APPENDIX C

EIGHT PEAK MASS SPECTRAL DATA

Eight peak spectra, indexed by name

Ions/Intensities	Mol.Wt.	Formula	Compound Name
190(100), 125(29), 134(28), 162(27), 91(14), 112(13), 191(12), 161(11)	278	$C_{16}H_{22}O_4$	abscisic acid, methyl ester
125(100), 167(27), 43(23), 96(14), 124(10), 126(8), 52(7), 80(5)	167	$C_8H_9NO_3$	acetanilide, 2,4-dihydroxy-
138(100), 153(73), 195(72), 43(31), 110(19), 52(13), 95(12), 139(11)	195	$C_{10}H_{13}NO_3$	acetanilide, 2,4-dimethoxy-
143(100), 43(42), 145(33), 185(19), 80(12), 51(10), 144(9), 114(9)	185	$C_8H_8NO_2Cl$	acetanilide, 2-hydroxy-4-chloro-
108(100), 123(80), 165(57), 43(42), 80(31), 52(21), 65(17), 92(8)	165	$C_9H_{11}NO_2$	acetanilide, 2-methoxy-
157(100), 142(92), 43(60), 199(53), 159(34), 144(32), 114(24), 201(19)	199	$C_9H_{10}NO_2Cl$	acetanilide, 2-methoxy-4-chloro-
125(100), 167(46), 43(33), 79(30), 52(12), 124(10), 126(8), 51(8)	167	$C_8H_9NO_3$	acetanilide, 3,4-dihydroxy-
138(100), 195(71), 153(31), 43(31), 110(24), 139(19), 15(9), 196(9)	195	$C_{10}H_{13}NO_3$	acetanilide, 3,4-dimethoxy-
154(100), 211(95), 43(40), 110(36), 169(34), 109(13), 212(11), 155(9)	211	$C_{10}H_{13}NO_2S$	acetanilide, 3-methylthio-4-methoxy-
108(100), 123(62), 165(56), 43(26), 80(10), 52(10), 122(10), 109(8)	165	$C_9H_{11}NO_2$	acetanilide, 4-methoxy-
43(100), 161(57), 163(35), 177(24), 179(15), 203(11), 162(10), 160(9)	219	$C_8H_7NO_2Cl_2$	acetanilide, N-hydroxy-3,4-dichloro-
43(100), 157(40), 126(31), 159(24), 127(21), 111(15), 142(13), 128(13)	199	$C_8H_8NO_2Cl$	acetanilide, N-hydroxy-4-chloro-
341(100), 282(58), 43(39), 42(34), 229(30), 59(23), 342(22), 204(17)	341	$C_{20}H_{23}NO_4$	acetyl codeine
136(100), 29(33), 52(30), 135(13), 53(12), 51(9), 137(7), 39(7)	136	$C_5H_4N_4O$	allopurinol
58(100), 59(18), 42(11), 30(8), 202(7), 203(5), 215(), 91(4)	277	$C_{20}H_{23}N$	amitryptaline
44(100), 91(6), 42(4), 65(4), 45(3), 39(3), 51(2), 120(2)	135	$C_9H_{13}N$	amphetamine
156(100), 141(60), 41(45), 157(33), 55(30), 43(30), 27(28), 29(22)	226	$C_{11}H_{18}N_2O_3$	amylobarbitone
148(100), 147(35), 77(22), 133(22), 117(22), 105(20), 121(18), 79(13)	148	$C_{10}H_{12}O$	anethole
106(100), 107(83), 77(32), 51(24), 39(23), 79(16), 65(15), 78(12)	107	C_7H_9N	aniline, N-methyl-
108(100), 65(95), 78(67), 39(46), 51(24), 77(22), 79(17), 93(16)	108	C_7H_8O	anisole
116(100), 43(88), 29(71), 85(59), 31(49), 44(46), 61(29), 42(28)	176	$C_6H_8O_6$	ascorbic acid
72(100), 30(57), 43(10), 56(9), 41(7), 57(6), 107(6), 73(5)	266	$C_{14}H_{22}N_2O_3$	atenolol
156(100), 141(76), 41(36), 27(33), 29(30), 39(30), 55(29), 98(22)	184	$C_8H_{12}N_2O_3$	barbitone
135(100), 136(69), 77(27), 92(14), 107(11), 39(10), 63(8), 65(8)	136	$C_8H_8O_2$	benzaldehyde, methoxy-
238(100), 223(31), 43(26), 192(19), 239(15), 191(11), 163(11), 39(10)	238	$C_{13}H_{18}O_4$	benzene, 2,3,4,5-tetramethoxy-allyl-
91(100), 92(89), 41(17), 65(13), 29(13), 39(12), 27(12), 105(9)	162	$C_{12}H_{18}$	benzene, n-hexyl
43(100), 171(89), 188(83), 230(61), 79(44), 52(19), 51(18), 95(16)	230	$C_8H_{10}N_2O_4S$	benzenesulfonamide, 3-hydroxy-4-acetylamino-
202(100), 244(75), 43(74), 138(42), 186(34), 92(25), 107(24), 79(12)	244	$C_9H_{12}N_2O_4S$	benzenesulfonamide, 3-methoxy-4-acetylamino-

Ions/Intensities	Mol.Wt.	Formula	Compound Name
43(100), 121(53), 202(24), 185(15), 64(9), 63(9), 122(8), 90(7)	242	$C_9H_{12}N_2O_4S$	benzenesulfonamide, N-methoxy-4-acetylamino-
43(100), 188(27), 172(21), 60(19), 107(18), 108(12), 92(9), 156(8)	230	$C_8H_{10}N_2O_4S$	benzenesulfonamide, N-OH-4-acetylamino-
120(100), 151(59), 193(38), 43(36), 65(20), 92(19), 121(11), 161(10)	193	$C_{10}H_{11}NO_3$	benzoic acid, N-acetyl-4-amino-, me. ester
105(100), 91(61), 77(39), 212(23), 51(22), 65(14), 106(11), 90(10)	212	$C_{14}H_{12}O_2$	benzyl benzoate
91(100), 57(46), 108(31), 192(27), 85(24), 41(15), 43(11), 92(8)	192	$C_{12}H_{16}O_2$	benzyl isopentanoate
91(100), 108(83), 57(34), 192(26), 85(25), 92(14), 65(12), 90(12)	192	$C_{12}H_{16}O_2$	benzyl pentanoate
169(100), 185(60), 43(47), 168(32), 211(28), 141(22), 167(21), 170(14)	227	$C_{14}H_{13}NO_2$	biphenyl, N-hydroxy-3-acetylamino-
169(100), 211(39), 168(30), 185(24), 43(23), 170(15), 141(11), 167(10)	227	$C_{14}H_{13}NO_2$	biphenyl, N-hydroxy-4-acetylamino-
199(100), 43(93), 168(51), 184(27), 200(17), 241(17), 169(16), 153(13)	241	$C_{15}H_{15}NO_2$	biphenyl, N-methoxy-3-acetylamino-
168(100), 199(77), 43(46), 169(40), 167(32), 198(30), 241(29), 141(22)	241	$C_{15}H_{15}NO_2$	biphenyl, N-methoxy-4-acetylamino-
69(100), 41(90), 93(85), 67(58), 94(53), 109(47), 79(45), 204(33)	204	$C_{15}H_{24}$	bisabolene, β-
43(100), 143(83), 85(67), 105(62), 81(60), 59(53), 134(49), 71(48)	238	$C_{15}H_{26}O_2$	bisabolol oxide B
143(100), 43(71), 93(43), 71(34), 125(34), 121(31), 68(30), 134(25)	238	$C_{15}H_{26}O_2$	bisabolol oxide B
43(100), 41(89), 69(80), 109(50), 119(40), 93(39), 55(35), 67(28)	222	$C_{15}H_{26}O$	bisabolol, α-
93(100), 141(87), 43(85), 94(62), 68(51), 121(49), 95(46), 41(39)	236	$C_{15}H_{24}O_2$	bisabolone oxide
95(100), 41(20), 110(17), 55(11), 43(10), 67(8), 93(8), 96(8)	154	$C_{10}H_{18}O$	borneol
95(100), 43(66), 93(38), 121(36), 136(33), 55(17), 69(16), 108(16)	196	$C_{12}H_{20}O_2$	bornyl acetate
41(100), 79(82), 67(82), 119(80), 55(68), 81(68), 84(65), 93(9)	280	$C_{16}H_{24}O_4$	Brefeldin A
317(100), 315(96), 236(92), 288(69), 78(57), 286(57), 77(56), 51(51)	315	$C_{14}H_{10}N_3OBr$	bromazepam
202(100), 200(18), 203(17), 101(11), 202(10), 88(6), 150(5), 100(4)	202	$C_{16}H_{10}$	butadiyne, 1,4-diphenyl-
59(100), 43(49), 31(42), 41(29), 39(14), 69(11), 42(7), 87(4)	102	$C_5H_{10}O_2$	butan-2-one, 3-hydroxy-3-methyl-
43(100), 105(43), 91(36), 148(28), 77(13), 79(12), 51(10), 67(9)	148	$C_{10}H_{12}O$	butan-2-one, 4-phenyl-
156(100), 141(94), 41(44), 29(40), 27(31), 39(21), 98(19), 142(15)	212	$C_{10}H_{16}N_2O_3$	butobarbitone
161(100), 134(58), 119(46), 105(45), 204(41), 41(34), 81(27), 91(25)	204	$C_{15}H_{24}$	cadinene, δ-
159(100), 160(13), 202(9), 129(7), 128(7), 131(5), 105(5), 144(4)	202	$C_{15}H_{22}$	calamenene
93(100), 121(67), 79(38), 41(38), 67(33), 91(28), 107(28), 39(27)	136	$C_{10}H_{16}$	camphene
43(100), 71(99), 69(48), 41(44), 67(33), 96(31), 84(28), 39(28)	154	$C_{10}H_{18}O$	camphene hydrate
108(100), 93(42), 95(25), 41(24), 109(19), 67(19), 91(13), 81(12)	152	$C_{19}H_{16}O$	campholene aldehyde, α-
95(100), 81(65), 41(61), 69(38), 108(35), 55(35), 83(33), 109(26)	152	$C_{10}H_{16}O$	camphor

Ions/Intensities	Mol.Wt.	Formula	Compound Name
295(100), 296(21), 238(12), 310(12), 26(8), 251(6), 27(6), 55(5)	310	$C_{21}H_{26}O_2$	cannabinol
140(100), 139(90), 91(65), 168(51), 51(36), 63(35), 77(30), 39(20)	168	$C_{12}H_8O$	capillin
193(100), 192(34), 236(23), 191(20), 165(16), 194(15), 63(7), 167(6)	236	$C_{15}H_{12}N_2O$	carbamazepine
186(100), 29(77), 114(68), 42(48), 72(45), 27(32), 113(31), 81(20)	186	$C_7H_{10}N_2O_2S$	carbimazole
93(100), 43(31), 91(31), 79(29), 77(29), 27(28), 80(22), 92(21)	136	$C_{10}H_{16}$	carene, Δ3-
161(100), 41(65), 84(49), 69(45), 55(41), 97(40), 43(39), 81(37)	222	$C_{15}H_{26}O$	carotol
135(100), 150(27), 91(20), 41(12), 77(11), 39(10), 136(10), 107(9)	150	$C_{10}H_{14}O$	carvacrol
84(100), 134(65), 41(50), 79(47), 109(47), 119(40), 55(39), 91(37)	152	$C_{10}H_{16}O$	carveol, *cis*-
109(100), 84(85), 41(46), 55(37), 119(35), 83(33), 91(33), 39(28)	152	$C_{10}H_{16}O$	carveol, *trans*-
43(100), 84(71), 119(55), 109(35), 134(35), 152(34), 41(29), 91(29)	194	$C_{12}H_{18}O$	carveyl acetate
82(100), 54(44), 39(34), 93(26), 108(25), 41(23), 53(17), 107(16)	150	$C_{10}H_{14}O$	carvone
41(100), 69(98), 93(94), 133(65), 79(61), 91(55), 107(39), 39(35)	204	$C_{15}H_{24}$	caryophyllene
124(100), 123(63), 78(48), 77(20), 51(19), 39(18), 55(10), 52(9)	124	$C_7H_8O_2$	catechol, 4-methyl-
119(100), 93(49), 41(34), 69(30), 105(28), 161(23), 204(20), 120(17)	204	$C_{15}H_{24}$	cedrene, α-
95(100), 151(84), 43(68), 150(61), 41(51), 69(44), 81(42), 152(35)	222	$C_{15}H_{26}O$	cedrol
184(100), 169(91), 183(26), 153(23), 155(22), 152(17), 185(15), 154(13)	184	$C_{14}H_{16}$	chamazulene
282(100), 283(80), 284(44), 285(25), 77(15), 220(13), 247(12), 219(11)	299	$C_{16}H_{14}N_3OCl$	chlordiazepoxide
86(100), 30(13), 58(11), 87(6), 41(6), 73(5), 42(5), 319(3)	319	$C_{18}H_{26}N_3Cl$	chloroquine
266(100), 264(76), 268(47), 109(25), 124(19), 98(14), 133(14), 62(12)	264	$C_8N_2Cl_4$	chlorothalonil
203(100), 58(92), 205(33), 72(26), 204(15), 42(13), 167(13), 202(12)	274	$C_{16}H_{19}N_2Cl$	chlorpheniramine
58(100), 86(21), 318(16), 85(8), 42(8), 272(6), 320(6), 232(5)	318	$C_{17}H_{19}N_2SCl$	chlorpromazine
43(100), 81(27), 55(26), 69(26), 71(22), 108(18), 84(18), 111(13)	154	$C_{10}H_{18}O$	cineole, 1,8-
123(100), 121(28), 150(27), 41(20), 93(19), 81(17), 43(17), 55(16)	316	$C_{20}H_{28}O_3$	cinerin I
121(100), 107(97), 149(65), 93(56), 167(55), 150(29), 91(25), 55(25)	360	$C_{21}H_{28}O_5$	cinerin II
131(100), 103(37), 176(30), 77(26), 51(15), 104(13), 132(12), 147(11)	176	$C_{11}H_{12}O_2$	cinnamic acid, ethyl ester
131(100), 162(58), 103(45), 77(24), 51(14), 102(11), 132(10), 163(6)	162	$C_{10}H_{10}O_2$	cinnamic acid, methyl ester
185(100), 185(57), 259(54), 43(54), 57(38), 29(27), 41(24), 157(22)	402	$C_{20}H_{34}O_8$	citric acid, acetyl-, tri-n-butyl ester
41(100), 69(81), 55(46), 95(36), 43(32), 56(29), 57(27), 39(21)	154	$C_{10}H_{18}O$	citronellal
41(100), 69(85), 55(42), 82(37), 67(34), 81(29), 71(25), 95(24)	156	$C_{10}H_{20}O$	citronellol

Ions/Intensities	Mol.Wt.	Formula	Compound Name
69(100), 41(95), 81(50), 82(47), 95(41), 67(28), 123(27), 68(22)	224	$C_{14}H_{24}O_2$	citronellyl butenoate
300(100), 77(85), 258(67), 51(58), 255(52), 259(47), 256(38), 283(38)	300	$C_{16}H_{13}N_2O_2Cl$	clobazepam
280(100), 286(72), 315(72), 288(56), 240(53), 234(53), 75(48), 287(44)	315	$C_{15}H_{10}N_3O_3Cl$	clonazepam
30(100), 229(48), 231(30), 172(19), 194(13), 174(12), 42(12), 230(8)	229	$C_9H_9N_3Cl_2$	clonidine
82(100), 182(45), 83(29), 105(21), 42(16), 77(13), 96(11), 97(8)	303	$C_{17}H_{21}NO_4$	cocaine
73(100), 371(76), 178(41), 196(39), 42(29), 372(23), 59(21), 70(21)	371	$C_{21}H_{29}NO_3Si$	codeine, trimethylsilyl derivative
119(100), 105(95), 161(94), 41(46), 93(65), 91(34), 55(28), 120(27)	204	$C_{15}H_{24}$	copaene, α-
161(100), 105(97), 119(93), 41(33), 81(32), 120(29), 91(29), 93(26)	204	$C_{15}H_{24}$	cubebene, α-
133(100), 105(66), 148(58), 77(39), 91(34), 79(34), 41(32), 119(32)	148	$C_{10}H_{12}O$	cuminic aldehyde, p-
135(100), 150(43), 105(42), 107(35), 79(32), 119(25), 91(23), 77(16)	150	$C_{10}H_{14}O$	cuminyl alcohol
83(100), 55(58), 41(38), 67(15), 43(13), 29(11), 168(11)	168	$C_{12}H_{24}$	cyclohexane, n-hexyl-
83(100), 55(71), 82(70), 41(38), 67(16), 29(16), 43(13), 154(12)	154	$C_{11}H_{22}$	cyclohexane, n-pentyl-
43(100), 135(53), 115(17), 132(14), 117(13), 65(8), 115(7), 39(6)	150	$C_{10}H_{14}O$	cymene-8-ol, p-
132(100), 117(81), 91(38), 115(33), 92(20), 39(19), 65(19), 131(15)	132	$C_{10}H_{12}$	cymenene
43(100), 248(75), 108(70), 290(63), 140(50), 58(27), 65(27), 92(23)	290	$C_{14}H_{14}N_2O_3S$	dapsone, acetyl-
151(100), 93(72), 43(43), 194(28), 136(25), 41(24), 133(14), 55(12)	238	$C_{15}H_{26}O_2$	daucol
74(100), 41(75), 43(74), 55(70), 110(50), 54(48), 67(45), 29(36)	184	$C_{11}C_{20}O_2$	dec-4-enoic acid, methyl ester
59(100), 271(48), 31(39), 150(36), 270(26), 42(23), 214(19), 30(16)	271	$C_{18}H_{25}NO$	dextromethorphan
58(100), 91(5), 57(5), 59(4), 42(3), 77(3), 105(2), 30(2)	339	$C_{22}H_{29}NO_2$	dextropropoxyphene
256(100), 283(81), 284(66), 255(42), 257(41), 285(41), 258(33), 286(22)	284	$C_{16}H_{13}N_2OCl$	diazepam
100(100), 44(17), 72(9), 101(7), 77(7), 29(7), 42(6), 56(4)	295	$C_{13}H_{19}NO$	diethylpropion
121(100), 43(74), 161(60), 123(38), 93(38), 136(36), 95(36), 119(33)	194	$C_{13}H_{22}O$	dihydro-β-ionone
29(100), 207(63), 137(34), 109(32), 41(31), 149(20), 189(18), 67(17)	222	$C_{15}H_{26}O$	dihydroagarofuran
121(100), 150(20), 77(8), 91(7), 78(5), 39(5), 122(4), 65(3),	150	$C_{10}H_{14}O$	dihydroanethole
95(100), 67(78), 68(66), 82(60), 81(54), 41(47), 152(43), 109(39)	152	$C_{10}H_{16}O$	dihydrocarvone
301(100), 44(40), 42(38), 59(37), 70(31), 164(26), 31(24), 302(21)	301	$C_{18}H_{23}NO_3$	dihydrocodeine
222(100), 177(31), 207(15), 98(13), 223(12), 51(11), 63(10), 192(10)	222	$C_{12}H_{14}O_4$	dillapiole
126(100), 41(82), 43(56), 168(45), 125(39), 55(36), 39(36), 69(35)	168	$C_{10}H_{16}O_2$	diosphenol
58(100), 73(80), 45(49), 44(22), 59(16), 42(14), 165(14), 167(11)	256	$C_{17}H_{21}NO$	diphenhydramine

Ions/Intensities	Mol.Wt.	Formula	Compound Name
43(100), 55(50), 69(40), 56(40), 41(38), 61(36), 83(34), 70(33)	228	$C_{14}H_{28}O_2$	dodecyl acetate
58(100), 71(60), 42(51), 44(26), 43(26), 51(22), 30(21), 27(11)	270	$C_{17}H_{22}N_2O$	doxylamine
81(100), 68(87), 93(69), 41(57), 67(48), 107(45), 55(41), 79(36)	204	$C_{15}H_{24}$	elemene, β-
121(100), 93(74), 107(47), 79(32), 94(29), 91(26), 81(26), 136(25)	204	$C_{15}H_{24}$	elemene, γ-
208(100), 194(54), 209(14), 77(13), 133(11), 91(11), 79(10), 177(10)	208	$C_{12}H_{16}O_3$	elemicin
59(100), 93(53), 41(45), 43(36), 161(33), 81(33), 107(29), 121(24)	222	$C_{15}H_{26}O$	elemol
58(100), 146(24), 42(21), 56(19), 77(16), 30(15), 105(14), 117(8)	165	$C_{10}H_{15}NO$	ephedrine
148(100), 147(42), 121(39), 117(30), 77(22), 133(21), 105(17), 51(15)	148	$C_{10}H_{12}O_2$	estragole
86(100), 58(23), 42(7), 29(6), 87(6), 30(5), 27(4), 51(3)	193	$C_{12}H_{19}NO$	etafedrine
313(100), 42(38), 59(29), 162(28), 314(19), 284(18), 124(18), 243(16)	313	$C_{19}H_{23}NO_3$	ethylmorphine
59(100), 109(36), 166(27), 41(18), 55(17), 95(17), 81(13), 96(13)	224	$C_{15}H_{28}O$	eudesman-11-ol, 4αH,5αH-
59(100), 109(27), 151(27), 95(21), 166(19), 41(18), 110(17), 55(13)	224	$C_{15}H_{28}O$	eudesman-11-ol, 4βH,5αH-
109(100), 95(87), 95(87), 55(85), 96(75), 81(69), 69(65), 83(65)	208	$C_{15}H_{28}$	eudesmane, 4αH,5αH-
59(100), 149(37), 164(27), 109(21), 108(20), 81(17), 41(17), 95(15)	222	$C_{15}H_{26}O$	eudesmol, β-
189(100), 204(69), 161(61), 59(50), 133(45), 105(32), 81(30), 107(26)	222	$C_{15}H_{26}O$	eudesmol, γ-
81(100), 80(50), 41(39), 71(31), 69(30), 43(28), 55(24), 84(21)	154	$C_{10}H_{18}O$	fenchol
81(100), 69(57), 41(24), 82(13), 152(12), 29(12), 80(10), 39(9)	152	$C_{10}H_{16}O$	fenchone
134(100), 41(36), 133(35), 69(31), 135(10), 107(9), 39(9), 77(6)	202	$C_{14}H_{18}O$	feniculin
312(100), 285(99), 286(67), 313(63), 266(48), 238(43), 283(40), 284(33)	313	$C_{16}H_{12}N_3O_3F$	flunitrazepam
181(100), 180(71), 223(57), 152(23), 43(21), 197(19), 182(16), 165(15)	239	$C_{15}H_{13}NO_2$	fluorene, N-hydroxy-2-acetylamino-
180(100), 181(63), 210(51), 179(39), 211(38), 43(37), 253(36), 165(33)	253	$C_{16}H_{15}NO_2$	fluorene, N-methoxy-2-acetylamino-
239(100), 180(62), 197(61), 196(51), 181(23), 152(21), 240(16), 168(14)	239	$C_{15}H_{13}NO_2$	fluorene-9-ol, 2-acetlamino-
86(100), 30(16), 87(10), 58(8), 99(8), 42(4), 56(4), 84(3)	387	$C_{21}H_{23}N_3OFCl$	flurazepam
69(100), 41(99), 114(26), 83(25), 123(13), 93(11), 105(10), 77(10)	182	$C_{11}H_{18}O_2$	geranic acid, methyl ester
161(100), 105(45), 91(41), 41(36), 119(30), 77(29), 55(27), 120(26)	204	$C_{15}H_{24}$	Germacrene D
56(100), 169(39), 43(28), 67(22), 82(16), 39(14), 171(13), 54(13)	494	$C_{23}H_{28}N_3O_5SCl$	glibenclamide
189(100), 117(87), 132(76), 160(40), 91(30), 115(29), 39(20), 77(19)	217	$C_{13}H_{15}NO_2$	glutethimide
105(100), 147(87), 41(85), 93(78), 79(58), 91(58), 204(56), 133(54)	204	$C_{15}H_{24}$	guaiene, α-
107(100), 108(99), 93(96), 41(83), 105(66), 79(62), 81(62), 95(61)	204	$C_{15}H_{24}$	guaiene, δ-

Ions/Intensities	Mol.Wt.	Formula	Compound Name
124(100), 109(56), 198(21), 77(18), 81(14), 122(11), 123(10), 52(9)	198	$C_{10}H_{14}O_4$	guaifenesin
161(100), 59(70), 107(57), 105(53), 93(42), 81(42), 41(39), 91(37)	222	$C_{15}H_{26}O$	guaiol
43(100), 41(61), 55(29), 69(27), 39(27), 108(16), 67(12), 111(11)	126	$C_8H_{14}O$	hept-5-en-2-one, trans 6-methyl-
55(100), 43(94), 41(88), 69(78), 83(70), 57(68), 56(60), 70(53)	238	$C_{17}H_{34}$	heptadec-8-ene, Z-
43(100), 57(87), 82(70), 55(59), 41(53), 96(48), 83(45), 69(44)	380	$C_{26}H_{52}O$	hexacosanal, n-
137(100), 109(26), 69(25), 41(23), 93(15), 55(12), 67(11), 39(11)	152	$C_{10}H_{16}O$	hexahydrobenzofuran, 3,6-dimethyl -
105(100), 77(66), 135(31), 51(26), 134(15), 106(8), 78(6), 161(4)	179	$C_9H_9NO_3$	hippuric acid
93(100), 41(34), 80(32), 121(29), 55(19), 43(17), 92(16), 69(15)	204	$C_{15}H_{24}$	humulene
160(100), 103(63), 76(30), 130(29), 131(25), 89(24), 115(23), 50(22)	160	$C_8H_8N_4$	hydralazine
163(100), 161(93), 91(68), 119(52), 206(45), 117(29), 41(28), 43(25)	206	$C_{13}H_{18}O_2$	ibuprofen
58(100), 235(58), 85(52), 234(44), 280(22), 193(20), 195(19), 208(16)	280	$C_{19}H_{24}N_2$	imipramine
144(100). 175(53), 116(17), 89(17), 145(11), 63(7), 176(6), 72(5)	175	$C_{10}H_9NO_2$	indole-2-carboxylic acid, methyl ester
164(100), 166(33), 223(23), 55(21), 43(21), 41(20), 99(17), 165(11)	223	$C_{11}H_{10}NO_2Cl$	indoleacetic acid, 4-chloro-, methyl ester
139(100), 141(37), 357(26), 111(23), 140(10), 358(9), 75(8), 113(8)	357	$C_{19}H_{16}NO_4Cl$	indomethacin
121(100), 93(80), 43(68), 136(59), 41(29), 91(27), 77(25), 109(23)	192	$C_{13}H_{20}O$	ionone, α-
177(100), 43(84), 41(26), 93(20), 91(15), 178(14), 121(12), 77(12)	192	$C_{13}H_{20}O$	ionone, β-
120(100), 41(42), 43(37), 138(31), 121(31), 39(28), 59(28), 55(28)	208	$C_{12}H_{16}O_3$	isoamyl salicylate
71(100), 43(93), 70(53), 41(24), 55(18), 27(13), 29(11), 42(11)	158	$C_9H_8O_2$	isobutyric acid, 2-methylbutyl ester
71(100), 43(99), 56(51), 57(45), 41(41), 29(24), 89(23), 27(17)	144	$C_8H_{16}O_2$	isobutyyl isobutyrate
112(100), 69(55), 41(53), 55(46), 139(33), 56(30), 70(28), 43(25)	154	$C_{10}H_{18}O$	isomenthone
74(100), 87(53), 43(48), 41(35), 55(30), 57(19), 69(18), 82(17)	158	$C_9H_{18}O_2$	isooctanoic acid, methyl ester
43(100), 60(60), 41(54), 57(48), 102(39), 61(25), 71(21), 228(19)	270	$C_{17}H_{24}O_2$	isopropyl myristate
123(100, 161(99), 133(95), 41(42), 162(31), 81(29), 91(26), 43(25),	328	$C_{21}H_{28}O_3$	isopyrethrin I
161(100), 133(92), 107(23), 91(22), 41(19), 105(18), 162(17), 93(15)	372	$C_{22}H_{28}O_5$	isopyrethrin II
123(100), 43(54), 41(34), 55(28), 81(23), 164(22), 93(22), 135(16)	330	$C_{21}H_{30}O_3$	jasmolin I
163(100), 135(89), 93(87), 107(79), 167(76), 55(55), 121(48), 41(43)	374	$C_{22}H_{30}O_5$	jasmolin II
43(100), 41(77),69(55), 109(44), 81(43), 55(36), 122(39), 107(32)	222	$C_{15}H_{26}O$	ledol
86(100), 30(17), 58(10), 87(6), 41(4), 72(3), 56(3), 27(3)	234	$C_{14}H_{22}N_2O$	lignocaine
68(100), 67(44), 93(35), 39(25), 79(24), 53(23), 94(18), 77(15)	136	$C_{10}H_{16}$	limonene

Ions/Intensities	Mol.Wt.	Formula	Compound Name
71(100), 43(74), 41(67), 69(47), 55(44), 27(33), 93(31), 39(28)	154	$C_{10}H_{18}O$	linalool
41(100), 93(93), 69(75), 43(42), 45(28), 121(22), 79(22), 77(19)	196	$C_{12}H_{20}O_2$	linalyl acetate
239(100), 284(72), 75(67), 276(49), 138(48), 302(46), 111(43), 304(35)	320	$C_{15}H_{20}N_2O_2Cl_2$	lorazepam
323(100), 221(81), 181(56), 222(45), 207(40), 72(37), 223(34), 196(24)	323	$C_{20}H_{25}N_3O$	lysergic acid diethylamide (LSD)
242(100), 207(94), 244(33), 270(20), 208(17), 165(16), 243(16), 269(13)	270	$C_{16}H_{15}N_2Cl$	medazepam
178(100), 134(96), 160(47), 78(28), 77(26), 51(26), 39(25), 135(23)	178	$C_{10}H_{10}O_3$	mellein
119(100), 91(74), 134(66), 41(30), 39(26), 77(21), 105(21), 92(17)	134	$C_{10}H_{14}$	mentha-1,3,9-triene, p-
71(100), 43(37), 41(16), 72(14), 58(14), 98(13), 55(11), 57(8)	156	$C_{10}H_{20}O$	menthan-1-ol, p-
113(100), 43(96), 95(66), 41(35), 99(32), 71(24), 55(20), 69(12)	156	$C_{10}H_{20}O$	menthan-4-ol, p-
59(100), 58(15), 55(13), 41(11), 43(8), 81(6), 60(5), 123(4)	156	$C_{10}H_{20}O$	menthan-8-ol, p-
55(100), 41(63), 97(61), 96(34), 27(21), 39(20), 43(17), 81(16)	140	$C_{10}H_{20}$	menthane, cis p-
108(100), 150(21), 79(17), 39(9), 109(8), 77(7), 41(6), 51(5)	150	$C_{10}H_{14}O$	menthofuran
71(100), 81(67), 41(62), 95(61), 55(48), 43(33), 82(33), 69(32)	156	$C_{10}H_{20}O$	menthol
69(100), 41(91), 109(58), 39(51), 81(50), 112(48), 55(42), 67(38)	186	$C_{10}H_{18}SO$	menthon-8-thiol, p-
112(100), 41(85), 69(67), 55(63), 56(39), 139(37), 70(36), 43(35)	154	$C_{10}H_{18}O$	menthone
95(100), 81(67), 138(52), 41(50), 55(44), 123(33), 43(31), 96(27)	198	$C_{12}H_{22}O_2$	menthyl acetate
235(100), 91(52), 250(42), 233(30), 65(25), 76(21), 236(16), 39(15)	250	$C_{16}H_{14}N_2O$	methaqualone
104(100), 91(91), 82(69), 105(43), 119(31), 39(28), 164(27), 77(25)	164	$C_{10}H_{12}O_2$	methyl 3-phenyl propanoate
316(100), 256(88), 241(52), 121(50), 136(42), 105(39), 213(37), 257(34)	316	$C_{21}H_{32}O_2$	methyl abietate
239(100), 299(20), 240(20), 314(14), 197(6), 173(5), 141(5), 143(4)	314	$C_{21}H_{30}O_2$	methyl dehydroabietate
83(100), 82(28), 153(26), 55(20), 156(19), 41(16), 67(12), 96(11)	226	$C_{13}H_{22}O_3$	methyl dihydrojasmonate
83(100), 41(53), 151(45), 67(33), 95(32), 55(29), 93(28), 224(23)	224	$C_{13}H_{20}O_3$	methyl jasmonate
55(100), 41(77), 69(69), 74(68), 83(43), 87(40), 84(34), 43(41)	268	$C_{17}H_{32}O_2$	methyl palmitoleate
121(100), 146(24), 55(23), 41(23), 180(22), 133(20), 316(20), 257(17)	316	$C_{21}H_{32}O_2$	methyl pimarate
58(100), 30(7), 91(5), 42(4), 59(4), 56(3), 65(3), 39(2)	149	$C_{10}H_{15}N$	methylamphetamine
84(100), 56(7), 85(6), 91(5), 55(4), 30(3), 39(2), 77(2)	233	$C_{14}H_{19}NO_2$	methylphenidate
155(100), 140(80), 83(58), 41(56), 98(54), 55(42), 29(26), 27(26)	183	$C_{10}H_{17}NO_2$	methyprylon
72(100), 30(55), 45(13), 43(7), 41(7), 56(7), 107(6), 57(5)	267	$C_{15}H_{25}NO_3$	metoprolol
54(100), 81(92), 53(81), 45(53), 124(50), 42(47), 27(44), 52(41)	171	$C_6H_9N_3O_3$	metromidazole

Ions/Intensities	Mol.Wt.	Formula	Compound Name
259(100), 161(62), 81(42), 163(10), 54(9), 89(8), 27(7), 160(7)	414	$C_{18}H_{14}N_2OCl_4$	miconazole
41(100), 93(91), 69(76), 39(34), 27(30), 53(21), 77(13), 29(12)	136	$C_{10}H_{16}$	myrcene
192(100), 91(24), 165(22), 119(16), 65(15), 39(14), 161(13), 193(12)	192	$C_{11}H_{12}O_3$	myristicine
69(100), 67(94), 93(91), 123(85), 41(83), 81(73), 82(70), 55(61)	154	$C_{10}H_{18}O$	myrtanol
43(100), 93(94), 82(71), 69(53), 121(45), 67(44), 41(44), 95(38)	196	$C_{12}H_{20}O_2$	myrtanyl acetate
79(100), 91(31), 108(17), 31(13), 77(12), 43(11), 41(11), 39(9)	152	$C_{10}H_{16}O$	myrtenol
173(100), 115(81), 142(80), 43(69), 215(46), 141(41), 127(35), 172(29)	215	$C_{11}H_{13}NO_2$	naphthalene, N-methoxy-2-acetylamino-
185(100), 230(48), 186(15), 141(14), 115(12), 170(11), 139(11), 153(8)	230	$C_{14}H_{14}O_3$	naproxen
185(100), 244(35), 186(17), 170(10), 141(7), 154(6), 245(6), 153(6)	244	$C_{15}H_{16}O_3$	naproxen, methyl ester
159(100), 142(73), 43(71), 115(70), 143(41), 201(37), 128(25), 140(22)	201	$C_{10}H_{11}NO_2$	napthalene, N-hydroxy-2-acetylamino-
69(100), 41(60), 68(19), 39(11), 93(10), 123(2), 67(8), 53(7)	154	$C_{10}H_{18}O$	nerol
84(100), 133(30), 162(21), 42(19), 161(18), 92(7), 119(7), 65(6)	162	$C_{10}H_{14}N_2$	nicotine
253(100), 280(99), 234(68), 206(66), 252(62), 281(59), 251(54), 77(51)	281	$C_{15}H_{11}N_3O_3$	nitrazepam
57(100), 43(21), 29(17), 72(14), 27(13), 55(10), 58(7), 39(7)	128	$C_8H_{16}O$	oct-1-en-3-ol
67(100), 68(89), 55(75), 43(65), 41(47), 27(41), 39(24), 82(22)	152	$C_{10}H_{16}O$	octa-1,4,6-trien-3-ol, 3,7-dimethyl-
59(100), 55(55), 41(48), 83(47), 31(31), 29(28), 43(22), 101(22)	130	$C_8H_{18}O$	octan-3-ol
43(100), 41(15), 55(13), 70(13), 56(11), 112(10), 57(9), 83(9)	172	$C_{10}H_{20}O_2$	octan-3-yl acetate
59(100), 72(51), 41(49), 55(41), 43(41), 29(23), 57(20), 81(12)	281	$C_{18}H_{35}NO$	oleamide
297(100), 42(53), 298(20), 296(19), 58(18), 283(17), 241(15), 240(15)	297	$C_{18}H_{19}NO_3$	oripavine
72(100), 30(78), 41(20), 56(13), 43(9), 57(6), 73(6), 39(5)	265	$C_{15}H_{23}NO_3$	oxprenolol
93(100), 199(89), 324(66), 77(56), 109(48), 55(45), 65(32), 41(31)	324	$C_{19}H_{20}N_2O_3$	oxyphenbutazone
324(100), 338(73), 339(62), 325(22), 308(20), 51(15), 293(14), 151(13)	339	$C_{20}H_{21}NO_4$	papaverine
140(100), 197(93), 155(86), 43(47), 51(11), 198(11), 156(10), 96(10)	197	$C_9H_{11}NO_2S$	paracetamol, 3-methythio-
43(100), 141(49), 183(28), 87(24), 42(22), 41(17), 140(10), 108(8)	312	$C_{13}H_{16}N_2O_5S$	paracetamol-3-mercapturic acid
135(100), 93(96), 107(86), 108(85), 204(51), 91(51), 105(50)	204	$C_{15}H_{24}$	patchoulene, α-
161(100), 119(66), 189(66), 93(60), 41(59), 105(55), 81(46), 204(45)	204	$C_{15}H_{24}$	patchoulene, β-
43(100), 41(99), 81(89), 83(88), 98(83), 55(69), 222(67), 138(59)	222	$C_{15}H_{26}O$	patchouli alcohol
55(100), 27(52), 43(21), 70(17), 44(10), 41(9), 56(8), 98(7)	98	$C_6H_{10}O$	pent-1-en-2-one, 4-methyl-
71(100), 42(82), 70(62), 57(49), 43(35), 103(26), 91(25), 247(23)	247	$C_{15}H_{21}NO_2$	pethidine

Ions/Intensities	Mol.Wt.	Formula	Compound Name
93(100), 77(33), 91(31), 92(23), 41(16), 136(13), 29(12), 39(10)	136	$C_{10}H_{16}$	phellandrene, α-
108(100), 109(86), 179(64), 137(42), 43(34), 81(11), 80(11), 180(7)	179	$C_{10}H_{13}NO_2$	phenacetin
124(100), 153(96), 125(69), 195(54), 43(38), 149(27), 96(20), 177(13)	195	$C_{10}H_{13}NO_3$	phenacetin, 2-hydroxy-
138(100), 209(72), 167(51), 43(31), 139(27), 124(21), 108(18), 152(11)	209	$C_{11}H_{15}NO_3$	phenacetin, 2-methoxy-
124(100), 195(52), 125(40), 43(34), 96(16), 153(7), 68(6), 196(6)	195	$C_{10}H_{13}NO_3$	phenacetin, 3-hydroxy-
138(100), 209(51), 139(36), 43(31), 110(121), 180(10), 210(7), 167(6)	209	$C_{11}H_{15}NO_3$	phenacetin, 3-methoxy-
108(100), 109(81), 179(64), 43(62), 137(44), 153(14), 136(14), 81(13)	195	$C_{10}H_{13}NO_3$	phenacetin, N-hydroxy-
108(100), 43(84), 138(64), 136(47), 167(39), 81(32), 107(30), 135(26)	209	$C_{11}H_{15}NO_3$	phenacetin, N-methoxy-
124(100), 153(76), 125(55), 96(16), 80(7), 154(7), 52(7), 53(4)	153	$C_8H_{11}NO_2$	phenetidine, 2-hydroxy
137(100), 108(70), 109(56), 207(47), 43(26), 138(10), 71(9), 110(9)	207	$C_{12}H_{17}NO_2$	phenetidine, N-butyryl-
137(100), 108(99), 109(91), 193(67), 52(9), 194(8), 81(8), 80(7)	193	$C_{11}H_{15}NO_2$	phenetidine, N-propionyl-
167(100), 138(95), 223(70), 139(25), 124(18), 29(15), 168(11), 152(10)	223	$C_{12}H_{17}NO_3$	phenetidine, N-propionyl-2-methoxy-
169(100), 58(70), 168(29), 72(17), 170(17), 167(13), 42(10), 30(6)	239	$C_{17}H_{21}N$	pheniramine
204(100), 117(35), 232(24), 51(20), 77(18), 161(17), 103(17), 146(16)	232	$C_{12}H_{12}N_2O_3$	phenobarbitone
232(100), 118(24), 146(23), 175(21), 117(18), 233(14), 91(9), 103(8)	260	$C_{14}H_{16}N_2O_3$	phenobarbitone, N,N-dimethyl
196(100), 198(89), 97(68), 132(37), 62(33), 200(30), 99(27), 61(26)	196	$C_6H_3OCl_3$	phenol, 2,4,6-trichloro-
162(100), 164(72), 63(49), 98(33), 99(12), 100(12), 62(12), 126(11)	162	$C_6H_4OCl_2$	phenol, 2,4-dichloro-
184(100), 63(65), 53(58), 30(47), 91(47), 107(32), 62(29), 92(26)	184	$C_6H_4N_2O_5$	phenol, 2,4-dinitro-
128(100), 64(71), 63(36), 130(31), 39(24), 65(22), 38(16), 92(13)	128	C_6H_5OCl	phenol, 2-chloro-
139(100), 39(63), 65(46), 63(36), 64(30), 81(24), 53(22), 38(21)	139	$C_6H_5NO_3$	phenol, 2-nitro-
107(100), 142(89), 77(45), 51(28), 144(25), 39(20), 78(14), 50(12)	142	C_7H_7OCl	phenol, 3-methyl-4-chloro-
266(100), 264(62), 268(60), 165(38), 167(35), 95(29), 60(21), 202(20)	264	C_6HOCl_5	phenol, pentachloro-
162(100), 164(66), 220(58), 22(39), 161(32), 133(28), 175(28), 163(27)	220	$C_8H_6Cl_2O_3$	phenoxyacetic acid, 2,4-dichloro-
234(100), 175(98), 199(68), 177(64), 236(59), 147(40), 145(37), 111(33)	234	$C_9H_8Cl_2O_3$	phenoxyacetic acid, 2,4-dichloro-, me.ester
180(100), 104(74), 77(66), 223(48), 209(43), 252(41), 51(39), 181(27)	252	$C_{15}H_{12}N_2O_2$	phentoin
105(100), 120(51), 77(51), 51(16), 39(9), 78(9), 106(8), 41(7)	176	$C_{12}H_{16}O$	phenyl-1-hexanone, 1-
77(100), 183(93), 308(44), 184(27), 105(19), 55(15), 51(14), 91(11)	308	$C_{19}H_{20}N_2O_2$	phenylbutazone
44(100), 45(3), 77(3), 42(3), 39(3), 95(2), 65(2), 43(1)	165	$C_9H_{13}NO_2$	phenylephrine
139(100), 140(68), 63(12), 62(9), 51(9), 141(7), 39(7), 114(6)	140	$C_{11}H_8$	phenylpenta-2,4-diyne, 1-

Ions/Intensities	Mol.Wt.	Formula	Compound Name
44(100), 77(6), 42(5), 79(4), 51(4), 45(3), 91(2), 105(2)	151	$C_9H_{13}NO$	phenylpropanolamine
114(100), 100(83), 42(14), 56(9), 115(8), 70(6), 101(6), 55(5)	398	$C_{23}H_{30}N_2O_4$	pholcodine
76(100), 50(78), 147(71), 104(69), 103(31), 74(29), 75(22), 38(17)	147	$C_8H_5NO_2$	phthalimide
30(100), 72(91), 133(73), 56(16), 43(15), 116(13), 41(12), 104(11)	248	$C_{14}H_{20}N_2O_2$	pindolol
93(100), 41(88), 43(58), 27(50), 69(47), 49(46), 77(42), 29(31)	136	$C_{10}H_{16}$	pinene, β-
70(100), 92(98), 41(97), 55(92), 83(89), 91(61), 69(54), 81(35)	152	$C_{10}H_{16}O$	pinocarveol, *trans-*
53(100), 41(88), 81(85), 108(57), 39(37), 69(37), 43(36), 79(32)	150	$C_{10}H_{14}O$	pinocarvone
84(100), 43(28), 41(27), 83(25), 93(24), 139(23), 55(18), 39(14)	156	$C_{10}H_{20}O$	piperitol, *cis-*
84(100), 41(27), 83(26), 93(25), 43(25), 139(24), 55(18), 39(15)	156	$C_{10}H_{20}O$	piperitol, *trans-*
82(100), 110(71), 39(33), 41(32), 95(28), 27(21), 54(19), 109(19)	152	$C_{10}H_{16}O$	piperitone
176(100), 177(36), 57(22), 45(18), 149(13), 29(12), 119(9)	338	$C_{19}H_{30}O_5$	piperonyl butoxide
233(100), 383(41), 259(30), 245(30), 95(29), 56(25), 43(19), 41(19)	383	$C_{18}H_{21}N_5O_4$	prazosin
77(100), 93(71), 91(68), 80(43), 147(37), 53(36), 105(33), 65(30)	162	$C_{12}H_{18}$	pregeijerene
146(100), 190(64), 117(50), 118(35), 30(22), 161(22), 189(22), 103(21)	218	$C_{12}H_{14}N_2O_2$	primidone
86(100), 99(19), 30(17), 69(14), 58(11), 41(11), 43(9), 120(9)	271	$C_{13}H_{22}N_3OCl$	procainamide
86(100), 99(25), 120(14), 30(10), 58(8), 87(6), 91(6), 92(5)	236	$C_{13}H_{20}N_2O_2$	procaine
113(100), 70(92), 43(51), 42(56), 373(39), 141(34), 26(28), 71(25)	373	$C_{20}H_{24}N_2SCl$	prochlorperazine
58(100), 86(21), 284(20), 238(10), 85(9), 199(8), 42(8), 198(7)	284	$C_{17}H_{20}N_2S$	promazine
137(100), 180(20), 122(13), 138(11), 43(7), 94(7), 51(5), 77(4)	180	$C_{10}H_{22}O_3$	propan-2-one, 1-(4-hydroxy-3-methoxyphenyl)-
43(100), 136(85), 165(82), 120(25), 57(23), 29(22), 162(15), 90(14)	207	$C_{11}H_{13}NO_3$	propiophenone, N-hydroxy-4-acetylamino-
179(100), 43(84), 150(56), 57(23), 119(16), 164(15), 134(12), 180(12)	221	$C_{12}H_{15}NO_3$	propiophenone, N-methoxy-4-acetylamino-
70(100), 44(67), 191(58), 189(13), 192(11), 165(8), 59(6), 71(5)	263	$C_{19}H_{21}N$	protryptyline
58(100), 30(10), 56(5), 42(5), 77(4), 59(4), 51(3), 57(2)	165	$C_{10}H_{15}NO$	pseudoephedrine
125(100), 43(95), 41(88), 168(75), 55(54), 39(43), 69(42), 153(39)	168	$C_{10}H_{16}O_2$	psi-diosphenol
81(100), 152(63), 67(63), 41(50), 109(46), 82(36), 39(28), 69(25)	152	$C_{10}H_{16}O$	pulegone
123(100), 41(34), 133(20), 162(18), 81(17), 91(17), 55(17), 105(12)	328	$C_{21}H_{28}O_3$	pyrethrin I
133(100), 160(77), 107(69), 161(68), 41(67), 167(58), 91(56), 105(41)	372	$C_{22}H_{28}O_5$	pyrethrin II
168(100), 167(85), 41(84), 43(71), 27(33), 97(29), 39(28), 29(26)	238	$C_{12}H_{18}N_2O_3$	quinalbarbitone
136(100), 41(13), 42(12), 137(12), 81(10), 55(9), 39(5), 117(5)	324	$C_{20}H_{24}N_2O_2$	quinine

Ions/Intensities	Mol.Wt.	Formula	Compound Name
184(100), 65(81), 39(68), 121(44), 69(39), 41(38), 94(35), 186(32)	364	$C_{18}H_{17}O_6Cl$	radicicol
59(100), 149(99), 81(44), 108(36), 93(30), 41(18), 43(16), 121(16)	222	$C_{15}H_{26}O$	rosifoliol
93(100), 77(31), 41(28), 43(25), 91(25), 79(21), 57(18), 94(13)	136	$C_{10}H_{16}$	sabinene
92(100), 91(77), 81(35), 41(35), 109(24), 79(23), 134(21), 27(21)	152	$C_{10}H_{16}O$	sabinol
91(100), 43(54), 92(43), 41(11), 119(9), 108(8), 39(6), 134(5)	194	$C_{12}H_{18}O_2$	sabinyl acetate
162(100), 104(58), 51(47), 77(47), 103(40), 131(40), 135(38), 43(33)	162	$C_{10}H_{10}O_2$	safrole
120(100), 92(81), 138(45), 39(36), 43(35), 64(35), 45(32), 63(21)	138	$C_7H_6O_3$	salicylic acid
121(100), 120(95), 92(70), 65(44), 195(28), 43(28), 39(26), 92(21)	195	$C_9H_9NO_4$	salicyluric acid
161(100), 122(71), 107(51), 204(51), 41(33), 105(31), 93(30), 121(29)	204	$C_{15}H_{24}$	selina-3,7(11)-diene
161(100), 204(86), 41(69), 91(51), 189(50), 105(48), 133(44), 135(43)	204	$C_{15}H_{24}$	selina-4(14),7(11)-diene
189(100), 204(76), 93(75), 81(64), 107(64), 41(63), 105(50), 91(45)	204	$C_{15}H_{24}$	selinene, α-
41(100), 105(90), 107(89), 204(88), 93(86), 81(78), 121(69), 79(68)	204	$C_{15}H_{24}$	selinene, β-
161(100), 189(98), 204(94), 41(40), 91(40), 105(39), 133(28), 81(24)	204	$C_{15}H_{24}$	selinene, δ-
233(100), 340(72), 341(59), 248(55), 247(32), 356(30), 139(29), 234(28)	356	$C_{20}H_{17}O_3SF$	sulindac
172(100), 92(95), 156(79), 65(75), 108(50), 39(25), 43(15), 63(14)	172	$C_6H_8N_2O_2S$	sulphanilamide
43(100), 109(51), 151(38), 65(20), 92(17), 45(15), 156(15), 108(13)	256	$C_{10}H_{12}N_2O_4S$	sulphanilamide, N1,N4-diacetyl-
109(100), 92(95), 65(67), 156(61), 108(56), 214(29), 39(23), 43(22)	214	$C_8H_{10}N_2O_3S$	sulphanilamide, N1-acetyl-
172(100), 43(90), 45(64), 156(46), 92(37), 214(33), 108(28), 65(25)	214	$C_8H_{10}N_2O_3S$	sulphanilamide, N4-acetyl-
77(100), 278(56), 78(36), 51(29), 105(23), 39(16), 279(15), 126(14)	404	$C_{23}H_{20}N_2O_3S$	sulphinpyrazone
271(100), 273(35), 77(24), 256(20), 300(19), 272(19), 255(14), 228(13)	300	$C_{16}H_{13}N_2O_2Cl$	temazepam
93(100), 43(36), 91(35), 77(35), 41(25), 121(24), 136(22), 92(21)	136	$C_{10}H_{16}$	terpinene, γ-
71(100), 93(46), 111(46), 41(34), 43(32), 86(26), 69(22), 55(18)	154	$C_{10}H_{18}O$	terpinene-4-ol
59(100), 93(50), 43(37), 121(35), 81(32), 136(32), 41(22), 67(16)	154	$C_{10}H_{18}O$	terpineol, α-
93(100), 121(91), 136(69), 91(46), 79(43), 77(40), 119(38), 41(36)	136	$C_{10}H_{16}$	terpinolene, α-
43(100), 121(88), 93(71), 136(57), 41(26), 59(22), 81(18), 68(16)	196	$C_{12}H_{20}O_2$	terpinyl acetate, α-
43(100), 55(68), 41(58), 69(57), 83(52), 57(48), 61(41), 70(36)	256	$C_{16}H_{32}O_2$	tetradecyl acetate
73(100), 69(50), 55(43), 43(32), 41(30), 70(20), 27(16), 56(8)	158	$C_{10}H_{22}O$	tetrahydrolinalool
180(100), 95(59), 68(48), 53(32), 41(32), 67(14), 42(11), 96(10)	180	$C_7H_8N_4O_2$	theophylline
98(100), 370(22), 126(14), 99(13), 70(12), 42(9), 371(5), 258(5)	370	$C_{21}H_{26}N_2S_2$	thioridazine

Ions/Intensities	Mol.Wt.	Formula	Compound Name
81(100), 41(81), 68(74), 110(66), 69(60), 67(49), 39(47), 109(42)	152	$C_{10}H_{16}O$	thujone
135(100), 150(26), 91(18), 39(10), 117(10), 115(10), 136(10), 77(8)	150	$C_{10}H_{14}O$	thymol
157(100), 43(55), 115(45), 203(21), 31(16), 42(15), 45(13), 111(10)	276	$C_{12}H_{20}O_6$	triethyl citrate
113(100), 70(94), 43(70), 42(44), 407(39), 71(33), 141(27), 58(22)	407	$C_{21}H_{24}N_3F_3S$	trifluoperazine
58(100), 249(37), 208(17), 193(14), 99(13), 248(11), 84(11), 234(10)	294	$C_{20}H_{26}N_2$	trimipramine
208(100), 209(86), 278(52), 84(28), 42(25), 96(24), 193(23), 194(21)	278	$C_{19}H_{22}N_2$	triprolidine
58(100), 43(70), 59(29), 71(28), 41(26), 55(14), 57(12), 85(5)	170	$C_{11}H_{22}O$	undecan-2-one
107(100), 135)88), 91(86), 41(68), 80(68), 39(61), 150(59), 79(49)	150	$C_{10}H_{14}O$	verbenone
41(100), 43(68), 69(63), 105(62), 79(61), 93(61), 81(55), 91(52)	222	$C_{15}H_{26}O$	viridiflorol
265(100), 43(46), 121(36), 308(29), 77(22), 187(17), 115(17), 266(17)	308	$C_{19}H_{16}O_4$	warfarin
202(100), 188(82), 135(60), 160(60), 136(57), 201(53), 119(47), 186(40)	219	$C_{10}H_{13}N_5O$	zeatin
93(100), 119(78), 41(44), 69(40), 77(26), 91(26), 56(18), 55(17)	204	$C_{15}H_{24}$	zingiberene

Eight peak spectra, indexed by major ions

Ions/Intensities	Mol.Wt.	Formula	Compound Name
29(100), 207(63), 137(34), 109(32), 41(31), 149(20), 189(18), 67(17)	222	$C_{15}H_{26}O$	dihydroagarofuran
30(100), 72(91), 133(73), 56(16), 43(15), 116(13), 41(12), 104(11)	248	$C_{14}H_{20}N_2O_2$	pindolol
30(100), 229(48), 231(30), 172(19), 194(13), 174(12), 42(12), 230(8)	229	$C_9H_9N_3Cl_2$	clonidine
41(100), 43(68), 69(63), 105(62), 79(61), 93(61), 81(55), 91(52)	222	$C_{15}H_{26}O$	viridiflorol
41(100), 69(81), 55(46), 95(36), 43(32), 56(29), 57(27), 39(21)	154	$C_{10}H_{18}O$	citronellal
41(100), 69(85), 55(42), 82(37), 67(34), 81(29), 71(25), 95(24)	156	$C_{10}H_{20}O$	citronellol
41(100), 69(98), 93(94), 133(65), 79(61), 91(55), 107(39), 39(35)	204	$C_{15}H_{24}$	caryophyllene
41(100), 79(82), 67(82), 119(80), 55(68), 81(68), 84(65), 93(9)	280	$C_{16}H_{24}O_4$	Brefeldin A
41(100), 93(91), 69(76), 39(34), 27(30), 53(21), 77(13), 29(12)	136	$C_{10}H_{16}$	myrcene
41(100), 93(93), 69(75), 43(42), 45(28), 121(22), 79(22), 77(19)	196	$C_{12}H_{20}O_2$	linalyl acetate
41(100), 105(90), 107(89), 204(88), 93(86), 81(78), 121(69), 79(68)	204	$C_{15}H_{24}$	selinene, β-
43(100), 41(15), 55(13), 70(13), 56(11), 112(10), 57(9), 83(9)	172	$C_{10}H_{20}O_2$	octan-3-yl acetate
43(100), 41(61), 55(29), 69(27), 39(27), 108(16), 67(12), 111(11)	126	$C_8H_{14}O$	hept-5-en-2-one, trans 6-methyl-
43(100), 41(77),69(55), 109(44), 81(43), 55(36), 122(39), 107(32)	222	$C_{15}H_{26}O$	ledol
43(100), 41(89), 69(80), 109(50), 119(40), 93(39), 55(35), 67(28)	222	$C_{15}H_{26}O$	bisabolol, α-
43(100), 41(99), 81(89), 83(88), 98(83), 55(69), 222(67), 138(59)	222	$C_{15}H_{26}O$	patchouli alcohol
43(100), 55(50), 69(40), 56(40), 41(38), 61(36), 83(34), 70(33)	228	$C_{14}H_{28}O_2$	dodecyl acetate
43(100), 55(68), 41(58), 69(57), 83(52), 57(48), 61(41), 70(36)	256	$C_{16}H_{32}O_2$	tetradecyl acetate
43(100), 57(87), 82(70), 55(59), 41(53), 96(48), 83(45), 69(44)	380	$C_{26}H_{52}O$	hexacosanal, n-
43(100), 60(60), 41(54), 57(48), 102(39), 61(25), 71(21), 228(19)	270	$C_{17}H_{24}O_2$	isopropyl myristate
43(100), 71(99), 69(48), 41(44), 67(33), 96(31), 84(28), 39(28)	154	$C_{10}H_{18}O$	camphene hydrate
43(100), 81(27), 55(26), 69(26), 71(22), 108(18), 84(18), 111(13)	154	$C_{10}H_{18}O$	cineole, 1,8-
43(100), 84(71), 119(55), 109(35), 134(35), 152(34), 41(29), 91(29)	194	$C_{12}H_{18}O$	carveyl acetate
43(100), 93(94), 82(71), 69(53), 121(45), 67(44), 41(44), 95(38)	196	$C_{12}H_{20}O_2$	myrtanyl acetate
43(100), 105(43), 91(36), 148(28), 77(13), 79(12), 51(10), 67(9)	148	$C_{10}H_{12}O$	butan-2-one, 4-phenyl-
43(100), 109(51), 151(38), 65(20), 92(17), 45(15), 156(15), 108(13)	256	$C_{10}H_{12}N_2O_4S$	sulphanilamide, N1,N4-diacetyl-
43(100), 121(88), 93(71), 136(57), 41(26), 59(22), 81(18), 68(16)	196	$C_{12}H_{20}O_2$	terpinyl acetate, α-
43(100), 121(53), 202(24), 185(15), 64(9), 63(9), 122(8), 90(7)	242	$C_9H_{12}N_2O_4S$	benzenesulfonamide, N-methoxy-4-acetylamino-

Ions/Intensities	Mol.Wt.	Formula	Compound Name
43(100), 135(53), 115(17), 132(14), 117(13), 65(8), 115(7), 39(6)	150	$C_{10}H_{14}O$	cymene-8-ol, p-
43(100), 136(85), 165(82), 120(25), 57(23), 29(22), 162(15), 90(14)	207	$C_{11}H_{13}NO_3$	propiophenone, N-hydroxy-4-acetylamino-
43(100), 141(49), 183(28), 87(24), 42(22), 41(17), 140(10), 108(8)	312	$C_{13}H_{16}N_2O_5S$	paracetamol-3-mercapturic acid
43(100), 143(83), 85(67), 105(62), 81(60), 59(53), 134(49), 71(48)	238	$C_{15}H_{26}O_2$	bisabolol oxide B
43(100), 157(40), 126(31), 159(24), 127(21), 111(15), 142(13), 128(13)	199	$C_8H_8NO_2Cl$	acetanilide, N-hydroxy-4-chloro-
43(100), 161(57), 163(35), 177(24), 179(15), 203(11), 162(10), 160(9)	219	$C_8H_7NO_2Cl_2$	acetanilide, N-hydroxy-3,4-dichloro-
43(100), 171(89), 188(83), 230(61), 79(44), 52(19), 51(18), 95(16)	230	$C_8H_{10}N_2O_4S$	benzenesulfonamide, 3-hydroxy-4-acetylamino-
43(100), 188(27), 172(21), 60(19), 107(18), 108(12), 92(9), 156(8)	230	$C_8H_{10}N_2O_4S$	benzenesulfonamide, N-OH-4-acetylamino-
43(100), 248(75), 108(70), 290(63), 140(50), 58(27), 65(27), 92(23)	290	$C_{14}H_{14}N_2O_3S$	dapsone, acetyl-
44(100), 45(3), 77(3), 42(3), 39(3), 95(2), 65(2), 43(1)	165	$C_9H_{13}NO_2$	phenylephrine
44(100), 77(6), 42(5), 79(4), 51(4), 45(3), 91(2), 105(2)	151	$C_9H_{13}NO$	phenylpropanolamine
44(100), 91(6), 42(4), 65(4), 45(3), 39(3), 51(2), 120(2)	135	$C_9H_{13}N$	amphetamine
53(100), 41(88), 81(85), 108(57), 39(37), 69(37), 43(36), 79(32)	150	$C_{10}H_{14}O$	pinocarvone
54(100), 81(92), 53(81), 45(53), 124(50), 42(47), 27(44), 52(41)	171	$C_6H_9N_3O_3$	metromidazole
55(100), 27(52), 43(21), 70(17), 44(10), 41(9), 56(8), 98(7)	98	$C_6H_{10}O$	pent-1-en-2-one, 4-methyl-
55(100), 41(63), 97(61), 96(34), 27(21), 39(20), 43(17), 81(16)	140	$C_{10}H_{20}$	menthane, cis p-
55(100), 41(77), 69(69), 74(68), 83(43), 87(40), 84(34), 43(41)	268	$C_{17}H_{32}O_2$	methyl palmitoleate
55(100), 43(94), 41(88), 69(78), 83(70), 57(68), 56(60), 70(53)	238	$C_{17}H_{34}$	heptadec-8-ene, *Z*-
56(100), 169(39), 43(28), 67(22), 82(16), 39(14), 171(13), 54(13)	494	$C_{23}H_{28}N_3O_5SCl$	glibenclamide
57(100), 43(21), 29(17), 72(14), 27(13), 55(10), 58(7), 39(7)	128	$C_8H_{16}O$	oct-1-en-3-ol
58(100), 30(10), 56(5), 42(5), 77(4), 59(4), 51(3), 57(2)	165	$C_{10}H_{15}NO$	pseudoephedrine
58(100), 30(7), 91(5), 42(4), 59(4), 56(3), 65(3), 39(2)	149	$C_{10}H_{15}N$	methylamphetamine
58(100), 43(70), 59(29), 71(28), 41(26), 55(14), 57(12), 85(5)	170	$C_{11}H_{22}O$	undecan-2-one
58(100), 59(18), 42(11), 30(8), 202(7), 203(5), 215(), 91(4)	277	$C_{20}H_{23}N$	amitryptaline
58(100), 71(60), 42(51), 44(26), 43(26), 51(22), 30(21), 27(11)	270	$C_{17}H_{22}N_2O$	doxylamine
58(100), 73(80), 45(49), 44(22), 59(16), 42(14), 165(14), 167(11)	256	$C_{17}H_{21}NO$	diphenhydramine
58(100), 86(21), 284(20), 238(10), 85(9), 199(8), 42(8), 198(7)	284	$C_{17}H_{20}N_2S$	promazine
58(100), 86(21), 318(16), 85(8), 42(8), 272(6), 320(6), 232(5)	318	$C_{17}H_{19}N_2SCl$	chlorpromazine
58(100), 91(5), 57(5), 59(4), 42(3), 77(3), 105(2), 30(2)	339	$C_{22}H_{29}NO_2$	dextropropoxyphene

Ions/Intensities	Mol.Wt.	Formula	Compound Name
58(100), 146(24), 42(21), 56(19), 77(16), 30(15), 105(14), 117(8)	165	$C_{10}H_{15}NO$	ephedrine
58(100), 235(58), 85(52), 234(44), 280(22), 193(20), 195(19), 208(16)	280	$C_{19}H_{24}N_2$	imipramine
58(100), 249(37), 208(17), 193(14), 99(13), 248(11), 84(11), 234(10)	294	$C_{20}H_{26}N_2$	trimipramine
59(100), 43(49), 31(42), 41(29), 39(14), 69(11), 42(7), 87(4)	102	$C_5H_{10}O_2$	butan-2-one, 3-hydroxy-3-methyl-
59(100), 55(55), 41(48), 83(47), 31(31), 29(28), 43(22), 101(22)	130	$C_8H_{18}O$	octan-3-ol
59(100), 58(15), 55(13), 41(11), 43(8), 81(6), 60(5), 123(4)	156	$C_{10}H_{20}O$	menthan-8-ol, p-
59(100), 72(51), 41(49), 55(41), 43(41), 29(23), 57(20), 81(12)	281	$C_{18}H_{35}NO$	oleamide
59(100), 93(53), 41(45), 43(36), 161(33), 81(33), 107(29), 121(24)	222	$C_{15}H_{26}O$	elemol
59(100), 93(50), 43(37), 121(35), 81(32), 136(32), 41(22), 67(16)	154	$C_{10}H_{18}O$	terpineol, α-
59(100), 109(27), 151(27), 95(21), 166(19), 41(18), 110(17), 55(13)	224	$C_{15}H_{28}O$	eudesman-11-ol, 4βH,5αH-
59(100), 109(36), 166(27), 41(18), 55(17), 95(17), 81(13), 96(13)	224	$C_{15}H_{28}O$	eudesman-11-ol, 4αH,5αH-
59(100), 149(99), 81(44), 108(36), 93(30), 41(18), 43(16), 121(16)	222	$C_{15}H_{26}O$	rosifoliol
59(100), 149(37), 164(27), 109(21), 108(20), 81(17), 41(17), 95(15)	222	$C_{15}H_{26}O$	eudesmol, β-
59(100), 271(48), 31(39), 150(36), 270(26), 42(23), 214(19), 30(16)	271	$C_{18}H_{25}NO$	dextromethorphan
67(100), 68(89), 55(75), 43(65), 41(47), 27(41), 39(24), 82(22)	152	$C_{10}H_{16}O$	octa-1,4,6-trien-3-ol, 3,7-dimethyl-
68(100), 67(44), 93(35), 39(25), 79(24), 53(23), 94(18), 77(15)	136	$C_{10}H_{16}$	limonene
69(100), 41(60), 68(19), 39(11), 93(10), 123(2), 67(8), 53(7)	154	$C_{10}H_{18}O$	nerol
69(100), 41(90), 93(85), 67(58), 94(53), 109(47), 79(45), 204(33)	204	$C_{15}H_{24}$	bisabolene, β-
69(100), 41(95), 81(50), 82(47), 95(41), 67(28), 123(27), 68(22)	224	$C_{14}H_{24}O_2$	citronellyl butenoate
69(100), 41(91), 109(58), 39(51), 81(50), 112(48), 55(42), 67(38)	186	$C_{10}H_{18}SO$	menthon-8-thiol, p-
69(100), 41(99), 114(26), 83(25), 123(13), 93(11), 105(10), 77(10)	182	$C_{11}H_{18}O_2$	geranic acid, methyl ester
69(100), 67(94), 93(91), 123(85), 41(83), 81(73), 82(70), 55(61)	154	$C_{10}H_{18}O$	myrtanol
70(100), 44(67), 191(58), 189(13), 192(11), 165(8), 59(6), 71(5)	263	$C_{19}H_{21}N$	protryptyline
70(100), 92(98), 41(97), 55(92), 83(89), 91(61), 69(54), 81(35)	152	$C_{10}H_{16}O$	pinocarveol, *trans*-
71(100), 42(82), 70(62), 57(49), 43(35), 103(26), 91(25), 247(23)	247	$C_{15}H_{21}NO_2$	pethidine
71(100), 43(74), 41(67), 69(47), 55(44), 27(33), 93(31), 39(28)	154	$C_{10}H_{18}O$	linalool
71(100), 43(37), 41(16), 72(14), 58(14), 98(13), 55(11), 57(8)	156	$C_{10}H_{20}O$	menthan-1-ol, p-
71(100), 43(99), 56(51), 57(45), 41(41), 29(24), 89(23), 27(17)	144	$C_8H_{16}O_2$	isobutyyl isobutyrate
71(100), 43(93), 70(53), 41(24), 55(18), 27(13), 29(11), 42(11)	158	$C_9H_8O_2$	isobutyric acid, 2-methylbutyl ester

Ions/Intensities	Mol.Wt.	Formula	Compound Name
71(100), 81(67), 41(62), 95(61), 55(48), 43(33), 82(33), 69(32)	156	$C_{10}H_{20}O$	menthol
71(100), 93(46), 111(46), 41(34), 43(32), 86(26), 69(22), 55(18)	154	$C_{10}H_{18}O$	terpinene-4-ol
72(100), 30(55), 45(13), 43(7), 41(7), 56(7), 107(6), 57(5)	267	$C_{15}H_{25}NO_3$	metoprolol
72(100), 30(57), 43(10), 56(9), 41(7), 57(6), 107(6), 73(5)	266	$C_{14}H_{22}N_2O_3$	atenolol
72(100), 30(78), 41(20), 56(13), 43(9), 57(6), 73(6), 39(5)	265	$C_{15}H_{23}NO_3$	oxprenolol
73(100), 69(50), 55(43), 43(32), 41(30), 70(20), 27(16), 56(8)	158	$C_{10}H_{22}O$	tetrahydrolinalool
73(100), 371(76), 178(41), 196(39), 42(29), 372(23), 59(21), 70(21)	371	$C_{21}H_{29}NO_3Si$	codeine, trimethylsilyl derivative
74(100), 41(75), 43(74), 55(70), 110(50), 54(48), 67(45), 29(36)	184	$C_{11}C_{20}O_2$	dec-4-enoic acid, methyl ester
74(100), 87(53), 43(48), 41(35), 55(30), 57(19), 69(18), 82(17)	158	$C_9H_{18}O_2$	isooctanoic acid, methyl ester
76(100), 50(78), 147(71), 104(69), 103(31), 74(29), 75(22), 38(17)	147	$C_8H_5NO_2$	phthalimide
77(100), 93(71), 91(68), 80(43), 147(37), 53(36), 105(33), 65(30)	162	$C_{12}H_{18}$	pregeijerene
77(100), 183(93), 308(44), 184(27), 105(19), 55(15), 51(14), 91(11)	308	$C_{19}H_{20}N_2O_2$	phenylbutazone
77(100), 278(56), 78(36), 51(29), 105(23), 39(16), 279(15), 126(14)	404	$C_{23}H_{20}N_2O_3S$	sulphinpyrazone
79(100), 91(31), 108(17), 31(13), 77(12), 43(11), 41(11), 39(9)	152	$C_{10}H_{16}O$	myrtenol
81(100), 152(63), 67(63), 41(50), 109(46), 82(36), 39(28), 69(25)	152	$C_{10}H_{16}O$	pulegone
81(100), 41(81), 68(74), 110(66), 69(60), 67(49), 39(47), 109(42)	152	$C_{10}H_{16}O$	thujone
81(100), 68(87), 93(69), 41(57), 67(48), 107(45), 55(41), 79(36)	204	$C_{15}H_{24}$	elemene, β-
81(100), 80(50), 41(39), 71(31), 69(30), 43(28), 55(24), 84(21)	154	$C_{10}H_{18}O$	fenchol
81(100), 69(57), 41(24), 82(13), 152(12), 29(12), 80(10), 39(9)	152	$C_{10}H_{16}O$	fenchone
82(100), 54(44), 39(34), 93(26), 108(25), 41(23), 53(17), 107(16)	150	$C_{10}H_{14}O$	carvone
82(100), 110(71), 39(33), 41(32), 95(28), 27(21), 54(19), 109(19)	152	$C_{10}H_{16}O$	piperitone
82(100), 182(45), 83(29), 105(21), 42(16), 77(13), 96(11), 97(8)	303	$C_{17}H_{21}NO_4$	cocaine
83(100), 41(53), 151(45), 67(33), 95(32), 55(29), 93(28), 224(23)	224	$C_{13}H_{20}O_3$	methyl jasmonate
83(100), 55(58), 41(38), 67(15), 43(13), 29(11), 168(11)	168	$C_{12}H_{24}$	cyclohexane, n-hexyl-
83(100), 55(71), 82(70), 41(38), 67(16), 29(16), 43(13), 154(12)	154	$C_{11}H_{22}$	cyclohexane, n-pentyl-
83(100), 82(28), 153(26), 55(20), 156(19), 41(16), 67(12), 96(11)	226	$C_{13}H_{22}O_3$	methyl dihydrojasmonate
84(100), 41(27), 83(26), 93(25), 43(25), 139(24), 55(18), 39(15)	156	$C_{10}H_{20}O$	piperitol, *trans*-
84(100), 43(28), 41(27), 83(25), 93(24), 139(23), 55(18), 39(14)	156	$C_{10}H_{20}O$	piperitol, *cis*-
84(100), 56(7), 85(6), 91(5), 55(4), 30(3), 39(2), 77(2)	233	$C_{14}H_{19}NO_2$	methylphenidate

Ions/Intensities	Mol.Wt.	Formula	Compound Name
84(100), 133(30), 162(21), 42(19), 161(18), 92(7), 119(7), 65(6)	162	$C_{10}H_{14}N_2$	nicotine
84(100), 134(65), 41(50), 79(47), 109(47), 119(40), 55(39), 91(37)	152	$C_{10}H_{16}O$	carveol, *cis*-
86(100), 30(13), 58(11), 87(6), 41(6), 73(5), 42(5), 319(3)	319	$C_{18}H_{26}N_3Cl$	chloroquine
86(100), 30(16), 87(10), 58(8), 99(8), 42(4), 56(4), 84(3)	387	$C_{21}H_{23}N_3OFCl$	flurazepam
86(100), 30(17), 58(10), 87(6), 41(4), 72(3), 56(3), 27(3)	234	$C_{14}H_{22}N_2O$	lignocaine
86(100), 58(23), 42(7), 29(6), 87(6), 30(5), 27(4), 51(3)	193	$C_{12}H_{19}NO$	etafedrine
86(100), 99(19), 30(17), 69(14), 58(11), 41(11), 43(9), 120(9)	271	$C_{13}H_{22}N_3OCl$	procainamide
86(100), 99(25), 120(14), 30(10), 58(8), 87(6), 91(6), 92(5)	236	$C_{13}H_{20}N_2O_2$	procaine
91(100), 43(54), 92(43), 41(11), 119(9), 108(8), 39(6), 134(5)	194	$C_{12}H_{18}O_2$	sabinyl acetate
91(100), 57(46), 108(31), 192(27), 85(24), 41(15), 43(11), 92(8)	192	$C_{12}H_{16}O_2$	benzyl isopentanoate
91(100), 92(89), 41(17), 65(13), 29(13), 39(12), 27(12), 105(9)	162	$C_{12}H_{18}$	benzene, n-hexyl
91(100), 108(83), 57(34), 192(26), 85(25), 92(14), 65(12), 90(12)	192	$C_{12}H_{16}O_2$	benzyl pentanoate
92(100), 91(77), 81(35), 41(35), 109(24), 79(23), 134(21), 27(21)	152	$C_{10}H_{16}O$	sabinol
93(100), 41(34), 80(32), 121(29), 55(19), 43(17), 92(16), 69(15)	204	$C_{15}H_{24}$	humulene
93(100), 41(88), 43(58), 27(50), 69(47), 49(46), 77(42), 29(31)	136	$C_{10}H_{16}$	pinene, β-
93(100), 43(31), 91(31), 79(29), 77(29), 27(28), 80(22), 92(21)	136	$C_{10}H_{16}$	carene, Δ3-
93(100), 43(36), 91(35), 77(35), 41(25), 121(24), 136(22), 92(21)	136	$C_{10}H_{16}$	terpinene, γ-
93(100), 77(31), 41(28), 43(25), 91(25), 79(21), 57(18), 94(13)	136	$C_{10}H_{16}$	sabinene
93(100), 77(33), 91(31), 92(23), 41(16), 136(13), 29(12), 39(10)	136	$C_{10}H_{16}$	phellandrene, α-
93(100), 119(78), 41(44), 69(40), 77(26), 91(26), 56(18), 55(17)	204	$C_{15}H_{24}$	zingiberene
93(100), 121(67), 79(38), 41(38), 67(33), 91(28), 107(28), 39(27)	136	$C_{10}H_{16}$	camphene
93(100), 121(91), 136(69), 91(46), 79(43), 77(40), 119(38), 41(36)	136	$C_{10}H_{16}$	terpinolene, α-
93(100), 141(87), 43(85), 94(62), 68(51), 121(49), 95(46), 41(39)	236	$C_{15}H_{24}O_2$	bisabolone oxide
93(100), 199(89), 324(66), 77(56), 109(48), 55(45), 65(32), 41(31)	324	$C_{19}H_{20}N_2O_3$	oxyphenbutazone
95(100), 41(20), 110(17), 55(11), 43(10), 67(8), 93(8), 96(8)	154	$C_{10}H_{18}O$	borneol
95(100), 43(66), 93(38), 121(36), 136(33), 55(17), 69(16), 108(16)	196	$C_{12}H_{20}O_2$	bornyl acetate
95(100), 67(78), 68(66), 82(60), 81(54), 41(47), 152(43), 109(39)	152	$C_{10}H_{16}O$	dihydrocarvone
95(100), 81(65), 41(61), 69(38), 108(35), 55(35), 83(33), 109(26)	152	$C_{10}H_{16}O$	camphor
95(100), 81(67), 138(52), 41(50), 55(44), 123(33), 43(31), 96(27)	198	$C_{12}H_{22}O_2$	menthyl acetate

Ions/Intensities	Mol.Wt.	Formula	Compound Name
95(100), 151(84), 43(68), 150(61), 41(51), 69(44), 81(42), 152(35)	222	$C_{15}H_{26}O$	cedrol
98(100), 370(22), 126(14), 99(13), 70(12), 42(9), 371(5), 258(5)	370	$C_{21}H_{26}N_2S_2$	thioridazine
100(100), 44(17), 72(9), 101(7), 77(7), 29(7), 42(6), 56(4)	295	$C_{13}H_{19}NO$	diethylpropion
104(100), 91(91), 82(69), 105(43), 119(31), 39(28), 164(27), 77(25)	164	$C_{10}H_{12}O_2$	methyl 3-phenyl propanoate
105(100), 77(66), 135(31), 51(26), 134(15), 106(8), 78(6), 161(4)	179	$C_9H_9NO_3$	hippuric acid
105(100), 91(61), 77(39), 212(23), 51(22), 65(14), 106(11), 90(10)	212	$C_{14}H_{12}O_2$	benzyl benzoate
105(100), 120(51), 77(51), 51(16), 39(9), 78(9), 106(8), 41(7)	176	$C_{12}H_{16}O$	phenyl-1-hexanone, 1-
105(100), 147(87), 41(85), 93(78), 79(58), 91(58), 204(56), 133(54)	204	$C_{15}H_{24}$	guaiene, α-
106(100), 107(83), 77(32), 51(24), 39(23), 79(16), 65(15), 78(12)	107	C_7H_9N	aniline, N-methyl-
107(100), 108(99), 93(96), 41(83), 105(66), 79(62), 81(62), 95(61)	204	$C_{15}H_{24}$	guaiene, δ-
107(100), 135)88), 91(86), 41(68), 80(68), 39(61), 150(59), 79(49)	150	$C_{10}H_{14}O$	verbenone
107(100), 142(89), 77(45), 51(28), 144(25), 39(20), 78(14), 50(12)	142	C_7H_7OCl	phenol, 3-methyl-4-chloro-
108(100), 43(84), 138(64), 136(47), 167(39), 81(32), 107(30), 135(26)	209	$C_{11}H_{15}NO_3$	phenacetin, N-methoxy-
108(100), 65(95), 78(67), 39(46), 51(24), 77(22), 79(17), 93(16)	108	C_7H_8O	anisole
108(100), 93(42), 95(25), 41(24), 109(19), 67(19), 91(13), 81(12)	152	$C_{19}H_{16}O$	campholene aldehyde, α-
108(100), 109(81), 179(64), 43(62), 137(44), 153(14), 136(14), 81(13)	195	$C_{10}H_{13}NO_3$	phenacetin, N-hydroxy-
108(100), 109(86), 179(64), 137(42), 43(34), 81(11), 80(11), 180(7)	179	$C_{10}H_{13}NO_2$	phenacetin
108(100), 123(62), 165(56), 43(26), 80(10), 52(10), 122(10), 109(8)	165	$C_9H_{11}NO_2$	acetanilide, 4-methoxy-
108(100), 123(80), 165(57), 43(42), 80(31), 52(21), 65(17), 92(8)	165	$C_9H_{11}NO_2$	acetanilide, 2-methoxy-
108(100), 150(21), 79(17), 39(9), 109(8), 77(7), 41(6), 51(5)	150	$C_{10}H_{14}O$	menthofuran
109(100), 84(85), 41(46), 55(37), 119(35), 83(33), 91(33), 39(28)	152	$C_{10}H_{16}O$	carveol, *trans*-
109(100), 92(95), 65(67), 156(61), 108(56), 214(29), 39(23), 43(22)	214	$C_8H_{10}N_2O_3S$	sulphanilamide, N1-acetyl-
109(100), 95(87), 95(87), 55(85), 96(75), 81(69), 69(65), 83(65)	208	$C_{15}H_{28}$	eudesmane, 4αH,5αH-
112(100), 41(85), 69(67), 55(63), 56(39), 139(37), 70(36), 43(35)	154	$C_{10}H_{18}O$	menthone
112(100), 69(55), 41(53), 55(46), 139(33), 56(30), 70(28), 43(25)	154	$C_{10}H_{18}O$	isomenthone
113(100), 43(96), 95(66), 41(35), 99(32), 71(24), 55(20), 69(12)	156	$C_{10}H_{20}O$	menthan-4-ol, p-
113(100), 70(92), 43(51), 42(56), 373(39), 141(34), 26(28), 71(25)	373	$C_{20}H_{24}N_2SCl$	prochlorperazine
113(100), 70(94), 43(70), 42(44), 407(39), 71(33), 141(27), 58(22)	407	$C_{21}H_{24}N_3F_3S$	trifluoperazine
114(100), 100(83), 42(14), 56(9), 115(8), 70(6), 101(6), 55(5)	398	$C_{23}H_{30}N_2O_4$	pholcodine

Ions/Intensities	Mol.Wt.	Formula	Compound Name
116(100), 43(88), 29(71), 85(59), 31(49), 44(46), 61(29), 42(28)	176	$C_6H_8O_6$	ascorbic acid
119(100), 91(74), 134(66), 41(30), 39(26), 77(21), 105(21), 92(17)	134	$C_{10}H_{14}$	mentha-1,3,9-triene, p-
119(100), 93(49), 41(34), 69(30), 105(28), 161(23), 204(20), 120(17)	204	$C_{15}H_{24}$	cedrene, α-
119(100), 105(95), 161(94), 41(46), 93(65), 91(34), 55(28), 120(27)	204	$C_{15}H_{24}$	copaene, α-
120(100), 41(42), 43(37), 138(31), 121(31), 39(28), 59(28), 55(28)	208	$C_{12}H_{16}O_3$	isoamyl salicylate
120(100), 92(81), 138(45), 39(36), 43(35), 64(35), 45(32), 63(21)	138	$C_7H_6O_3$	salicylic acid
120(100), 151(59), 193(38), 43(36), 65(20), 92(19), 121(11), 161(10)	193	$C_{10}H_{11}NO_3$	benzoic acid, N-acetyl-4-amino-, me. ester
121(100), 43(74), 161(60), 123(38), 93(38), 136(36), 95(36), 119(33)	194	$C_{13}H_{22}O$	dihydro-β-ionone
121(100), 93(80), 43(68), 136(59), 41(29), 91(27), 77(25), 109(23)	192	$C_{13}H_{20}O$	ionone, α-
121(100), 93(74), 107(47), 79(32), 94(29), 91(26), 81(26), 136(25)	204	$C_{15}H_{24}$	elemene, γ-
121(100), 107(97), 149(65), 93(56), 167(55), 150(29), 91(25), 55(25)	360	$C_{21}H_{28}O_5$	cinerin II
121(100), 120(95), 92(70), 65(44), 195(28), 43(28), 39(26), 92(21)	195	$C_9H_9NO_4$	salicyluric acid
121(100), 146(24), 55(23), 41(23), 180(22), 133(20), 316(20), 257(17)	316	$C_{21}H_{32}O_2$	methyl pimarate
121(100), 150(20), 77(8), 91(7), 78(5), 39(5), 122(4), 65(3),	150	$C_{10}H_{14}O$	dihydroanethole
123(100), 41(34), 133(20), 162(18), 81(17), 91(17), 55(17), 105(12)	328	$C_{21}H_{28}O_3$	pyrethrin I
123(100), 43(54), 41(34), 55(28), 81(23), 164(22), 93(22), 135(16)	330	$C_{21}H_{30}O_3$	jasmolin I
123(100), 121(28), 150(27), 41(20), 93(19), 81(17), 43(17), 55(16)	316	$C_{20}H_{28}O_3$	cinerin I
123(100), 161(99), 133(95), 41(42), 162(31), 81(29), 91(26), 43(25),	328	$C_{21}H_{28}O_3$	isopyrethrin I
124(100), 109(56), 198(21), 77(18), 81(14), 122(11), 123(10), 52(9)	198	$C_{10}H_{14}O_4$	guaifenesin
124(100), 123(63), 78(48), 77(20), 51(19), 39(18), 55(10), 52(9)	124	$C_7H_8O_2$	catechol, 4-methyl-
124(100), 153(76), 125(55), 96(16), 80(7), 154(7), 52(7), 53(4)	153	$C_8H_{11}NO_2$	phenetidine, 2-hydroxy
124(100), 153(96), 125(69), 195(54), 43(38), 149(27), 96(20), 177(13)	195	$C_{10}H_{13}NO_3$	phenacetin, 2-hydroxy-
124(100), 195(52), 125(40), 43(34), 96(16), 153(7), 68(6), 196(6)	195	$C_{10}H_{13}NO_3$	phenacetin, 3-hydroxy-
125(100), 43(95), 41(88), 168(75), 55(54), 39(43), 69(42), 153(39)	168	$C_{10}H_{16}O_2$	psi-diosphenol
125(100), 167(46), 43(33), 79(30), 52(12), 124(10), 126(8), 51(8)	167	$C_8H_9NO_3$	acetanilide, 3,4-dihydroxy-
125(100), 167(27), 43(23), 96(14), 124(10), 126(8), 52(7), 80(5)	167	$C_8H_9NO_3$	acetanilide, 2,4-dihydroxy-
126(100), 41(82), 43(56), 168(45), 125(39), 55(36), 39(36), 69(35)	168	$C_{10}H_{16}O_2$	diosphenol
128(100), 64(71), 63(36), 130(31), 39(24), 65(22), 38(16), 92(13)	128	C_6H_5OCl	phenol, 2-chloro-
131(100), 103(37), 176(30), 77(26), 51(15), 104(13), 132(12), 147(11)	176	$C_{11}H_{12}O_2$	cinnamic acid, ethyl ester

Ions/Intensities	Mol.Wt.	Formula	Compound Name
131(100), 162(58), 103(45), 77(24), 51(14), 102(11), 132(10), 163(6)	162	$C_{10}H_{10}O_2$	cinnamic acid, methyl ester
132(100), 117(81), 91(38), 115(33), 92(20), 39(19), 65(19), 131(15)	132	$C_{10}H_{12}$	cymenene
133(100), 105(66), 148(58), 77(39), 91(34), 79(34), 41(32), 119(32)	148	$C_{10}H_{12}O$	cuminic aldehyde, p-
133(100), 160(77), 107(69), 161(68), 41(67), 167(58), 91(56), 105(41)	372	$C_{22}H_{28}O_5$	pyrethrin II
134(100), 41(36), 133(35), 69(31), 135(10), 107(9), 39(9), 77(6)	202	$C_{14}H_{18}O$	feniculin
135(100), 93(96), 107(86), 108(85), 204(51), 91(51), 105(50)	204	$C_{15}H_{24}$	patchoulene, α-
135(100), 136(69), 77(27), 92(14), 107(11), 39(10), 63(8), 65(8)	136	$C_8H_8O_2$	benzaldehyde, methoxy-
135(100), 150(26), 91(18), 39(10), 117(10), 115(10), 136(10), 77(8)	150	$C_{10}H_{14}O$	thymol
135(100), 150(27), 91(20), 41(12), 77(11), 39(10), 136(10), 107(9)	150	$C_{10}H_{14}O$	carvacrol
135(100), 150(43), 105(42), 107(35), 79(32), 119(25), 91(23), 77(16)	150	$C_{10}H_{14}O$	cuminyl alcohol
136(100), 29(33), 52(30), 135(13), 53(12), 51(9), 137(7), 39(7)	136	$C_5H_4N_4O$	allopurinol
136(100), 41(13), 42(12), 137(12), 81(10), 55(9), 39(5), 117(5)	324	$C_{20}H_{24}N_2O_2$	quinine
137(100), 108(70), 109(56), 207(47), 43(26), 138(10), 71(9), 110(9)	207	$C_{12}H_{17}NO_2$	phenetidine, N-butyryl-
137(100), 108(99), 109(91), 193(67), 52(9), 194(8), 81(8), 80(7)	193	$C_{11}H_{15}NO_2$	phenetidine, N-propionyl-
137(100), 109(26), 69(25), 41(23), 93(15), 55(12), 67(11), 39(11)	152	$C_{10}H_{16}O$	hexahydrobenzofuran, 3,6-dimethyl -
137(100), 180(20), 122(13), 138(11), 43(7), 94(7), 51(5), 77(4)	180	$C_{10}H_{22}O_3$	propan-2-one, 1-(4-hydroxy-3-methoxyphenyl)-
138(100), 153(73), 195(72), 43(31), 110(19), 52(13), 95(12), 139(11)	195	$C_{10}H_{13}NO_3$	acetanilide, 2,4-dimethoxy-
138(100), 195(71), 153(31), 43(31), 110(24), 139(19), 15(9), 196(9)	195	$C_{10}H_{13}NO_3$	acetanilide, 3,4-dimethoxy-
138(100), 209(51), 139(36), 43(31), 110(121), 180(10), 210(7), 167(6)	209	$C_{11}H_{15}NO_3$	phenacetin, 3-methoxy-
138(100), 209(72), 167(51), 43(31), 139(27), 124(21), 108(18), 152(11)	209	$C_{11}H_{15}NO_3$	phenacetin, 2-methoxy-
139(100), 39(63), 65(46), 63(36), 64(30), 81(24), 53(22), 38(21)	139	$C_6H_5NO_3$	phenol, 2-nitro-
139(100), 140(68), 63(12), 62(9), 51(9), 141(7), 39(7), 114(6)	140	$C_{11}H_8$	phenylpenta-2,4-diyne, 1-
139(100), 141(37), 357(26), 111(23), 140(10), 358(9), 75(8), 113(8)	357	$C_{19}H_{16}NO_4Cl$	indomethacin
140(100), 139(90), 91(65), 168(51), 51(36), 63(35), 77(30), 39(20)	168	$C_{12}H_8O$	capillin
140(100), 197(93), 155(86), 43(47), 51(11), 198(11), 156(10), 96(10)	197	$C_9H_{11}NO_2S$	paracetamol, 3-methythio-
143(100), 43(71), 93(43), 71(34), 125(34), 121(31), 68(30), 134(25)	238	$C_{15}H_{26}O_2$	bisabolol oxide B
143(100), 43(42), 145(33), 185(19), 80(12), 51(10), 144(9), 114(9)	185	$C_8H_8NO_2Cl$	acetanilide, 2-hydroxy-4-chloro-
144(100). 175(53), 116(17), 89(17), 145(11), 63(7), 176(6), 72(5)	175	$C_{10}H_9NO_2$	indole-2-carboxylic acid, methyl ester
146(100), 190(64), 117(50), 118(35), 30(22), 161(22), 189(22), 103(21)	218	$C_{12}H_{14}N_2O_2$	primidone

Ions/Intensities	Mol.Wt.	Formula	Compound Name
148(100), 147(35), 77(22), 133(22), 117(22), 105(20), 121(18), 79(13)	148	$C_{10}H_{12}O$	anethole
148(100), 147(42), 121(39), 117(30), 77(22), 133(21), 105(17), 51(15)	148	$C_{10}H_{12}O_2$	estragole
151(100), 93(72), 43(43), 194(28), 136(25), 41(24), 133(14), 55(12)	238	$C_{15}H_{26}O_2$	daucol
154(100), 211(95), 43(40), 110(36), 169(34), 109(13), 212(11), 155(9)	211	$C_{10}H_{13}NO_2S$	acetanilide, 3-methylthio-4-methoxy-
155(100), 140(80), 83(58), 41(56), 98(54), 55(42), 29(26), 27(26)	183	$C_{10}H_{17}NO_2$	methyprylon
156(100), 141(76), 41(36), 27(33), 29(30), 39(30), 55(29), 98(22)	184	$C_8H_{12}N_2O_3$	barbitone
156(100), 141(94), 41(44), 29(40), 27(31), 39(21), 98(19), 142(15)	212	$C_{10}H_{16}N_2O_3$	butobarbitone
156(100), 141(60), 41(45), 157(33), 55(30), 43(30), 27(28), 29(22)	226	$C_{11}H_{18}N_2O_3$	amylobarbitone
157(100), 43(55), 115(45), 203(21), 31(16), 42(15), 45(13), 111(10)	276	$C_{12}H_{20}O_6$	triethyl citrate
157(100), 142(92), 43(60), 199(53), 159(34), 144(32), 114(24), 201(19)	199	$C_9H_{10}NO_2Cl$	acetanilide, 2-methoxy-4-chloro-
159(100), 142(73), 43(71), 115(70), 143(41), 201(37), 128(25), 140(22)	201	$C_{10}H_{11}NO_2$	napthalene, N-hydroxy-2-acetylamino-
159(100), 160(13), 202(9), 129(7), 128(7), 131(5), 105(5), 144(4)	202	$C_{15}H_{22}$	calamenene
160(100), 103(63), 76(30), 130(29), 131(25), 89(24), 115(23), 50(22)	160	$C_8H_8N_4$	hydralazine
161(100), 41(65), 84(49), 69(45), 55(41), 97(40), 43(39), 81(37)	222	$C_{15}H_{26}O$	carotol
161(100), 59(70), 107(57), 105(53), 93(42), 81(42), 41(39), 91(37)	222	$C_{15}H_{26}O$	guaiol
161(100), 105(45), 91(41), 41(36), 119(30), 77(29), 55(27), 120(26)	204	$C_{15}H_{24}$	Germacrene D
161(100), 105(97), 119(93), 41(33), 81(32), 120(29), 91(29), 93(26)	204	$C_{15}H_{24}$	cubebene, α-
161(100), 119(66), 189(66), 93(60), 41(59), 105(55), 81(46), 204(45)	204	$C_{15}H_{24}$	patchoulene, β-
161(100), 122(71), 107(51), 204(51), 41(33), 105(31), 93(30), 121(29)	204	$C_{15}H_{24}$	selina-3,7(11)-diene
161(100), 133(92), 107(23), 91(22), 41(19), 105(18), 162(17), 93(15)	372	$C_{22}H_{28}O_5$	isopyrethrin II
161(100), 134(58), 119(46), 105(45), 204(41), 41(34), 81(27), 91(25)	204	$C_{15}H_{24}$	cadinene, δ-
161(100), 189(98), 204(94), 41(40), 91(40), 105(39), 133(28), 81(24)	204	$C_{15}H_{24}$	selinene, δ-
161(100), 204(86), 41(69), 91(51), 189(50), 105(48), 133(44), 135(43)	204	$C_{15}H_{24}$	selina-4(14),7(11)-diene
162(100), 104(58), 51(47), 77(47), 103(40), 131(40), 135(38), 43(33)	162	$C_{10}H_{10}O_2$	safrole
162(100), 164(72), 63(49), 98(33), 99(12), 100(12), 62(12), 126(11)	162	$C_6H_4OCl_2$	phenol, 2,4-dichloro-
162(100), 164(66), 220(58), 22(39), 161(32), 133(28), 175(28), 163(27)	220	$C_8H_6Cl_2O_3$	phenoxyacetic acid, 2,4-dichloro-
163(100), 135(89), 93(87), 107(79), 167(76), 55(55), 121(48), 41(43)	374	$C_{22}H_{30}O_5$	jasmolin II
163(100), 161(93), 91(68), 119(52), 206(45), 117(29), 41(28), 43(25)	206	$C_{13}H_{18}O_2$	ibuprofen
164(100), 166(33), 223(23), 55(21), 43(21), 41(20), 99(17), 165(11)	223	$C_{11}H_{10}NO_2Cl$	indoleacetic acid, 4-chloro-, methyl ester

Ions/Intensities	Mol.Wt.	Formula	Compound Name
167(100), 138(95), 223(70), 139(25), 124(18), 29(15), 168(11), 152(10)	223	$C_{12}H_{17}NO_3$	phenetidine, N-propionyl-2-methoxy-
168(100), 167(85), 41(84), 43(71), 27(33), 97(29), 39(28), 29(26)	238	$C_{12}H_{18}N_2O_3$	quinalbarbitone
168(100), 199(77), 43(46), 169(40), 167(32), 198(30), 241(29), 141(22)	241	$C_{15}H_{15}NO_2$	biphenyl, N-methoxy-4-acetylamino-
169(100), 58(70), 168(29), 72(17), 170(17), 167(13), 42(10), 30(6)	239	$C_{17}H_{21}N$	pheniramine
169(100), 185(60), 43(47), 168(32), 211(28), 141(22), 167(21), 170(14)	227	$C_{14}H_{13}NO_2$	biphenyl, N-hydroxy-3-acetylamino-
169(100), 211(39), 168(30), 185(24), 43(23), 170(15), 141(11), 167(10)	227	$C_{14}H_{13}NO_2$	biphenyl, N-hydroxy-4-acetylamino-
172(100), 43(90), 45(64), 156(46), 92(37), 214(33), 108(28), 65(25)	214	$C_8H_{10}N_2O_3S$	sulphanilamide, N4-acetyl-
172(100), 92(95), 156(79), 65(75), 108(50), 39(25), 43(15), 63(14)	172	$C_6H_8N_2O_2S$	sulphanilamide
173(100), 115(81), 142(80), 43(69), 215(46), 141(41), 127(35), 172(29)	215	$C_{11}H_{13}NO_2$	naphthalene, N-methoxy-2-acetylamino-
176(100), 177(36), 57(22), 45(18), 149(13), 29(12), 119(9)	338	$C_{19}H_{30}O_5$	piperonyl butoxide
177(100), 43(84), 41(26), 93(20), 91(15), 178(14), 121(12), 77(12)	192	$C_{13}H_{20}O$	ionone, β-
178(100), 134(96), 160(47), 78(28), 77(26), 51(26), 39(25), 135(23)	178	$C_{10}H_{10}O_3$	mellein
179(100), 43(84), 150(56), 57(23), 119(16), 164(15), 134(12), 180(12)	221	$C_{12}H_{15}NO_3$	propiophenone, N-methoxy-4-acetylamino-
180(100), 95(59), 68(48), 53(32), 41(32), 67(14), 42(11), 96(10)	180	$C_7H_8N_4O_2$	theophylline
180(100), 104(74), 77(66), 223(48), 209(43), 252(41), 51(39), 181(27)	252	$C_{15}H_{12}N_2O_2$	phentoin
180(100), 181(63), 210(51), 179(39), 211(38), 43(37), 253(36), 165(33)	253	$C_{16}H_{15}NO_2$	fluorene, N-methoxy-2-acetylamino-
181(100), 180(71), 223(57), 152(23), 43(21), 197(19), 182(16), 165(15)	239	$C_{15}H_{13}NO_2$	fluorene, N-hydroxy-2-acetylamino-
184(100), 63(65), 53(58), 30(47), 91(47), 107(32), 62(29), 92(26)	184	$C_6H_4N_2O_5$	phenol, 2,4-dinitro-
184(100), 65(81), 39(68), 121(44), 69(39), 41(38), 94(35), 186(32)	364	$C_{18}H_{17}O_6Cl$	radicicol
184(100), 169(91), 183(26), 153(23), 155(22), 152(17), 185(15), 154(13)	184	$C_{14}H_{16}$	chamazulene
185(100), 185(57), 259(54), 43(54), 57(38), 29(27), 41(24), 157(22)	402	$C_{20}H_{34}O_8$	citric acid, acetyl-, tri-n-butyl ester
185(100), 230(48), 186(15), 141(14), 115(12), 170(11), 139(11), 153(8)	230	$C_{14}H_{14}O_3$	naproxen
185(100), 244(35), 186(17), 170(10), 141(7), 154(6), 245(6), 153(6)	244	$C_{15}H_{16}O_3$	naproxen, methyl ester
186(100), 29(77), 114(68), 42(48), 72(45), 27(32), 113(31), 81(20)	186	$C_7H_{10}N_2O_2S$	carbimazole
189(100), 117(87), 132(76), 160(40), 91(30), 115(29), 39(20), 77(19)	217	$C_{13}H_{15}NO_2$	glutethimide
189(100), 204(76), 93(75), 81(64), 107(64), 41(63), 105(50), 91(45)	204	$C_{15}H_{24}$	selinene, α-
189(100), 204(69), 161(61), 59(50), 133(45), 105(32), 81(30), 107(26)	222	$C_{15}H_{26}O$	eudesmol, γ-
190(100), 125(29), 134(28), 162(27), 91(14), 112(13), 191(12), 161(11)	278	$C_{16}H_{22}O_4$	abscisic acid, methyl ester
192(100), 91(24), 165(22), 119(16), 65(15), 39(14), 161(13), 193(12)	192	$C_{11}H_{12}O_3$	myristicine

Ions/Intensities	Mol.Wt.	Formula	Compound Name
193(100), 192(34), 236(23), 191(20), 165(16), 194(15), 63(7), 167(6)	236	$C_{15}H_{12}N_2O$	carbamazepine
196(100), 198(89), 97(68), 132(37), 62(33), 200(30), 99(27), 61(26)	196	$C_6H_3OCl_3$	phenol, 2,4,6-trichloro-
199(100), 43(93), 168(51), 184(27), 200(17), 241(17), 169(16), 153(13)	241	$C_{15}H_{15}NO_2$	biphenyl, N-methoxy-3-acetylamino-
202(100), 188(82), 135(60), 160(60), 136(57), 201(53), 119(47), 186(40)	219	$C_{10}H_{13}N_5O$	zeatin
202(100), 200(18), 203(17), 101(11), 202(10), 88(6), 150(5), 100(4)	202	$C_{16}H_{10}$	butadiyne, 1,4-diphenyl-
202(100), 244(75), 43(74), 138(42), 186(34), 92(25), 107(24), 79(12)	244	$C_9H_{12}N_2O_4S$	benzenesulfonamide, 3-methoxy-4-acetylamino-
203(100), 58(92), 205(33), 72(26), 204(15), 42(13), 167(13), 202(12)	274	$C_{16}H_{19}N_2Cl$	chlorpheniramine
204(100), 117(35), 232(24), 51(20), 77(18), 161(17), 103(17), 146(16)	232	$C_{12}H_{12}N_2O_3$	phenobarbitone
208(100), 194(54), 209(14), 77(13), 133(11), 91(11), 79(10), 177(10)	208	$C_{12}H_{16}O_3$	elemicin
208(100), 209(86), 278(52), 84(28), 42(25), 96(24), 193(23), 194(21)	278	$C_{19}H_{22}N_2$	triprolidine
222(100), 177(31), 207(15), 98(13), 223(12), 51(11), 63(10), 192(10)	222	$C_{12}H_{14}O_4$	dillapiole
232(100), 118(24), 146(23), 175(21), 117(18), 233(14), 91(9), 103(8)	260	$C_{14}H_{16}N_2O_3$	phenobarbitone, N,N-dimethyl
233(100), 340(72), 341(59), 248(55), 247(32), 356(30), 139(29), 234(28)	356	$C_{20}H_{17}O_3SF$	sulindac
233(100), 383(41), 259(30), 245(30), 95(29), 56(25), 43(19), 41(19)	383	$C_{18}H_{21}N_5O_4$	prazosin
234(100), 175(98), 199(68), 177(64), 236(59), 147(40), 145(37), 111(33)	234	$C_9H_8Cl_2O_3$	phenoxyacetic acid, 2,4-dichloro-, me.ester
235(100), 91(52), 250(42), 233(30), 65(25), 76(21), 236(16), 39(15)	250	$C_{16}H_{14}N_2O$	methaqualone
238(100), 223(31), 43(26), 192(19), 239(15), 191(11), 163(11), 39(10)	238	$C_{13}H_{18}O_4$	benzene, 2,3,4,5-tetramethoxy-allyl-
239(100), 180(62), 197(61), 196(51), 181(23), 152(21), 240(16), 168(14)	239	$C_{15}H_{13}NO_2$	fluorene-9-ol, 2-acetlamino-
239(100), 284(72), 75(67), 276(49), 138(48), 302(46), 111(43), 304(35)	320	$C_{15}H_{20}N_2O_2Cl_2$	lorazepam
239(100), 299(20), 240(20), 314(14), 197(6), 173(5), 141(5), 143(4)	314	$C_{21}H_{30}O_2$	methyl dehydroabietate
242(100), 207(94), 244(33), 270(20), 208(17), 165(16), 243(16), 269(13)	270	$C_{16}H_{15}N_2Cl$	medazepam
253(100), 280(99), 234(68), 206(66), 252(62), 281(59), 251(54), 77(51)	281	$C_{15}H_{11}N_3O_3$	nitrazepam
256(100), 283(81), 284(66), 255(42), 257(41), 285(41), 258(33), 286(22)	284	$C_{16}H_{13}N_2OCl$	diazepam
259(100), 161(62), 81(42), 163(10), 54(9), 89(8), 27(7), 160(7)	414	$C_{18}H_{14}N_2OCl_4$	miconazole
265(100), 43(46), 121(36), 308(29), 77(22), 187(17), 115(17), 266(17)	308	$C_{19}H_{16}O_4$	warfarin
266(100), 264(62), 268(60), 165(38), 167(35), 95(29), 60(21), 202(20)	264	C_6HOCl_5	phenol, pentachloro-
266(100), 264(76), 268(47), 109(25), 124(19), 98(14), 133(14), 62(12)	264	$C_8N_2Cl_4$	chlorothalonil
271(100), 273(35), 77(24), 256(20), 300(19), 272(19), 255(14), 228(13)	300	$C_{16}H_{13}N_2O_2Cl$	temazepam
280(100), 286(72), 315(72), 288(56), 240(53), 234(53), 75(48), 287(44)	315	$C_{15}H_{10}N_3O_3Cl$	clonazepam

Ions/Intensities	Mol.Wt.	Formula	Compound Name
282(100), 283(80), 284(44), 285(25), 77(15), 220(13), 247(12), 219(11)	299	$C_{16}H_{14}N_3OCl$	chlordiazepoxide
295(100), 296(21), 238(12), 310(12), 26(8), 251(6), 27(6), 55(5)	310	$C_{21}H_{26}O_2$	cannabinol
297(100), 42(53), 298(20), 296(19), 58(18), 283(17), 241(15), 240(15)	297	$C_{18}H_{19}NO_3$	oripavine
300(100), 77(85), 258(67), 51(58), 255(52), 259(47), 256(38), 283(38)	300	$C_{16}H_{13}N_2O_2Cl$	clobazepam
301(100), 44(40), 42(38), 59(37), 70(31), 164(26), 31(24), 302(21)	301	$C_{18}H_{23}NO_3$	dihydrocodeine
312(100), 285(99), 286(67), 313(63), 266(48), 238(43), 283(40), 284(33)	313	$C_{16}H_{12}N_3O_3F$	flunitrazepam
313(100), 42(38), 59(29), 162(28), 314(19), 284(18), 124(18), 243(16)	313	$C_{19}H_{23}NO_3$	ethylmorphine
316(100), 256(88), 241(52), 121(50), 136(42), 105(39), 213(37), 257(34)	316	$C_{21}H_{32}O_2$	methyl abietate
317(100), 315(96), 236(92), 288(69), 78(57), 286(57), 77(56), 51(51)	315	$C_{14}H_{10}N_3OBr$	bromazepam
323(100), 221(81), 181(56), 222(45), 207(40), 72(37), 223(34), 196(24)	323	$C_{20}H_{25}N_3O$	lysergic acid diethylamide (LSD)
324(100), 338(73), 339(62), 325(22), 308(20), 51(15), 293(14), 151(13)	339	$C_{20}H_{21}NO_4$	papaverine
341(100), 282(58), 43(39), 42(34), 229(30), 59(23), 342(22), 204(17)	341	$C_{20}H_{23}NO_4$	acetyl codeine

Eight peak spectra, indexed by molecular weight

Ions/Intensities	Mol.Wt.	Formula	Compound Name
55(100), 27(52), 43(21), 70(17), 44(10), 41(9), 56(8), 98(7)	98	$C_6H_{10}O$	pent-1-en-2-one, 4-methyl-
59(100), 43(49), 31(42), 41(29), 39(14), 69(11), 42(7), 87(4)	102	$C_5H_{10}O_2$	butan-2-one, 3-hydroxy-3-methyl-
106(100), 107(83), 77(32), 51(24), 39(23), 79(16), 65(15), 78(12)	107	C_7H_9N	aniline, N-methyl-
108(100), 65(95), 78(67), 39(46), 51(24), 77(22), 79(17), 93(16)	108	C_7H_8O	anisole
124(100), 123(63), 78(48), 77(20), 51(19), 39(18), 55(10), 52(9)	124	$C_7H_8O_2$	catechol, 4-methyl-
43(100), 41(61), 55(29), 69(27), 39(27), 108(16), 67(12), 111(11)	126	$C_8H_{14}O$	hept-5-en-2-one, trans 6-methyl-
57(100), 43(21), 29(17), 72(14), 27(13), 55(10), 58(7), 39(7)	128	$C_8H_{16}O$	oct-1-en-3-ol
128(100), 64(71), 63(36), 130(31), 39(24), 65(22), 38(16), 92(13)	128	C_6H_5OCl	phenol, 2-chloro-
59(100), 55(55), 41(48), 83(47), 31(31), 29(28), 43(22), 101(22)	130	$C_8H_{18}O$	octan-3-ol
132(100), 117(81), 91(38), 115(33), 92(20), 39(19), 65(19), 131(15)	132	$C_{10}H_{12}$	cymenene
119(100), 91(74), 134(66), 41(30), 39(26), 77(21), 105(21), 92(17)	134	$C_{10}H_{14}$	mentha-1,3,9-triene, p-
44(100), 91(6), 42(4), 65(4), 45(3), 39(3), 51(2), 120(2)	135	$C_9H_{13}N$	amphetamine
136(100), 29(33), 52(30), 135(13), 53(12), 51(9), 137(7), 39(7)	136	$C_5H_4N_4O$	allopurinol
135(100), 136(69), 77(27), 92(14), 107(11), 39(10), 63(8), 65(8)	136	$C_8H_8O_2$	benzaldehyde, methoxy-
93(100), 121(67), 79(38), 41(38), 67(33), 91(28), 107(28), 39(27)	136	$C_{10}H_{16}$	camphene
93(100), 43(31), 91(31), 79(29), 77(29), 27(28), 80(22), 92(21)	136	$C_{10}H_{16}$	carene, Δ3-
68(100), 67(44), 93(35), 39(25), 79(24), 53(23), 94(18), 77(15)	136	$C_{10}H_{16}$	limonene
41(100), 93(91), 69(76), 39(34), 27(30), 53(21), 77(13), 29(12)	136	$C_{10}H_{16}$	myrcene
93(100), 77(33), 91(31), 92(23), 41(16), 136(13), 29(12), 39(10)	136	$C_{10}H_{16}$	phellandrene, α-
93(100), 41(88), 43(58), 27(50), 69(47), 49(46), 77(42), 29(31)	136	$C_{10}H_{16}$	pinene, β-
93(100), 77(31), 41(28), 43(25), 91(25), 79(21), 57(18), 94(13)	136	$C_{10}H_{16}$	sabinene
93(100), 43(36), 91(35), 77(35), 41(25), 121(24), 136(22), 92(21)	136	$C_{10}H_{16}$	terpinene, γ-
93(100), 121(91), 136(69), 91(46), 79(43), 77(40), 119(38), 41(36)	136	$C_{10}H_{16}$	terpinolene, α-
120(100), 92(81), 138(45), 39(36), 43(35), 64(35), 45(32), 63(21)	138	$C_7H_6O_3$	salicylic acid
139(100), 39(63), 65(46), 63(36), 64(30), 81(24), 53(22), 38(21)	139	$C_6H_5NO_3$	phenol, 2-nitro-
55(100), 41(63), 97(61), 96(34), 27(21), 39(20), 43(17), 81(16)	140	$C_{10}H_{20}$	menthane, cis p-
139(100), 140(68), 63(12), 62(9), 51(9), 141(7), 39(7), 114(6)	140	$C_{11}H_8$	phenylpenta-2,4-diyne, 1-
107(100), 142(89), 77(45), 51(28), 144(25), 39(20), 78(14), 50(12)	142	C_7H_7OCl	phenol, 3-methyl-4-chloro-

Ions/Intensities	Mol.Wt.	Formula	Compound Name
71(100), 43(99), 56(51), 57(45), 41(41), 29(24), 89(23), 27(17)	144	$C_8H_{16}O_2$	isobutyyl isobutyrate
76(100), 50(78), 147(71), 104(69), 103(31), 74(29), 75(22), 38(17)	147	$C_8H_5NO_2$	phthalimide
148(100), 147(35), 77(22), 133(22), 117(22), 105(20), 121(18), 79(13)	148	$C_{10}H_{12}O$	anethole
43(100), 105(43), 91(36), 148(28), 77(13), 79(12), 51(10), 67(9)	148	$C_{10}H_{12}O$	butan-2-one, 4-phenyl-
133(100), 105(66), 148(58), 77(39), 91(34), 79(34), 41(32), 119(32)	148	$C_{10}H_{12}O$	cuminic aldehyde, p-
148(100), 147(42), 121(39), 117(30), 77(22), 133(21), 105(17), 51(15)	148	$C_{10}H_{12}O_2$	estragole
58(100), 30(7), 91(5), 42(4), 59(4), 56(3), 65(3), 39(2)	149	$C_{10}H_{15}N$	methylamphetamine
135(100), 150(27), 91(20), 41(12), 77(11), 39(10), 136(10), 107(9)	150	$C_{10}H_{14}O$	carvacrol
82(100), 54(44), 39(34), 93(26), 108(25), 41(23), 53(17), 107(16)	150	$C_{10}H_{14}O$	carvone
135(100), 150(43), 105(42), 107(35), 79(32), 119(25), 91(23), 77(16)	150	$C_{10}H_{14}O$	cuminyl alcohol
43(100), 135(53), 115(17), 132(14), 117(13), 65(8), 115(7), 39(6)	150	$C_{10}H_{14}O$	cymene-8-ol, p-
121(100), 150(20), 77(8), 91(7), 78(5), 39(5), 122(4), 65(3),	150	$C_{10}H_{14}O$	dihydroanethole
108(100), 150(21), 79(17), 39(9), 109(8), 77(7), 41(6), 51(5)	150	$C_{10}H_{14}O$	menthofuran
53(100), 41(88), 81(85), 108(57), 39(37), 69(37), 43(36), 79(32)	150	$C_{10}H_{14}O$	pinocarvone
135(100), 150(26), 91(18), 39(10), 117(10), 115(10), 136(10), 77(8)	150	$C_{10}H_{14}O$	thymol
107(100), 135)88), 91(86), 41(68), 80(68), 39(61), 150(59), 79(49)	150	$C_{10}H_{14}O$	verbenone
44(100), 77(6), 42(5), 79(4), 51(4), 45(3), 91(2), 105(2)	151	$C_9H_{13}NO$	phenylpropanolamine
108(100), 93(42), 95(25), 41(24), 109(19), 67(19), 91(13), 81(12)	152	$C_{19}H_{16}O$	campholene aldehyde, α-
95(100), 81(65), 41(61), 69(38), 108(35), 55(35), 83(33), 109(26)	152	$C_{10}H_{16}O$	camphor
84(100), 134(65), 41(50), 79(47), 109(47), 119(40), 55(39), 91(37)	152	$C_{10}H_{16}O$	carveol, *cis*-
109(100), 84(85), 41(46), 55(37), 119(35), 83(33), 91(33), 39(28)	152	$C_{10}H_{16}O$	carveol, *trans*-
95(100), 67(78), 68(66), 82(60), 81(54), 41(47), 152(43), 109(39)	152	$C_{10}H_{16}O$	dihydrocarvone
81(100), 69(57), 41(24), 82(13), 152(12), 29(12), 80(10), 39(9)	152	$C_{10}H_{16}O$	fenchone
137(100), 109(26), 69(25), 41(23), 93(15), 55(12), 67(11), 39(11)	152	$C_{10}H_{16}O$	hexahydrobenzofuran, 3,6-dimethyl -
79(100), 91(31), 108(17), 31(13), 77(12), 43(11), 41(11), 39(9)	152	$C_{10}H_{16}O$	myrtenol
67(100), 68(89), 55(75), 43(65), 41(47), 27(41), 39(24), 82(22)	152	$C_{10}H_{16}O$	octa-1,4,6-trien-3-ol, 3,7-dimethyl-
70(100), 92(98), 41(97), 55(92), 83(89), 91(61), 69(54), 81(35)	152	$C_{10}H_{16}O$	pinocarveol, *trans*-
82(100), 110(71), 39(33), 41(32), 95(28), 27(21), 54(19), 109(19)	152	$C_{10}H_{16}O$	piperitone
81(100), 152(63), 67(63), 41(50), 109(46), 82(36), 39(28), 69(25)	152	$C_{10}H_{16}O$	pulegone

Ions/Intensities	Mol.Wt.	Formula	Compound Name
92(100), 91(77), 81(35), 41(35), 109(24), 79(23), 134(21), 27(21)	152	$C_{10}H_{16}O$	sabinol
81(100), 41(81), 68(74), 110(66), 69(60), 67(49), 39(47), 109(42)	152	$C_{10}H_{16}O$	thujone
124(100), 153(76), 125(55), 96(16), 80(7), 154(7), 52(7), 53(4)	153	$C_8H_{11}NO_2$	phenetidine, 2-hydroxy
95(100), 41(20), 110(17), 55(11), 43(10), 67(8), 93(8), 96(8)	154	$C_{10}H_{18}O$	borneol
43(100), 71(99), 69(48), 41(44), 67(33), 96(31), 84(28), 39(28)	154	$C_{10}H_{18}O$	camphene hydrate
43(100), 81(27), 55(26), 69(26), 71(22), 108(18), 84(18), 111(13)	154	$C_{10}H_{18}O$	cineole, 1,8-
41(100), 69(81), 55(46), 95(36), 43(32), 56(29), 57(27), 39(21)	154	$C_{10}H_{18}O$	citronellal
83(100), 55(71), 82(70), 41(38), 67(16), 29(16), 43(13), 154(12)	154	$C_{11}H_{22}$	cyclohexane, n-pentyl-
81(100), 80(50), 41(39), 71(31), 69(30), 43(28), 55(24), 84(21)	154	$C_{10}H_{18}O$	fenchol
112(100), 69(55), 41(53), 55(46), 139(33), 56(30), 70(28), 43(25)	154	$C_{10}H_{18}O$	isomenthone
71(100), 43(74), 41(67), 69(47), 55(44), 27(33), 93(31), 39(28)	154	$C_{10}H_{18}O$	linalool
112(100), 41(85), 69(67), 55(63), 56(39), 139(37), 70(36), 43(35)	154	$C_{10}H_{18}O$	menthone
69(100), 67(94), 93(91), 123(85), 41(83), 81(73), 82(70), 55(61)	154	$C_{10}H_{18}O$	myrtanol
69(100), 41(60), 68(19), 39(11), 93(10), 123(2), 67(8), 53(7)	154	$C_{10}H_{18}O$	nerol
71(100), 93(46), 111(46), 41(34), 43(32), 86(26), 69(22), 55(18)	154	$C_{10}H_{18}O$	terpinene-4-ol
59(100), 93(50), 43(37), 121(35), 81(32), 136(32), 41(22), 67(16)	154	$C_{10}H_{18}O$	terpineol, α-
41(100), 69(85), 55(42), 82(37), 67(34), 81(29), 71(25), 95(24)	156	$C_{10}H_{20}O$	citronellol
71(100), 43(37), 41(16), 72(14), 58(14), 98(13), 55(11), 57(8)	156	$C_{10}H_{20}O$	menthan-1-ol, p-
113(100), 43(96), 95(66), 41(35), 99(32), 71(24), 55(20), 69(12)	156	$C_{10}H_{20}O$	menthan-4-ol, p-
59(100), 58(15), 55(13), 41(11), 43(8), 81(6), 60(5), 123(4)	156	$C_{10}H_{20}O$	menthan-8-ol, p-
71(100), 81(67), 41(62), 95(61), 55(48), 43(33), 82(33), 69(32)	156	$C_{10}H_{20}O$	menthol
84(100), 43(28), 41(27), 83(25), 93(24), 139(23), 55(18), 39(14)	156	$C_{10}H_{20}O$	piperitol, *cis*-
84(100), 41(27), 83(26), 93(25), 43(25), 139(24), 55(18), 39(15)	156	$C_{10}H_{20}O$	piperitol, *trans*-
71(100), 43(93), 70(53), 41(24), 55(18), 27(13), 29(11), 42(11)	158	$C_9H_8O_2$	isobutyric acid, 2-methylbutyl ester
74(100), 87(53), 43(48), 41(35), 55(30), 57(19), 69(18), 82(17)	158	$C_9H_{18}O_2$	isooctanoic acid, methyl ester
73(100), 69(50), 55(43), 43(32), 41(30), 70(20), 27(16), 56(8)	158	$C_{10}H_{22}O$	tetrahydrolinalool
160(100), 103(63), 76(30), 130(29), 131(25), 89(24), 115(23), 50(22)	160	$C_8H_8N_4$	hydralazine
91(100), 92(89), 41(17), 65(13), 29(13), 39(12), 27(12), 105(9)	162	$C_{12}H_{18}$	benzene, n-hexyl
131(100), 162(58), 103(45), 77(24), 51(14), 102(11), 132(10), 163(6)	162	$C_{10}H_{10}O_2$	cinnamic acid, methyl ester

Ions/Intensities	Mol.Wt.	Formula	Compound Name
84(100), 133(30), 162(21), 42(19), 161(18), 92(7), 119(7), 65(6)	162	$C_{10}H_{14}N_2$	nicotine
162(100), 164(72), 63(49), 98(33), 99(12), 100(12), 62(12), 126(11)	162	$C_6H_4OCl_2$	phenol, 2,4-dichloro-
77(100), 93(71), 91(68), 80(43), 147(37), 53(36), 105(33), 65(30)	162	$C_{12}H_{18}$	pregeijerene
162(100), 104(58), 51(47), 77(47), 103(40), 131(40), 135(38), 43(33)	162	$C_{10}H_{10}O_2$	safrole
104(100), 91(91), 82(69), 105(43), 119(31), 39(28), 164(27), 77(25)	164	$C_{10}H_{12}O_2$	methyl 3-phenyl propanoate
108(100), 123(80), 165(57), 43(42), 80(31), 52(21), 65(17), 92(8)	165	$C_9H_{11}NO_2$	acetanilide, 2-methoxy-
108(100), 123(62), 165(56), 43(26), 80(10), 52(10), 122(10), 109(8)	165	$C_9H_{11}NO_2$	acetanilide, 4-methoxy-
58(100), 146(24), 42(21), 56(19), 77(16), 30(15), 105(14), 117(8)	165	$C_{10}H_{15}NO$	ephedrine
44(100), 45(3), 77(3), 42(3), 39(3), 95(2), 65(2), 43(1)	165	$C_9H_{13}NO_2$	phenylephrine
58(100), 30(10), 56(5), 42(5), 77(4), 59(4), 51(3), 57(2)	165	$C_{10}H_{15}NO$	pseudoephedrine
125(100), 167(27), 43(23), 96(14), 124(10), 126(8), 52(7), 80(5)	167	$C_8H_9NO_3$	acetanilide, 2,4-dihydroxy-
125(100), 167(46), 43(33), 79(30), 52(12), 124(10), 126(8), 51(8)	167	$C_8H_9NO_3$	acetanilide, 3,4-dihydroxy-
140(100), 139(90), 91(65), 168(51), 51(36), 63(35), 77(30), 39(20)	168	$C_{12}H_8O$	capillin
83(100), 55(58), 41(38), 67(15), 43(13), 29(11), 168(11)	168	$C_{12}H_{24}$	cyclohexane, n-hexyl-
126(100), 41(82), 43(56), 168(45), 125(39), 55(36), 39(36), 69(35)	168	$C_{10}H_{16}O_2$	diosphenol
125(100), 43(95), 41(88), 168(75), 55(54), 39(43), 69(42), 153(39)	168	$C_{10}H_{16}O_2$	psi-diosphenol
58(100), 43(70), 59(29), 71(28), 41(26), 55(14), 57(12), 85(5)	170	$C_{11}H_{22}O$	undecan-2-one
54(100), 81(92), 53(81), 45(53), 124(50), 42(47), 27(44), 52(41)	171	$C_6H_9N_3O_3$	metromidazole
43(100), 41(15), 55(13), 70(13), 56(11), 112(10), 57(9), 83(9)	172	$C_{10}H_{20}O_2$	octan-3-yl acetate
172(100), 92(95), 156(79), 65(75), 108(50), 39(25), 43(15), 63(14)	172	$C_6H_8N_2O_2S$	sulphanilamide
144(100). 175(53), 116(17), 89(17), 145(11), 63(7), 176(6), 72(5)	175	$C_{10}H_9NO_2$	indole-2-carboxylic acid, methyl ester
116(100), 43(88), 29(71), 85(59), 31(49), 44(46), 61(29), 42(28)	176	$C_6H_8O_6$	ascorbic acid
131(100), 103(37), 176(30), 77(26), 51(15), 104(13), 132(12), 147(11)	176	$C_{11}H_{12}O_2$	cinnamic acid, ethyl ester
105(100), 120(51), 77(51), 51(16), 39(9), 78(9), 106(8), 41(7)	176	$C_{12}H_{16}O$	phenyl-1-hexanone, 1-
178(100), 134(96), 160(47), 78(28), 77(26), 51(26), 39(25), 135(23)	178	$C_{10}H_{10}O_3$	mellein
105(100), 77(66), 135(31), 51(26), 134(15), 106(8), 78(6), 161(4)	179	$C_9H_9NO_3$	hippuric acid
108(100), 109(86), 179(64), 137(42), 43(34), 81(11), 80(11), 180(7)	179	$C_{10}H_{13}NO_2$	phenacetin
137(100), 180(20), 122(13), 138(11), 43(7), 94(7), 51(5), 77(4)	180	$C_{10}H_{22}O_3$	propan-2-one, 1-(4-hydroxy-3-methoxyphenyl)-
180(100), 95(59), 68(48), 53(32), 41(32), 67(14), 42(11), 96(10)	180	$C_7H_8N_4O_2$	theophylline

Ions/Intensities	Mol.Wt.	Formula	Compound Name
69(100), 41(99), 114(26), 83(25), 123(13), 93(11), 105(10), 77(10)	182	$C_{11}H_{18}O_2$	geranic acid, methyl ester
155(100), 140(80), 83(58), 41(56), 98(54), 55(42), 29(26), 27(26)	183	$C_{10}H_{17}NO_2$	methyprylon
156(100), 141(76), 41(36), 27(33), 29(30), 39(30), 55(29), 98(22)	184	$C_8H_{12}N_2O_3$	barbitone
184(100), 169(91), 183(26), 153(23), 155(22), 152(17), 185(15), 154(13)	184	$C_{14}H_{16}$	chamazulene
74(100), 41(75), 43(74), 55(70), 110(50), 54(48), 67(45), 29(36)	184	$C_{11}C_{20}O_2$	dec-4-enoic acid, methyl ester
184(100), 63(65), 53(58), 30(47), 91(47), 107(32), 62(29), 92(26)	184	$C_6H_4N_2O_5$	phenol, 2,4-dinitro-
143(100), 43(42), 145(33), 185(19), 80(12), 51(10), 144(9), 114(9)	185	$C_8H_8NO_2Cl$	acetanilide, 2-hydroxy-4-chloro-
186(100), 29(77), 114(68), 42(48), 72(45), 27(32), 113(31), 81(20)	186	$C_7H_{10}N_2O_2S$	carbimazole
69(100), 41(91), 109(58), 39(51), 81(50), 112(48), 55(42), 67(38)	186	$C_{10}H_{18}SO$	menthon-8-thiol, p-
91(100), 57(46), 108(31), 192(27), 85(24), 41(15), 43(11), 92(8)	192	$C_{12}H_{16}O_2$	benzyl isopentanoate
91(100), 108(83), 57(34), 192(26), 85(25), 92(14), 65(12), 90(12)	192	$C_{12}H_{16}O_2$	benzyl pentanoate
121(100), 93(80), 43(68), 136(59), 41(29), 91(27), 77(25), 109(23)	192	$C_{13}H_{20}O$	ionone, α-
177(100), 43(84), 41(26), 93(20), 91(15), 178(14), 121(12), 77(12)	192	$C_{13}H_{20}O$	ionone, β-
192(100), 91(24), 165(22), 119(16), 65(15), 39(14), 161(13), 193(12)	192	$C_{11}H_{12}O_3$	myristicine
120(100), 151(59), 193(38), 43(36), 65(20), 92(19), 121(11), 161(10)	193	$C_{10}H_{11}NO_3$	benzoic acid, N-acetyl-4-amino-, me. ester
86(100), 58(23), 42(7), 29(6), 87(6), 30(5), 27(4), 51(3)	193	$C_{12}H_{19}NO$	etafedrine
137(100), 108(99), 109(91), 193(67), 52(9), 194(8), 81(8), 80(7)	193	$C_{11}H_{15}NO_2$	phenetidine, N-propionyl-
43(100), 84(71), 119(55), 109(35), 134(35), 152(34), 41(29), 91(29)	194	$C_{12}H_{18}O$	carveyl acetate
121(100), 43(74), 161(60), 123(38), 93(38), 136(36), 95(36), 119(33)	194	$C_{13}H_{22}O$	dihydro-β-ionone
91(100), 43(54), 92(43), 41(11), 119(9), 108(8), 39(6), 134(5)	194	$C_{12}H_{18}O_2$	sabinyl acetate
138(100), 153(73), 195(72), 43(31), 110(19), 52(13), 95(12), 139(11)	195	$C_{10}H_{13}NO_3$	acetanilide, 2,4-dimethoxy-
138(100), 195(71), 153(31), 43(31), 110(24), 139(19), 15(9), 196(9)	195	$C_{10}H_{13}NO_3$	acetanilide, 3,4-dimethoxy-
124(100), 153(96), 125(69), 195(54), 43(38), 149(27), 96(20), 177(13)	195	$C_{10}H_{13}NO_3$	phenacetin, 2-hydroxy-
124(100), 195(52), 125(40), 43(34), 96(16), 153(7), 68(6), 196(6)	195	$C_{10}H_{13}NO_3$	phenacetin, 3-hydroxy-
108(100), 109(81), 179(64), 43(62), 137(44), 153(14), 136(14), 81(13)	195	$C_{10}H_{13}NO_3$	phenacetin, N-hydroxy-
121(100), 120(95), 92(70), 65(44), 195(28), 43(28), 39(26), 92(21)	195	$C_9H_9NO_4$	salicyluric acid
95(100), 43(66), 93(38), 121(36), 136(33), 55(17), 69(16), 108(16)	196	$C_{12}H_{20}O_2$	bornyl acetate
41(100), 93(93), 69(75), 43(42), 45(28), 121(22), 79(22), 77(19)	196	$C_{12}H_{20}O_2$	linalyl acetate
43(100), 93(94), 82(71), 69(53), 121(45), 67(44), 41(44), 95(38)	196	$C_{12}H_{20}O_2$	myrtanyl acetate

Ions/Intensities	Mol.Wt.	Formula	Compound Name
196(100), 198(89), 97(68), 132(37), 62(33), 200(30), 99(27), 61(26)	196	$C_6H_3OCl_3$	phenol, 2,4,6-trichloro-
43(100), 121(88), 93(71), 136(57), 41(26), 59(22), 81(18), 68(16)	196	$C_{12}H_{20}O_2$	terpinyl acetate, α-
140(100), 197(93), 155(86), 43(47), 51(11), 198(11), 156(10), 96(10)	197	$C_9H_{11}NO_2S$	paracetamol, 3-methythio-
124(100), 109(56), 198(21), 77(18), 81(14), 122(11), 123(10), 52(9)	198	$C_{10}H_{14}O_4$	guaifenesin
95(100), 81(67), 138(52), 41(50), 55(44), 123(33), 43(31), 96(27)	198	$C_{12}H_{22}O_2$	menthyl acetate
157(100), 142(92), 43(60), 199(53), 159(34), 144(32), 114(24), 201(19)	199	$C_9H_{10}NO_2Cl$	acetanilide, 2-methoxy-4-chloro-
43(100), 157(40), 126(31), 159(24), 127(21), 111(15), 142(13), 128(13)	199	$C_8H_8NO_2Cl$	acetanilide, N-hydroxy-4-chloro-
159(100), 142(73), 43(71), 115(70), 143(41), 201(37), 128(25), 140(22)	201	$C_{10}H_{11}NO_2$	napthalene, N-hydroxy-2-acetylamino-
202(100), 200(18), 203(17), 101(11), 202(10), 88(6), 150(5), 100(4)	202	$C_{16}H_{10}$	butadiyne, 1,4-diphenyl-
159(100), 160(13), 202(9), 129(7), 128(7), 131(5), 105(5), 144(4)	202	$C_{15}H_{22}$	calamenene
134(100), 41(36), 133(35), 69(31), 135(10), 107(9), 39(9), 77(6)	202	$C_{14}H_{18}O$	feniculin
69(100), 41(90), 93(85), 67(58), 94(53), 109(47), 79(45), 204(33)	204	$C_{15}H_{24}$	bisabolene, β-
161(100), 134(58), 119(46), 105(45), 204(41), 41(34), 81(27), 91(25)	204	$C_{15}H_{24}$	cadinene, δ-
41(100), 69(98), 93(94), 133(65), 79(61), 91(55), 107(39), 39(35)	204	$C_{15}H_{24}$	caryophyllene
119(100), 93(49), 41(34), 69(30), 105(28), 161(23), 204(20), 120(17)	204	$C_{15}H_{24}$	cedrene, α-
119(100), 105(95), 161(94), 41(46), 93(65), 91(34), 55(28), 120(27)	204	$C_{15}H_{24}$	copaene, α-
161(100), 105(97), 119(93), 41(33), 81(32), 120(29), 91(29), 93(26)	204	$C_{15}H_{24}$	cubebene, α-
81(100), 68(87), 93(69), 41(57), 67(48), 107(45), 55(41), 79(36)	204	$C_{15}H_{24}$	elemene, β-
121(100), 93(74), 107(47), 79(32), 94(29), 91(26), 81(26), 136(25)	204	$C_{15}H_{24}$	elemene, γ-
161(100), 105(45), 91(41), 41(36), 119(30), 77(29), 55(27), 120(26)	204	$C_{15}H_{24}$	Germacrene D
105(100), 147(87), 41(85), 93(78), 79(58), 91(58), 204(56), 133(54)	204	$C_{15}H_{24}$	guaiene, α-
107(100), 108(99), 93(96), 41(83), 105(66), 79(62), 81(62), 95(61)	204	$C_{15}H_{24}$	guaiene, δ-
93(100), 41(34), 80(32), 121(29), 55(19), 43(17), 92(16), 69(15)	204	$C_{15}H_{24}$	humulene
135(100), 93(96), 107(86), 108(85), 204(51), 91(51), 105(50)	204	$C_{15}H_{24}$	patchoulene, α-
161(100), 119(66), 189(66), 93(60), 41(59), 105(55), 81(46), 204(45)	204	$C_{15}H_{24}$	patchoulene, β-
161(100), 122(71), 107(51), 204(51), 41(33), 105(31), 93(30), 121(29)	204	$C_{15}H_{24}$	selina-3,7(11)-diene
161(100), 204(86), 41(69), 91(51), 189(50), 105(48), 133(44), 135(43)	204	$C_{15}H_{24}$	selina-4(14),7(11)-diene
189(100), 204(76), 93(75), 81(64), 107(64), 41(63), 105(50), 91(45)	204	$C_{15}H_{24}$	selinene, α-
41(100), 105(90), 107(89), 204(88), 93(86), 81(78), 121(69), 79(68)	204	$C_{15}H_{24}$	selinene, β-

Ions/Intensities	Mol.Wt.	Formula	Compound Name
161(100), 189(98), 204(94), 41(40), 91(40), 105(39), 133(28), 81(24)	204	$C_{15}H_{24}$	selinene, δ-
93(100), 119(78), 41(44), 69(40), 77(26), 91(26), 56(18), 55(17)	204	$C_{15}H_{24}$	zingiberene
163(100), 161(93), 91(68), 119(52), 206(45), 117(29), 41(28), 43(25)	206	$C_{13}H_{18}O_2$	ibuprofen
137(100), 108(70), 109(56), 207(47), 43(26), 138(10), 71(9), 110(9)	207	$C_{12}H_{17}NO_2$	phenetidine, N-butyryl-
43(100), 136(85), 165(82), 120(25), 57(23), 29(22), 162(15), 90(14)	207	$C_{11}H_{13}NO_3$	propiophenone, N-hydroxy-4-acetylamino-
208(100), 194(54), 209(14), 77(13), 133(11), 91(11), 79(10), 177(10)	208	$C_{12}H_{16}O_3$	elemicin
109(100), 95(87), 95(87), 55(85), 96(75), 81(69), 69(65), 83(65)	208	$C_{15}H_{28}$	eudesmane, 4αH,5αH-
120(100), 41(42), 43(37), 138(31), 121(31), 39(28), 59(28), 55(28)	208	$C_{12}H_{16}O_3$	isoamyl salicylate
138(100), 209(72), 167(51), 43(31), 139(27), 124(21), 108(18), 152(11)	209	$C_{11}H_{15}NO_3$	phenacetin, 2-methoxy-
138(100), 209(51), 139(36), 43(31), 110(121), 180(10), 210(7), 167(6)	209	$C_{11}H_{15}NO_3$	phenacetin, 3-methoxy-
108(100), 43(84), 138(64), 136(47), 167(39), 81(32), 107(30), 135(26)	209	$C_{11}H_{15}NO_3$	phenacetin, N-methoxy-
154(100), 211(95), 43(40), 110(36), 169(34), 109(13), 212(11), 155(9)	211	$C_{10}H_{13}NO_2S$	acetanilide, 3-methylthio-4-methoxy-
105(100), 91(61), 77(39), 212(23), 51(22), 65(14), 106(11), 90(10)	212	$C_{14}H_{12}O_2$	benzyl benzoate
156(100), 141(94), 41(44), 29(40), 27(31), 39(21), 98(19), 142(15)	212	$C_{10}H_{16}N_2O_3$	butobarbitone
109(100), 92(95), 65(67), 156(61), 108(56), 214(29), 39(23), 43(22)	214	$C_8H_{10}N_2O_3S$	sulphanilamide, N1-acetyl-
172(100), 43(90), 45(64), 156(46), 92(37), 214(33), 108(28), 65(25)	214	$C_8H_{10}N_2O_3S$	sulphanilamide, N4-acetyl-
173(100), 115(81), 142(80), 43(69), 215(46), 141(41), 127(35), 172(29)	215	$C_{11}H_{13}NO_2$	naphthalene, N-methoxy-2-acetylamino-
189(100), 117(87), 132(76), 160(40), 91(30), 115(29), 39(20), 77(19)	217	$C_{13}H_{15}NO_2$	glutethimide
146(100), 190(64), 117(50), 118(35), 30(22), 161(22), 189(22), 103(21)	218	$C_{12}H_{14}N_2O_2$	primidone
43(100), 161(57), 163(35), 177(24), 179(15), 203(11), 162(10), 160(9)	219	$C_8H_7NO_2Cl_2$	acetanilide, N-hydroxy-3,4-dichloro-
202(100), 188(82), 135(60), 160(60), 136(57), 201(53), 119(47), 186(40)	219	$C_{10}H_{13}N_5O$	zeatin
162(100), 164(66), 220(58), 22(39), 161(32), 133(28), 175(28), 163(27)	220	$C_8H_6Cl_2O_3$	phenoxyacetic acid, 2,4-dichloro-
179(100), 43(84), 150(56), 57(23), 119(16), 164(15), 134(12), 180(12)	221	$C_{12}H_{15}NO_3$	propiophenone, N-methoxy-4-acetylamino-
43(100), 41(89), 69(80), 109(50), 119(40), 93(39), 55(35), 67(28)	222	$C_{15}H_{26}O$	bisabolol, α-
161(100), 41(65), 84(49), 69(45), 55(41), 97(40), 43(39), 81(37)	222	$C_{15}H_{26}O$	carotol
95(100), 151(84), 43(68), 150(61), 41(51), 69(44), 81(42), 152(35)	222	$C_{15}H_{26}O$	cedrol
29(100), 207(63), 137(34), 109(32), 41(31), 149(20), 189(18), 67(17)	222	$C_{15}H_{26}O$	dihydroagarofuran
222(100), 177(31), 207(15), 98(13), 223(12), 51(11), 63(10), 192(10)	222	$C_{12}H_{14}O_4$	dillapiole
59(100), 93(53), 41(45), 43(36), 161(33), 81(33), 107(29), 121(24)	222	$C_{15}H_{26}O$	elemol

Ions/Intensities	Mol.Wt.	Formula	Compound Name
59(100), 149(37), 164(27), 109(21), 108(20), 81(17), 41(17), 95(15)	222	$C_{15}H_{26}O$	eudesmol, β-
189(100), 204(69), 161(61), 59(50), 133(45), 105(32), 81(30), 107(26)	222	$C_{15}H_{26}O$	eudesmol, γ-
161(100), 59(70), 107(57), 105(53), 93(42), 81(42), 41(39), 91(37)	222	$C_{15}H_{26}O$	guaiol
43(100), 41(77),69(55), 109(44), 81(43), 55(36), 122(39), 107(32)	222	$C_{15}H_{26}O$	ledol
43(100), 41(99), 81(89), 83(88), 98(83), 55(69), 222(67), 138(59)	222	$C_{15}H_{26}O$	patchouli alcohol
59(100), 149(99), 81(44), 108(36), 93(30), 41(18), 43(16), 121(16)	222	$C_{15}H_{26}O$	rosifoliol
41(100), 43(68), 69(63), 105(62), 79(61), 93(61), 81(55), 91(52)	222	$C_{15}H_{26}O$	viridiflorol
164(100), 166(33), 223(23), 55(21), 43(21), 41(20), 99(17), 165(11)	223	$C_{11}H_{10}NO_2Cl$	indoleacetic acid, 4-chloro-, methyl ester
167(100), 138(95), 223(70), 139(25), 124(18), 29(15), 168(11), 152(10)	223	$C_{12}H_{17}NO_3$	phenetidine, N-propionyl-2-methoxy-
69(100), 41(95), 81(50), 82(47), 95(41), 67(28), 123(27), 68(22)	224	$C_{14}H_{24}O_2$	citronellyl butenoate
59(100), 109(36), 166(27), 41(18), 55(17), 95(17), 81(13), 96(13)	224	$C_{15}H_{28}O$	eudesman-11-ol, 4αH,5αH-
59(100), 109(27), 151(27), 95(21), 166(19), 41(18), 110(17), 55(13)	224	$C_{15}H_{28}O$	eudesman-11-ol, 4βH,5αH-
83(100), 41(53), 151(45), 67(33), 95(32), 55(29), 93(28), 224(23)	224	$C_{13}H_{20}O_3$	methyl jasmonate
156(100), 141(60), 41(45), 157(33), 55(30), 43(30), 27(28), 29(22)	226	$C_{11}H_{18}N_2O_3$	amylobarbitone
83(100), 82(28), 153(26), 55(20), 156(19), 41(16), 67(12), 96(11)	226	$C_{13}H_{22}O_3$	methyl dihydrojasmonate
169(100), 185(60), 43(47), 168(32), 211(28), 141(22), 167(21), 170(14)	227	$C_{14}H_{13}NO_2$	biphenyl, N-hydroxy-3-acetylamino-
169(100), 211(39), 168(30), 185(24), 43(23), 170(15), 141(11), 167(10)	227	$C_{14}H_{13}NO_2$	biphenyl, N-hydroxy-4-acetylamino-
43(100), 55(50), 69(40), 56(40), 41(38), 61(36), 83(34), 70(33)	228	$C_{14}H_{28}O_2$	dodecyl acetate
30(100), 229(48), 231(30), 172(19), 194(13), 174(12), 42(12), 230(8)	229	$C_9H_9N_3Cl_2$	clonidine
43(100), 171(89), 188(83), 230(61), 79(44), 52(19), 51(18), 95(16)	230	$C_8H_{10}N_2O_4S$	benzenesulfonamide, 3-hydroxy-4-acetylamino-
202(100), 244(75), 43(74), 138(42), 186(34), 92(25), 107(24), 79(12)	244	$C_9H_{12}N_2O_4S$	benzenesulfonamide, 3-methoxy-4-acetylamino-
43(100), 188(27), 172(21), 60(19), 107(18), 108(12), 92(9), 156(8)	230	$C_8H_{10}N_2O_4S$	benzenesulfonamide, N-OH-4-acetylamino-
185(100), 230(48), 186(15), 141(14), 115(12), 170(11), 139(11), 153(8)	230	$C_{14}H_{14}O_3$	naproxen
204(100), 117(35), 232(24), 51(20), 77(18), 161(17), 103(17), 146(16)	232	$C_{12}H_{12}N_2O_3$	phenobarbitone
84(100), 56(7), 85(6), 91(5), 55(4), 30(3), 39(2), 77(2)	233	$C_{14}H_{19}NO_2$	methylphenidate
86(100), 30(17), 58(10), 87(6), 41(4), 72(3), 56(3), 27(3)	234	$C_{14}H_{22}N_2O$	lignocaine
234(100), 175(98), 199(68), 177(64), 236(59), 147(40), 145(37), 111(33)	234	$C_9H_8Cl_2O_3$	phenoxyacetic acid, 2,4-dichloro-, me.ester
93(100), 141(87), 43(85), 94(62), 68(51), 121(49), 95(46), 41(39)	236	$C_{15}H_{24}O_2$	bisabolone oxide
193(100), 192(34), 236(23), 191(20), 165(16), 194(15), 63(7), 167(6)	236	$C_{15}H_{12}N_2O$	carbamazepine

Ions/Intensities	Mol.Wt.	Formula	Compound Name
86(100), 99(25), 120(14), 30(10), 58(8), 87(6), 91(6), 92(5)	236	$C_{13}H_{20}N_2O_2$	procaine
238(100), 223(31), 43(26), 192(19), 239(15), 191(11), 163(11), 39(10)	238	$C_{13}H_{18}O_4$	benzene, 2,3,4,5-tetramethoxy-allyl-
43(100), 143(83), 85(67), 105(62), 81(60), 59(53), 134(49), 71(48)	238	$C_{15}H_{26}O_2$	bisabolol oxide B
143(100), 43(71), 93(43), 71(34), 125(34), 121(31), 68(30), 134(25)	238	$C_{15}H_{26}O_2$	bisabolol oxide B
151(100), 93(72), 43(43), 194(28), 136(25), 41(24), 133(14), 55(12)	238	$C_{15}H_{26}O_2$	daucol
55(100), 43(94), 41(88), 69(78), 83(70), 57(68), 56(60), 70(53)	238	$C_{17}H_{34}$	heptadec-8-ene, *Z*-
168(100), 167(85), 41(84), 43(71), 27(33), 97(29), 39(28), 29(26)	238	$C_{12}H_{18}N_2O_3$	quinalbarbitone
181(100), 180(71), 223(57), 152(23), 43(21), 197(19), 182(16), 165(15)	239	$C_{15}H_{13}NO_2$	fluorene, N-hydroxy-2-acetylamino-
239(100), 180(62), 197(61), 196(51), 181(23), 152(21), 240(16), 168(14)	239	$C_{15}H_{13}NO_2$	fluorene-9-ol, 2-acetlamino-
169(100), 58(70), 168(29), 72(17), 170(17), 167(13), 42(10), 30(6)	239	$C_{17}H_{21}N$	pheniramine
199(100), 43(93), 168(51), 184(27), 200(17), 241(17), 169(16), 153(13)	241	$C_{15}H_{15}NO_2$	biphenyl, N-methoxy-3-acetylamino-
168(100), 199(77), 43(46), 169(40), 167(32), 198(30), 241(29), 141(22)	241	$C_{15}H_{15}NO_2$	biphenyl, N-methoxy-4-acetylamino-
43(100), 121(53), 202(24), 185(15), 64(9), 63(9), 122(8), 90(7)	242	$C_9H_{12}N_2O_4S$	benzenesulfonamide, N-methoxy-4-acetylamino-
185(100), 244(35), 186(17), 170(10), 141(7), 154(6), 245(6), 153(6)	244	$C_{15}H_{16}O_3$	naproxen, methyl ester
71(100), 42(82), 70(62), 57(49), 43(35), 103(26), 91(25), 247(23)	247	$C_{15}H_{21}NO_2$	pethidine
30(100), 72(91), 133(73), 56(16), 43(15), 116(13), 41(12), 104(11)	248	$C_{14}H_{20}N_2O_2$	pindolol
235(100), 91(52), 250(42), 233(30), 65(25), 76(21), 236(16), 39(15)	250	$C_{16}H_{14}N_2O$	methaqualone
180(100), 104(74), 77(66), 223(48), 209(43), 252(41), 51(39), 181(27)	252	$C_{15}H_{12}N_2O_2$	phentoin
180(100), 181(63), 210(51), 179(39), 211(38), 43(37), 253(36), 165(33)	253	$C_{16}H_{15}NO_2$	fluorene, N-methoxy-2-acetylamino-
58(100), 73(80), 45(49), 44(22), 59(16), 42(14), 165(14), 167(11)	256	$C_{17}H_{21}NO$	diphenhydramine
43(100), 109(51), 151(38), 65(20), 92(17), 45(15), 156(15), 108(13)	256	$C_{10}H_{12}N_2O_4S$	sulphanilamide, N1,N4-diacetyl-
43(100), 55(68), 41(58), 69(57), 83(52), 57(48), 61(41), 70(36)	256	$C_{16}H_{32}O_2$	tetradecyl acetate
232(100), 118(24), 146(23), 175(21), 117(18), 233(14), 91(9), 103(8)	260	$C_{14}H_{16}N_2O_3$	phenobarbitone, N,N-dimethyl
70(100), 44(67), 191(58), 189(13), 192(11), 165(8), 59(6), 71(5)	263	$C_{19}H_{21}N$	protryptyline
266(100), 264(76), 268(47), 109(25), 124(19), 98(14), 133(14), 62(12)	264	$C_8N_2Cl_4$	chlorothalonil
266(100), 264(62), 268(60), 165(38), 167(35), 95(29), 60(21), 202(20)	264	C_6HOCl_5	phenol, pentachloro-
72(100), 30(78), 41(20), 56(13), 43(9), 57(6), 73(6), 39(5)	265	$C_{15}H_{23}NO_3$	oxprenolol
72(100), 30(57), 43(10), 56(9), 41(7), 57(6), 107(6), 73(5)	266	$C_{14}H_{22}N_2O_3$	atenolol
72(100), 30(55), 45(13), 43(7), 41(7), 56(7), 107(6), 57(5)	267	$C_{15}H_{25}NO_3$	metoprolol

Ions/Intensities	Mol.Wt.	Formula	Compound Name
55(100), 41(77), 69(69), 74(68), 83(43), 87(40), 84(34), 43(41)	268	$C_{17}H_{32}O_2$	methyl palmitoleate
58(100), 71(60), 42(51), 44(26), 43(26), 51(22), 30(21), 27(11)	270	$C_{17}H_{22}N_2O$	doxylamine
43(100), 60(60), 41(54), 57(48), 102(39), 61(25), 71(21), 228(19)	270	$C_{17}H_{24}O_2$	isopropyl myristate
242(100), 207(94), 244(33), 270(20), 208(17), 165(16), 243(16), 269(13)	270	$C_{16}H_{15}N_2Cl$	medazepam
59(100), 271(48), 31(39), 150(36), 270(26), 42(23), 214(19), 30(16)	271	$C_{18}H_{25}NO$	dextromethorphan
86(100), 99(19), 30(17), 69(14), 58(11), 41(11), 43(9), 120(9)	271	$C_{13}H_{22}N_3OCl$	procainamide
203(100), 58(92), 205(33), 72(26), 204(15), 42(13), 167(13), 202(12)	274	$C_{16}H_{19}N_2Cl$	chlorpheniramine
157(100), 43(55), 115(45), 203(21), 31(16), 42(15), 45(13), 111(10)	276	$C_{12}H_{20}O_6$	triethyl citrate
58(100), 59(18), 42(11), 30(8), 202(7), 203(5), 215(), 91(4)	277	$C_{20}H_{23}N$	amitryptaline
190(100), 125(29), 134(28), 162(27), 91(14), 112(13), 191(12), 161(11)	278	$C_{16}H_{22}O_4$	abscisic acid, methyl ester
208(100), 209(86), 278(52), 84(28), 42(25), 96(24), 193(23), 194(21)	278	$C_{19}H_{22}N_2$	triprolidine
41(100), 79(82), 67(82), 119(80), 55(68), 81(68), 84(65), 93(9)	280	$C_{16}H_{24}O_4$	Brefeldin A
58(100), 235(58), 85(52), 234(44), 280(22), 193(20), 195(19), 208(16)	280	$C_{19}H_{24}N_2$	imipramine
253(100), 280(99), 234(68), 206(66), 252(62), 281(59), 251(54), 77(51)	281	$C_{15}H_{11}N_3O_3$	nitrazepam
59(100), 72(51), 41(49), 55(41), 43(41), 29(23), 57(20), 81(12)	281	$C_{18}H_{35}NO$	oleamide
256(100), 283(81), 284(66), 255(42), 257(41), 285(41), 258(33), 286(22)	284	$C_{16}H_{13}N_2OCl$	diazepam
58(100), 86(21), 284(20), 238(10), 85(9), 199(8), 42(8), 198(7)	284	$C_{17}H_{20}N_2S$	promazine
43(100), 248(75), 108(70), 290(63), 140(50), 58(27), 65(27), 92(23)	290	$C_{14}H_{14}N_2O_3S$	dapsone, acetyl-
58(100), 249(37), 208(17), 193(14), 99(13), 248(11), 84(11), 234(10)	294	$C_{20}H_{26}N_2$	trimipramine
100(100), 44(17), 72(9), 101(7), 77(7), 29(7), 42(6), 56(4)	295	$C_{13}H_{19}NO$	diethylpropion
297(100), 42(53), 298(20), 296(19), 58(18), 283(17), 241(15), 240(15)	297	$C_{18}H_{19}NO_3$	oripavine
282(100), 283(80), 284(44), 285(25), 77(15), 220(13), 247(12), 219(11)	299	$C_{16}H_{14}N_3OCl$	chlordiazepoxide
300(100), 77(85), 258(67), 51(58), 255(52), 259(47), 256(38), 283(38)	300	$C_{16}H_{13}N_2O_2Cl$	clobazepam
271(100), 273(35), 77(24), 256(20), 300(19), 272(19), 255(14), 228(13)	300	$C_{16}H_{13}N_2O_2Cl$	temazepam
301(100), 44(40), 42(38), 59(37), 70(31), 164(26), 31(24), 302(21)	301	$C_{18}H_{23}NO_3$	dihydrocodeine
82(100), 182(45), 83(29), 105(21), 42(16), 77(13), 96(11), 97(8)	303	$C_{17}H_{21}NO_4$	cocaine
77(100), 183(93), 308(44), 184(27), 105(19), 55(15), 51(14), 91(11)	308	$C_{19}H_{20}N_2O_2$	phenylbutazone
265(100), 43(46), 121(36), 308(29), 77(22), 187(17), 115(17), 266(17)	308	$C_{19}H_{16}O_4$	warfarin
295(100), 296(21), 238(12), 310(12), 26(8), 251(6), 27(6), 55(5)	310	$C_{21}H_{26}O_2$	cannabinol

Ions/Intensities	Mol.Wt.	Formula	Compound Name
43(100), 141(49), 183(28), 87(24), 42(22), 41(17), 140(10), 108(8)	312	$C_{13}H_{16}N_2O_5S$	paracetamol-3-mercapturic acid
313(100), 42(38), 59(29), 162(28), 314(19), 284(18), 124(18), 243(16)	313	$C_{19}H_{23}NO_3$	ethylmorphine
312(100), 285(99), 286(67), 313(63), 266(48), 238(43), 283(40), 284(33)	313	$C_{16}H_{12}N_3O_3F$	flunitrazepam
239(100), 299(20), 240(20), 314(14), 197(6), 173(5), 141(5), 143(4)	314	$C_{21}H_{30}O_2$	methyl dehydroabietate
317(100), 315(96), 236(92), 288(69), 78(57), 286(57), 77(56), 51(51)	315	$C_{14}H_{10}N_3OBr$	bromazepam
280(100), 286(72), 315(72), 288(56), 240(53), 234(53), 75(48), 287(44)	315	$C_{15}H_{10}N_3O_3Cl$	clonazepam
123(100), 121(28), 150(27), 41(20), 93(19), 81(17), 43(17), 55(16)	316	$C_{20}H_{28}O_3$	cinerin I
316(100), 256(88), 241(52), 121(50), 136(42), 105(39), 213(37), 257(34)	316	$C_{21}H_{32}O_2$	methyl abietate
121(100), 146(24), 55(23), 41(23), 180(22), 133(20), 316(20), 257(17)	316	$C_{21}H_{32}O_2$	methyl pimarate
58(100), 86(21), 318(16), 85(8), 42(8), 272(6), 320(6), 232(5)	318	$C_{17}H_{19}N_2SCl$	chlorpromazine
86(100), 30(13), 58(11), 87(6), 41(6), 73(5), 42(5), 319(3)	319	$C_{18}H_{26}N_3Cl$	chloroquine
239(100), 284(72), 75(67), 276(49), 138(48), 302(46), 111(43), 304(35)	320	$C_{15}H_{20}N_2O_2Cl_2$	lorazepam
323(100), 221(81), 181(56), 222(45), 207(40), 72(37), 223(34), 196(24)	323	$C_{20}H_{25}N_3O$	lysergic acid diethylamide (LSD)
93(100), 199(89), 324(66), 77(56), 109(48), 55(45), 65(32), 41(31)	324	$C_{19}H_{20}N_2O_3$	oxyphenbutazone
136(100), 41(13), 42(12), 137(12), 81(10), 55(9), 39(5), 117(5)	324	$C_{20}H_{24}N_2O_2$	quinine
123(100, 161(99), 133(95), 41(42), 162(31), 81(29), 91(26), 43(25),	328	$C_{21}H_{28}O_3$	isopyrethrin I
123(100), 41(34), 133(20), 162(18), 81(17), 91(17), 55(17), 105(12)	328	$C_{21}H_{28}O_3$	pyrethrin I
123(100), 43(54), 41(34), 55(28), 81(23), 164(22), 93(22), 135(16)	330	$C_{21}H_{30}O_3$	jasmolin I
176(100), 177(36), 57(22), 45(18), 149(13), 29(12), 119(9)	338	$C_{19}H_{30}O_5$	piperonyl butoxide
58(100), 91(5), 57(5), 59(4), 42(3), 77(3), 105(2), 30(2)	339	$C_{22}H_{29}NO_2$	dextropropoxyphene
324(100), 338(73), 339(62), 325(22), 308(20), 51(15), 293(14), 151(13)	339	$C_{20}H_{21}NO_4$	papaverine
341(100), 282(58), 43(39), 42(34), 229(30), 59(23), 342(22), 204(17)	341	$C_{20}H_{23}NO_4$	acetyl codeine
233(100), 340(72), 341(59), 248(55), 247(32), 356(30), 139(29), 234(28)	356	$C_{20}H_{17}O_3SF$	sulindac
139(100), 141(37), 357(26), 111(23), 140(10), 358(9), 75(8), 113(8)	357	$C_{19}H_{16}NO_4Cl$	indomethacin
121(100), 107(97), 149(65), 93(56), 167(55), 150(29), 91(25), 55(25)	360	$C_{21}H_{28}O_5$	cinerin II
184(100), 65(81), 39(68), 121(44), 69(39), 41(38), 94(35), 186(32)	364	$C_{18}H_{17}O_6Cl$	radicicol
98(100), 370(22), 126(14), 99(13), 70(12), 42(9), 371(5), 258(5)	370	$C_{21}H_{26}N_2S_2$	thioridazine
73(100), 371(76), 178(41), 196(39), 42(29), 372(23), 59(21), 70(21)	371	$C_{21}H_{29}NO_3Si$	codeine, trimethylsilyl derivative
161(100), 133(92), 107(23), 91(22), 41(19), 105(18), 162(17), 93(15)	372	$C_{22}H_{28}O_5$	isopyrethrin II

Ions/Intensities	Mol.Wt.	Formula	Compound Name
133(100), 160(77), 107(69), 161(68), 41(67), 167(58), 91(56), 105(41)	372	$C_{22}H_{28}O_5$	pyrethrin II
113(100), 70(92), 43(51), 42(56), 373(39), 141(34), 26(28), 71(25)	373	$C_{20}H_{24}N_2SCl$	prochlorperazine
163(100), 135(89), 93(87), 107(79), 167(76), 55(55), 121(48), 41(43)	374	$C_{22}H_{30}O_5$	jasmolin II
43(100), 57(87), 82(70), 55(59), 41(53), 96(48), 83(45), 69(44)	380	$C_{26}H_{52}O$	hexacosanal, n-
233(100), 383(41), 259(30), 245(30), 95(29), 56(25), 43(19), 41(19)	383	$C_{18}H_{21}N_5O_4$	prazosin
86(100), 30(16), 87(10), 58(8), 99(8), 42(4), 56(4), 84(3)	387	$C_{21}H_{23}N_3OFCl$	flurazepam
114(100), 100(83), 42(14), 56(9), 115(8), 70(6), 101(6), 55(5)	398	$C_{23}H_{30}N_2O_4$	pholcodine
185(100), 185(57), 259(54), 43(54), 57(38), 29(27), 41(24), 157(22)	402	$C_{20}H_{34}O_8$	citric acid, acetyl-, tri-n-butyl ester
77(100), 278(56), 78(36), 51(29), 105(23), 39(16), 279(15), 126(14)	404	$C_{23}H_{20}N_2O_3S$	sulphinpyrazone
113(100), 70(94), 43(70), 42(44), 407(39), 71(33), 141(27), 58(22)	407	$C_{21}H_{24}N_3F_3S$	trifluoperazine
259(100), 161(62), 81(42), 163(10), 54(9), 89(8), 27(7), 160(7)	414	$C_{18}H_{14}N_2OCl_4$	miconazole
56(100), 169(39), 43(28), 67(22), 82(16), 39(14), 171(13), 54(13)	494	$C_{23}H_{28}N_3O_5SCl$	glibenclamide